

A STUDY OF UNBALANCED MORPHOLOGICAL UNDERSTANDING:
MORPHOLOGICAL LAND USE PATTERNS ANALYSIS OF U.S. MEGAREGIONS

A Dissertation

by

YOUNGHO KO

Submitted to the Office of Graduate Studies of
Texas A&M University
in partial fulfillment of the requirements for the degree of

DOCTOR OF PHILOSOPHY

May 2012

Major Subject: Urban and Regional Sciences

A Study of Unbalanced Morphological Understanding:
Morphological Land Use Patterns Analysis of U.S. Megaregions

Copyright 2012 Youngho Ko

A STUDY OF UNBALANCED MORPHOLOGICAL UNDERSTANDING:
MORPHOLOGICAL LAND USE PATTERNS ANALYSIS OF U.S. MEGAREGIONS

A Dissertation

by

YOUNGHO KO

Submitted to the Office of Graduate Studies of
Texas A&M University
in partial fulfillment of the requirements for the degree of

DOCTOR OF PHILOSOPHY

Approved by:

Chair of Committee,	Elise M. Bright
Committee Members,	Shannon S. Van Zandt
	Dudley L. Poston
	Raghavan Srinivasan
Head of Department,	Forster Ndubisi

May 2012

Major Subject: Urban and Regional Sciences

ABSTRACT

A Study of Unbalanced Morphological Understanding:
Morphological Land Use Patterns Analysis of U.S. Megaregions.

(May 2012)

Youngho Ko, B.E., Handong University, Pohang, S.Korea;

M.U.P., Texas A&M University, College Station, TX

Chair of Advisory Committee: Dr. Elise M. Bright

This study identifies problems in the definitions of U.S. megaregions which have given too much importance to functional relationships and overlooked morphological characteristics. This study, therefore, examines morphological characteristics of the 11 U.S. megaregions to represent morphologically-oriented U.S. megaregions. A primary research hypothesis is that the 11 U.S. megaregions spatially examined by morphological characteristics may not be equal to the current representation of the 11 U.S. megaregions. The research hypothesis is tested by two distinct scale analyses which spatially examine the morphological characteristics at global and local levels. The global scale spatial analysis was conducted using the density-based sprawl index, spatial scattering pattern index, and spatial clustering pattern index. Local scale spatial patterns were examined by the Getis-Ord G_i^* hot spots analysis and the Anselin Local Moran's I cluster and outlier analysis. Representing the megaregion scale urban built environment, the morphological characteristics were examined by 2000 total population,

2000 population density, 2001 impervious land cover, and 2000 nighttime light emissions.

Megaregional morphology is important for considering the built environment, the urban form, and the urban fabric at the megaregion scale. The consideration for the megaregional morphology describes the space for human behavior moving from one place to another within a regional boundary. Morphological clusterings and spatial boundaries of the clustering areas, therefore, are critical for defining U.S. megaregions to identify the spatial limits of megaregion scale human behavior. Theoretical and empirical literature reviews, however, recognized that most megaregion studies focused on functional relationships and, as such, characterized the megaregions as the economically dominant and functionally interconnected polycentric urban structures.

The analysis results found that global scale spatial distributions of morphological characteristics had been inconsistently concentrated and clustered in high density subareas of each U.S. megaregion. The morphological clustering representation of the 11 U.S. megaregions, as the final result, concluded that the morphologically identified U.S. megaregions were not the same as the current U.S. megaregions. This study asks the urban and regional planning profession to balance the perspective between functional relationships and morphological characteristics in identifying U.S. megaregions.

ACKNOWLEDGEMENTS

I would like to thank my committee chair, Dr. Bright, and my committee members, Dr. VanZandt, Dr. Srinivasan, and Dr. Poston, for their guidance and support throughout the course of this research.

Thanks also go to my friends and colleagues and the department faculty and staff for making my time at Texas A&M University a great experience.

Finally, thanks to my wife and family for their patience and love.

TABLE OF CONTENTS

	Page
ABSTRACT	iii
ACKNOWLEDGEMENTS	v
TABLE OF CONTENTS	vi
LIST OF FIGURES	ix
LIST OF TABLES	xiv
CHAPTER	
I INTRODUCTION.....	1
1. Statement of the problem	1
2. Purpose of the study	2
3. Research questions and hypotheses.....	2
4. Importance of the study	4
II LITERATURE REVIEW.....	7
1. Various definitions of megaregions in theoretical efforts	7
1.1. Megalopolis – the first concept of megaregions	8
1.2. Contemporary megaregion concepts.....	15
1.3. Findings in theoretical reviews of U.S. megaregion concepts	22
2. Various features of the megaregion in empirical studies	24
2.1. Contemporary megaregion features	24
2.2. Findings in empirical reviews of U.S. megaregion features	27
3. Conclusion.....	29
III RESEARCH METHODOLOGY	31
1. Morphological characteristics and land use patterns of U.S. megaregions	31
1.1. Functional and the morphological features of megaregions	32
1.2. Land use patterns.....	34

CHAPTER	Page
2. Dimensions to examine U.S. megaregion morphological characteristics	35
2.1. Density dimension	38
2.2. Spatial scattering dimension	40
2.3. Spatial clustering dimension	41
2.4. Measurement scale	42
3. Indices to evaluate morphological dimension at a megaregion scale	43
3.1. Density-based sprawl index	44
3.2. Spatial scattering pattern index	45
3.3. Spatial clustering pattern index	46
3.4. Local scale spatial association	47
4. Description of the data and the data treatment	52
4.1. Description of morphological data	52
4.2. Data treatment for density-based sprawl index	54
4.3. Data treatment for spatial scattering pattern index	56
4.4. Data treatment for spatial clustering pattern index	62
4.5. Data treatment for local scale spatial analyses	66
 IV RESULTS	 69
1. Spatial patterns analysis results	69
1.1. Density-based sprawl index	69
1.2. Spatial scattering pattern index	71
1.3. Spatial clustering pattern index	76
2. Local spatial clustering analysis results	82
2.1. The Northeast megaregion	82
2.2. The Texas Triangle megaregion	98
2.3. The Great Lakes megaregion	115
2.4. The Piedmont Atlantic megaregion	134
2.5. The Florida megaregion	152
2.6. The Gulf Coast megaregion	168
2.7. The Front Range megaregion	184
2.8. The Arizona Sun Corridor megaregion	199
2.9. The Northern California megaregion	213
2.10. The Southern California megaregion	228
2.11. The Cascadia megaregion	242
3. Results summary for research hypotheses	257
3.1. Spatial patterns of the 11 U.S. megaregions	257
3.2. Spatial associations of the 11 U.S. megaregions	259
3.3. Morphological characteristics of the 11 U.S. megaregions ..	262

CHAPTER	Page
V CONCLUSION	270
1. Summary	270
2. Conclusions	273
3. Limitations and further research.....	274
4. Urban and regional planning implications	276
REFERENCES	280
APPENDIX A	286
APPENDIX B	297
VITA	308

LIST OF FIGURES

FIGURE	Page
1 U.S. megaregion identified by Gottmann.....	9
2 U.S. megaregions identified by the Metropolitan Institute	19
3 U.S. megaregions identified by the RPA	19
4 Density dimension – high-density land use pattern and low-density land use pattern.....	39
5 Spatial scattering dimension – highly concentrated land use pattern and equally scattered land use pattern.....	41
6 Spatial clustering dimension – monocentric land use pattern, polycentric land use pattern, and decentralized land use pattern	42
7 Four different types of local spatial associations	51
8 Calculation results of density-based sprawl index	70
9 Calculation results of spatial scattering pattern index.....	72
10 Calculation results of spatial clustering pattern index	77
11 The Northeast megaregion local clustering analysis results by 2000 population density	83
12 The Northeast megaregion local clustering analysis results by 2001 impervious land cover	86
13 The Northeast megaregion local clustering analysis results by 2000 nighttime light emissions	90
14 Local clusterings of morphological features in the Northeast megaregion	94
15 Morphological clusterings of the Northeast megaregion	96
16 The Texas Triangle megaregion local clustering analysis results by 2000 population density	99

	Page
17 The Texas Triangle megaregion local clustering analysis results by 2001 impervious land cover	103
18 The Texas Triangle megaregion local clustering analysis results by 2000 nighttime light emissions	107
19 Local clusterings of morphological features in the Texas Triangle megaregion	110
20 Morphological clusterings of the Texas Triangle megaregion.....	112
21 The Great Lakes megaregion local clustering analysis results by 2000 population density	116
22 The Great Lakes megaregion local clustering analysis results by 2001 impervious land cover	121
23 The Great Lakes megaregion local clustering analysis results by 2000 nighttime light emissions	125
24 Local clusterings of morphological features in the Great Lakes megaregion.....	128
25 Morphological clusterings of the Great Lakes megaregion	130
26 The Piedmont Atlantic megaregion local clustering analysis results by 2000 population density	135
27 The Piedmont Atlantic megaregion local clustering analysis results by 2001 impervious land cover	139
28 The Piedmont Atlantic megaregion local clustering analysis results by 2000 nighttime light emissions	143
29 Local clusterings of morphological features in the Piedmont Atlantic megaregion.....	146
30 Morphological clusterings of the Piedmont Atlantic megaregion	148
31 The Florida megaregion local clustering analysis results by 2000 population density	153

	Page
32 The Florida megaregion local clustering analysis results by 2001 impervious land cover	156
33 The Florida megaregion local clustering analysis results by 2000 nighttime light emissions	159
34 Local clusterings of morphological features in the Florida megaregion....	163
35 Morphological clusterings of the Florida megaregion	165
36 The Gulf Coast megaregion local clustering analysis results by 2000 population density	169
37 The Gulf Coast megaregion local clustering analysis results by 2001 impervious land cover	173
38 The Gulf Coast megaregion local clustering analysis results by 2000 nighttime light emissions	176
39 Local clusterings of morphological features in the Gulf Coast megaregion...	179
40 Morphological clusterings of the Gulf Coast megaregion	181
41 The Front Range megaregion local clustering analysis results by 2000 population density	185
42 The Front Range megaregion local clustering analysis results by 2001 impervious land cover	188
43 The Front Range megaregion local clustering analysis results by 2000 nighttime light emissions	192
44 Local clusterings of morphological features in the Front Range megaregion	195
45 Morphological clusterings of the Front Range megaregion.....	197
46 The Arizona Sun Corridor megaregion local clustering analysis results by 2000 population density	201
47 The Arizona Sun Corridor megaregion local clustering analysis results by 2001 impervious land cover	204

	Page
48 The Arizona Sun Corridor megaregion local clustering analysis results by 2000 nighttime light emissions	207
49 Local clusterings of morphological features in the Arizona Sun Corridor megaregion	209
50 Morphological clusterings of the Arizona Sun Corridor megaregion	211
51 The Northern California megaregion local clustering analysis results by 2000 population density	214
52 The Northern California megaregion local clustering analysis results by 2001 impervious land cover	218
53 The Northern California megaregion local clustering analysis results by 2000 nighttime light emissions	221
54 Local clusterings of morphological features in the Northern California megaregion	224
55 Morphological clusterings of the Northern California megaregion	226
56 The Southern California megaregion local clustering analysis results by 2000 population density	229
57 The Southern California megaregion local clustering analysis results by 2001 impervious land cover	232
58 The Southern California megaregion local clustering analysis results by 2000 nighttime light emissions	235
59 Local clusterings of morphological features in the Southern California megaregion	238
60 Morphological clusterings of the Southern California megaregion	240
61 The Cascadia megaregion local clustering analysis results by 2000 population density	244
62 The Cascadia megaregion local clustering analysis results by 2001 impervious land cover	247

	Page
63 The Cascadia megaregion local clustering analysis results by 2000 nighttime light emissions	250
64 Local clusterings of morphological features in the Cascadia megaregion.	253
65 Morphological clusterings of the Cascadia megaregion	255
66 Proportional extents of morphological clusterings in terms of morphological elements of the 11 U.S. megaregions	265
67 The 11 U.S. megaregions morphological clusterings	267

LIST OF TABLES

TABLE		Page
1	A summary of contemporary megaregion concepts.....	16
2	Components used to define U.S. megaregions by two institutions	20
3	Transformation of the concept of megaregions in theoretical studies.....	21
4	Megaregion features empirically developed in contemporary megaregion studies.....	25
5	Dimensions of other land use patterns studies	36
6	Northeast 2000 population density hot spots descriptors.....	84
7	Northeast 2000 population density HH spatial associations descriptors....	85
8	Northeast 2001 impervious land cover hot spots descriptors.....	87
9	Northeast 2001 impervious land cover HH spatial associations descriptors.....	88
10	Northeast 2000 nighttime light emissions hot spots descriptors	91
11	Northeast 2000 nighttime light emissions HH spatial associations descriptors.....	92
12	The Northeast megaregion morphological clusterings descriptors	97
13	Texas Triangle 2000 population density hot spots descriptors	100
14	Texas Triangle 2000 population density HH spatial associations descriptors.....	101
15	Texas Triangle 2000 population density clustering descriptors.....	102
16	Texas Triangle 2001 impervious land cover hot spots descriptors	104
17	Texas Triangle 2001 impervious land cover HH spatial associations descriptors.....	105

	Page
18 Texas Triangle 2001 impervious land cover clustering descriptors.....	106
19 Texas Triangle 2000 nighttime light emissions hot spots descriptors	108
20 Texas Triangle 2000 nighttime light emissions HH spatial associations descriptors.....	109
21 The Texas Triangle megaregion morphological clusterings descriptors ...	113
22 Great Lakes 2000 population density hot spots descriptors.....	117
23 Great Lakes 2000 population density HH spatial associations descriptors.....	118
24 Great Lakes 2000 population density clustering descriptors	119
25 Great Lakes 2001 impervious land cover hot spots descriptors.....	122
26 Great Lakes 2001 impervious land cover HH spatial associations descriptors.....	123
27 Great Lakes 2001 impervious land cover clustering descriptors	123
28 Great Lakes 2000 nighttime light emissions hot spots descriptors	126
29 Great Lakes 2000 nighttime light emissions HH spatial associations descriptors.....	127
30 The Great Lakes megaregion morphological clusterings descriptors	131
31 Piedmont Atlantic 2000 population density hot spots descriptors	136
32 Piedmont Atlantic 2000 population density HH spatial associations descriptors.....	137
33 Piedmont Atlantic 2000 population density clustering descriptors.....	138
34 Piedmont Atlantic 2001 impervious land cover hot spots descriptors.....	140
35 Piedmont Atlantic 2001 impervious land cover HH spatial associations descriptors.....	141

	Page
36 Piedmont Atlantic 2001 impervious land cover clustering descriptors.....	142
37 Piedmont Atlantic 2000 nighttime light emissions hot spots descriptors ..	144
38 Piedmont Atlantic 2000 nighttime light emissions HH spatial associations descriptors.....	145
39 The Piedmont Atlantic megaregion morphological clusterings descriptors.	149
40 Florida 2000 population density hot spots descriptors.....	152
41 Florida 2000 population density HH spatial associations descriptors.....	154
42 Florida 2000 population density clustering descriptors	155
43 Florida 2001 impervious land cover hot spots descriptors.....	157
44 Florida 2001 impervious land cover HH spatial associations descriptors .	158
45 Florida 2001 impervious land cover clustering descriptors	160
46 Florida 2000 nighttime light emissions hot spots descriptors	161
47 Florida 2000 nighttime light emissions HH spatial associations descriptors	162
48 The Florida megaregion morphological clusterings descriptors	166
49 Gulf Coast 2000 population density hot spots descriptors.....	170
50 Gulf Coast 2000 population density HH spatial associations descriptors.....	171
51 Gulf Coast 2000 population density clustering descriptors	172
52 Gulf Coast 2001 impervious land cover hot spots descriptors.....	174
53 Gulf Coast 2001 impervious land cover HH spatial associations descriptors.....	174
54 Gulf Coast 2001 impervious land cover clustering descriptors	175
55 Gulf Coast 2000 nighttime light emissions hot spots descriptors	177

	Page
56 Gulf Coast 2000 nighttime light emissions HH spatial associations descriptors.....	178
57 The Gulf Coast megaregion morphological clusterings descriptors	182
58 Front Range 2000 population density hot spots descriptors	186
59 Front Range 2000 population density HH spatial associations descriptors.....	187
60 Front Range 2001 impervious land cover hot spots descriptors	189
61 Front Range 2001 impervious land cover HH spatial associations descriptors.....	190
62 Front Range 2001 impervious land cover clustering descriptors.....	191
63 Front Range 2000 nighttime light emissions hot spots descriptors.....	193
64 Front Range 2000 nighttime light emissions HH spatial associations descriptors.....	194
65 The Front Range megaregion morphological clusterings descriptors.....	198
66 Arizona Sun Corridor 2000 population density hot spots descriptors	200
67 Arizona Sun Corridor 2000 population density HH spatial associations descriptors.....	202
68 Arizona Sun Corridor 2001 impervious land cover hot spots descriptors .	203
69 Arizona Sun Corridor 2001 impervious land cover HH spatial associations descriptors.....	205
70 Arizona Sun Corridor 2000 nighttime light emissions hot spots descriptors	206
71 Arizona Sun Corridor 2000 nighttime light emissions HH spatial associations descriptors.....	208
72 The Arizona Sun Corridor megaregion morphological clusterings descriptors.....	212

	Page
73 Northern California 2000 population density hot spots descriptors.....	215
74 Northern California 2000 population density HH spatial associations descriptors.....	216
75 Northern California 2001 impervious land cover hot spots descriptors.....	217
76 Northern California 2001 impervious land cover HH spatial associations descriptors.....	219
77 Northern California 2001 impervious land cover clustering descriptors ...	220
78 Northern California 2000 nighttime light emissions hot spots descriptors	222
79 Northern California 2000 nighttime light emissions HH spatial associations descriptors.....	223
80 The Northern California megaregion morphological clusterings descriptors.....	227
81 Southern California 2000 population density hot spots descriptors.....	228
82 Southern California 2000 population density HH spatial associations descriptors.....	230
83 Southern California 2001 impervious land cover hot spots descriptors.....	231
84 Southern California 2001 impervious land cover HH spatial associations descriptors.....	233
85 Southern California 2000 nighttime light emissions hot spots descriptors	236
86 Southern California 2000 nighttime light emissions HH spatial associations descriptors.....	237
87 The Southern California megaregion morphological clusterings descriptors.....	241
88 Cascadia 2000 population density hot spots descriptors.....	243
89 Cascadia 2000 population density HH spatial associations descriptors.....	245

	Page
90 Cascadia 2001 impervious land cover hot spots descriptors.....	246
91 Cascadia 2001 impervious land cover HH spatial associations descriptors.	248
92 Cascadia 2001 impervious land cover clustering descriptors	249
93 Cascadia 2000 nighttime light emissions hot spots descriptors	251
94 Cascadia 2000 nighttime light emissions HH spatial associations descriptors.....	252
95 The Cascadia megaregion morphological clusterings descriptors	256
96 A summary of morphological clustering extent of the 11 U.S. megaregions ...	264

CHAPTER I

INTRODUCTION

1. Statement of the problem

This study identifies problems in the definitions of United States (U.S.) megaregions which have given too much importance to functional relationships and overlooked morphological characteristics. A concept of megaregion has been initially developed in the U.S. northeastern seaboard, naming it a megalopolis, as a new urban morphology that interconnects metropolitan areas through transportation bringing people, money, and services from one place to another (Gottmann, 1961). Inspired from the concept of the megalopolis, the Regional Plan Association (RPA, 2006) and Metropolitan Institute at Virginia Tech (Lang & Dhavale, 2005) have identified the 11 U.S. megaregions. The 11 U.S. megaregions have been representing a new urban geography that interconnects traditional metropolitan and urban areas across traditional jurisdictional boundaries. Most contemporary research of U.S. megaregions has considered megaregional economic advantage based primarily on functionally interconnected and integrated regional relationships (Banerjee, 2009; Carbonell & Yaro, 2005; Contant & de Nie, 2009; Cowell, 2010; Feser & Hewings, 2007; Florida, Gulden, & Mellander, 2008; Glaeser, 2007; Green, 2007; Lang & Nelson, 2007, 2009; Meijers & Burger, 2009; Priemus & Hall, 2004; Rodrigue, 2004; Ross, 2009a; Ross & Woo, 2009; Taylor, Evans, & Pain, 2008; Zhang & Chen, 2009; Zhang, Steiner, & Butler, 2007).

This dissertation follows the style of *Journal of the American Planning Association*.

Other research, however, has expressed concern about the indiscreetly popularized concept of megaregions. These arguments have been vague rather than defining clear concepts (Rodríguez-Pose, 2008), applying the megaregion concept to practical planning without full identification of megaregion components (Dewar & Epstein, 2007) and placing too much importance on both functional aspects and related benefits of megaregions (Hoyler, Kloosterman, & Sokol, 2008). The megaregions need both conceptual clarity and detailed empirical evidence and, as such, have been accepted on a fuzzy basis combining both morphological characteristics and functional relationships. These two components should have been distinctly observed because of obviously different empirical dimensions from each other (Hoyler et al., 2008).

2. Purpose of the study

This study examines morphological characteristics of U.S. megaregions to represent morphologically-oriented U.S. megaregions in comparison with U.S. megaregions primarily identified based on functional relationships of U.S. megaregions by RPA. By comparing the morphologically-oriented U.S. megaregions and RPA's U.S. megaregions, this study encourages urban and regional planning professionals to reconsider their definitions of U.S. megaregions and related advantage.

3. Research questions and hypotheses

A primary research question is what do morphological characteristics of U.S. megaregions represent on relation to current geographic boundaries of the U.S.

megaregions? The primary research emphasis is to identify problems in identification of U.S. megaregions that is currently biased toward megaregional functions and, as such, is a problematic representation. A primary hypothesis is, therefore, that U.S. megaregions spatially examined by morphological characteristics may not be equal to current representations of U.S. megaregions. Assumptions for the hypothesis state that current U.S. megaregions of RPA may be function-oriented representations which may be different from morphologically-oriented representations of the region. This study, however, will not attempt to object to existence of U.S. megaregions and to their functional relationships and advantages. This study, rather, will attempt to identify spatial structures and spatial associations within U.S. megaregions, focusing on morphological characteristics. The primary problem, therefore, may infer two sub-problems.

The first research sub-question is what do spatial patterns of morphological characteristics of U.S. megaregions represent concerning variations of morphological characteristics spatial distribution? The first research sub-question therefore is to identify areas of inconsistency in spatial patterns of morphological characteristics. A hypothesis of the first research sub-question is that spatial patterns of morphological characteristics of U.S. megaregions may not represent a common spatial structure in cross-comparison with the spatial patterns of each U.S. megaregion. An assumption for the first research hypothesis is that regions which have been demonstrated to share common functional features may represent common spatial distribution patterns of morphological characteristics within the boundaries of U.S. megaregions.

The second research sub-question asks what spatial associations of morphological characteristics of U.S. megaregions represent concerning spatial interconnections of the spatial associations of morphological characteristics within the boundaries of U.S. megaregions. The second research sub-question concerns problems in the spatial isolation of spatial associations of morphological characteristics. A hypothesis of the second research question states that the spatial associations of morphological characteristics of U.S. megaregions may not be spatially interconnected within the boundaries of U.S. megaregions. An assumption for the second research hypothesis is that regions which have been functionally interconnected may represent morphological characteristics that are spatially interconnected.

4. Importance of the study

The growth of megaregional knowledge has been limited to the functional relationships of megaregions, primarily highlighting advantages that the interconnected regional economic entities have produced. This unbalanced attention has been accused of vagueness of conceptual clarity (Rodríguez-Pose, 2008) and insufficiently detailed empirical evidence (Hoyler et al., 2008), invoking the consideration of megaregional morphology. The understanding of megaregional morphology needs systematic evidence using flexible geographies of megaregions and their influence on the structure of megaregions (Hoyler et al., 2008).

As an extended understanding of urban morphology to megaregion scale, the megaregional morphology study may be concerned with the built environment

representing urban form and urban fabric consisting of the space in which human beings are able to move from one place to another within regional boundaries (Jiang & Claramunt, 2002; Levy, 1999; Whitehand & Morton, 2004). Traditional studies of urban morphology have been conducted at a city or metropolitan scale observation of individual buildings, streets, constructed areas, and open space for example. In order to look at the built environment on a megaregion scale, however, a larger scale observation is required than for traditional scales. It is recommended to create data sets that are able to observe the morphology on a larger scale. The data sets also have the characteristics of urban morphology associated with built environment, urban form, and urban fabric, representing the regional boundary.

Adding to the importance of morphological study on a megaregion scale, this study analyzes morphological clustering. Concerning the geographic variation of urban environments, morphological clustering indicates a spatial aggregation and its boundary, meaning the excess of events or values within the geographical boundary (Jacquez, 2008, 2009). When the spatial associations of morphological features and the boundaries of the spatial clustering are considered, they reflect the morphological characteristics for each megaregion, compared to the functional relationship oriented megaregion boundary of RPA.

This study, therefore, expects to show the imbalanced emphasis of current megaregion scale planning and policies. The theoretical review may represent fundamental aspects of the megaregion concept. The empirical review may show subjects which necessarily need to be highlighted. The dimensions for measuring

morphological characteristics of U.S. megaregions may be extended to applied study of megaregional morphology, combining them with functional relationships within U.S. megaregions. The results of this study may inspire practical urban planners to focus on, or at least not ignore, morphological characteristics of megaregions. For those who work for the Texas megaregion particularly, this study may provoke the reconsideration of ongoing Texas megaregion studies and planning to check their perspectives of the region. Consideration of morphological characteristics may encourage urban sprawl management or urban spatial structure planning in regions which have suffered from traditional urban issues and have been ignored because of being included in a megaregion with more favorable regions.

CHAPTER II

LITERATURE REVIEW

This literature review identifies the unbalanced perspectives which have been defined in the theoretical efforts and examinations of empirical studies. The unbalanced theoretical definitions of megaregions will become apparent in this literature review which explains how megaregional features have variously been researched in past empirical studies.

1. Various definitions of megaregions in theoretical efforts

A concept of megaregion was derived from observations of broadly connected urban components and the resulting expansion of regional boundaries crossing neighboring jurisdictions (Carbonell & Yaro, 2005; Dewar & Epstein, 2007; Hall, 2007; Lang & Knox, 2009; Priemus & Hall, 2004; Regional Plan Association, 2006; Rodríguez-Pose, 2008; Ross, 2009b; Sokol, Van Egeraat, & Williams, 2008; Todorovich, 2009; Turok, 2009). Contemporary studies have produced the concept of megaregions observing their own interests in such areas as business networks (Taylor et al., 2008) or transportation connections (Rodrigue, 2004; Zhang & Chen, 2009) in newly defined large regions. The studies, in turn, have called for a new governance framework to take care of each region's own interests. It would be difficult, however, to deliver effective governance to the large megaregions because they are so large and diverse that residents do not easily identify themselves as coming from a megaregion whereas little sense of

common cultural and political identity exists (Dewar & Epstein, 2007). Urban scholars have focused on megaregional features in many different ways. Contemporary urban studies are newly defining megaregions in order to fully understand their contexts and diverse regional interests.

1.1. Megalopolis – the first concept of megaregions

Conceptual evolution of megaregions started from a French geographer Jean Gottmann's (1961) book *Megalopolis: the urbanized northeastern seaboard of the United States*. Naming the 1960s urbanized northeastern seaboard area of the U.S. a megalopolis, Gottmann described a new urban morphology as metropolitan areas interconnected through transportation bringing people, money, and services from one place to another. The book includes historical observations of the northeastern seaboard area – revolution in land use and density changes in manufacturing, commercial, and transportation systems and changes in neighborhoods. Even though Gottmann's megalopolis was limited to the northeastern seaboard area of the 11 New England states (see Figure 1), the concept of interconnected metropolitan areas was enough to inspire a new regional concept for subsequent megaregion studies (Banerjee, 2009; Contant & de Nie, 2009; Cowell, 2010; Dewar & Epstein, 2007; Florida et al., 2008; Hoyler et al., 2008; Lang & Dhavale, 2005; Lang & Knox, 2009; Lang & Nelson, 2007, 2009; Rodrigue, 2004; Ross, 2008; Ross & Woo, 2009; Todorovich, 2009; Vicino, Hanlon, & Short, 2007; Zhang & Chen, 2009).

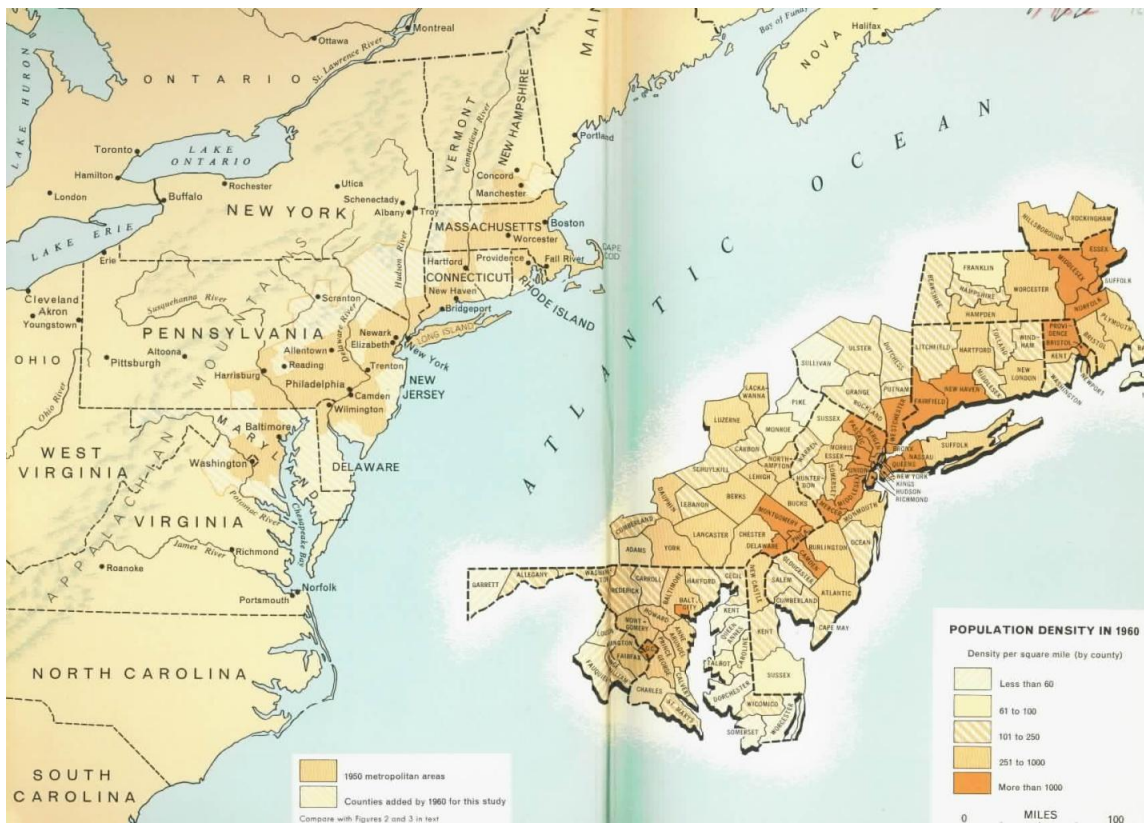


Figure 1 U.S. megaregion identified by Gottmann (1961, inside front cover)

Subsequent megaregion studies have considered how the concept of megalopolis has been influenced theoretically and empirically. Analyzing the features identified by Gottmann's megalopolis, this study recognizes how the contemporary concept of megaregions has developed and attempted to discover what has been neglected. In the following discussions megalopolis, as a term, only identifies the northeastern seaboard area of the U.S. that was observed by Gottmann (1961) whereas megaregion or megaregions represents other regions that have subsequently been incorporated in the megalopolis.

Features of Gottmann's megalopolis may be divided into such subjects as development of urban centers; interconnection; transportation; deconcentration, reconcentration, and integration; nebulous morphology; social and economic contrasts; and need for a new framework.

1) Development of urban centers

As a harbor area, the region had been the principal entrance for immigrants coming into the U.S. with New York City being the chief port of entry. As an economic attraction, the main cities of megalopolis offered satisfactory economic opportunities to a massively increasing number of people. International trade concentrated in the region brought prosperity and, in turn, the higher population densities coincided with higher income.

2) Interconnection

Urbanized areas and their residences with other forms of activity scattered widely and rapidly throughout the region outside the old urban areas. As a result, a new and shifting map of land use emerged throughout the region. Communities which originally depended on the old main urban centers also became orbits of other urbanized areas, expanding outside and overlapping each other in a complicated manner. The interconnections grew more and more entangled as more specialization developed in the labor force in certain districts, and as the means of travel and communication between these various urban centers were constantly being improved. As a whole, the

megalopolis region was made up of many inter-dependent parts, and the increase in population and human movement through the area affected other not-yet-urbanized sections of the region.

3) Transportation

The proximity of the various towns in megalopolis created rivalries and competition leading to a historical process of selection of some areas rather than others for the localization of certain functions leading to rapid growth. As more major urban centers of the megalopolis became crowded, a finer division of labor and space took shape, and more coordination and tighter links between more and more places were required. The era of the automobile helped the metropolis to explode over the countryside while still remaining coherent. Roads were good enough to make traffic relatively easy between the various towns of southern New England, parts of New York, and surrounding Philadelphia. A great deal of transportation went by water, roads played a part, and railroads carried a good deal of traffic. Because of its network of overseas relationships and domestic transportation technology and manufacturing, the megalopolis was able to rise quickly to eminence in the international economic system.

4) Deconcentration, reconcentration, and integration

Given development of domestic transportation systems and technology in the megalopolis, manufacturing became a less important component of the large urban centers. The proximity of a large agglomeration of available labor also became a less

important factor in determining industrial plant location while the consumer market kept its attraction in the urban centers. Such trends contributed to the decentralization of physical production plants, pushing them into suburban areas or satellite towns, in turn, increasing the average occupation density on the fringes of metropolitan areas, consolidating the megalopolis in some regions and expanding its limits. At the same time, newly created and rapidly developing economic activities appeared much more interconnected because they used more narrowly specialized personnel. Many companies discovered the advantage of locating their financial headquarters close to institutions serving their various needs. This kind of re-concentration caused the growth of business districts in central cities, and similar entanglements also concentrated various activities of the mass-media market in the megalopolis. In process of deconcentration and reconcentration, the metropolitan regions of megalopolis grew toward each other, joined, and even penetrated one another. The integration became an indisputable fact for megalopolis, deeply penetrating the social and economic structure of the region and its various parts. The unity of megalopolis as an urban region, as a result, was founded on the relative integration of contiguous standard metropolitan areas along the northeastern seaboard.

5) Nebulous morphology

Between and around the urban centers territory was classified as metropolitan but rural, or even as nonmetropolitan. The rapid expansion of the area devoted to urban use of the land had been a prime factor in imposing urbanization as the essential force that directed land use throughout the whole region. The expansion of the urban areas created

dense interurban and peripheral growth along the axial belt joining the main historic urban centers with the resultant distribution of densities contributing to a considerable expansion of the territory. The urban centers and their suburban areas grew together and became one great urban system. The megalopolis sprawl came about because residences followed industrial or commercial establishments out of the old urban territory, and also because retail and wholesale trade establishments followed their customers toward new residential areas. Since the dispersal of both residences and industries required well-organized means of access, they became dependent on a network of highways. In the era of the automobile it became much easier to decentralize and scatter people as well as trade and light industry than previously when the attraction of rail lines or major waterways had been stronger. The resultant distribution of urban uses of the land in megalopolis developed a nebulous character fostered by many people wishing to have their residences in rural landscapes; also by the vogue of the suburban way of life among certain categories of urbanites; and by the advantage of decentralized locations of new industrial or even bureaucratic establishments. The functions of the neatly delimited downtowns and uptowns of the past mingled in disconcerting fashion with farming, woodlands, or just highly populated suburbs.

6) Social and economic contrasts

As great wealth has always been a neighbor of slums and poverty in great cities, the contrast of megalopolis was also striking. The contrast between wealth and poverty was sharpened by differences in level of education which made social mobility more

difficulty. Racial discrimination added further to the contrast. In megalopolis the growing population made good use of relatively obsolete structures when newcomers in search of work and economic opportunity opened the door to the spread of blight and slums in the heart of the central cities. The desire for a homogeneous neighborhood often caused large groups to move to another district in the community once they thought their territory had been infiltrated by newcomers of an undesirable race, creed, or social status. At the same time, the smaller cities of megalopolis decayed more rapidly, and the average income of their residents declined in both absolute and relative terms in contrast to a general rise throughout the region and the nation.

7) Need for a new framework

The future of land use in the megalopolis region, and in each of its growing and changing cities, was likely to be accompanied by great fluidity. Thus it became obvious that land use patterns which were changing rapidly in the megalopolis were not able to be identified or administered according to simple formulas dealing with location, density of occupation, or immediate profits to be earned. Land use needed to be described in broad terms and major categories. The inner details and the orientation of their evolution had to be considered in the light of full understanding of the region's activities and modes of life and the economic and social structure of its component communities. The revolution which occurred in land use in megalopolis stemmed from deep changes in the ways and means that the local society applied to the use of the land. This pointed to new functions arising in the hub of the main metropolis in megalopolis.

Summing up the above features, the megalopolis has been defined as metropolitan regions interconnected with their hinterlands by transportation networks. The interconnected regions were developed on the basis of economic power of urban centers incorporating deconcentration, reconcentration, and integration processes. Their synthesized morphology has been difficult to delineate because the processes of deconcentration and reconcentration have continuously occurred, even though the interconnected, and thus integrated, regions have been developed based on networks of constituent metropolitan areas where jurisdictional boundaries have been clearly distinct. These features of megalopolis, therefore, call for a new governance framework combining social and economic contrasts.

The megalopolis concept of Gottmann (1961) seems to include almost every attribute of historic urban regions, adding the characteristic of functional interconnections between urban centers. The concept synthesizes social, economic, demographic, infrastructural, and environmental aspects. The megalopolis functions on the basis of coordination and integration between various roles of metropolitan regions, representing a characteristic of ambiguous morphology on the basis of rapid and repeated expansion of areas devoted to urban land use.

1.2. Contemporary megaregion concepts

Incorporating the above features identified in the megalopolis, this literature review investigates contemporary megaregion studies influenced by Gottmann's (1961) megalopolis to see how the features of the megalopolis have been considered in

contemporary megaregion studies. In other words, given the theoretical influences on definitions of contemporary megaregions, this section will review how megalopolis features have been transformed and highlighted in contemporary megaregion concepts. Because there are too many megaregion studies to directly address in the text of this study, tabulation seems to be the best way to examine how other researchers have defined a megaregion. The tabulation of various definitions and the comparison of the tabulated features (see Table 1) will show which parts of contemporary megaregions have been focused on and which have not.

Table 1 A summary of contemporary megaregion concepts

Contemporary Megaregion Concepts	Related Megalopolis Features
A megaregion is a functional link of Information and Communication Technology (ICT) networks and traffic networks to develop a multimodal long-distance network hub (Priemus & Hall, 2004).	<ul style="list-style-type: none"> • Interconnection
A megaregion is a structural and functional entity, logistically integrating regions of production, consumption and distribution as the main structure behind the international division of labor and production (Rodrigue, 2004).	<ul style="list-style-type: none"> • Interconnection • Integration
A megaregion is a response to congested transportation networks which have interrupted the economic vitality and quality of life for contemporary U.S. regions. A megaregion, therefore, is a model for cooperating and complementing among cities and regions connected with each other to facilitate economic growth and job creation through transportation, economic development, environmental protection, and equity as a new urban form (Carbonell & Yaro, 2005).	<ul style="list-style-type: none"> • Integration
A megaregion is large area of connected settlements that shows a changing metropolitan form. Characteristics of megaregions depend on economic, environmental, and demographic facts with little sense of common cultural and political identity (Dewar & Epstein, 2007).	<ul style="list-style-type: none"> • Interconnection

Table 1 continued.

<p>A megaregion is a response to the decentralized nature of the U.S. economy, reflecting the changing patterns of location for people and firms in order to link the old employment centers of proximate metropolitan areas (Glaeser, 2007).</p>	<ul style="list-style-type: none"> • Interconnection • Deconcentration
<p>A megaregion is a polycentric development coming from simultaneous decentralization at a regional scale, and recentralization at a more local scale as overlapping commuter fields served by the car (Hall, 2007)</p>	<ul style="list-style-type: none"> • Deconcentration, & reconcentration • Interconnection • Transportation
<p>A megaregion is a new type of urban form composed of a number of cities within reasonable commuting distance, having polycentric structure to display crisscross commuting patterns, sometimes resulting in traffic congestion. The polycentric space is intricate comprising more than one central city and its direct hinterlands (Hoyler et al., 2008).</p>	<ul style="list-style-type: none"> • Interconnection
<p>A megaregion is a polycentric economic unit qualitatively differing from constituent metropolitan regions as an integrated set of cities and suburban hinterlands across large populations, markets, significant economic capacity, substantial innovative activity and highly skilled labor (Florida et al., 2008).</p>	<ul style="list-style-type: none"> • Interconnection • Integration
<p>A megaregion is a coincidence of human activity with systems of cities in geographical proximity, interacting between urban cores and semi-urban and rural hinterlands. The boundaries of a megaregion do not necessarily have to match existing administrative boundaries (Rodríguez-Pose, 2008).</p>	<ul style="list-style-type: none"> • Interconnection • Integration • Nebulous morphology
<p>A megaregion is a system of dynamic places that are not fixed by census data, rather places that need to be measured for their changes in settlement patterns focusing on rank-size distribution or concentration / deconcentration (Banerjee, 2009).</p>	<ul style="list-style-type: none"> • Deconcentration & reconcentration
<p>As the most appropriate unit for interdependent social and economic coordination, a megaregion is a spatial and functional network of metropolitan centers and surrounding areas across environmental, economic, and infrastructure interactions (Ross, 2009a).</p>	<ul style="list-style-type: none"> • Interconnection
<p>A megaregion is a linked network tied to metropolitan areas as a functional unit to serve economic, social, and population dynamics within boundaries of the natural, economic, and social connections between cities, metropolitan areas, and rural places (Contant & de Nie, 2009).</p>	<ul style="list-style-type: none"> • Interconnection
<p>A megaregion is a postindustrial form of urban agglomeration composed of polycentric metropolitan regions that constitute a metropolitan network of cities (Meijers & Burger, 2009).</p>	<ul style="list-style-type: none"> • Urban core development • Interconnection
<p>As an integrator of the spaces of flows, a megaregion is a new spatial and temporal pattern of urbanity that is a polycentric, shifting, and dynamic multi-metropolis. Its urban space is networked across economic fields reflecting urban patterns to social patterns (Neuman & Hull, 2009).</p>	<ul style="list-style-type: none"> • Interconnection • Nebulous morphology

Table 1 continued.

A megaregion is large, complex, and dynamic agglomeration of functional metropolitan areas and its new geography shows linked regional economies as demonstrated by commuter patterns (Lang & Nelson, 2009).	<ul style="list-style-type: none"> • Interconnection • Transportation • Integration
A megaregion is a functionally integrated network of urban cores (metropolitan centers) and adjacent areas of influence in social, environmental, economic, and infrastructure relationships (Ross & Woo, 2009).	<ul style="list-style-type: none"> • Interconnection • Integration
Lacking fixed boundaries, a megaregion is a common attribute among transportation, environmental, economic, and cultural relationships of each component city with various population and city size (Todorovich, 2009).	<ul style="list-style-type: none"> • Integration • Nebulous morphology
A megaregion is a complementary functional geography interacted through commuting, trade, information or other flows, integrating different levels of functional government across economic, social, and environmental objectives (Turok, 2009).	<ul style="list-style-type: none"> • Interconnection • Integration
A megaregion is a new geographical unit containing trans-metropolitan clusters with a network that flows between cities based on economic globalization (Zhang & Chen, 2009).	<ul style="list-style-type: none"> • Interconnection

When the most representative planning organizations for identifying U.S. megaregions are additionally referenced, it will be apparent how the current megaregion concept has been derived and developed. The most current conception for U.S. megaregions was observed by both RPA (2006) and the Metropolitan Institute at Virginia Tech (Lang & Dhavale, 2005). The Metropolitan Institute defined 10 U.S. megaregions (see Figure 2) as clusters of counties with more than two combined metropolitan areas and a total population of more than 10 million by 2040 (Lang & Dhavale, 2005). RPA (2006) also identified U.S. megaregions and defined them as agglomerations of metropolitan regions with integrated labor markets, infrastructure, and land use systems. Given the definitions they designated the 11 U.S. megaregions according to their own criteria (see Figure 3).



Figure 2 U.S. megaregions identified by the Metropolitan Institute (Lang & Dhavale, 2005, p. 13)

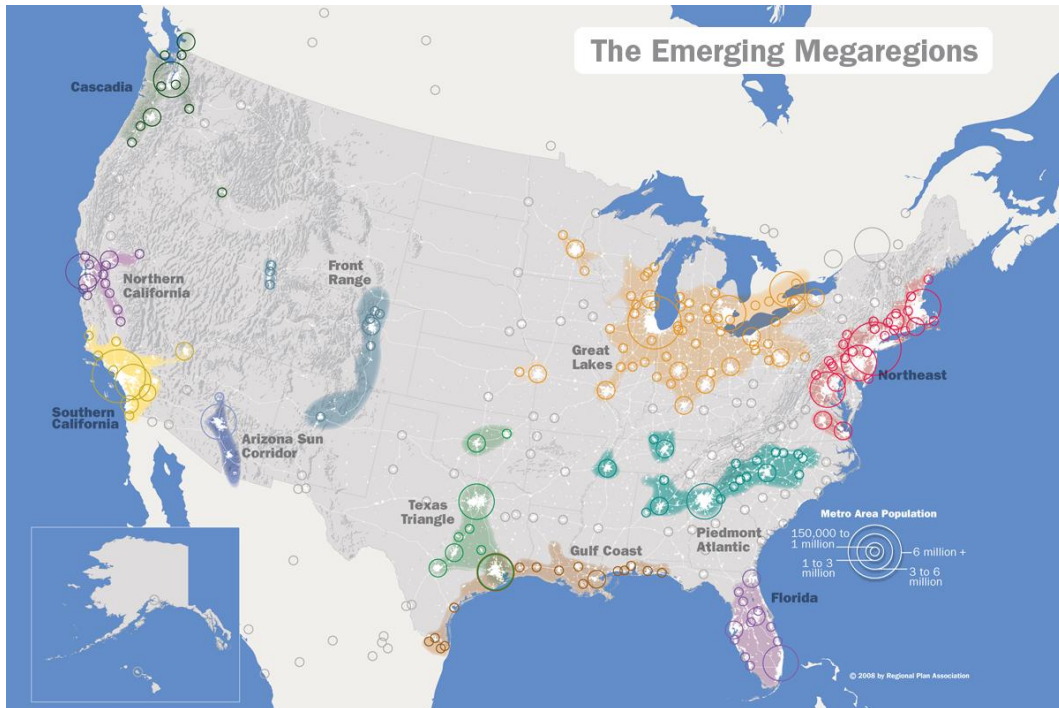


Figure 3 U.S. megaregions identified by the RPA (RPA, 2006, pp. 10-11)

Table 2 Components used to define U.S. megaregions by two institutions (Ross, 2008, p. 39)

	Metropolitan Institute	Regional Plan Association
Requirements of megaregions	More than 2 metropolitan areas & 10 million population by 2040	N/A
Analysis Criteria	<ul style="list-style-type: none"> • Population size • Contiguity • Cultural and historical geography • Physical environment • Links of large centers • Growth projections • Goods and service flows 	<ul style="list-style-type: none"> • Environmental systems and topography • Infrastructure system • Economic linkage • Settlement patterns and land use • Shared culture and history

These two most recent definitions of U.S. megaregions have been compared by the Center for Quality Growth and Regional Development (Ross, 2008). The components used to define U.S. megaregions by the Metropolitan Institute and RPA are described in Table 2. Given the definitions and components for U.S. megaregions, the two institutions have produced two maps to represent U.S. megaregions (see Figures 2 and 3). The delineated areas overlapped each other except the Front Range and the Texas megaregion.

The next tabulation (see Table 3) shows how the megalopolis features identified by Gottmann (1961) have been transformed and developed in contemporary megaregion studies in light of theoretical efforts to define the concept of megaregions.

As seen in the table, Gottmann's (1961) megalopolis concept focused on development of urban centers, interconnection, transportation, deconcentration-reconcentration-integration, nebulous morphology, social and economic contrasts, and need for a new framework. In an effort to define the concept of megaregions, the

subsequent contemporary megaregion studies have emphasized polycentric structure, interaction and integration between core cities and functionally tied neighboring regions, and coordination across social, economic, infrastructural, and environmental aspects.

Table 3 Transformation of the concept of megaregions in theoretical studies

Gottmann's Megalopolis	Theoretical Emphasis of Contemporary Megaregions	
Development of urban centers	Functional interconnection & integration	Megaregions in contemporary studies have been defined as polycentric network structures with coordination, interconnection, and integration between metropolitan areas and hinterland regions. Contemporary megaregions have also been dominant economic entities based on growth of population, flow of goods and services, and links to large centers.
Interconnection		
Deconcentration- Reconcentration- Integration		
Transportation	Transportation Network	Based on infrastructural coordination, constituent areas of contemporary megaregions have been interconnected through transportation networks or sometimes Information and Communication Technology networks.
Needs for new framework	New framework	Because of the growth of interconnection and integration through networks of urban centers, suburban areas, and hinterlands and because of new social, economic, environmental issues resulting from interconnection and integration, contexts of megaregions are difficult to integrate within historic metropolitan scale governance; rather those need to be considered using a bigger scale approach, megaregion scale planning and governance.
Social and economic contrasts	N/A	
Nebulous morphology	Flexible boundary	Flexible boundaries of megaregions have been expanding due to population expansion and resultant land consumption.

Polycentric coordination and functional integration have required transportation links and sometimes Information and Communication Technology networks as well. Few studies have added the feature of flexible boundary to their concept of megaregions. Social and economic contrasts were missing in the theoretical efforts to define megaregions. Additionally, recent definitions of megaregion seem to include particular criteria such as population size, links among large centers, goods and service flows, economic linkage, etc.

1.3. Findings in theoretical reviews of U.S. megaregion concepts

The above definitions and theoretical characterizations for megaregions in contemporary studies are likely to partially coincide with Gottmann's (1961) findings in megalopolis. Most contemporary megaregion studies have agreed with such features of the megalopolis as interconnection, transportation, and integration in their megaregion concepts. In order to expand the features of megalopolis, other elements such as development of urban centers and deconcentration-reconcentration should be considered. This study argues, therefore, that contemporary megaregion studies seem to include such features of Gottmann's (1961) megalopolis as development of urban centers, deconcentration-reconcentration-integration, interconnection, and transportation. This study also finds that most megaregion studies have been producing conclusions calling for new governance systems for megaregions to coordinate their various but integrated components. Additionally this study finds that most megaregion studies, in their theories defining megaregion concepts, have emphasized two dominant features which

are polycentric urban structures and dominant economic entities. Other megaregion studies have used a vague term for megaregions but have also identified the two common features of contemporary megaregion concepts through their theoretical efforts (Cowell, 2010; Davoudi, 2008; Green, 2007; Meijers & Burger, 2009; Parr, 2005).

Whereas contemporary megaregion studies have agreed with many features of Gottmann's (1961) megalopolis and even transformed the features by adding other characteristics such as polycentric and economic bodies, they seem to have overlooked other megalopolis features such as social and economic contrasts and nebulous morphology in their theoretical emphasis. Contemporary megaregion studies also seem to have understood the urban centers development, the interconnection, and the deconcentration-reconcentration-integration features only as functional relationships. These features, however, originated both from repeated land use development (or consumption) and, consequently, urbanized area expansion. When the foundation of the features are considered, it is questionable why contemporary megaregion studies have not reflected the interconnection and the deconcentration-reconcentration-integration features on the basis of physical linkages such as spatial structures interconnection or spatial patterns integration. When the fact is considered that megaregions are based on urbanized metropolitan areas and their connections, contemporary megaregion studies ought to take into account physically connected urbanized areas in their theoretical definitions for megaregions. The flexible boundary issue of megaregions pointed out by Gottmann (1961) calling it nebulous morphology, may be less nebulous when the

physically connected urbanized area networks in a megaregion are considered in theoretical efforts.

2. Various features of the megaregion in empirical studies

Keeping in mind the above evaluation of theoretical efforts in defining the megaregion concept, the next step is an empirical review of contemporary megaregion studies to evaluate how the features highlighted in the theoretical efforts to define the megaregion concept have been examined empirically. The evaluation of empirical attention in light of the megaregional features theoretically developed, therefore, determines whether empirical studies have only confirmed the limited theoretical megaregion features or rather the practical efforts have complemented the other features theoretically overlooked.

2.1. Contemporary megaregion features

The following tabulation (see Table 4) summarizes the empirical megaregion studies selected by the author. The evaluation of empirical efforts will be different from the previous evaluation over theoretical efforts to define the concept of megaregions. The following evaluation table recognizes particular aspects empirically examined in contemporary megaregion studies in comparison with such megaregion features identified from the theoretical efforts as functional interconnection and integration; economically oriented polycentric structure; transportation network; new framework; social and economic contrasts; and nebulous morphology.

Table 4 Megaregion features empirically developed in contemporary megaregion studies

Empirical emphasis areas of contemporary megaregion studies	FII	EPS	TN	SEC	NF	NM
Examination of U.S. northeastern megaregion freight systems such as terminals and distribution centers to consider megaregions as logistically integrated entities (Rodrigue, 2004)	√		√			
Examination of network connectivity and polycentricity for advanced producer service firms and their office networks in European megaregions (Taylor et al., 2008)	√	√				
Examination of income / economic productivity and growth rates for U.S. megaregions to show regionally different growth patterns according to their different land use regulations (Glaeser, 2007)		√			√	
Examination of U.S. southern California socioeconomic densities by municipality such as residential density and foreign-born population to consider megaregions as systems of places different from the artifacts of census data (Banerjee, 2009)		√				
Examination of economic inequality, racial diversity, neighborhood segregation, and concentrated poverty to argue limitations of U.S. megaregion scale planning approaches (Fainstein & Fainstein, 2009)				√	√	
Examination of employment, job densities, workplace, and commuter patterns to show conflicts between local needs and regional growth interests in Europe megaregions (Turok, 2009)				√	√	
Examination of commuting patterns and network densities to show functional polycentricity in European megaregions (Green, 2007)	√	√				
Examination of total amount of travel demand by year 2050 and distribution of mobility demand to prove future transportation investment needs in the U.S. Texas Triangle megaregion (Zhang & Chen, 2009)	√		√			
Examination of size, dispersion, polycentricity, capital-labor ratio, and educational attainment of U.S. metropolitan areas to show effect of polycentricity on labor productivity compared to a single larger city (Meijers & Burger, 2009)		√				
Examination of correspondence of diverse economic profiles of case areas to show complementarity of polycentric megaregions (Cowell, 2010)		√				

Table 4 continued.

Examination of principal components of U.S. northeastern megaregion after Gottmann’s megalopolis of 50 years to show socio-spatial transformations in terms of population and economic activity with more decentralized and suburbanized agglomeration and with more multiracial and multiethnic than 50 years before (Vicino et al., 2007)				√		
Examination of economic structure with export industries, daily flights, internet routes, county-to-county goods flows, watersheds, and principal census facts for the U.S. Texas Triangle megaregion to show future transportation demand in the region (Zhang et al., 2007)	√	√	√		√	
Examination of interregional trade of U.S. Midwest megaregion and industry value chains clustering and concentration of U.S. to show spatially dispersed industrial clustering trends (Feser & Hewings, 2007)	√					
Examination of hot and cold areas in combined terms of median rent, below poverty rate, educational attainment, and employment rate to show patterns of new investment in areas of the U.S. Northeastern megaregion, considering transit connections between hot and cold regions to harmonize economic and environmental imbalances and to redirect misguided vacant use consumption (Yaro & Carbonell, 2007)			√	√		√

- FII : Functional interconnection and integration
- EPS : Economically oriented polycentric structure
- TN : Transportation network
- SEC : Social and economic contrasts
- NF : New framework
- NM : Nebulous morphology

Given the above observation of empirical emphasis areas in contemporary megaregion studies, it is apparent that functional interconnection and integration (FII) and economically oriented polycentric structure (EPS) are most frequently examined. This finding follows conceptual popularity in the previous theoretical focuses. More specifically, some studies have examined the FII and the EPS features together (Green, 2007; Taylor et al., 2008) or each feature alone (Banerjee, 2009; Cowell, 2010; Feser & Hewings, 2007; Meijers & Burger, 2009). Some other studies have examined one of the two features with the transportation network (TN) feature (Rodrigue, 2004; Zhang & Chen, 2009). Examinations of the TN feature are relatively fewer than the two dominant FII and EPS features as always considered together with FII. It is interesting that examinations of social and economic contrasts (SEC) are observed in the empirical review whereas that feature has been totally overlooked in theoretical efforts to define megaregion concepts. The new framework (NF) feature has been examined together with other features such as the FII (Zhang et al., 2007), the EPS (Glaeser, 2007), and the SEC (Fainstein & Fainstein, 2009; Turok, 2009). An empirical examination of nebulous morphology (NM) has been difficult to find.

2.2. Findings in empirical reviews of U.S. megaregion features

This review section of empirical megaregion studies finds that contemporary studies have paid attention to topological features primarily concerned with functional interconnection-integration and economically oriented polycentric structure. The focuses on the two topological features of megaregions seem to have been derived from

such features of Gottmann's (1961) megalopolis as development of urban centers, and interconnection, deconcentration-reconcentration-integration. Transportation network has also been important in empirical studies because this feature has enabled the megaregional topological relationships to function. Social and economic contrast has been underlined in empirical studies but has not been observed in the previous theoretical review. New framework has been included in concluding sections of several empirical studies. Examination of nebulous morphology has seldom been observed by this empirical review.

Given the empirical review of megaregion studies, however, this study asks why the transportation network has been considered as only a facilitator to serve both functional interconnection-integration and economically oriented polycentric structures. In other words, contemporary megaregion studies seem to consider the transportation network only as a topological feature of functional relationships, while the network system is also likely to be considered as a topographical feature for evaluating physical connections among various land uses. In the same manner, the economically oriented polycentric structures may be examined not only as a topological dimension, but also as a topographical factor. The evaluation of polycentric structure based on land use may be a good example for topographical understanding. Given the bias in empirical examinations of the above features, it seems that ignorance of the nebulous morphology feature in the empirical studies for its topographical characteristic is reasonable. The perspectives of megaregions are unbalanced and, as such, are primarily dependent on topological functions and relations which overlook topographical aspects.

3. Conclusion

This literature review has explored how contemporary U.S. megaregions have been defined in theoretical efforts and examined in empirical studies, concerning balances in studying functional relationships and morphological characteristics of U.S. megaregions. The review would like to conclude that contemporary megaregion studies have showed a limited focus on the morphological characteristics in identifying megaregion concepts and examining megaregional features. These studies have attempted to understand the functional relationships of megaregions so that topological aspects have been more considered than topographical megaregions.

Megaregions have been considered as interconnected and, consequently, integrated urbanized areas using transportation networks and functioning as integrated economic entities across jurisdictional boundaries of traditional cities, counties, and metropolitan areas. Two features, the polycentric urban structure and the dominant economic entities, have been theoretically popularized. Focus on the two features has continued in empirical studies as primarily examining the functional interconnection-integration and the economically oriented polycentric structure. Most subjects of contemporary studies have been dependent on topological functions and relations in understanding megaregions.

Unbiased perspectives of megaregions encourage the study of morphological characteristics of U.S. megaregions such as topographical features and patterns in a megaregional structure. The theoretical review shows that the interconnection and the deconcentration-reconcentration-integration features ought to consider spatial

connections of urbanized areas on the basis of repeated expansion of land development. The empirical review confirms that dominant dimensions mainly depended on functional relationships in examining megaregional components and, as such, have failed to overcome theoretical ignorance regarding topographical features such as physical links among urban structures in megaregions.

CHAPTER III

RESEARCH METHODOLOGY

This section describes how the morphological characteristics of U.S. megaregions are examined through various types of land use patterns data. This chapter is divided into two parts. The first section studies the use of megaregional morphology examination to provide a theoretical foundation for land use patterns data analysis. The second section adds evaluation dimensions on a megaregion scale for land use patterns data analysis.

1. Morphological characteristics and land use patterns of U.S. megaregions

Contemporary studies seem to have merged the functional relationships and morphological characteristics of megaregions (Hoyler et al., 2008). Topology and topography are two main structures which have also been incorporated in megaregion contexts (Banerjee, 2009; Green, 2007; Regional Plan Association, 2006). Topology relates to interconnected polycentric structures and topography indicates how interconnectedness is expressed in geography (Hoyler et al., 2008). Even though the effects between functions and morphologies or between topologies and topographies have been combined in the process of deconcentration-reconcentration of urban regions, they should have been observed distinctly, because of obviously different dimensions (Hoyler et al., 2008). This study, therefore, considers that megaregional morphology has

distinct characteristics from megaregional functions, and that land use patterns analysis may become a practical method to observe morphological characteristics.

1.1. Functional and the morphological features of megaregions

The functions of megaregions seem to have been established through polycentric interconnections between distinct roles of constituent urban regions and suburban areas (Davoudi, 2008; Green, 2007; Hoyler et al., 2008; Parr, 2005). The main reasons for increased interconnections are likely to be globalization; continued growth of metropolitan areas and their suburbanized regions in terms of population and socio-economic activities; and resultant competition with other urbanized areas that have been autonomous (Amin, 2002; Carbonell & Yaro, 2005; Dewar & Epstein, 2007; Regional Plan Association, 2006; Rodríguez-Pose, 2008; Ross, 2009a). The interconnections are primarily served by transportation networks (Neuman & Hull, 2009; Rodrigue, 2004; Zhang & Chen, 2009; Zhang et al., 2007). The results of functional interconnections appear to increase economic capacity and financing resources (RPA, 2006). The functions of megaregions are to be considered within a new regional framework based on the interconnection of historic urban centers through transportation networks to produce increased economic capacity and financing ability. In other words, contemporary megaregions represent polycentric structures which perform complementary functions synthesizing historically distinct roles of urban centers (Lang & Knox, 2009; Pain, 2006; Sokol et al., 2008).

The morphology of megaregions, on the other hand, seems to have been established through polycentric interconnections of expanded historic urban areas and their sprawling neighboring areas (Parr, 2005). Given the transportation infrastructure to connect historic urban regions and their suburbanized areas, particular directions and forms of the polycentric interconnections seem to have been established topographically ranging from centralized to dispersed and from monocentric to polycentric (Meijers, 2008; Meijers & Burger, 2009). Even though one can identify the existence of interconnections between particular regions, for example freight distribution or business branches (Rodrigue, 2004; Zhang et al., 2007), it is difficult to identify exact geographic boundaries of the interconnections and influences. The fact is, therefore, that the delineation of most megaregions does not fall on historic jurisdictional boundaries but more often across others' geographic limits (de Vries & Priemus, 2003; Priemus & Hall, 2004; Vicino et al., 2007). It is difficult, therefore, to determine where the morphology of megaregions starts and ends as it is transforming (Davoudi, 2008; Dewar & Epstein, 2007; Neuman & Hull, 2009; Parr, 2005).

In spite of the differences in morphological and functional understanding, the conclusion of previous researchers shows that contemporary megaregional understanding has primarily relied on megaregional functions such as economically oriented polycentric structure and functional interconnection–integration. The megaregion studies have also shown theoretical and empirical failure to consider megaregional features with morphological characteristics. The economically–oriented polycentric structure of megaregions may be examined not only by a business network

(Taylor et al., 2008) but also by an urbanized area network regarding the polycentric structure as a spatial structure. The functional interconnection-integration may not only be evaluated by transportation connections (Rodrigue, 2004; Zhang & Chen, 2009) but also by land use connections regarding the interconnection-integration as a morphological link.

1.2. Land use patterns

U.S. megaregions have been studied to show various spatial forms and scales depending on how they exhibit themselves and how they spread into vast areas (Lang & Knox, 2009). U.S. megaregions have been placed, in terms of their spatial forms, on a continuum ranging from the galactic megaregional form to the corridor feature megaregion (Dewar & Epstein, 2007) and on a quadrant that has a galaxy-corridor axis and the mosaic-network axis (Banerjee, 2009). Attempts to categorize U.S. megaregions according to their spatial forms, however, have difficulty understanding morphological characteristics such as urbanized area structure and land use connections for their arbitrary categorization based on intangible dimensions and lack of consideration of the patterns of urbanity that represent the morphological characteristics of megaregions (Neuman & Hull, 2009).

Given the limitations in understanding megaregional morphology, land use patterns seem to provide a good dimension for the patterns of urbanity and non-arbitrary examination. Land use patterns, which refer to the arrangement of the urbanized areas for civic activities (Galster et al., 2001), have been utilized as means for morphological

understanding of urban regions in other studies (Jiang & Claramunt, 2002; Levy, 1999; Sargent, 1972; Whitehand & Morton, 2004) based on the importance of land use development recognized as an irreversible influence on urban environments (Dewar & Epstein, 2007). Land use patterns, as a result, can be considered as a non-arbitrary, tangible means to produce empirical evidence for morphological characteristics at a megaregion scale.

2. Dimensions to examine U.S. megaregion morphological characteristics

This section explores other empirical land use pattern studies and, as such, determines applicable dimensions for a land use pattern analysis to represent U.S. megaregion morphological characteristics.

Table 5 summarizes the authors of empirical land use patterns studies, their measurement scales, and main dimensions of their examinations. Whereas some megaregion studies have shown some differences in explaining what each dimension measures and how each measurement represents land use patterns, most studies have attempted to understand land use patterns within a common boundary to measure morphological characteristics. The dimensions explored in this study are density, land use mix, scattering, clustering, continuity, accessibility, and proximity.

Table 5 Dimensions of other land use patterns studies

Studies	Measure Scale	Density	Land Mix	Scatter	Cluster	Continuity	Access	Proximity
Lopez & Hynes, 2003	Metropolitan area (Primary)	Density						
Ewing, Pendall, & Chen, 2002	Metropolitan area (MSAs; CMSAs; NECMAs)	Density	Land use mix		Centeredness		Street	
Tsai, 2005	Metropolitan area	Density		Equal distribution (Gini)	Clustering (Moran)			
Frenkel & Ashkenazi, 2008	Israel town scale	Density	Land use mix	Scatter				
Wolman et al., 2005	Extended Urban Area	Density		Concentration	Clustering; Centrality (CBD); Nuclearity			Proximity
Galster et al., 2001	Urbanized Area	Density	(Concept) Land use mix	Concentration	Clustering; Centrality (CBD); Nuclearity	(Concept) Continuity		Proximity
Torrens & Alberti, 2000	(Conceptual dimensions)	Density gradients		Geometry of scatter		Surfaces of sprawl	Accessibility	
Torrens, 2008	Austin, TX	Density gradients	Diversity in activities		Decentralization (Moran)		Accessibility	

Table 5 continued.

Cutsinger, Galster, Wolman, Hanson, & Towns, 2005	Extended Urban Area	Density	Mixed use	Concentration	Centrality; Nuclearity	Continuity		Proximity
Malpezzi & Guo, 2001	Metropolitan area (MSA)	Density & Density gradients		Dispersion in tract density (Gini)	Spatial autocorrelation (Moran); Compactness	Discontinuity	Gravity based model	
Glaeser & Kahn, 2004	Metropolitan area (MSA)	Density (ZIP code level)			Share of employment and population			
Lang, 2003	Urbanized area; Metropolitan area	Density & Density change						

These empirical dimensions for land use patterns analysis, in fact, can be divided by two groups according to what factor each dimension proposes to measure (Tsai, 2005). First is the urban sprawl measurement group. Even though it is still controversial because of the lack of a clear definition of urban sprawl and its characteristics (producing a clear definition of urban sprawl and characterizing the urban phenomenon are not the interest of this study), it is obvious that housing and places where people live represent a major portion of land use (Lopez & Hynes, 2003). Density and land use mix dimensions in Table 5, therefore, fall in the urban sprawl group.

The second group measures the spatial structure of urbanization. Characterizing the overall shape of land use phenomena, the spatial structure of urbanization represents the spatial pattern of human activities, in other words, morphology (Tsai, 2005). The scattering and the clustering dimensions in Table 5 seem to be included in the spatial structure of the urbanization measurement group. It is expected that it will be difficult for the other dimensions in Table 5 such as continuity, accessibility, and proximity, to be applied to megaregion scale evaluation. In their empirical applications, the other dimensions seem to be highly correlated with former dimensions such as clustering (Cutsinger et al., 2005; Ewing et al., 2002; Galster et al., 2001; Wolman et al., 2005). This study, therefore, focuses on density, scattering, and clustering dimensions.

2.1. Density dimension

The density dimension has been used in almost every land use patterns analysis (Cutsinger et al., 2005; Ewing et al., 2002; Frenkel & Ashkenazi, 2008; Galster et al.,

2001; Glaeser & Kahn, 2004; Lang, 2003; Lopez & Hynes, 2003; Malpezzi & Guo, 2001; Torrens, 2008; Torrens & Alberti, 2000; Tsai, 2005; Wolman et al., 2005). In fact population density measures the total population of an area divided by the amount of the land area and, as such, represents the degree to which a unit land area is occupied by a large population or by a small population. When the entire region density is considered, including constituent subareas densities, the density dimension is able to evaluate a pattern of land consumption showing how the different land areas are variously occupied (Galster et al., 2001). In terms of a sprawl measurement dimension, a high level of sprawl in a region is evident when most constituent sub-areas show relatively even low densities. A low level of sprawl in a region is apparent when most sub-areas have relatively uneven high densities (Frenkel & Ashkenazi, 2008; Lopez & Hynes, 2003). Figure 4 is a conceptual illustration of the density dimension.

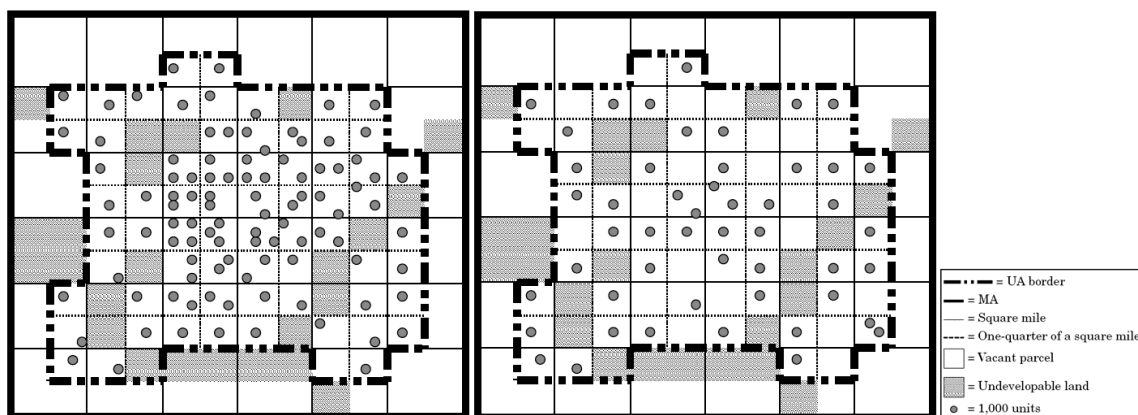


Figure 4 Density dimension – high-density land use pattern (left) and low-density land use pattern (right) (Galster et al., 2001, p. 689)

This study, additionally, considers the density gradient dimension as a version of the population density dimension because the density gradients examine proportional change of population densities according to distance from the central area in a region, or proportional change of population densities during a certain time period.

2.2. Spatial scattering dimension

The spatial scattering dimension measures the spatial structure of a region, addressing the extent to which the urbanized areas are equally distributed or concentrated in a few parts of an area (Malpezzi & Guo, 2001; Tsai, 2005; Wolman et al., 2005). The spatial scattering dimension can be distinguished from the above sprawl measurement dimensions by its capacity to measure spatial relationship (Galster et al., 2001; Tsai, 2005). The degree of various population sizes per a unit land area (i.e., density) and the degree of diverse land uses in an area (i.e., land use mix) function only to capture the extent of diversity in urban activities for the various population sizes in a given area. In terms of a measurement for the spatial structure of urbanization, however, the spatial scattering dimension evaluates the degree to which urban activities are equally or unequally distributed, showing spatial structure in a given area (Tsai, 2005). For example, evenly scattered urban areas or continuously developed urban areas may all be high density areas or all low density areas and, as such, both evenly scattered and unevenly scattered urban areas may consist of the same types of land uses or all different types of land uses. The concerns of spatial scattering patterns of urban structure, as a

result, are beyond those of the sprawl measurement dimensions. Figure 5 is a conceptual illustration for the spatial scattering dimension.



Figure 5 Spatial scattering dimension – highly concentrated land use pattern (left) and equally scattered land use pattern (right) (Galster et al., 2001, p. 692)

2.3. Spatial clustering dimension

The spatial clustering dimension has been used to evaluate the degree to which the urbanized areas are tightly bunched or decentralized in a given region (Galster et al., 2001), determining a land use pattern among monocentric, polycentric, and decentralized urbanization (Tsai, 2005). The spatial clustering dimension needs to be distinguished from the above sprawl measurement dimensions for the same reason as the spatial scattering dimension, the capacity to measure the spatial relationship (Galster et al., 2001; Tsai, 2005). In terms of a measurement for the spatial structure of urbanization, the spatial clustering dimension evaluates the degree to which unevenly distributed urban activities measured by the spatial scattering dimension are clustered or randomly distributed (Tsai, 2005). For example, urban areas may be dense and concentrated and

still not be clustered, being uniformly spread throughout a given region or urban areas may have low densities and a low concentration but high clustering, showing tightly bunched urban land use. Figure 6 is a conceptual illustration for the spatial clustering dimension.

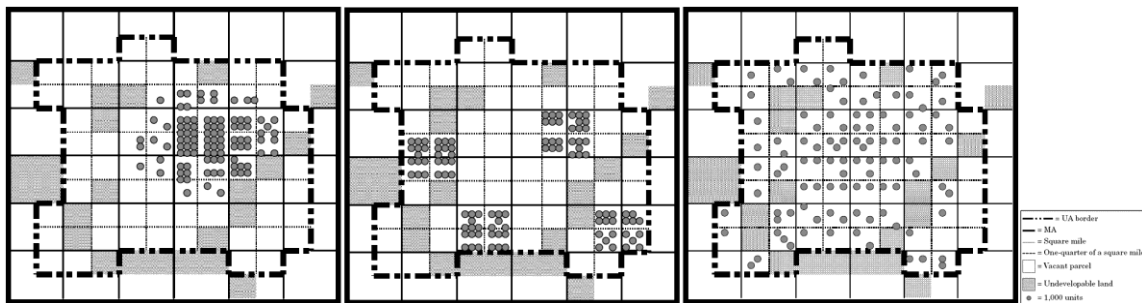


Figure 6 Spatial clustering dimension – monocentric land use pattern (left), polycentric land use pattern (middle), and decentralized land use pattern (right) (Galster et al., 2001, p. 693 & 696)

2.4. Measurement scale

The dimensions described above should be operationalized and, consequently, applicable to examine megaregion scale land use patterns. This study examines morphological characteristics in terms of land use patterns at a megaregion scale. The best dimensions for this study, therefore, seem to be measurements that are operationalized for a megaregion scale or are scale-independent by themselves. Most land use pattern examinations, however, have used empirical dimensions at a metropolitan scale (Ewing et al., 2002; Glaeser & Kahn, 2004; Lopez & Hynes, 2003; Malpezzi & Guo, 2001; Tsai, 2005), an urbanized area scale (Galster et al., 2001), or multi-scale combining the former areas (Cutsinger et al., 2005; Torrens, 2008; Wolman

et al., 2005). The measurement scale has been studied for the dimensions to determine differences according to metropolitan structure, sub-metropolitan structure, and community-level structure (Knaap, Song, Ewing, & Clifton, 2005). Any of these, however, may not be directly applicable to this megaregion scale study.

This study proposes to consider census tract level as a unit of measurement for megaregion scale land use patterns analysis. The census tract is designed to contain relatively homogeneous units with respect to population characteristics, economic status, and living conditions at the time it is established and, as such, the census tract boundaries are delineated with the intention of being stable over many decades, generally following relatively permanent visible features (Poston, 2010). Census tract level observations, therefore, seem to provide more consistent and stable evaluations than county level observations or block group level observations. The county level observation that has been used in current megaregion studies (Ross, 2008) may be too general to capture morphological differences within a county. The block group level observation is expected to be too specific to operationalize for megaregion scale evaluation within given times and budget limits.

3. Indices to evaluate morphological dimension at a megaregion scale

Considering the above issues in developing dimensions, this section operationalizes dimensions for megaregion land use patterns analysis as population density-based sprawl, spatial scattering, and spatial clustering.

3.1. Density-based sprawl index

The density-based sprawl index (DSI) measures the degree of land consumption by population densities per square mile in comparison between a high-density census tract group and a low-density census tract group. In terms of sprawl measurement, the extent of differences in population densities is expected to represent the sprawl level of a megaregion. The low differences in population densities between the high and low-density groups refer to a low level of sprawl. Highly different population densities between two census tract groups indicate a high level of sprawl.

The DSI can be calculated on the basis of the sprawl index of Lopez & Hynes (2003) as follows

$$DSI = \left(\frac{S\%_i - D\%_i}{100} + 1 \right) \times 50,$$

where

$D\%_i$ = percentage of the total population in high-density (over 3,500 / sq. mi) census tracts i , and

$S\%_i$ = percentage of the total population in low-density (between 3,500 / sq. mi and 200 / sq. mi) census tracts i .

The threshold for cutting off the high density census tract group is greater than 3,500 persons per square mile, and for the low density census tract group fewer than 3,500 and greater than 200 persons per square mile (fewer than 200 persons per square mile for the rural area is excluded) (Lopez & Hynes, 2003). The theoretically possible calculation results range from 0 to 100 (i.e., $0 \leq DSI \leq 100$), representing that all

megapolitan population lives entirely in high-density areas as 0 of the DSI, and that all megapolitan population lives entirely in low-density areas as 100 of the DSI.

The advantage in using the DSI is its independence from the measurement scale for the census tract level measurement unit. A defect of the DSI is that the thresholds to cut off the high and low density groups have been taken from the metropolitan scale. Other thresholds to distinguish high and low density groups for the megaregion scale may be questionable.

3.2. Spatial scattering pattern index

The spatial scattering pattern index (SPI) measures the degree to which the spatial pattern of urbanization is equally or unequally scattered in a megaregion. In terms of an urban structure measurement, the extent of spatial inequality in the distribution of urbanized land areas represents spatial scattering of urban structures. The more evenly distributed spatial pattern is indicated by a lower degree of the SPI, and the more unevenly distributed spatial pattern (somewhat concentrated spatial pattern) is represented by a higher degree of SPI.

The SPI can be calculated on the basis of the Gini coefficient modified by Tsai (2005) as follows

$$SPI = 0.5 \sum_{i=1}^N |X_i - Y_i|,$$

where

N = the number of census tracts in a megaregion,

X_i = the proportion of the megaregion land area in census tract i , and

Y_i = the proportion of population in census tract i .

The theoretical calculation results range from 0 to 1 (i.e., $0 \leq \text{SPI} \leq 1$), representing that urban structures are evenly distributed as 0 of the SPI, and that urban structures are extremely concentrated in fewer areas as 1 of the SPI.

The advantage in using the SPI is the ability to describe a spatial pattern without representing it on maps and, as such, to show small differences between urban structures through calculation results. A drawback of SPI as a spatial structure measurement is that SPI cannot determine whether the spatial structure is monocentric, polycentric, or randomly decentralized. This weakness requires the inclusion of the clustered spatial structure index to compensate it.

3.3. Spatial clustering pattern index

The spatial clustering pattern index (CPI) measures the degree to which the spatial pattern of urbanization is clustered or randomly distributed in a megaregion. In terms of an urban structure measurement, the extent of spatial constellation of urbanized land areas represents the spatial clustering of urban structures. Poorly clustered urban land areas denote more randomly distributed spatial patterns of urbanization, and highly clustered urban land areas evince more monocentric-like spatial patterns of urbanization.

The CPI can be calculated on the basis of Moran's (1950) I coefficient modified by Tsai (2005) as follows

$$\text{CPI} = \frac{N \sum_{i=1}^N \sum_{j=1}^N W_{ij} (X_i - \bar{X})(X_j - \bar{X})}{\left(\sum_{i=1}^N \sum_{j=1}^N W_{ij} \right) (X_i - \bar{X})^2},$$

where

N = the number of census tracts in a megaregion,

X_i = population in census tract i ,

Y_j = population in census tract j ,

\bar{X} = the mean of population in all of census tracts, and

W_{ij} = spatial adjacency between census tract i and census tract j .

The theoretical calculation results range from -1 to 1 (i.e., $0 \leq \text{CPI} \leq 1$), representing the chessboard pattern of urban structure as -1 of the CPI, the randomly scattered pattern of urban structure as 0 of the CPI, and the closely clustered pattern of urban structure as 1 of the CPI.

The advantage in using the CPI is the ability to describe a spatial pattern without representing it as maps and, as such, to show small differences between urban structures through calculation results. A drawback of the CPI is the difficulty to clearly differentiate the monocentric urban structure from the polycentric urban structure. A megaregion seems to have a more monocentric-like urban structure when the CPI calculation result reaches 1; however, it is hard to define the exact range for the monocentric urban structure and the polycentric urban structure.

3.4. Local scale spatial association

As stated above, the CPI is a global scale measurement. The CPI came from Moran's I coefficient, and as such provides one statistic to determine the spatial association of the morphological features in a megaregion as statistically significant spatial clustering or dispersion. The CPI, however, cannot identify where the clusters or

the dispersions are on the map at a local scale, nor does the measurement identify how it varies from a local scale spatial association of a morphological feature to other morphological features within the same megaregion boundary. It is difficult, therefore, to determine from the measurement result whether an urbanized spatial pattern of a morphological feature is monocentric or polycentric (Allen, 2009; Getis & Ord, 1992; Jacquez, 2008; Ord & Getis, 1995; Scott & Janikas, 2010; Tsai, 2005; Zhang, Luo, Xu, & Ledwith, 2008).

Compensating for limitations of the CPI, this study uses local scale indicators of spatial autocorrelation such as Cluster and Outlier Analysis (Anselin Local Moran's I) tool and Hot Spots Analysis (Getis-Ord G_i^*) tool to measure spatial association and clustering at a local level and to represent the spatial patterns on the map. The representation of local clusters for each megaregion, as a result, may be a circular shape, an elliptical shape, or a fractal structure. Associating the presence of a local cluster in a particular area with an excess of values (Jacquez, 2008, 2009), the final map representation for local clusters of each megaregion can be interpreted to show an excess of population with a high level of land consumption in an area of clusters in terms of the 2000 population density cluster. Using 2001 impervious land cover data, the local cluster analysis can represent excess urbanization. The 2000 nighttime light emissions data and local cluster analysis also can indicate areas where nighttime urban activities are concentrated. When the spatial concentrations of urban morphological features are tabulated and overlapped for each megaregion, a pattern of megaregional morphology can be constructed.

1) Hot spots analysis (Getis-Ord G_i^*)

Given a set of weighted attribute values for each morphological feature of a megaregion, Getis-Ord (Getis & Ord, 1992) G_i^* statistic can identify the local spatial association of the weighted features distinguishing between high value local clusters and low value local clusters. In the same manner the hot spots analysis tool of ArcMAP represents the spatial associations of features on the map. The hot spots analysis (Getis-Ord G_i^*) tool compares the attribute values of each morphological feature with the neighboring attribute values within a threshold distance band. The specific calculation to produce Getis-Ord G_i^* statistic is

$$G_i^*(d) = \frac{\sum_{j=1, j \neq i}^n w_{ij}(d)x_j}{\sum_{j=1, j \neq i}^n x_j},$$

where

$w_{ij}(d)$ = the spatial weight between census tract i and j determined as a fixed distance by Ripley's K function for the most significant clustering distance from census tract i to all the other census tracts.

The above calculation represents the ratio of the sum of attribute values of census tracts located within a radius of the threshold distance to the sum of all attribute values of census tracts including value of the origin census tract. A positive G_i^* statistic shows clusters of high values (hot spots) and a negative calculation result shows clusters of low values (cold spots) (Allen, 2009; Anselin, 1995; Getis & Ord, 1992; Scott & Janikas, 2010).

2) Cluster and outlier analysis (Anselin Local Moran's I)

Anselin (1995) Local Moran's I identifies local clusters of high or low values given a set of weighted features. The Anselin Local Moran's I analysis uses the cluster and outlier analysis tool of ArcMAP for this study. Based on a comparison with neighboring features, the Anselin Local Moran's I tool quantifies and visualizes spatial autocorrelation and clustering by location as well as by values similar in magnitude (Allen, 2009; Anselin, 1995; Scott & Janikas, 2010; Zhang et al., 2008). The calculation for the cluster and outlier analysis (Anselin Local Moran's I) tool in this study is

$$I_i = \frac{x_i - \bar{X}}{S_i^2} \sum_{j=1, j \neq i}^n w_{ij} (x_j - \bar{X}),$$

where

x_i is an attribute of each morphological feature for census tract i ,

\bar{X} = the mean of the corresponding attribute,

x_j = an attribute of each morphological feature for all the other census tracts

(where $j \neq i$),

S_i^2 = variance of the attribute of each morphological feature, and

w_{ij} = the spatial weight between census tract i and j determined as a fixed

distance by Ripleys K function for the most significant clustering

distance from census tract i to all the other census tracts.

Following above calculation, the Anselin Local Moran's I shows how morphological features that are assigned to each census tract differ from the morphological features within a megaregion as a whole, comparing each attribute of a

morphological feature for a census tract to the mean value for all attributes of the morphological feature within a megaregion. Calculating z-values and p-values for morphological features in terms of each census tract, the Anselin Local Moran's *I* tool quantifies statistically significant clusters of high or low value as well as spatial outliers based on attributes of each morphological feature. Clusters represented on the map are distinguished between clusters of high values (HH), clusters of low values (LL), outlier high values surrounded primarily by low values (HL), and outlier low values surrounded primarily by high values (LH). Figure 7 represents the four different types of spatial associations in the cluster and outlier analysis. (Allen, 2009; Anselin, 1995; Scott & Janikas, 2010; C. Zhang et al., 2008).

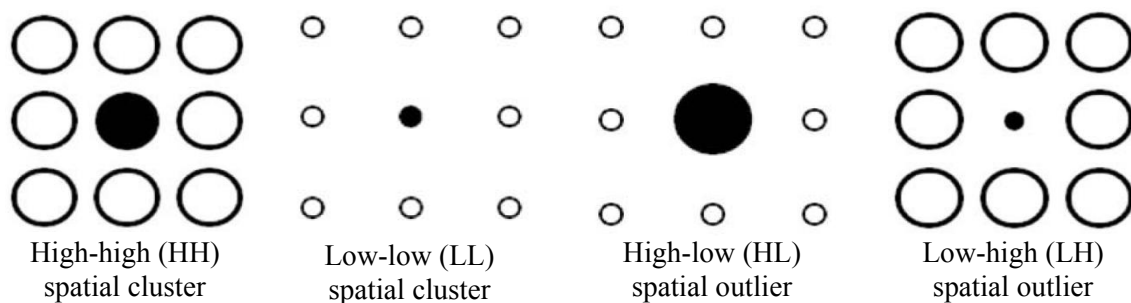


Figure 7 Four different types of local spatial associations (C. Zhang et al., 2008, p. 214)

The above two spatial local clustering analysis tools, therefore, represent excessive morphological characteristics on maps at the local scale. Considering each morphological characteristic in this study, a spatial cluster (or hot spot) by the population density identifies the regional concentration of effective land consumption per capita. A spatial cluster (or hot spot) by the impervious land cover pinpoints places

where urbanized built environments are concentrated. A spatial cluster (or hot spot) by nighttime light emissions detects urban development fabrics that consist mainly of urban socio-economic activities.

When an area is considered to be spatially clustered by both tools in terms of a morphological feature, the area can be more significant, than other areas identified as spatial clustering by only one of them to represent the excess of the morphological feature within the clustering boundary. When an area is considered to be spatially clustered with numerous characteristics of megaregional morphology, one area can be more significant, than other areas identified as being spatially clustered with only one characteristic, to represent the excess of the morphological characteristics within the clustering boundary.

4. Description of the data and the data treatment

This section explains how data sources can be obtained and treated to evaluate morphological dimension indices. All the data is secondary data already that exist.

4.1. Description of morphological data

The data used in this study represents morphological characteristics at the megaregion scale. The data include the 2000 total population, 2000 population density, 2001 impervious land cover, and 2000 nighttime light emissions (DMSP-OLS). The following descriptions show where each piece of data can be obtained and how each can represent a morphological characteristic at the megaregion scale.

1) Population density data

Population density has been popular in land use pattern analysis studies (Cutsinger et al., 2005; Ewing et al., 2002; Frenkel & Ashkenazi, 2008; Galster et al., 2001; Glaeser & Kahn, 2004; Lang, 2003; Lopez & Hynes, 2003; Malpezzi & Guo, 2001; Torrens, 2008; Torrens & Alberti, 2000; Tsai, 2005; Wolman et al., 2005). Population density refers to land consumption primarily by residential land use so that urban development related morphological urban patterns can be examined by the population density dataset.

2) Impervious land cover data

Impervious surfaces refer to a type of land cover which prevents water infiltration into the soil and, as such, are observed in most urbanized land use (Arnold & Gibbons, 1996). Urbanization changes the natural landscape to such urban forms as roads, rooftops, sidewalks, patios, and compacted soils. Impervious surfaces and their proportion in a given amount of land area have been considered to be effective indicators to measure urbanization and various features of urbanization (Arnold & Gibbons, 1996; Barnes, Morgan, & Roberge, 2002; Brabec, Schulte, & Richards, 2002; Hasse & Lathrop, 2003; Lu & Weng, 2006; Morse, Huryn, & Cronan, 2003; Stankowski & Trenton, 1972; Yuan & Bauer, 2007). In examining the megaregion morphological characteristics the impervious land cover is likely to represent urbanized land areas, not determining exactly what land is used for, but reflecting patterns of urban activities.

3) Nighttime light emissions (DMSP-OLS) data

Unlike economic and cultural variables, the nighttime light emissions are a measurable physical quantity for examining the extent of urbanization (Florida et al., 2008; Imhoff, Lawrence, Stutzer, & Elvidge, 1997). Florida et al. (2008) have tried to identify boundaries of world megaregions based on nighttime light emissions data, defining the megaregions in terms of contiguously lighted areas as seen from space at night. Identification of world megaregions in terms of nighttime light emissions was not for identifying functional relationships in spatial observation, but for observing spatial development patterns resulting from functional relationships.

4.2. Data treatment for density-based sprawl index

The first step is to delineate the 11 U.S. megaregions using a census tract as a measurement unit. The Regional Plan Association (RPA) has defined the U.S. megaregions based on counties (Hagler, 2009; RPA, 2008), however, this study follows the spatial definition of the 11 megaregions at census tract level.

The U.S. Census Bureau provided both the 2000 Census TIGER/Line shape files and the 2000 Census attribute files. The shape files are for topographical data including ArcGIS features. For this study, features of states, counties, and census tracts are necessary. The attribute files provide information for each feature of the shape files. For this study, Census 2000 Summary File 1 100-percent data P1 was used. Total Population is selected for census tract level feature data. The downloaded attribute tables were modified to have a field name TotPOP00 and to export to ArcMAP. The

modified attribute files, then, are joined to shape feature files according to the census tract identification code field (CTIDF00).

Total land areas for each census tract are given as square meter unit in the attribute files. ArcMAP recalculates the total land areas of each census tract as square mile units (1 sq. mi = 2,589,988.11 sq. meters), adding a new field (ALANDsqmi) to the census tracts attribute table of each megaregion and using the field calculator as “ALANDsqmi = ALAND00 / 2589988.11”.

Population density of each census tract for the 11 U.S. megaregions can be calculated by dividing total population of each census tract by the newly generated square mile unit land area of the census tract. ArcMAP is used, adding a new field (PopDen00) and using the field calculator as “PopDen00 = TotPOP / ALANDsqmi”.

The 2000 census tracts of a megaregion are categorized as high density census tracts when the 2000 population density of a census tract is greater than 3,500. When a census tract is greater than 200 and less than or equal to 3,500, it is regarded as a low density census tract.

The low or high density census tracts are then used to calculate $D\%$ _{*i*} and $S\%$ _{*i*}. $D\%$ _{*i*} refers to percentage of the total population in high density (over 3,500 / sq. mi) census tracts *i*. $D\%$ _{*i*} can be calculated by dividing the sum of the 2000 total population of high density group census tracts by the sum of the 2000 total population of every census tract of a megaregion and multiplying by 100. $S\%$ _{*i*} refers to percentage of the total population in low density (between 3,500 and 200 / sq. mi) census tracts *i*. $S\%$ _{*i*} can be calculated by dividing the sum of the 2000 total population of low density group census tracts by the

sum of the 2000 total population of every census tract of a megaregion and multiplying 100.

The density-based sprawl index value of a megaregion, finally, can be generated by subtracting $D\%_i$ from $S\%_i$, dividing the difference by 100, then adding 1, and multiplying 50.

4.3. Data treatment for spatial scattering pattern index

The spatial scattering pattern index (SPI) measures the degree of scattering patterns of urbanization in a megaregion. Considering the patterns of urbanization, this study uses 2000 total population, 2000 population density, 2001 impervious land cover, and 2000 nighttime light emissions. The SPI then is produced for the degrees of total population scattering, population density scattering, impervious land cover scattering, and nighttime light emissions scattering.

To produce the SPI in terms of four different datasets, this study generates the proportion of land area in census tract i (X_i), the proportion of total population in census tract i (Pop_Y_i), the proportion of population density in census tract i (Den_Y_i), the proportion of impervious land cover in census tract i ($ImpS_Y_i$), and the proportion of nighttime light emissions in census tract i ($DMSP_Y_i$).

1) Total population and population density data treatment

The proportion of land area for each census tract (X_i) is calculated by dividing land

area of a census tract by the sum of land areas of every census tract in a megaregion. The proportion of total population for each census tract (Pop_Y_i) is calculated by dividing total population of a census tract by the sum of total population of every census tract in a megaregion. The proportion of population density for each census tract (Den_Y_i) is calculated by dividing population density of a census tract by the sum of population density of every census tract in a megaregion.

The next step calculates the absolute difference between the proportion of land area for each census tract (X_i) and the proportion of total population for each census tract (Pop_Y_i) (i.e., $|X_i - Pop_Y_i|$) and the absolute difference between the proportion of land area for each census tract (X_i) and the proportion of population density for each census tract (Den_Y_i) (i.e., $|X_i - Den_Y_i|$). This calculation is easily done by using an MS Excel sheet. After producing the absolute differences for every census tract in a megaregion, these differences are summed up and divided by 2 to produce the SPI of total population and the SPI of population density of a megaregion.

In comparison with the above calculations for the SPI of total population and for the SPI of population density, this study needs to make preliminary arrangements to produce the proportion of impervious land cover in each census tract and the proportion of nighttime light emissions in each census tract.

2) Impervious land cover data treatment

First, this study needs to consider the thresholds of imperviousness percentages and nighttime light emissions values to represent urbanized spatial patterns. Impervious

land cover, greater than or equal to 20 percent of imperviousness, is considered the threshold to distinguish urbanized spatial patterns from other impervious land covers (Arnold & Gibbons, 1996). Nighttime light emissions greater than 80 percent are considered the threshold to distinguish urbanized spatial patterns from other nighttime light emissions (Imhoff et al., 1997).

Impervious land cover data was obtained from the National Land Cover Database (NLCD) at <http://www.mrlc.gov/nlcd2001.php>. The data includes 2001 percentage developed imperviousness at a 30-meter resolution for the 50 U.S. states. Using the ArcMap Raster Projection tool, U.S. scale raw impervious land cover data was projected according to a UTM coordinate system that corresponds to each megaregion. Using the ArcMap Clips tool, the impervious land cover raster set for each megaregion was generated according to each megaregion shape feature. Each clipped impervious land cover data, then, is reclassified according to the threshold for distinguishing urbanized impervious surfaces from other impervious surfaces. The Con of the Spatial Analysts Tools of ArcMAP was used. Each input conditional raster is clipped and projected impervious land cover data. Expression is $VALUE \geq 20$ AND $VALUE \leq 100$. Constant value for true raster is 1 and for false raster is 0. Following the above steps, each piece of clipped and projected impervious land cover data is reclassified as raster value 1 referring to urbanized impervious surfaces and raster value 0 referring to other impervious surfaces.

The Zonal Statistics as Table of ArcMAP produced an attribute table summing up all the raster value 1s within a census tract of a megaregion. Feature zone data is each

megaregion shape feature. Zone field is the census tract identification code (CTIDF00). Input value raster is VALUE. Statistics type is SUM. The attribute table produced by the Zonal Statistics as Table for each megaregion is, then, joined to the corresponding shape feature megaregion according to the CTIDF00. The proportion of impervious land cover for each census tract of a megaregion ($ImpS_Y_i$), finally, can be calculated by dividing the resulted sum of impervious surface (i.e., sum of raster value 1s within a census tract) by the sum of every impervious surface (i.e., total sum of raster value 1s within a megaregion).

The next step calculates the absolute difference between the proportion of land area for each census tract (X_i) and the proportion of impervious land cover for each census tract ($ImpS_Y_i$) (i.e., $|X_i - ImpS_Y_i|$). This calculation is easily done by using an MS Excel sheet. After producing the absolute differences for every census tract in a megaregion, these differences are summed up and divided by 2 to produce the SPI of impervious land cover for a megaregion.

3) Nighttime light emissions data treatment

The 2000 nighttime light emissions data was obtained from the Defense Meteorological Satellite Program – Operational Linescan System (DMSP-OLS) archive at <http://www.ngdc.noaa.gov/dmsp/downloadV4composites.html>. The data included 2000 nighttime light emissions at 30 arc second grids resolution (approximately 1km resolution) for the world.

Using the ArcMap Raster Projection tool, the world scale raw DMSP-OLS data is projected according to a UTM coordinate system that corresponds to each megaregion. Using the ArcMap Clips tool, the DMSP-OLS raster set for each megaregion is generated according to each megaregion shape feature.

The particular resolution for rasterizing each piece of shape feature megaregion data is different because the DMSP-OLS raw data uses the WGS coordinate system and the resolution is projected differently according to each megaregion UTM coordinate system. The diverse cell size caused by the coordinate system relocation for each megaregion ranges from approximately 800 to 950 meters. All different cell resolutions can be problematic in this study not only because a fixed and identical cell resolution for every megaregion analysis is preferable, but also because the Zonal Statistics as Table tool assigns 0 value of DMSP-OLS to a census tract that has a smaller land area than the corresponding DMSP-OLS cell. The projected and clipped DMSP-OLS raster set for each megaregion is, therefore, required to have a fixed resolution that is sufficient to be covered by the smallest census tract land area. Using a 30-meter resolution scale that is identical to the resolution of impervious land cover, a fixed and small enough DMSP-OLS raster data set is generated by the ArcMAP Resample tool.

Each piece of clipped DMSP-OLS data, then, is reclassified according to the threshold for distinguishing urbanized nighttime light emissions from other nighttime light emissions. The Con of the Spatial Analyst Tools of ArcMAP is used. Input conditional raster is each piece of clipped and projected DMSP-OLS data. Expression is $VALUE > 55.44$ (88% of cutting line for maximum nighttime light emission value).

Constant value for true raster is 1 and for false raster is 0. Following the above steps, each piece of clipped and projected DMSP-OLS data is reclassified as raster value 1 referring to nighttime light emissions from urbanized areas and raster value 0 referring to nighttime light emissions from other areas.

The Zonal Statistics as Table of ArcMAP produces an attribute table summing up all the raster value 1s within a census tract of a megaregion. Feature zone data is the megaregion shape feature. Zone field is the census tract identification code (CTIDF00). Input value raster is VALUE. Statistics type is SUM. The attribute table produced by the Zonal Statistics as Table for each megaregion is then joined to the corresponding shape feature megaregion according to the CTIDF00. The proportion of nighttime light emission for each census tract of a megaregion (DMSP_Y_i), finally, can be calculated by dividing resulted sum of nighttime light emissions (i.e., sum of raster value 1s within a census tract) by sum of every nighttime light emission (i.e., total sum of raster value 1s within a megaregion).

The next step calculates the absolute difference between the proportion of land area for each census tract (X_i) and the proportion of nighttime light emissions for each census tract (DMSP_Y_i) (i.e., |X_i – DMSP_Y_i|). This calculation is easily done by using an MS Excel sheet. After producing the absolute differences for every census tract in a megaregion, the absolute differences are summed up and divided by 2 in order to produce the SPI of nighttime light emissions for a megaregion.

4.4. Data treatment for spatial clustering pattern index

The clustered spatial pattern index (CPI) measures the degree of clustering patterns of urbanization in a megaregion. Considering the pattern of urbanization, this study uses 2000 total population, 2000 population density, 2001 impervious land cover, and 2000 nighttime light emissions. The CPI, as a result, is produced for the degrees of total population clustering, population density clustering, impervious land cover clustering, and nighttime light emissions clustering.

In order to produce the CPI in terms of four different datasets, this study utilized the Spatial Autocorrelation (Moran's I) tool of ArcMap. The Spatial Autocorrelation function perfectly matches the CPI in generating Moran's I coefficient as a result of the analysis. In order to realize the maximum clustering distance for each potential clustering in a megaregion, this study also used the Multi-Distance Spatial Cluster Analysis (Ripley's K Function) tool of ArcMap.

The Multi-Distance Spatial Cluster Analysis (Ripley's K Function) tool measures distance where the most significant clustering can be detected in a given spatial dataset (Allen, 2009; Scott & Janikas, 2010). The K function tool, therefore, can determine the maximum clustering distance from a census tract of a megaregion to all neighboring census tracts in the megaregion, weighting each piece of morphological data (i.e., the total population of each census tract, population density of each census tract, urbanized impervious land cover of each census tract, and urbanized nighttime light emissions).

The total population and the population density datasets have only one value for each corresponding census tract in a megaregion. The impervious land cover and

nighttime light emissions data, however, have various values for each corresponding census tract in a megaregion because the resolution of the two datasets is typically smaller than a census tract land area. In order to resolve this issue, this study has used mean of imperviousness percentage values in a census tract and mean of nighttime light emissions values in a census tract as well.

1) Total population and population density data treatment

Once the DSI was produced, this study contained shape feature megaregion datasets at the census tract level including the 2000 total population (TotPOP00) and the 2000 population density (PopDen00) for each census tract in attribute tables of the shape feature megaregion datasets. Using the two fields, the Multi-Distance Spatial Cluster Analysis (Ripleys K Function) produces the maximum clustering distance for each potential clustering in a megaregion (see Appendix A). Input feature class is census tract level shape feature megaregion data. Weight field is TotPOP00 for total population based clustering analysis and PopDen00 for population density based clustering analysis. Distance at the maximum difference between expected K and observed K, as a result, is the maximum clustering distance for each potential clustering in a megaregion.

The Spatial Autocorrelation (Moran's I) of ArcMap produces the CPI using the resulted maximum distance by Ripleys K Function. Input feature class is a census tract level shape feature megaregion data. Input field is TotPOP00 for total population CPI and PopDen00 for population density CPI. Fixed distance is selected for conceptualization of spatial relationships in this study. Having row standardization for

various sizes of census tracts with fewer distributed near the edge of a megaregion (in order to avoid the exaggeration of differences or similarities between values of census tracts due to unevenly distributed and unevenly sized census tracts near the edge of a megaregion), the maximum clustering distance produced by Ripley's K Function is inserted for threshold distance.

2) Impervious land cover data treatment

Preparation steps for the impervious land cover data in the CPI are similar to those for the SPI. Using 20 percent threshold, the function of Extract by Attributes of ArcMAP can extract impervious land cover values that are greater than or equal to 20 and less than or equal to 100. The input raster is the clipped and projected impervious land cover raw data. The where clause is $VALUE \geq 20$ AND $VALUE \leq 100$.

It is not necessary in the CPI for the conditional function to reclassify urbanized impervious land cover (i.e., $20 \leq \text{value} \leq 100$) to 1 and other impervious land cover (i.e., $20 > \text{value}$ or $100 < \text{value}$) to 0. The CPI rather needs raw imperviousness values ranging between 20 and 100 percent for the formula to distinguish urbanized impervious land cover areas from other impervious land cover areas.

Having megaregion shape feature data for the feature zone data, the Zonal Statistics as Table produces the attribute table. The statistics type for the CPI is MEAN unlike the SUM of the SPI. Because the 30-meter raster resolution of impervious land cover data is smaller than the typical census tract land area size, various values of impervious land cover are located in a census tract. For this issue, the mean statistics

type for the Zonal Statistics as Table is more likely to be a representative value of impervious land cover for a census tract than the sum statistics type. Zone field is the census tract identification code (CTIDF00). Input value raster is VALUE. Having the mean statistics type, the result attribute table of the Zonal Statistics as Table is then joined to the corresponding shape feature megaregion according to the CTIDF00. As a result, the joined attribute table of the shape feature megaregion includes the MEAN field.

The next step generates the CPI of impervious land cover for each megaregion. The maximum clustering distance for each potential clustering in terms of the impervious land cover needs to be prepared by Multi-Distance Spatial Cluster Analysis (Ripleys K Function). Input feature class is a census tract level shape feature megaregion which is created in the previous step. Weight field is MEAN. Distance at the maximum difference between expected K and observed K, as a result, is the maximum clustering distance for each potential clustering in terms of impervious land cover.

The Spatial Autocorrelation (Moran's *I*) of ArcMAP produces the CPI using the resulted maximum distance generated by Ripleys K Function. Input feature class is a census tract level shape feature megaregion data. Input field is MEAN. Fixed distance is selected for conceptualization of spatial relationships in this study. Having row standardization for various sizes of census tracts with fewer distributed near the edge of a megaregion (in order to avoid the exaggeration of differences or similarities between values of census tracts due to unevenly distributed and unevenly sized census tracts near

the edge of a megaregion), the maximum clustering distance produced by Ripley's K Function is inserted for threshold distance.

3) Nighttime light emissions data treatment

The nighttime light emissions data treatment is basically the same as the one for the impervious land cover data except threshold value used for distinguishing urbanized area nighttime light emissions from rural area nighttime light emissions. Using 88% threshold, the Extract by Attributes of ArcMAP, input raster is the clipped and projected nighttime light emissions raw data. The where clause is $VALUE > 55.44$ (55.44 is the 88% cutting value).

The other steps for the CPI of nighttime light emissions data are same as those for the CPI of impervious land cover data.

4.5. Data treatment for local scale spatial analyses

Getis-Ord G_i^* hot spots analysis and Anselin Local Moran's I cluster and outlier analysis have the same data treatment.

1) Total population and population density data treatment

The local level spatial association analysis for total population and population density uses the census tract level shape feature megaregion datasets that include the 2000 total population (TotPOP00) attribute and 2000 population density (PopDen00) attribute.

For the hot spots analysis (Getis-Ord G_i^*) parameters, input feature class is the census tract level shape feature. Input field is TotPOP00 for observing local level spatial clustering patterns of total population and PopDen00 for population density. This study used fixed distance band for the conceptualization of spatial relationships. Threshold distance is the distance that resulted from Ripley's K function for each morphological feature data.

For the cluster and outlier analysis (Anselin Local Moran's I), every input parameter is identical to the hot spots analysis (Getis-Ord G_i^*), except the row standardization setting.

2) Impervious land cover and nighttime light emissions data treatment

Local scale spatial clustering pattern analysis for impervious land cover data and nighttime light emissions data used census tract level shape feature megaregion datasets that included the mean value attribute of each census tract on impervious land cover ranging between 20 and 100 and on nighttime light emissions ranging above 55.44 (88%).

For hot spots analysis (Getis-Ord G_i^*) parameters, input feature class is the census tract level shape feature megaregion dataset. Input field is the MEAN field for each morphological feature. The fixed distance band was selected for spatial relationships. The distance resulting from Ripley's K function was used for threshold distance.

For the cluster and outlier analysis (Anselin Local Moran's I), every input parameter was identical to the hot spots analysis (Getis-Ord G_i^*), except the row standardization setting.

CHAPTER IV

RESULTS

The following analysis results can be divided into spatial pattern analysis results and local spatial association analysis results according to the research sub-questions. The first part includes the results of the density-based sprawl index (DSI), the spatial scattering pattern index (SPI), and the spatial clustering pattern index (CPI). The second part includes the results of Getis-Ord G_i^* hot spots analysis and Anselin Local Moran's I cluster and outlier analysis.

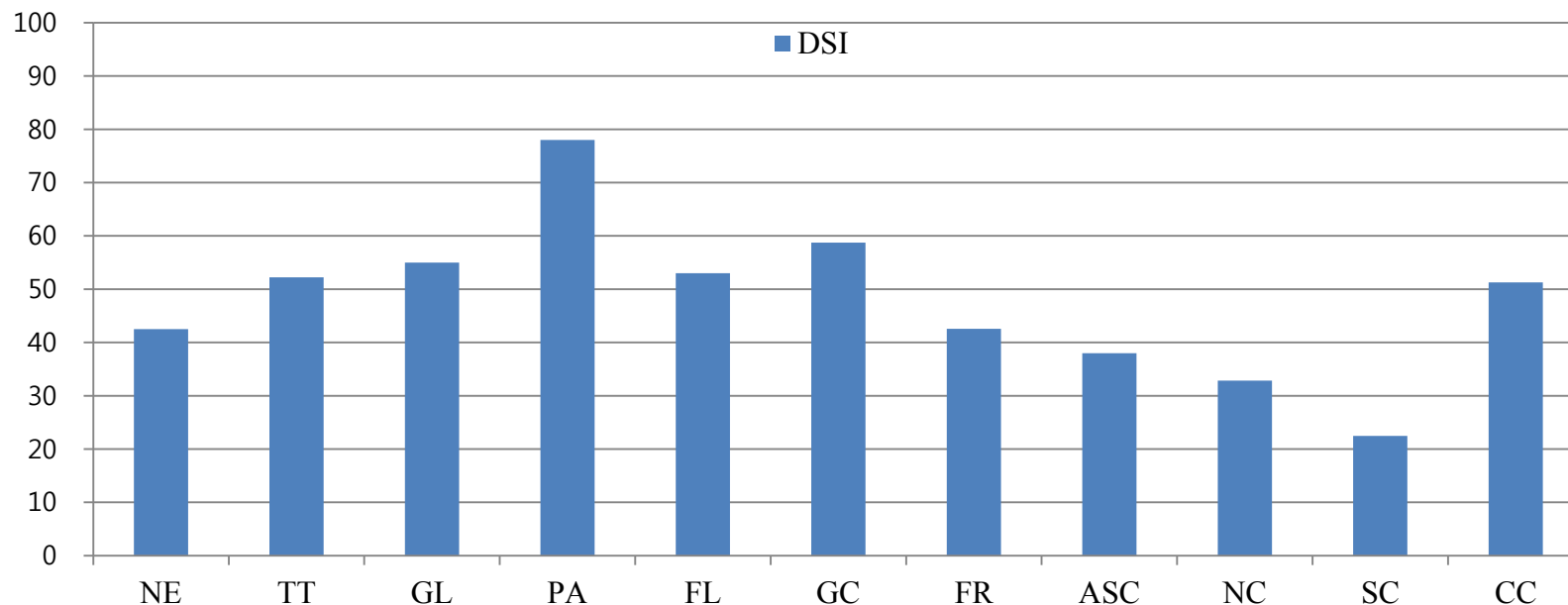
1. Spatial patterns analysis results

1.1. Density-based sprawl index

The result of calculations for the density-based sprawl index (DSI) is given in Figure 8. The DSI values can be interpreted to show that all populations of a megaregion live entirely in high density areas (i.e., low level of sprawl) when the DSI value approaches zero (0). From the DSI values, it can be also determined that the entire population of a megaregion lives in low density areas (i.e., high level of sprawl) when the value approaches 100 (one hundred). All megaregions were analyzed based on census tract levels using the 2000 census data and ArcMAP data.

The Piedmont Atlantic megaregion shows the highest level of population density sprawl at around 80 DSI value, meaning that residents of that megaregion have sprawled into low density areas to a greater extent compared to other U.S. megaregion residents.

Density-based Sprawl Index (DSI) (2000 CenTract level)



Close to 0 (zero) – All populations of a megaregion live entirely in high density areas (i.e., low level of sprawl)

Close to 100 (one hundred) – All populations of a megaregion live entirely in low density areas (i.e., high level of sprawl)

	NE	TT	GL	PA	FL	GC	FR	ASC	NC	SC	CC
DSI	42.5144	52.2155	54.9773	77.9855	53.0072	58.7292	42.5595	37.9969	32.8417	22.4713	51.2634

NE – Northeast

TT – Texas Triangle

GL – Great Lakes

PA – Piedmont Atlantic

FL – Florida

GC – Gulf Coast

FR – Front Range

ASC – Arizona Sun Corridor

NC – Northern California

SC – Southern California

CC – Cascadia

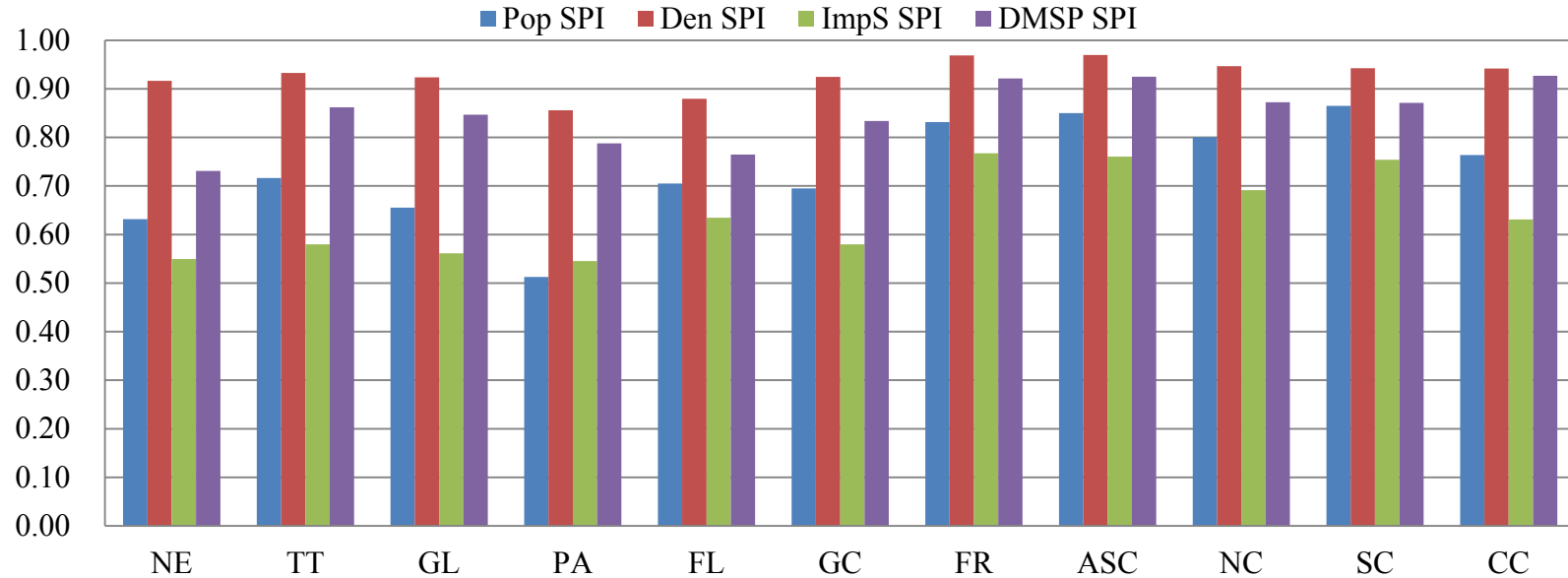
Figure 8 Calculation results of density-based sprawl index

In 2000, the Southern California megaregion had the lowest level of population density sprawl at about 22 DSI, meaning that residents of that megaregion lived in high density areas to a greater extent than residents of other U.S. megaregion. Compared to the DSI mean value which is around 48, the Northeast megaregion, where the concept of megaregion originated, shows about a 43 DSI value, meaning that inhabitants of that megaregion have less sprawl than the average level of sprawl for the 11 U.S. megaregions in 2000. Six megaregions including the Texas Triangle, Great Lakes, Piedmont Atlantic, Florida, Gulf Coast, and Cascadia show above mean population density sprawl. It means that the 6 megaregions have a higher level of land consumption per capita than the average land consumption per capita of the 11 U.S. megaregions in 2000. Every other megaregion, including the Northeast, Front Range, Arizona Sun Corridor, Northern California, and Southern California, shows below mean population density sprawl. It means that in 2000 the 5 megaregions had a lower level of land consumption per capita than average land consumption per capita of the 11 U.S. megaregions.

1.2. Spatial scattering pattern index

The results of calculations for the spatial scattering pattern index (SPI) are given in Figure 9. The calculations were conducted to identify the spatial scattering patterns of morphological characteristics for the 11 U.S. megaregions. The observation determined whether the 11 U.S. megaregions share common spatial scattering patterns of morphological characteristics. SPI was produced using the 2000 total population, 2000 population density, 2001 impervious land cover, and 2000 nighttime light emissions.

Spatial Scattering Pattern Index (SPI) (2000 CenTract level)



Close to 0 (zero) – Each morphological feature is evenly distributed in a megaregion

Close to 1 (one) – Each morphological feature density is extremely high in fewer areas in a megaregion

	NE	TT	GL	PA	FL	GC	FR	ASC	NC	SC	CC
Pop SPI	0.6317	0.7162	0.6554	0.5128	0.7051	0.6948	0.8315	0.8499	0.8003	0.8650	0.7636
Den SPI	0.9166	0.9327	0.9237	0.8559	0.8795	0.9246	0.9687	0.9698	0.9466	0.9425	0.9418
ImpS SPI	0.5496	0.5797	0.5613	0.5453	0.6346	0.5799	0.7672	0.7604	0.6914	0.7540	0.6309
DMSP SPI	0.7309	0.8621	0.8467	0.7877	0.7648	0.8337	0.9212	0.9251	0.8726	0.8711	0.9269

NE – Northeast

TT – Texas Triangle

GL – Great Lakes

PA – Piedmont Atlantic

FL – Florida

GC – Gulf Coast

FR – Front Range

ASC – Arizona Sun Corridor

NC – Northern California

SC – Southern California

CC – Cascadia

Figure 9 Calculation results of spatial scattering pattern index

SPI, therefore, measures spatial scattering patterns of four different morphological characteristics – 2000 total population scattering spatial pattern index (Pop SPI), 2000 population density scattering spatial pattern index (Den SPI), 2001 impervious land cover scattering spatial pattern index (ImpS SPI), and 2000 nighttime light emissions scattering spatial pattern index (DMSP SPI).

The SPI values can be interpreted as follows: each morphological feature (i.e., 2000 total population, 2000 population density, 2001 impervious land cover, and 2000 nighttime light emissions) is evenly distributed within a megaregion when an SPI value approaches 0; each morphological feature density is extremely high in fewer areas within a megaregion when a value of the SPI approaches 1. The SPI value can be interpreted as a relative term in comparison with other SPI values because of the lack of thresholds to determine the absolute extent of spatial scattering based on a single value. Observations of spatial scattering patterns, therefore, are conducted in terms of each morphological characteristic for the 11 U.S. megaregions and each megaregion for morphological characteristics.

As observations in terms of each morphological characteristic show, the 2000 total population spatial scattering indicates that the Southern California megaregion has the highest Pop SPI at around 0.87 and the Arizona Sun Corridor megaregion has the second highest Pop SPI at around 0.85. This means that populations in the megaregions in 2000 were extremely concentrated in fewer areas. For spatial scattering of the 2000 population density, the Arizona Sun Corridor megaregion shows the highest Den SPI at around 0.97. Northern and Southern California and Cascadia megaregions show the

second highest Den SPI, at approximately 0.94. It means for the megaregions that land consumption per capita was extremely concentrated in fewer areas in 2000. For the spatial scattering of the 2001 impervious land cover, the Front Range and Arizona Sun Corridor megaregions show the highest value of SPI at around 0.77 and 0.76 respectively. It means that megaregions with urbanized built environments represented by impervious land cover were extremely concentrated in fewer areas in the year 2001. For the spatial scattering of the 2000 nighttime light emissions, the Arizona Sun Corridor and Front Range megaregions showed the highest SPI value at around 0.93 and 0.92 respectively. It means that in the megaregions urbanized social activities, which are represented by nighttime light emissions, were extremely concentrated in fewer areas in 2000.

The above results show that morphological characteristics observed in this study have a distinct spatial scattering pattern from each other for the 11 U.S. megaregions. Among the morphological characteristics, spatial scattering patterns identified by 2000 population density represent the most extreme spatial concentration in fewer areas at around the 0.93 mean of the 11 U.S. megaregions Den SPIs. The spatial scattering patterns identified by 2000 nighttime light emissions also show an extreme spatial concentration in fewer areas at about the 0.85 mean of the 11 U.S. megaregions DMSP SPIs. The spatial scattering patterns of the 2000 total population demonstrate relatively low spatial concentration in fewer areas at about the 0.73 mean of the 11 U.S. megaregions Pop SPIs. Spatial scattering patterns of 2001 impervious land cover

represent the lowest degree of spatial concentration in fewer areas at about the 0.64 mean of 11 the U.S. megaregions ImpS SPIs.

In terms of each megaregion, the 11 U.S. megaregions have the greatest deviation in the 2000 total population and the smallest deviation in 2000 population density. Observations also show the greatest deviation of SPIs in the Northeast megaregion and the smallest deviation of SPIs in the Southern California megaregion. Spatial scattering of morphological characteristics represents such a general pattern as the highest SPI at 2000 population density, the second highest SPI at 2000 nighttime light emissions, the third highest SPI at 2000 total population, and the lowest SPI at 2001 impervious land cover. The Piedmont Atlantic megaregion represents a lower Pop SPI than the ImpS SPI, even though every other megaregion has a higher Pop SPI than the ImpS SPI. The Southern California megaregion is also exceptional in that the Pop SPI is the same as the DMSP SPI, contrasted to other megaregions where the Pop SPI is smaller than the DMSP SPI.

The overall observations for spatial scattering patterns show that such morphological characteristics of the 11 U.S. megaregions as population, density, impervious land cover, and nighttime light emissions are distributed unevenly in fewer areas. It means that megaregion scale urban structures and human habitat spatially converge in fewer areas. It is difficult to say, however, that the 11 U.S. megaregions share common patterns of spatial scattering of morphological characteristics based on inconsistencies in the Piedmont Atlantic and Southern California megaregions. It does not mean that the spatial distribution of morphological characteristics is a random

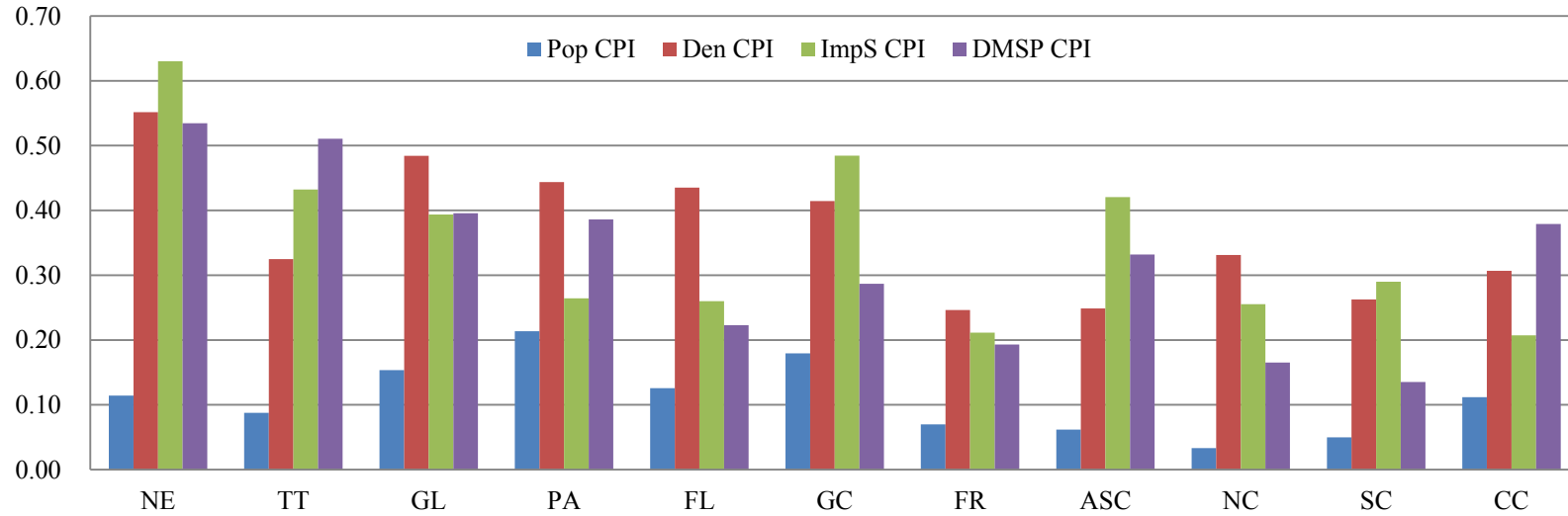
scattering of the 11 U.S. megaregions, but that spatial distribution is inconsistently concentrated in fewer areas according to morphological characteristics. The spatial scattering pattern index, however, has no power to determine whether the concentrated spatial distribution in fewer areas is clustered or not.

1.3. Spatial clustering pattern index

The results of calculations for the spatial clustering pattern index (CPI) are given in Figure 10. The CPI was calculated using the 2000 total population, 2000 population density, 2001 impervious land cover, and 2000 nighttime light emissions. The CPI, therefore, has measured spatial clustering patterns of four different morphological characteristics which are the 2000 total population spatial clustering pattern index (Pop CPI), 2000 population density spatial clustering pattern index (Den CPI), 2001 impervious land cover spatial clustering pattern index (ImpS CPI), and 2000 nighttime light emissions spatial clustering pattern index (DMSP CPI).

The CPI values can be interpreted to demonstrate that each morphological feature (i.e., 2000 total population, 2000 population density, 2001 impervious land cover, and 2000 nighttime light emissions) is randomly distributed within a megaregion when the value of CPI approaches 0, and that each morphological feature is closely clustered in subareas within a megaregion when the value of CPI approaches 1. A value of the CPI can be interpreted as a relative term in comparison with other values of CPI because of the lack of thresholds to determine the absolute extent of spatial clustering for a single value. Observations of spatial clustering patterns, therefore, are conducted in terms of

Spatial Clustering Pattern Index (CPI) (2000 CenTract level)



Close to -1 (negative one) – Chessboard pattern

Close to 0 (zero) – Random scattering

Close to 1 (positive one) – High density subareas are closely clustered

	NE	TT	GL	PA	FL	GC	FR	ASC	NC	SC	CC
Pop CPI	0.1142	0.0877	0.1536	0.2135	0.1256	0.1795	0.0698	0.0619	0.0332	0.0498	0.1118
Den CPI	0.5515	0.3249	0.4842	0.4438	0.4351	0.4145	0.2464	0.2486	0.3312	0.2627	0.3068
ImpS CPI	0.6301	0.4323	0.3937	0.2644	0.2600	0.4845	0.2113	0.4206	0.2552	0.2900	0.2073
DMSP CPI	0.5345	0.5107	0.3958	0.3862	0.2229	0.2869	0.1930	0.3319	0.1652	0.1351	0.3791

NE – Northeast

TT – Texas Triangle

GL – Great Lakes

PA – Piedmont Atlantic

FL – Florida

GC – Gulf Coast

FR – Front Range

ASC – Arizona Sun Corridor

NC – Northern California

SC – Southern California

CC – Cascadia

Figure 10 Calculation results of spatial clustering pattern index

each morphological characteristic for the 11 U.S. megaregions and each megaregion for morphological characteristics.

In terms of each morphological characteristic, the 2000 total population spatial clustering indicates that most megaregions show highly random clustering spatial patterns at around the 0.11 mean of the 11 U.S. megaregions Pop CPIs. Piedmont Atlantic and Gulf Coast are the two top megaregions which show the most spatial clustering patterns among the U.S. megaregions at around 0.21 and 0.18 Pop CPI, respectively. The Pop CPIs for the two top megaregions do not necessarily represent the spatial clustering of the 2000 total population because of low absolute values. The Northern and the Southern California megaregions show the lowest Pop CPIs at around 0.03 and 0.05, respectively. The spatial patterns of 2000 total population for the 11 U.S. megaregions, therefore, are not likely to be closely clustered in high density subareas. For the spatial clustering of the 2000 population density, the mean value of the Den CPI is around 0.37 which means for the 11 U.S. megaregions that the spatial patterns of 2000 population density are three times more closely clustered in high density subareas than those of 2000 total population. The Northeast megaregion shows the highest level of clustering at around 0.55 Den CPI, signifying that the spatial distribution of 2000 population density of the Northeast megaregion is the most closely clustered in high density subareas among the 11 US megaregions. The Den CPIs also show that megaregions including the Great Lakes, Piedmont Atlantic, Florida, and Gulf Coast have, compared with other megaregions, relatively closely clustered population density spatial patterns in high density subareas at around 0.48, 0.44, 0.44, and 0.41, respectively. The

Front Range and Arizona Sun Corridor megaregions show the lowest population density clustering spatial patterns at around 0.25 for both regions. This means that the spatial distributions of 2000 population density in the megaregions are randomly scattered and less likely to be closely clustered into high density subareas. For the spatial clustering of 2001 impervious land cover, the mean value of the ImpS CPI is around 0.35 which indicates that for the 11 U.S. megaregions the spatial patterns of 2001 impervious land cover are nearly three times more closely clustered in high density subareas than those of 2000 total population. It also means that for the 11 U.S. megaregions the spatial clustering patterns of 2001 impervious land cover are similar to those of 2000 population density. The Northeast megaregion shows the highest ImpS CPI at around 0.63, suggesting that the spatial distribution of 2001 impervious land cover of the Northeast megaregion is the most closely clustered in high density subareas among the 11 U.S. megaregions. Megaregions including the Gulf Coast, Texas Triangle, Arizona Sun Corridor, and Great Lakes were in the second highest ImpS CPI group at around 0.48, 0.43, 0.42, and 0.39, respectively. The Cascadia and Front Range megaregions show the lowest ImpS CPI at around 0.21 in both cases. Thus, for the Cascadia and Front Range megaregions, the spatial distributions of 2001 impervious surface land cover are randomly scattered and less likely to be closely clustered in high density subareas. For the spatial clustering of 2000 nighttime light emissions, the mean value of the DMSP CPI is around 0.32. This indicates that for the 11 U.S. megaregions the spatial patterns of 2000 nighttime light emissions are nearly three times more closely clustered in high density subareas than those of 2000 total population. It also means for the 11 U.S.

megaregions that the spatial clustering patterns of 2000 nighttime light emissions are similar to those of 2000 population density and 2001 impervious land cover. The Northeast megaregion shows the highest DMSP CPI at around 0.53, meaning that the spatial distribution of 2000 nighttime light emissions of the Northeast megaregion are the most closely clustered in high density subareas among the 11 U.S. megaregions. The Texas Triangle megaregion also shows a high degree of spatial clustering in 2000 nighttime light emissions at around 0.51. The next highest DMSP CPI group includes the Great Lakes megaregion at around 0.40, the Piedmont Atlantic megaregion at around 0.38, and the Cascadia megaregion at around 0.37. The Southern and Northern California megaregions show the lowest DMSP CPIs at around 0.06 and 0.11, respectively. For the two California megaregions the spatial distributions of 2000 nighttime light emissions are randomly scattered and less likely to be closely clustered in high density subareas.

In terms of each megaregion, the 11 U.S. megaregions have the greatest deviation in 2000 nighttime light emissions and the smallest deviation in 2000 population density. The observations also show the greatest deviation of CPIs in the Northeast megaregion and the smallest deviation of CPIs in the Front Range megaregion. The spatial clustering of the morphological characteristics does not represent a general pattern such as the highest CPI of a particular morphological characteristic and the second highest CPI of the other morphological characteristics. The CPIs of the 11 U.S. megaregions, rather, irregularly rank the CPIs from top to bottom. Only the Pop CPIs of the 11 U.S.

megaregions show a pattern indicating the lowest CPI among the CPIs of the megaregions.

The overall observations for spatial clustering patterns show that such morphological characteristics of the 11 U.S. megaregions as population, density, impervious land cover, and nighttime light emissions are spatially clustered in high density subareas to some extent within each responding megaregion boundary. This means that megaregion scale urban structures and human habitats are spatially clustered in high density subareas. It is difficult to say, however, that the 11 U.S. megaregions share common patterns of spatial clustering of morphological characteristics based on inconsistent CPIs in the megaregions. It does not mean that the spatial distribution of morphological characteristics is randomly scattered for the 11 U.S. megaregions, but that the spatial distribution is clustered in high density subareas to an irregular extent by each morphological characteristic.

Compensating for the limitation of the spatial scattering index, the concentrated spatial distribution of morphological features on fewer areas is now determined to be clustered to some extent. The spatial clustering index, however, still has less power to determine whether the concentrated and clustered spatial distribution of morphological features of fewer high density subareas has monocentric clustering patterns or polycentric clustering patterns because the spatial clustering index is a global scale measurement.

2. Local spatial clustering analysis results

The following figures show the local clustering analysis results in terms of the 2000 population density, 2001 impervious land cover, and 2000 nighttime light emissions (DMSP-OLS). Each figure contains the raw morphological data representation, the hot spots produced by the Getis-Ord G_i^* , the clusters and outliers of the spatial association produced by the Anselin Local Moran's I , and each morphological feature clustering that overlaps statistically significant hot spots with statistically significant high-high (HH) spatial association.

2.1. The Northeast megaregion

1) Local clustering of 2000 population density

Figure 11 shows local clustering analysis results produced by using 2000 population density. Following the threshold of Density-based Sprawl Index, 2000 population density is categorized into three groups: rural areas population density (i.e., less than 200 persons per square mile), low population density areas (i.e., between 200 and 3,500 persons per square mile), and high population density areas (i.e., greater than 3,500 persons per square mile) (top left of figure). The general observation of the distribution of 2000 population density shows that the low population density areas represent a fractal but a linearly connected distribution. The high population density areas are likely to pinpoint urbanized areas such as Boston, Massachusetts, New York City, New York, Philadelphia, Pennsylvania, Baltimore, Maryland, and Washington, DC.

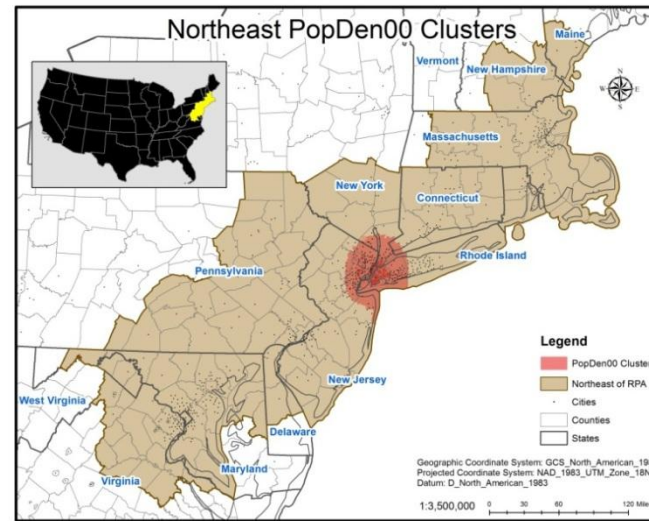
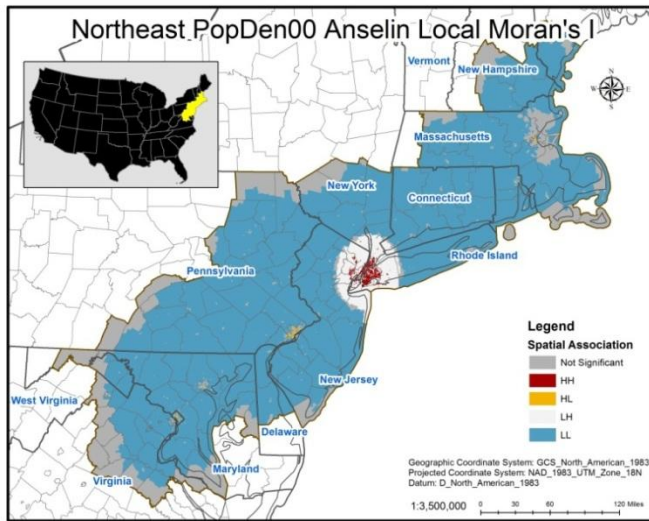
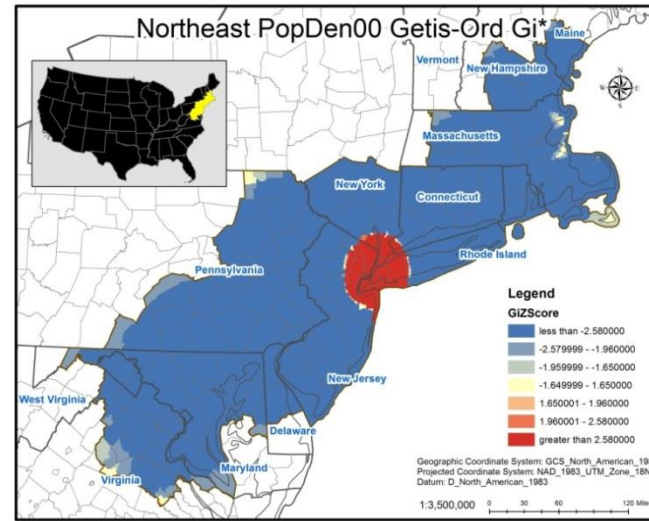
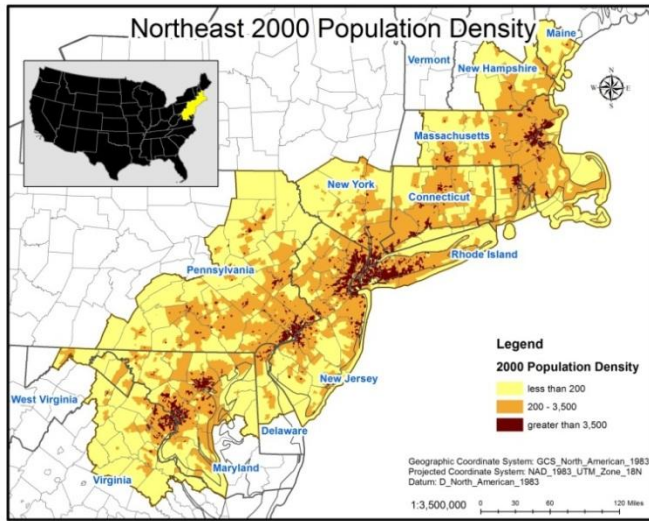


Figure 11 The Northeast megaregion local clustering analysis results by 2000 population density

The statistically significant hot spots at the 0.05 alpha level, as a result of Getis-Ord G_i^* analysis in terms of 2000 population density, represent monocentric clustering (top right of figure). Hot spots are spatially concentrated in the areas around New York City including some parts of New Jersey, New York, Connecticut, and Rhode Island. Table 6 shows hot spots descriptors of 2000 population density for Northeast. The mean of 2000 population density for hot spot areas is around 32,889.96 in comparison with the mean value of approximately 13,914.65 for the Northeast megaregion. This shows that the levels of land use per capita are similarly high within the hot spot boundary.

Table 6 Northeast 2000 population density hot spots descriptors

Clustering Areas	Census Tracts	Land Area (sq. mi)	2000 Total Population
		11,697 (100%)	60,382.64 (100%)
New York City	3,699 (31.62%)	1,958.43 (3.24%)	14,701,831 (29.71%)

The HH spatial associations, as a result of Anselin Local Moran's I analysis in terms of 2000 population density, also represent monocentric clustering in New York City (bottom left of figure). Table 7 shows HH spatial associations descriptors of 2000 population density for Northeast. The mean of 2000 population density for HH spatial associations is around 50,850.19 in comparison with the mean value of approximately 13,914.65 for the Northeast megaregion. Resulted HH spatial associations, therefore, indicate that a high level of land use per capita is clustered with other similarly high levels of land use per capita within the resulted areas.

Table 7 Northeast 2000 population density HH spatial associations descriptors

Clustering Areas	Census Tracts	Land Area (sq. mi)	2000 Total Population
		11,697 (100%)	60,382.64 (100%)
New York City	2,214 (18.93%)	219.67 (0.36%)	8,883,866 (17.95%)

Morphological clustering, as a result of overlapping two analysis results in terms of 2000 population density, has the same clustering boundary as Getis-Ord G_i^* analysis result (bottom right of figure). The clustering extent of 2000 population density for the Northeast megaregion, therefore, is identical to the extent of hot spot clustering. The overlapping of the two clustering analysis results shows that the clustering pattern of 2000 population density is monocentric around New York City, including some areas of New Jersey, New York, Connecticut, and Rhode Island. The clustering pattern of 2000 population density also shows that the concentration of clusters is located only in New York City. The morphological clustering map represents, therefore, that the levels of land use per capita are similarly high and clustered within the clustering boundary. In terms of clustering by 2000 population density, the Northeast megaregion identified by RPA seems to have an exaggerated boundary.

2) Local clustering of 2001 impervious land cover

Figure 12 shows local clustering analysis results produced by using 2001 impervious land cover. The general observation of the distribution of 2001 impervious land cover is that the highest degree of imperviousness in 2001 was likely concentrated in areas where high population density is located (top left of figure). The highly

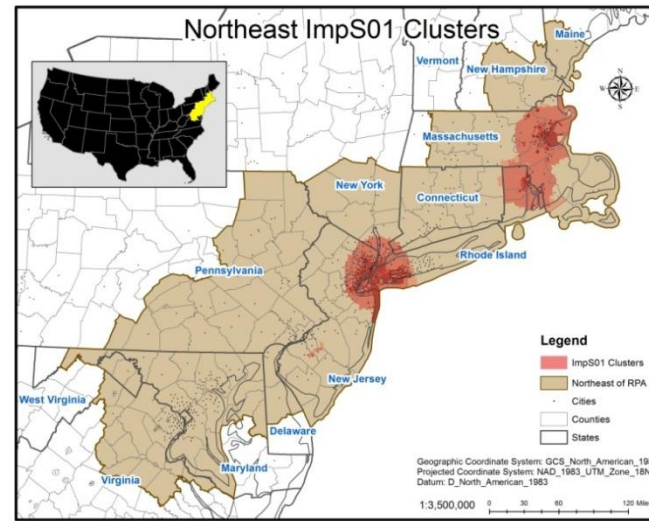
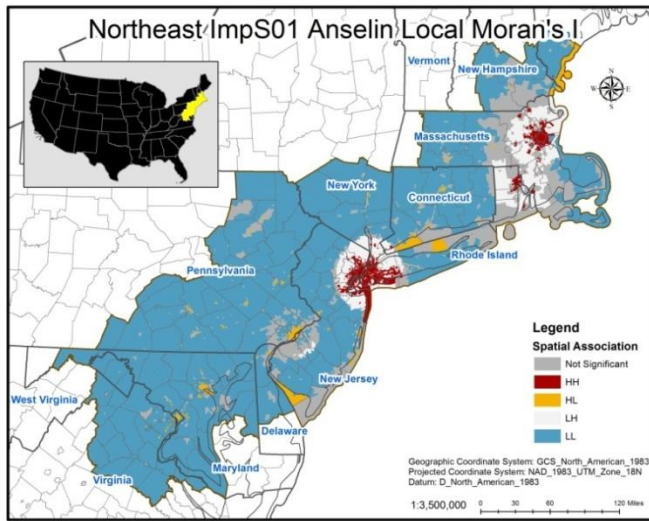
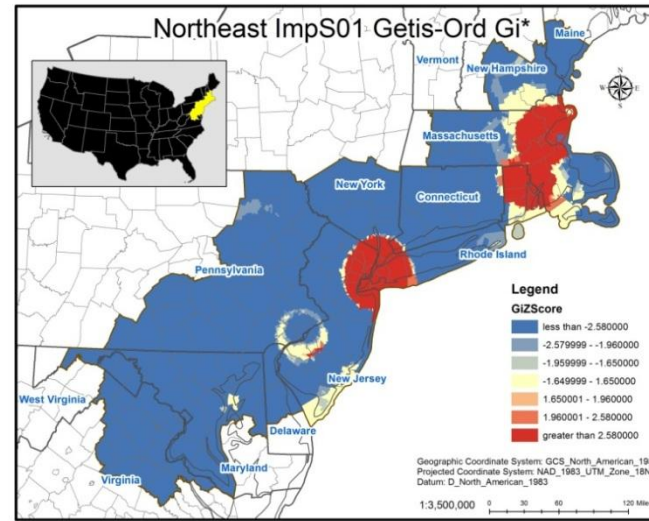
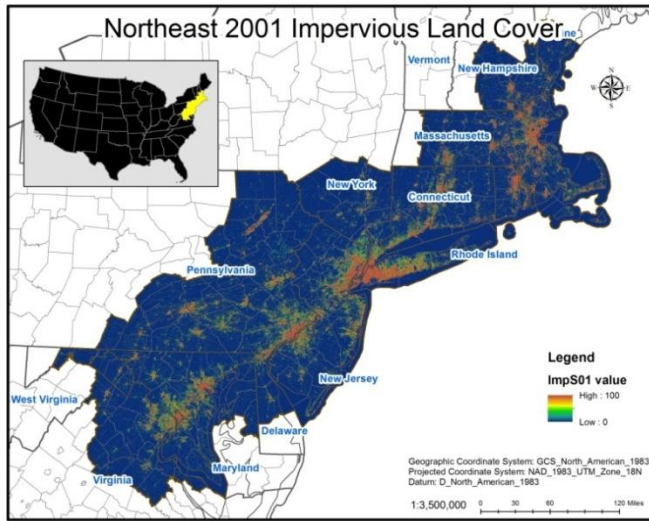


Figure 12 The Northeast megaregion local clustering analysis results by 2001 impervious land cover

impervious areas are most likely to be clustered around areas such as New York City, Boston, Philadelphia, Baltimore, and Washington, DC.

The statistically significant hot spots at the 0.05 alpha level, as a result of Getis-Ord G_i^* analysis in terms of 2001 impervious land cover, represent tri-centric clustering (top right of figure). They are spatially concentrated in the areas around New York City including some parts of New Jersey, New York, Connecticut, and Rhode Island in the clustering; the areas around Boston – Providence including some parts of Massachusetts, Connecticut, and Rhode Island in the clustering; and the areas around Williamstown, New Jersey. Table 8 shows hot spots descriptors of 2001 impervious land cover for Northeast. The mean of 2001 impervious land cover for hot spot areas is around 67.71% in comparison with the mean value of approximately 38.33% for the Northeast megaregion. Resulted hot spots, therefore, indicate that the urbanization levels of built environments are similarly high within the hot spot boundary.

Table 8 Northeast 2001 impervious land cover hot spots descriptors

Clustering Areas	Census Tracts	Land Area (sq. mi)	2000 Total Population
	11,697 (100%)	60,382.64 (100%)	49,481,012 (100%)
New York City	3,731 (31.9%)	1,964.48 (3.25%)	14,851,774 (30.02%)
Boston – Providence	1,067 (9.12%)	3,149.07 (5.22%)	5,031,679 (10.17%)
Williamstown	12 (0.1%)	62.76 (0.1%)	61,244 (0.12%)
Total	4,810 (41.12%)	5,176.31 (8.57%)	19,944,697 (40.31%)

The HH spatial association, as a result of Anselin Local Moran's I analysis in terms of 2001 impervious land cover, represents tri-centric clustering located in the areas around New York City, Boston, and Providence, Connecticut (bottom left of figure). The clustering areas separating Boston and Providence are the one clustering area in Getis-Ord G_i^* analysis result. The clustering around Williamstown, New Jersey resulted by Getis-Ord G_i^* analysis disappears in the result of Anselin Local Moran's I . Table 9 shows HH spatial associations descriptors of 2001 impervious land cover for Northeast. The mean of 2001 impervious land cover for HH spatial associations is around 76.4% in comparison with the mean value of approximately 38.33% for the Northeast megaregion. Resulted HH spatial associations, therefore, indicate that a high level of urbanization for built environments is clustered with other similarly highly urbanized built environments within the resulted areas.

Table 9 Northeast 2001 impervious land cover HH spatial associations descriptors

Clustering Areas	Census Tracts	Land Area (sq. mi)	2000 Total Population
		11,697 (100%)	60,382.64 (100%)
New York City	2,791 (23.86%)	626.31 (1.04%)	10,787,450 (21.8%)
Boston	395 (3.38%)	209.08 (0.35%)	1,700,800 (3.44%)
Providence	130 (1.11%)	80.8 (0.13%)	541,013 (1.09%)
Total	3,316 (28.35%)	916.19 (1.52%)	13,029,263 (26.33%)

Morphological clustering, as a result of overlapping two analysis results in terms of 2001 impervious land cover, has the same clustering boundary as Getis-Ord G_i^*

analysis result (bottom right of figure). The extent of 2001 impervious land cover clustering of the Northeast megaregion, therefore, is identical to the extent of hot spot clustering. The overlapping of the two clustering analysis results shows that the clustering pattern of the 2001 impervious land cover is polycentric around New York City, including some areas of New Jersey, New York, Connecticut, and Rhode Island; around Boston – Providence, including some areas of Massachusetts, Connecticut, and Rhode Island; and around Williamstown, New Jersey. The clustering pattern of 2001 impervious land cover also shows that the concentration of clusters is located both around Boston and Providence, distinguishing two morphological cores from the Boston – Providence clustering area. The concentration of clusters around New York City represents a west-to-east axial pattern crossing from Perth Amboy, New Jersey to Long Beach, New York. The morphological clustering map represents, therefore, that the urbanization levels of these built environments are high and clustered within the clustering boundary. In terms of the clustering of 2001 impervious land cover, the Northeast megaregion identified by RPA seems to have an exaggerated boundary.

3) Local clustering of 2000 nighttime light emissions (DMSP-OLS)

Figure 13 shows local clustering analysis results produced by using 2000 nighttime light emissions (DMSP-OLS). The general observation of the distribution of 2000 nighttime light emissions indicates that highest degree of nighttime light emissions in 2000 is likely to be located in areas of high population density (top left of figure). The distribution of nighttime light emissions is likely to follow a linear axis from Virginia to

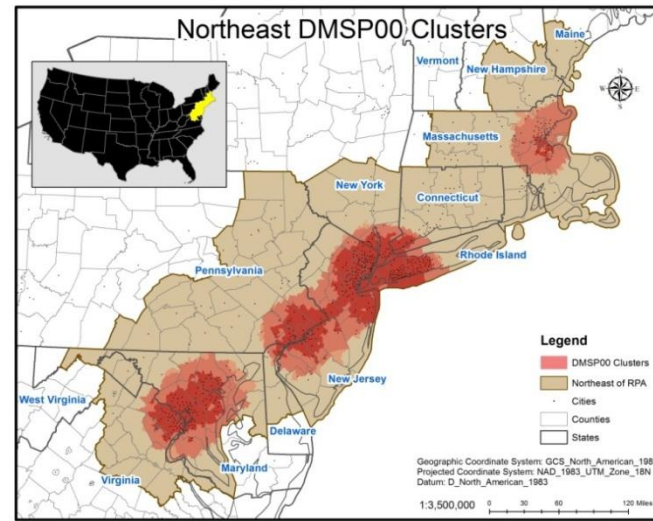
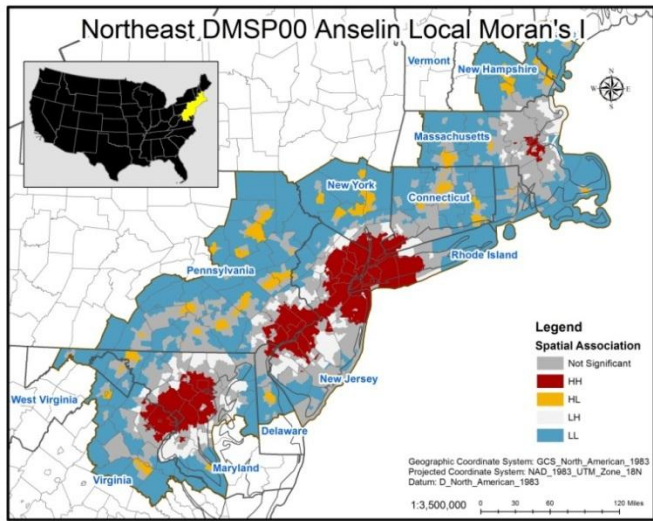
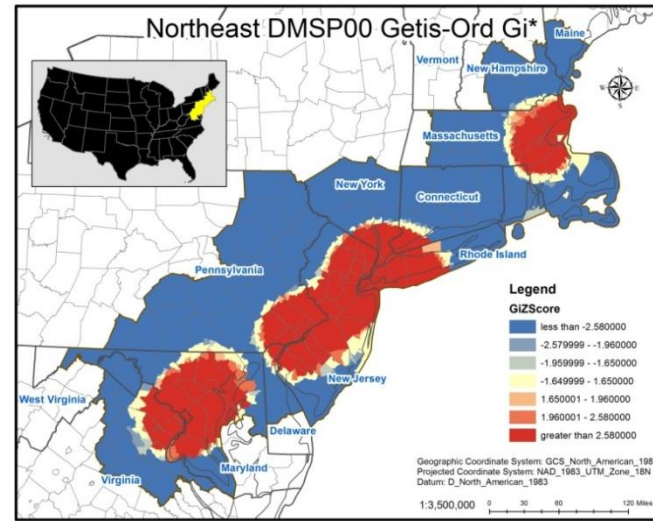
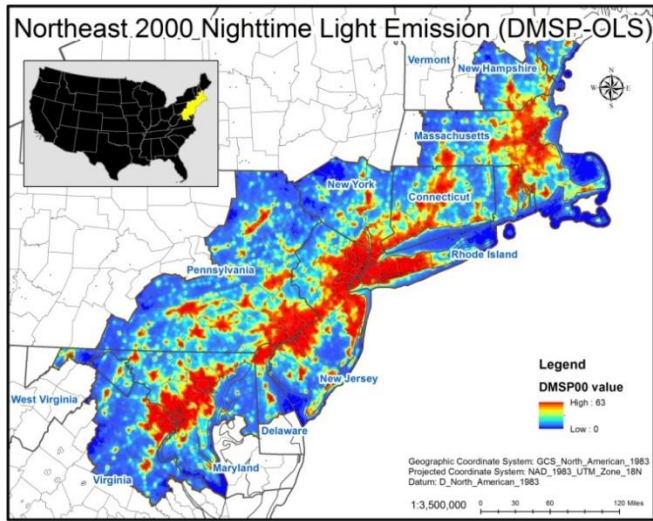


Figure 13 The Northeast megaregion local clustering analysis results by 2000 nighttime light emissions

Connecticut with a cluster around Massachusetts, Rhode Island, and New Hampshire. The general form of distribution is also likely to be similar to the distribution of impervious land cover.

The statistically significant hot spots at the 0.05 alpha level, as a result of Getis-Ord G_i^* analysis in terms of 2000 nighttime light emissions, represent tri-centric clustering (top right of figure). They are spatially concentrated in the areas around New York City – Philadelphia, crossing New York, Rhode Island, New Jersey, Delaware, and Pennsylvania; around Baltimore – Washington, DC, crossing Maryland and Virginia; and around Boston, Massachusetts. Table 10 shows hot spots descriptors of 2000 nighttime light emissions for Northeast. The mean of 2000 nighttime light emissions for hot spot areas is around 60.76% in comparison with the mean value of approximately 55.32% for the Northeast megaregion. Resulted hot spots, therefore, indicate that the urban development levels caused by nighttime socio-economic activities are similarly high within the hot spot boundary.

Table 10 Northeast 2000 nighttime light emissions hot spots descriptors

Clustering Areas	Census Tracts	Land Area (sq. mi)	2000 Total Population
	11,697 (100%)	60,382.64 (100%)	49,481,012 (100%)
New York City – Philadelphia	5,935 (50.74%)	8,704.55 (14.42%)	23,843,798 (48.19%)
Baltimore – Washington, DC	1,521 (13%)	5,062.35 (8.38%)	6,734,985 (13.61%)
Boston	839 (7.17%)	2,163.74 (3.58%)	4,012,932 (8.11%)
Total	8,295 (70.92%)	15,930.64 (26.38%)	34,591,715 (69.91%)

The HH spatial association, as a result of Anselin Local Moran's *I* analysis in terms of 2000 nighttime light emissions, represents tri-centric clustering located in the areas where the hot spot clustering is located (bottom left of figure). The extent of clustering shown in the result of Anselin Local Moran's *I* analysis is smaller than the clustering in the hot spots analysis result. The connection between the clustering area around New York City and the other clustering area around Philadelphia is likely to be narrow compared to a round clustering form in the region. Table 11 shows HH spatial associations descriptors of 2000 nighttime light emissions for Northeast. The mean of 2000 nighttime light emissions for HH spatial associations is around 62.67% in comparison with the mean value of approximately 55.32% for the Northeast megaregion. Resulted HH spatial associations, therefore, indicate that a high level of urban development caused by nighttime socio-economic activities is clustered with other similarly high levels of nighttime socio-economic urban activities within the resulted areas.

Table 11 Northeast 2000 nighttime light emissions HH spatial associations descriptors

Clustering Areas	Census Tracts	Land Area (sq. mi)	2000 Total Population
		11,697 (100%)	60,382.64 (100%)
New York City – Philadelphia	5,431 (43.43%)	4,777.82 (7.91%)	21,734,518 (43.92%)
Baltimore – Washington, DC	1,319 (11.28%)	2,119.18 (3.51%)	5,795,963 (11.71%)
Boston	248 (2.12%)	186.15 (0.31%)	1,082,074 (2.19%)
Total	6,998 (59.83%)	7,083.14 (11.73%)	28,612,555 (57.83%)

Morphological clustering, as a result of overlapping two analysis results in terms of 2000 nighttime light emissions, has the same clustering boundary as Getis-Ord G_i^* analysis result (bottom right of figure). The extent of 2000 nighttime light emissions clustering of the Northeast megaregion, therefore, is identical to the extent of hot spot clustering. The overlapping of the two clustering analysis results shows that the clustering pattern of 2000 nighttime light emissions is polycentric around New York City – Philadelphia, including some areas of New Jersey, Delaware, Pennsylvania, New York, Connecticut, and Rhode Island; and around Baltimore – Washington DC, including Maryland and Virginia; and around Boston, Massachusetts. The clustering pattern of 2000 nighttime light emissions also shows a connection between clustering core areas located in round clustering around New York City. The areas around Baltimore – Washington, DC are expected to be another round shape clustering. The clustering around Boston, however, has a core area around Boston. The morphological clustering map shows that the levels of urban development caused by nighttime socio-economic activities are similarly high and clustered within the clustering boundary. In terms of the clustering by 2000 nighttime light emissions, the Northeast megaregion identified by RPA seems to have an exaggerated boundary.

4) Morphological local clustering

Figure 14 represents results only produced by overlapping every clustering of the Getis-Ord G_i^* hot spots analysis (top of figure) and only by overlapping every HH spatial cluster of the Anselin Local Moran's I spatial cluster and outlier analysis (bottom

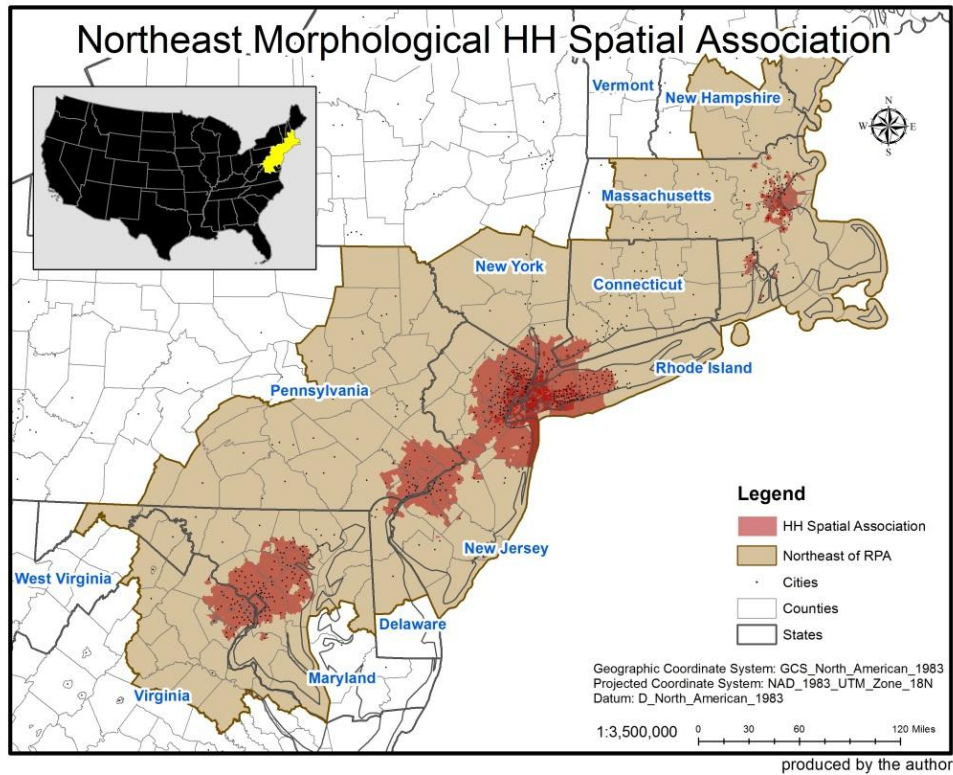
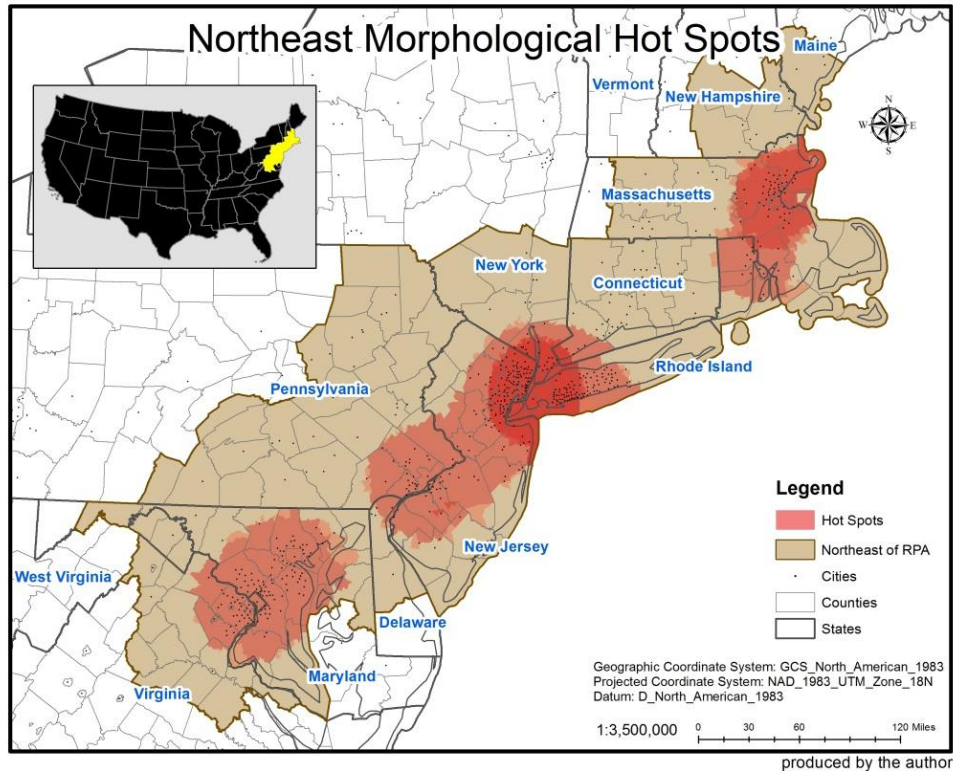


Figure 14 Local clusterings of morphological features in the Northeast megaregion

of figure). As the final representation for the Northeast megaregion morphological clustering, Figure 15 represents a result produced by overlapping the results separately represented in Figure 14. Table 12 summarizes the Northeast megaregion morphological clustering descriptors.

Representing polycentric morphological clustering for the Northeast megaregion, the clusterings around New York City, Philadelphia, Baltimore – Washington, DC, Providence, and Boston are highlighted, meaning that the cities and the surrounding areas have an excess of morphological characteristics such as population density, impervious land cover, and nighttime light emissions (see Figure 15). The clustering connection between New York City and Philadelphia represents a linear axis, meaning that the excess of morphological characteristics makes a connection between the two round shape clustering areas. The clustering around Providence and Boston, however, appears to be weakly connected compared to the strong clustering connection between New York City and Philadelphia even though Providence and Boston are located in a same clustering area. The Baltimore – Washington, DC clustering area is likely to become one region. The overlapping observation of every local clustering analysis result also shows that there is a disconnection between clustering areas. The disconnection between the clustering area around New York City – Philadelphia and the clustering area around Baltimore – Washington, DC seems to be weaker than the disconnection between the clustering area around New York City – Philadelphia and the clustering area around Boston – Providence. The observation additionally indicates that the morphological clustering boundary of the Northeast megaregion does not follow the

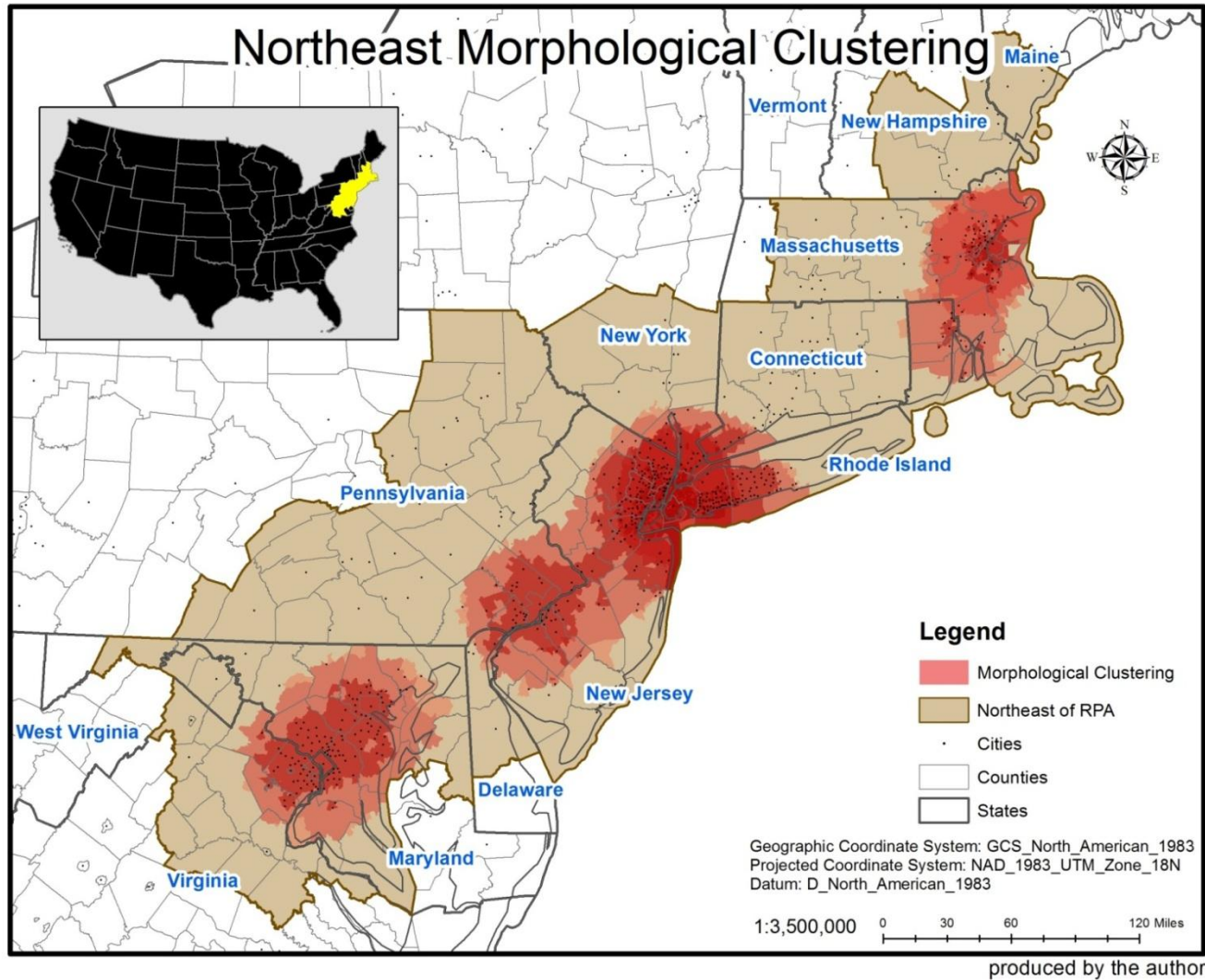


Figure 15 Morphological clusterings of the Northeast megaregion

Table 12 The Northeast megaregion morphological clusterings descriptors

Data Type	Clustering Area	Analysis	Northeast Morphological Clusterings Descriptors		
			Census Tract	Land Areas (sq. mi)	2000 Total Population
			11,697 (100%)	60,382.64 (100%)	49,481,012 (100%)
PopDen00	New York City	Hot Spot	3,699 (31.62%)	1,958.43 (3.24%)	14,701,831 (29.71%)
		HH Cluster	2,214 (18.93%)	219.67 (0.36%)	8,883,866 (17.95%)
	Clustering Total		3,699 (31.62%)	1,958.43 (3.24%)	14,701,831 (29.71%)
ImpS01	New York City	Hot Spot	3,731 (31.9%)	1,964.48 (3.25%)	14,851,774 (30.02%)
		HH Cluster	2,791 (23.86%)	626.31 (1.04%)	10,787,450 (21.80%)
	Boston - Providence	Hot Spot	1,067 (9.12%)	3,149.07 (5.22%)	5,031,679 (10.17%)
		HH Cluster*	395 (3.38%)	209.08 (0.35%)	1,700,800 (3.44%)
		HH Cluster**	130 (1.11%)	80.80 (0.13%)	541,013 (1.09%)
	Williamstown	Hot Spot	12 (0.1%)	62.76 (0.1%)	61,244 (0.12%)
		HH Cluster	n/a	n/a	n/a
	Subtotal	Hot Spot	4,810 (41.12%)	5,176.31 (8.57%)	19,944,697 (40.31%)
		HH Cluster	3,316 (28.35%)	916.19 (1.52%)	13,029,263 (26.33%)
Clustering Total		4,810 (41.12%)	5,176.31 (8.57%)	19,944,697 (40.31%)	
DMSP00	New York City - Philadelphia	Hot Spot	5,935 (50.74%)	8,704.55 (14.42%)	23,843,798 (48.19%)
		HH Cluster	5,431 (46.43%)	4,777.82 (7.91%)	21,734,518 (43.92%)
	Baltimore - Washington, DC	Hot Spot	1,521 (13%)	5,062.35 (8.38%)	6,734,985 (13.61%)
		HH Cluster	1,319 (11.28%)	2,119.18 (3.51%)	5,795,963 (11.71%)
	Boston	Hot Spot	839 (7.17%)	2,163.74 (3.58%)	4,012,932 (8.11%)
		HH Cluster	248 (2.12%)	186.15 (0.31%)	1,082,074 (2.19%)
	Subtotal	Hot Spot	8,295 (70.92%)	15,930.64 (26.38%)	34,591,715 (69.91%)
		HH Cluster	6,998 (59.83%)	7,083.14 (11.73%)	28,612,555 (57.83%)
Clustering Total		8,295 (70.92%)	15,930.64 (26.38%)	34,591,715 (69.91%)	
The Northeast Subtotal		Hot Spot	8,558 (73.16%)	17,191.49 (28.47%)	35,791,991 (72.33%)
		HH	7,356 (62.89%)	7,295.38 (12.08%)	30,166,764 (60.97%)
The Northeast Morphological Clusterings Total			8,558 (73.16%)	17,191.49 (28.47%)	35,791,991 (72.33%)

HH Cluster* - Clustering around Boston

HH Cluster** - Clustering around Providence

delineation of RPA. The total extent of Northeast clustering in terms of all morphological features analyzed thus far includes 8,558 census tracts being around 73.16% of the total Northeast census tracts; about 17,191.49 square miles equal approximately 28.47% of the total Northeast land area; and 35,791,991 total population being around 72.33% of the total population of the Northeast megaregion.

The Northeast morphological clustering map resulted finally represents the locations where high levels of land use per capita, urbanized built environment, and nighttime socio-economic urban activities are clustered. The clustering areas of New York City – Philadelphia and Baltimore – Washington, DC seem to have morphological connections being physically close. The clustering area of Boston – Providence, however, is not likely to be connected to other clustering areas because of its physically distant location. The final map also represents an exaggerated boundary for the Northeast megaregion in the morphological observation.

2.2. The Texas Triangle megaregion

1) Local clustering of 2000 population density

Figure 16 shows local clustering analysis results produced by using 2000 population density. Following the threshold of Density-based Sprawl Index, 2000 population density is categorized into three groups: rural areas population density (i.e., less than 200 persons per square mile), low population density areas (i.e., between 200 and 3,500 persons per square mile), and high population density areas (i.e., greater than 3,500 persons per square mile) (top left of figure). The general observation of the

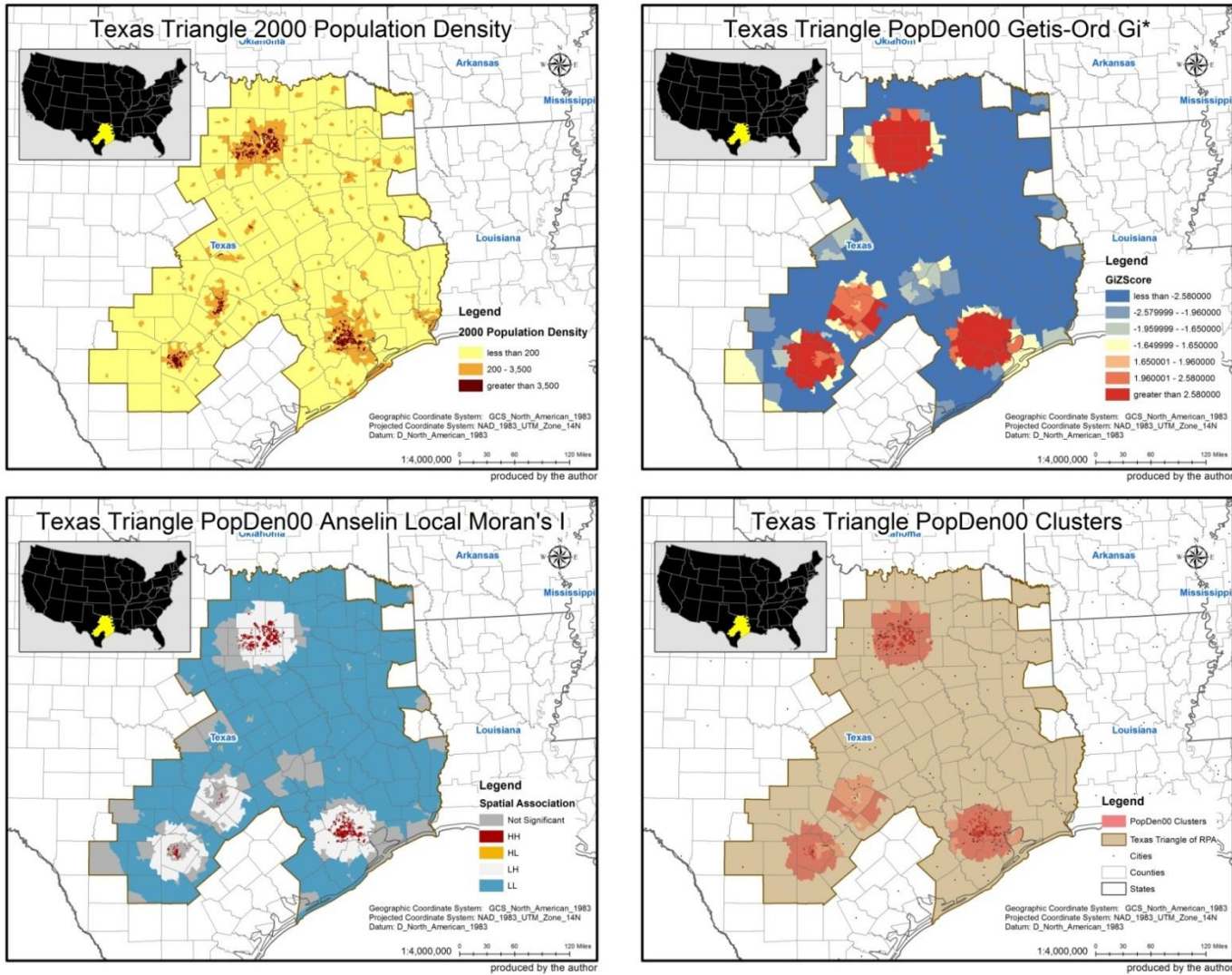


Figure 16 The Texas Triangle megaregion local clustering analysis results by 2000 population density

distribution of 2000 population density shows that the low population density areas represent such concentration areas in Dallas – Fort Worth, Houston, Austin, and San Antonio. High population density areas are centered for these low population density areas.

The statistically significant hot spots at the 0.05 alpha level, as a result of Getis-Ord G_i^* analysis in terms of 2000 population density, represent polycentric clustering (top right of figure). Hot Spots are spatially concentrated in the areas around Dallas – Fort Worth, Houston, Austin, and San Antonio. Table 13 shows hot spots descriptors of 2000 population density for Texas Triangle. The mean of 2000 population density for hot spot areas is around 4,011.49 in comparison with the mean value of approximately 3,078.04 for the Texas Triangle megaregion. Resulted hot spots, therefore, indicate that the levels of land use per capita are similarly high within the hot spot boundary.

Table 13 Texas Triangle 2000 population density hot spots descriptors

Clustering Areas	Census Tracts	Land Area (sq. mi)	2000 Total Population
	3,256 (100%)	82,981.12 (100%)	16,051,142 (100%)
Dallas – Fort Worth	897 (27.55%)	3,619.58 (4.36%)	4,454,617 (27.75%)
Houston	759 (23.31%)	3,288.93 (3.96%)	4,068,498 (25.35%)
San Antonio	300 (9.21%)	2,627.95 (3.17%)	1,516,626 (9.45%)
Austin	179 (5.5%)	2,290.51 (2.76%)	920,943 (5.74%)
Total	2,135 (65.57%)	11,826.96 (14.25%)	10,960,684 (68.29%)

The HH spatial associations, as a result of Anselin Local Moran's I analysis in terms of 2000 population density, also represent polycentric clustering in Dallas – Fort

Worth, Houston, Austin, and San Antonio (bottom left of figure). Compared to above hot spots analysis result, the clustering extents are smaller and clustering patterns are more fractal. Table 14 shows HH spatial associations descriptors of 2000 population density for Texas Triangle. The mean of 2000 population density for HH spatial associations is around 6,758.68 in comparison with the mean value of approximately 3,078.04 for the Texas Triangle megaregion. Resulted HH spatial associations, therefore, indicate that a high level of land use per capita is clustered with other similarly high levels of land use per capita within the resulted areas.

Table 14 Texas Triangle 2000 population density HH spatial associations descriptors

Clustering Areas	Census Tracts 3,256 (100%)	Land Area (sq. mi) 82,981.12 (100%)	2000 Total Population 16,051,142 (100%)
Dallas – Fort Worth	462 (14.19%)	408.93 (0.49%)	2,329,099 (14.51%)
Houston	351 (10.78%)	333.02 (0.4%)	2,023,745 (12.61%)
San Antonio	73 (2.24%)	59.01 (0.07%)	402,776 (2.51%)
Austin	28 (0.86%)	14.87 (0.02%)	139,169 (0.87%)
Total	914 (28.07%)	815.84 (0.98%)	4,894,789 (30.49%)

Morphological clustering, as a result of overlapping two analysis results in terms of 2000 population density, has the mostly same clustering boundary as Getis- Ord G_i^* analysis result (bottom right of figure). Only 8 census tracts resulted by HH spatial associations are not included in hot spots analysis result. Seven census tracts locate in central Austin and 1 census tract locates in western Fort Worth. The overlapping of the two clustering analysis results shows that the clustering pattern of 2000 population

density is polycentric around Dallas – Fort Worth, Houston, San Antonio, and Austin. The result of overlapping also shows that the concentration of 2000 population density clusters is located repeatedly in the central areas of Dallas – Fort Worth and Houston. Table 15 shows the total extent of 2000 population density clustering descriptors for Texas Triangle. The morphological clustering map represents, therefore, that the levels of land use per capita are similarly high and clustered within the clustering boundary. In terms of clustering by 2000 population density, the Texas Triangle megaregion identified by RPA seems to have an exaggerated boundary.

Table 15 Texas Triangle 2000 population density clustering descriptors

Clustering Total	Census Tracts	Land Area (sq. mi)	2000 Total Population
	3,256 (100%)	82,981.12 (100%)	16,051,142 (100%)
2000 population density	2,143 (65.82%)	11,830.81 (14.26%)	11,004,181 (68.56%)

2) Local clustering of 2001 impervious land cover

Figure 17 shows local clustering analysis results produced by using 2001 impervious land cover. The general observation of the distribution of 2001 impervious land cover is that the highest degree of imperviousness in 2001 was likely concentrated in areas where low and high population density areas are located (top left of figure). The highly impervious areas are most likely to be clustered around areas such as Dallas – Fort Worth, Houston, San Antonio, and Austin.

The statistically significant hot spots at the 0.05 alpha level, as a result of Getis-Ord G_i^* analysis in terms of 2001 impervious land cover, represent polycentric clustering

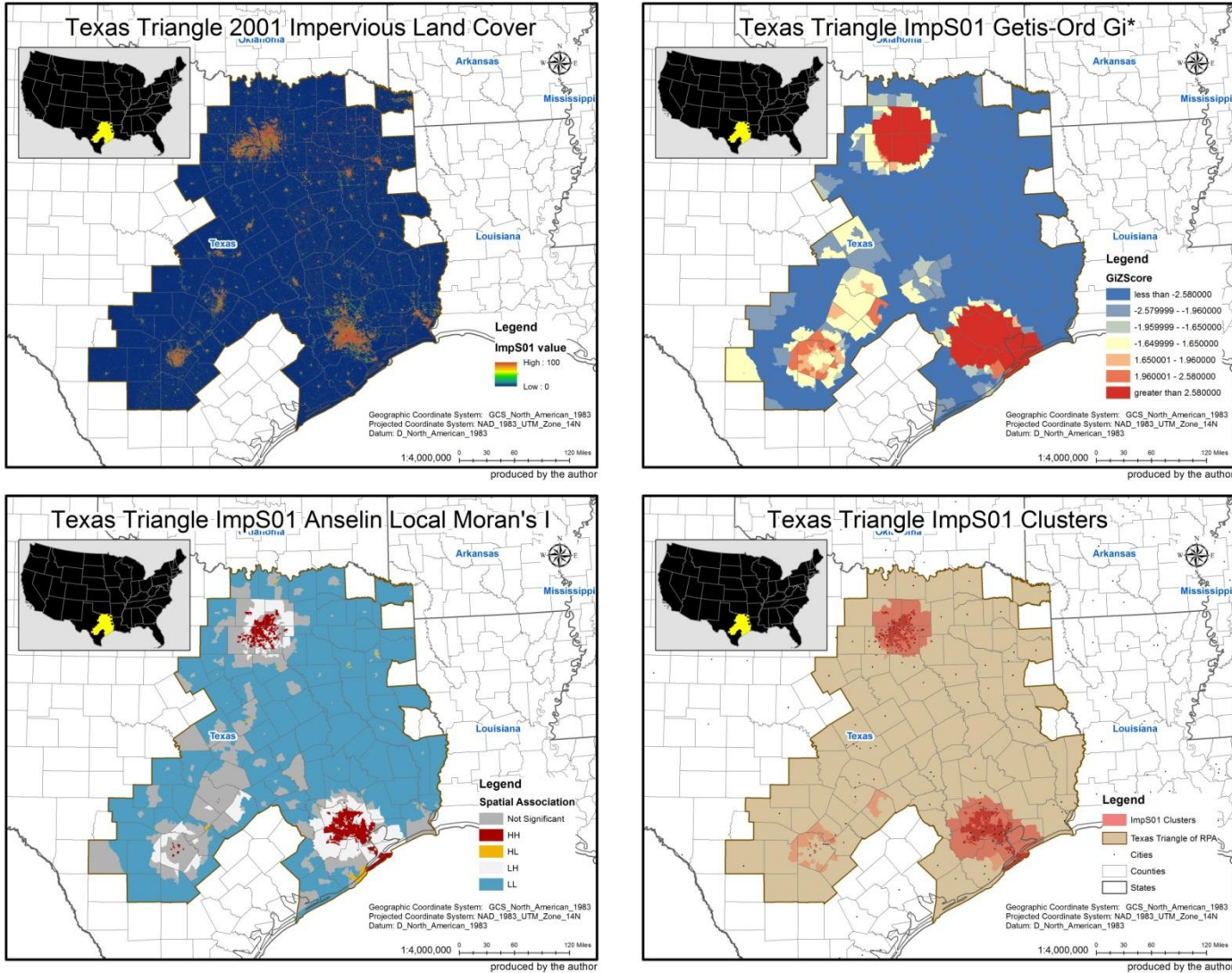


Figure 17 The Texas Triangle megaregion local clustering analysis results by 2001 impervious land cover

which consists of two large clusterings and two fragmented clustering pieces (top right of figure). Hot spots are spatially concentrated in the areas around Dallas – Fort Worth and Houston – Galveston, and the outskirts of San Antonio and Austin. Table 16 shows hot spots descriptors of 2001 impervious land cover for Texas Triangle. The mean of 2001 impervious land cover for hot spot areas is around 54.49% in comparison with the mean value of approximately 28.1% for the Texas Triangle megaregion. Resulted hot spots, therefore, indicate that the urbanization levels of built environments are similarly high within the hot spot boundary.

Table 16 Texas Triangle 2001 impervious land cover hot spots descriptors

Clustering Areas	Census Tracts	Land Area (sq. mi)	2000 Total Population
		3,256 (100%)	82,981.12 (100%)
Dallas – Fort Worth	829 (25.46%)	3,000.81 (3.62%)	4,157,065 (25.9%)
Houston – Galveston	817 (25.09%)	4,402.25 (5.31%)	4,310,989 (26.86%)
San Antonio	38 (1.17%)	1,039.35 (1.25%)	191,943 (1.2%)
Austin	3 (0.09%)	292.82 (0.36%)	20,920 (0.13%)
Total	1,687 (51.81%)	8,742.23 (10.54%)	8,680,917 (54.08%)

The HH spatial association, as a result of Anselin Local Moran's *I* analysis in terms of 2001 impervious land cover, represents polycentric clustering located in the areas around Dallas – Fort Worth and Houston – Galveston (bottom left of figure). The HH spatial associations located around Austin and San Antonio appears tiny dots. Table 17 shows HH spatial associations descriptors of 2001 impervious land cover for Texas Triangle. The mean of 2001 impervious land cover for HH spatial associations is around

61.99% in comparison with the mean value of approximately 28.1% for the Texas Triangle megaregion. Resulted HH spatial associations, therefore, indicate that a high level of urbanization for built environments is clustered with other similarly highly urbanized built environments within the resulted areas.

Table 17 Texas Triangle 2001 impervious land cover HH spatial associations descriptors

Clustering Areas	Census Tracts	Land Area (sq. mi)	2000 Total Population
		3,256 (100%)	82,981.12 (100%)
Dallas – Fort Worth	344 (10.57%)	671.17 (0.81%)	1,687,813 (10.52%)
Houston – Galveston	589 (18.09%)	1,149.45 (1.39%)	3,119,366 (19.43%)
San Antonio	25 (0.77%)	32.79 (0.04%)	78,817 (0.49%)
Austin	4 (0.12%)	2.55 (0.003%)	12,041 (0.08%)
Total	962 (29.55%)	1,855.97 (2.24%)	4,898,037 (30.52%)

Morphological clustering, as a result of overlapping two analysis results in terms of 2001 impervious land cover, has the similar clustering boundary with Getis-Ord G_i^* analysis result (bottom right of figure). The areas around Austin and San Antonio are not likely to be clustered compared to the areas around Dallas – Fort Worth and Houston – Galveston. The central Dallas – Fort Worth areas are highlighted again by 2001 impervious land cover, representing a core of clustering. The clustering areas around Houston – Galveston also bridge the central areas of two cities. Table 18 shows the total extent of 2001 impervious land cover clustering descriptors for Texas Triangle. The morphological clustering map represents, therefore, that the urbanization levels of these

built environments are similarly high and clustered within the clustering boundary. In terms of the clustering by 2001 impervious land cover, the Texas Triangle megaregion identified by RPA seems to have an exaggerated boundary.

Table 18 Texas Triangle 2001 impervious land cover clustering descriptors

Clustering Total	Census Tracts	Land Area (sq. mi)	2000 Total Population
	3,256 (100%)	82,981.12 (100%)	16,051,142 (100%)
2001 impervious land cover	1,720 (52.83%)	8,779.46 (10.58%)	8,770,967 (54.64%)

3) Local clustering of 2000 nighttime light emissions (DMSP-OLS)

Figure 18 shows local clustering analysis results produced by using 2000 nighttime light emissions (DMSP-OLS). The general observation of the distribution of 2000 nighttime light emissions is that the highest degree of nighttime light emissions in 2000 is likely to be clustered around Dallas – Fort Worth and Houston – Galveston (top left of figure). It is noticeable for the clustering and interconnection between the areas around San Antonio and Austin.

The statistically significant hot spots at the 0.05 alpha level, as a result of Getis-Ord G_i^* analysis in terms of 2000 nighttime light emissions, represent polycentric clustering (top right of figure). They are spatially concentrated in the areas around Dallas – Fort Worth, Houston – Galveston, San Antonio, and Georgetown – San Marcos across Austin. Table 19 shows hot spots descriptors of 2000 nighttime light emissions for Texas Triangle. The mean of 2000 nighttime light emissions for hot spot areas is around 59.51% in comparison with the mean value of approximately 50.3% for the Texas Triangle

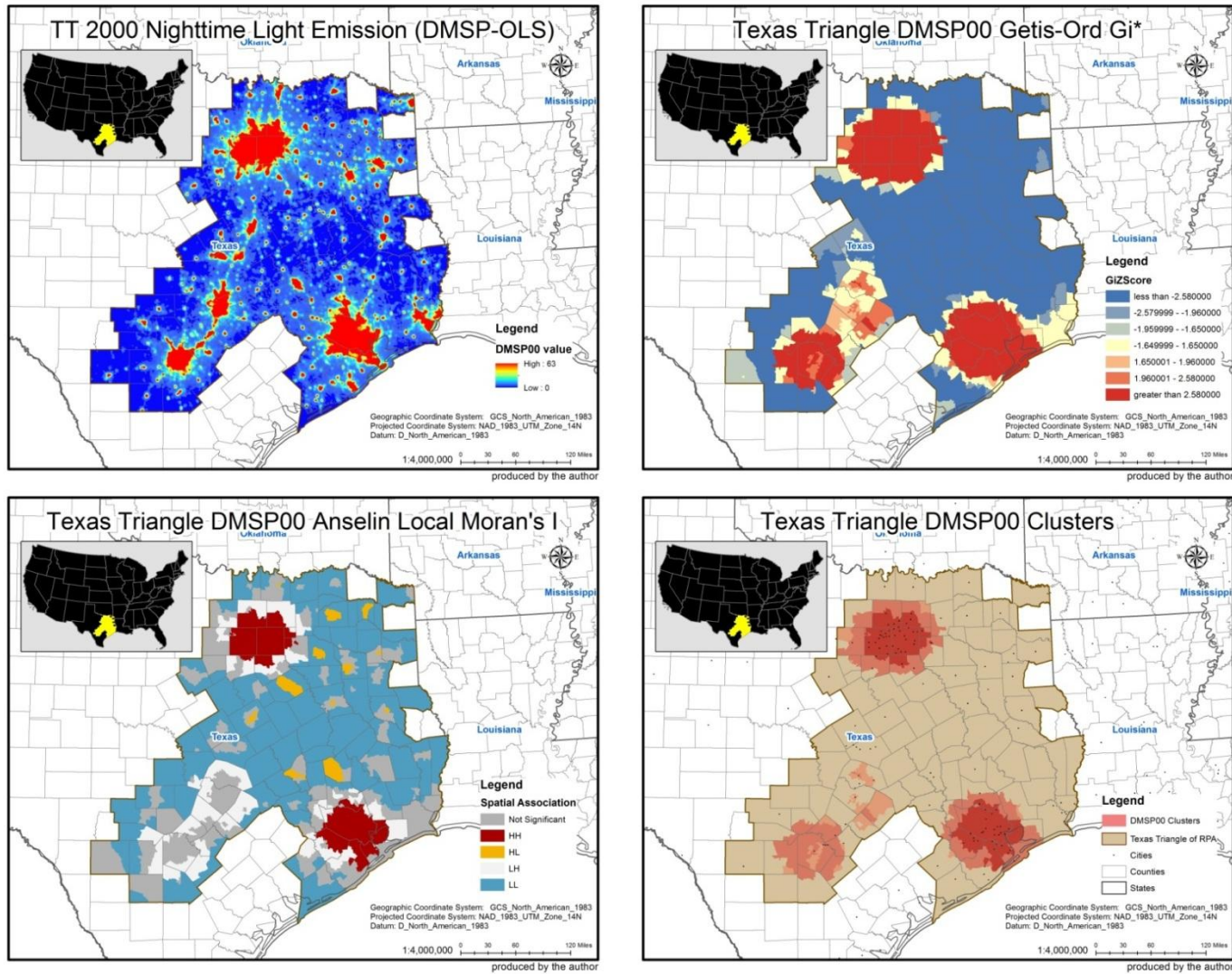


Figure 18 The Texas Triangle megaregion local clustering analysis results by 2000 nighttime light emissions

megaregion. Resulted hot spots, therefore, indicate that the urban development levels caused by nighttime socio-economic activities are similarly high within the hot spot boundary.

Table 19 Texas Triangle 2000 nighttime light emissions hot spots descriptors

Clustering Areas	Census Tracts	Land Area (sq. mi)	2000 Total Population
		3,256 (100%)	82,981.12 (100%)
Dallas – Fort Worth	1,019 (31.3%)	6,731.23 (8.11%)	5,051,971 (31.47%)
Houston – Galveston	847 (26.01%)	5,631.33 (6.79%)	4,470,687 (27.85%)
San Antonio	320 (9.83%)	3,783.54 (4.56%)	1,625,634 (10.13%)
Georgetown – San Marcos	72 (2.21%)	1,384.42 (1.67%)	343,065 (2.14%)
Total	2,258 (69.35%)	17,530.52 (21.13%)	11,491,355 (71.59%)

The HH spatial association, as a result of Anselin Local Moran's *I* analysis in terms of 2000 nighttime light emissions, represents dual-centric clustering located in the areas around Dallas – Fort Worth and Houston – Galveston, excluding San Antonio and Austin from the hot spots analysis result (bottom left of figure). Table 20 shows HH spatial associations descriptors of 2000 nighttime light emissions for Texas Triangle. The mean of 2000 nighttime light emissions for HH spatial associations is around 62.47% in comparison with the mean value of approximately 50.3% for the Texas Triangle megaregion. Resulted HH spatial associations, therefore, indicate that a high level of urban development caused by nighttime socio-economic activities is clustered with other similarly high levels of nighttime socio-economic urban activities within the resulted areas.

Table 20 Texas Triangle 2000 nighttime light emissions HH spatial associations descriptors

Clustering Areas	Census Tracts	Land Area (sq. mi)	2000 Total Population
		3,256 (100%)	82,981.12 (100%)
Dallas – Fort Worth	950 (29.18%)	2,931 (3.53%)	4,644,402 (28.94%)
Houston – Galveston	775 (23.8%)	2,882.66 (3.47%)	4,127,283 (25.71%)
Total	1,725 (52.98%)	5,813.66 (7.01%)	8,771,685 (54.65%)

Morphological clustering, as a result of overlapping two analysis results in terms of 2000 nighttime light emissions, has the same clustering boundary as Getis-Ord G_i^* analysis result (bottom right of figure). The extent of 2000 nighttime light emissions clustering of the Texas Triangle megaregion, therefore, is identical to the extent of hot spot clustering. The overlapping of the two clustering analysis results shows that the clustering pattern of 2000 nighttime light emissions has two large clustering areas around Dallas – Fort Worth and Houston – Galveston. Central areas of the clusterings are resulted to be morphologically clustered by the two spatial pattern analysis tools. The clustering areas around San Antonio and Georgetown – San Marcos, however, are resulted to be morphologically clustered only by the hot spots analysis tool. The morphological clustering map shows that the levels of urban development caused by nighttime socio-economic activities are similarly high and clustered within the clustering boundary. In terms of the clustering by 2000 nighttime light emissions, the Texas Triangle megaregion identified by RPA seems to have an exaggerated boundary.

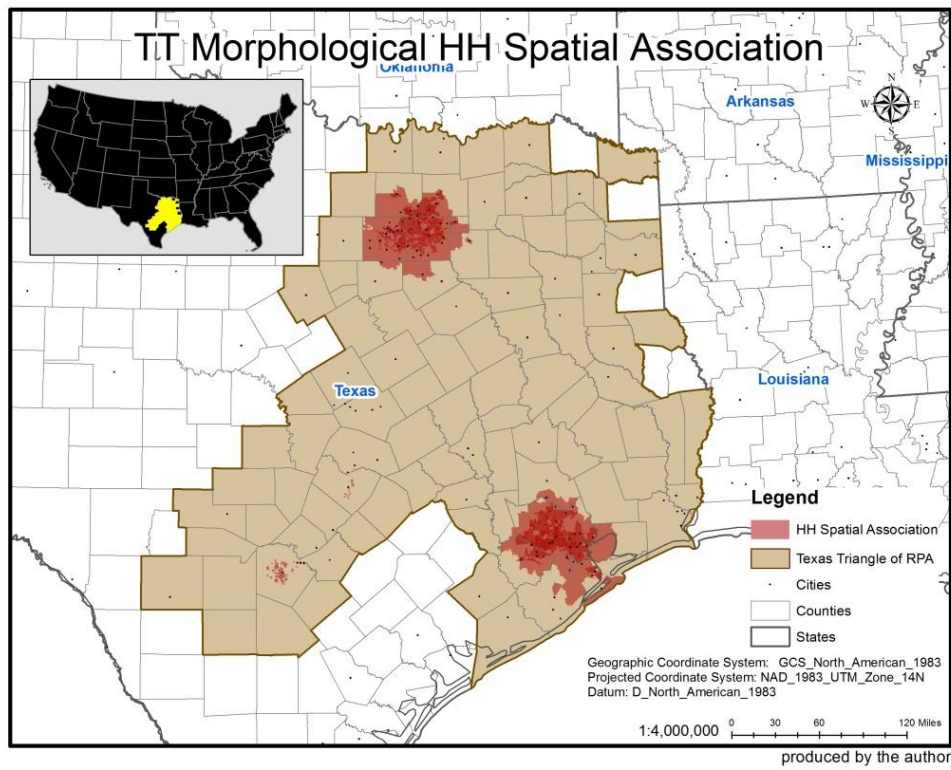
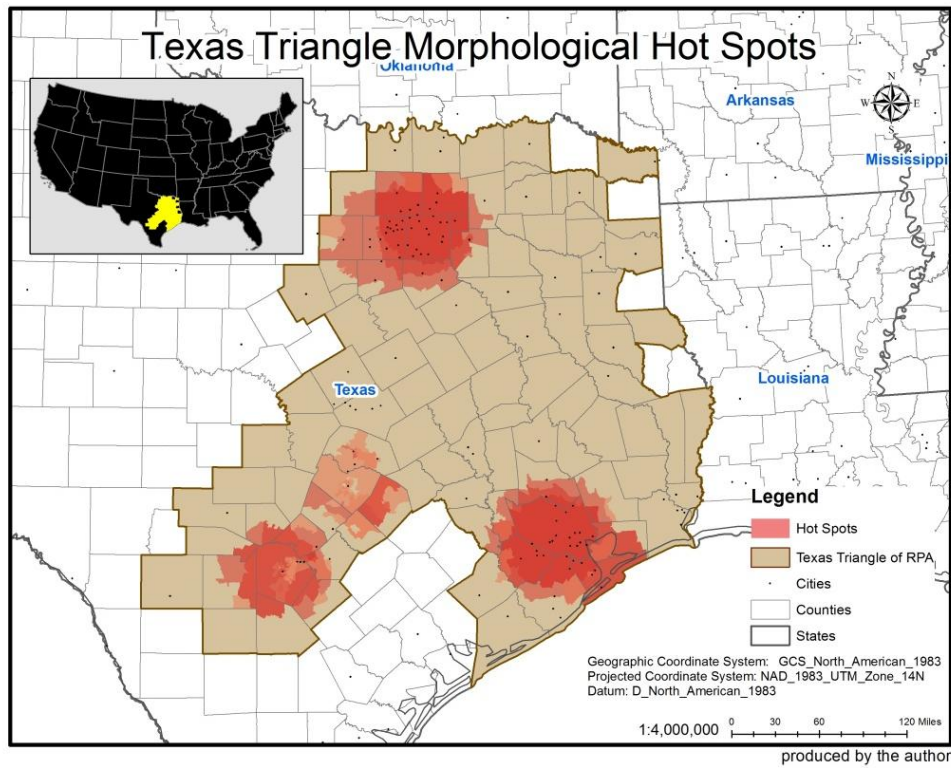


Figure 19 Local clusterings of morphological features in the Texas Triangle megaregion

4) Morphological local clustering

Figure 19 represents results only produced by overlapping every clustering of the Getis-Ord G_i^* hot spots analysis (top of figure) and only by overlapping every HH spatial cluster of the Anselin Local Moran's I spatial cluster and outlier analysis (bottom of figure). As the final representation for Texas Triangle megaregion morphological clustering, Figure 20 represents a result produced by overlapping the results separately represented in Figure 19. Table 21 summarizes the Texas Triangle megaregion morphological clustering descriptors.

Representing polycentric morphological clustering for the Texas Triangle megaregion, the clustering around Dallas – Fort Worth, Houston – Galveston, San Antonio are highlighted, meaning that the cities and the surrounding areas have an excess of morphological characteristics such as population density, impervious land cover, and nighttime light emissions (see Figure 20). The clustering areas around Dallas – Fort Worth and Houston – Galveston appear to become clustering cores, meaning that an excess of morphological characteristics are more concentrated in the areas. The clustering areas around Austin seem to be weakly clustered than other clustering areas. The attachment of the Austin clustering areas to the San Antonio clustering areas is more likely to happen than separating the two morphological clusters apart. Concerning the megaregion boundary of RPA, in terms of morphological clustering, the Texas Triangle megaregion seems to be problematic to consider morphological interconnections or integrations within the regional boundary. The total extent of Texas Triangle clustering in terms of all morphological features analyzed thus far includes 2,395 census tracts

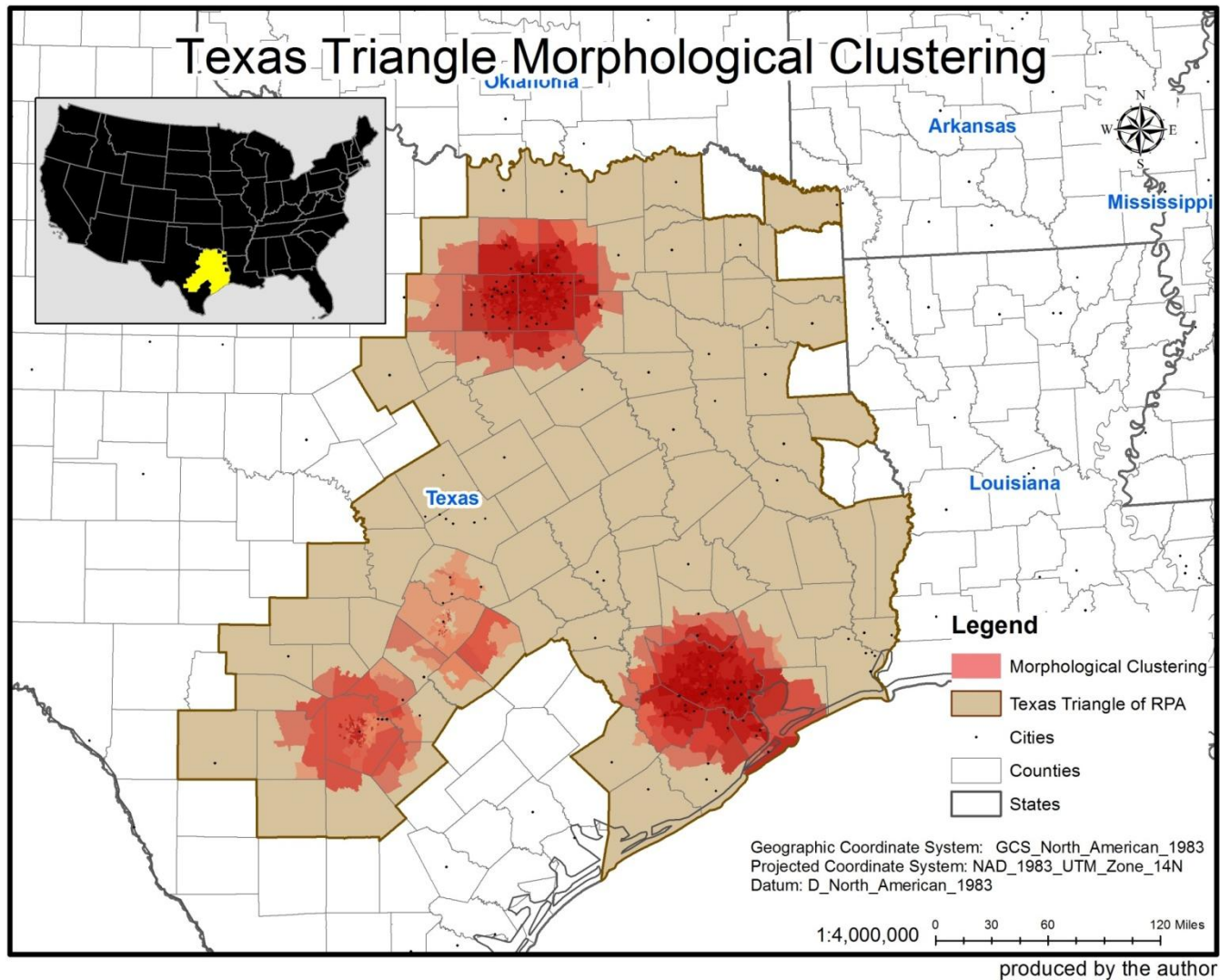


Figure 20 Morphological clusterings of the Texas Triangle megaregion

Table 21 The Texas Triangle megaregion morphological clusterings descriptors

Data Type	Clustering Area	Analysis	Texas Triangle Morphological Clusterings Descriptors		
			Census Tracts	Land Areas (sq. mi)	2000 Total Population
			3,256 (100%)	82,981.12 (100%)	16,051,142 (100%)
PopDen00	Dallas - Fort Worth	Hot Spot	897 (27.55%)	3,619.58 (4.36%)	4,454,617 (27.75%)
		HH Cluster	462 (14.19%)	408.93 (0.49%)	2,329,099 (14.51%)
	Houston	Hot Spot	759 (23.31%)	3,288.93 (3.96%)	4,068,498 (25.35%)
		HH Cluster	351 (10.78%)	333.02 (0.4%)	2,023,745 (12.61%)
	San Antonio	Hot Spot	300 (9.21%)	2,627.95 (3.17%)	1,516,626 (9.45%)
		HH Cluster	73 (2.24%)	59.01 (0.07%)	402,776 (2.51%)
	Austin	Hot Spot	179 (5.5%)	2,290.51 (2.76%)	920,943 (5.74%)
		HH Cluster	28 (0.86%)	14.87 (0.02%)	139,169 (0.87%)
	Subtotal	Hot Spot	2,135 (65.57%)	11,826.96 (14.25%)	10,960,684 (68.29%)
		HH Cluster	914 (28.07%)	815.84 (0.98%)	4,894,789 (30.49%)
Clustering Total			2,143 (65.82%)	11,830.81 (14.26%)	11,004,181 (68.56%)
ImpS01	Dallas - Fort Worth	Hot Spot	829 (25.46%)	3,000.81 (3.62%)	4,157,065 (25.90%)
		HH Cluster	344 (10.57%)	671.17 (0.81%)	1,687,813 (10.52%)
	Houston - Galveston	Hot Spot	817 (25.09%)	4,402.25 (5.31%)	4,310,989 (26.86%)
		HH Cluster	589 (18.09%)	1,149.45 (1.39%)	3,119,366 (19.43%)
	San Antonio	Hot Spot	38 (1.17%)	1,039.35 (1.25%)	191,943 (1.20%)
		HH Cluster	25 (0.77%)	32.79 (0.04%)	78,817 (0.49%)
	Austin	Hot Spot	3 (0.09%)	299.82 (0.36%)	20,920 (0.13%)
		HH Cluster	4 (0.12%)	2.55 (0.003%)	12,041 (0.08%)
	Subtotal	Hot Spot	1,687 (51.81%)	8,742.23 (10.54%)	8,680,917 (54.08%)
		HH Cluster	962 (29.55%)	1,855.97 (2.24%)	4,898,037 (30.52%)
Clustering Total			1,720 (52.83%)	8,779.46 (10.58%)	8,770,967 (54.64%)

Table 21 continued.

DMSP00	Dallas - Fort Worth	Hot Spot	1,019 (31.3%)	6,731.23 (8.11%)	5,051,971 (31.47%)
		HH Cluster	950 (29.18%)	2,931.00 (3.53%)	4,644,402 (28.94%)
	Houston - Galveston	Hot Spot	847 (26.01%)	5,631.33 (6.79%)	4,470,685 (27.85%)
		HH Cluster	775 (23.8%)	2,882.66 (3.47%)	4,127,283 (25.71%)
	San Antonio	Hot Spot	320 (9.83%)	3,783.54 (4.56%)	1,625,634 (10.13%)
		HH Cluster	n/a	n/a	n/a
	Georgetown - San Marcos	Hot Spot	72 (2.21%)	1,384.42 (1.67%)	343,065 (2.14%)
		HH Cluster	n/a	n/a	n/a
	Subtotal	Hot Spot	2,258 (69.35%)	17,530.52 (21.13%)	11,491,355 (71.59%)
		HH Cluster	1,725 (52.98%)	5,813.66 (7.01%)	8,771,685 (54.65%)
Clustering Total			2,258 (69.35%)	17,530.52 (21.13%)	11,491,355 (71.59%)
The Texas Triangle Subtotal		Hot Spot	2,393 (73.50%)	18,854.42 (22.72%)	12,190,191 (75.95%)
		HH Cluster	1,862 (57.19%)	5,945.00 (7.16%)	9,416,651 (58.67%)
The Texas Triangle Morphological Clusterings Total			2,395 (73.56%)	18,855.64 (22.72%)	12,199,780 (76.01%)

being around 73.56% of the total Texas Triangle census tracts; about 18,855.64 square miles equal approximately 22.72% of the total Texas Triangle land area; and 12,199,780 total population being around 76.01% of the total population of the Texas Triangle megaregion.

The Texas Triangle morphological clustering map resulted finally represents the locations where high levels of land uses per capita, urbanized built environment, and nighttime socio-economic urban activities are clustered. The clustering areas of Austin and San Antonio seem to have morphological connections being physically close. The clustering areas of Dallas – Fort Worth and Houston – Galveston seem to be difficult to consider morphological connections to other clustering areas because of their physically distant locations. The final map also represents an exaggerated boundary for the Texas Triangle megaregion in the morphological observation.

2.3. The Great Lakes megaregion

1) Local clustering of 2000 population density

Figure 21 shows local clustering analysis results produced by using 2000 population density. Following the threshold of Density-based Sprawl Index, 2000 population density is categorized into three groups: rural areas population density (i.e., less than 200 persons per square mile), low population density areas (i.e., between 200 and 3,500 persons per square mile), and high population density areas (i.e., greater than 3,500 persons per square mile) (top left of figure). The general observation of the distribution of 2000 population density shows that the low population density areas

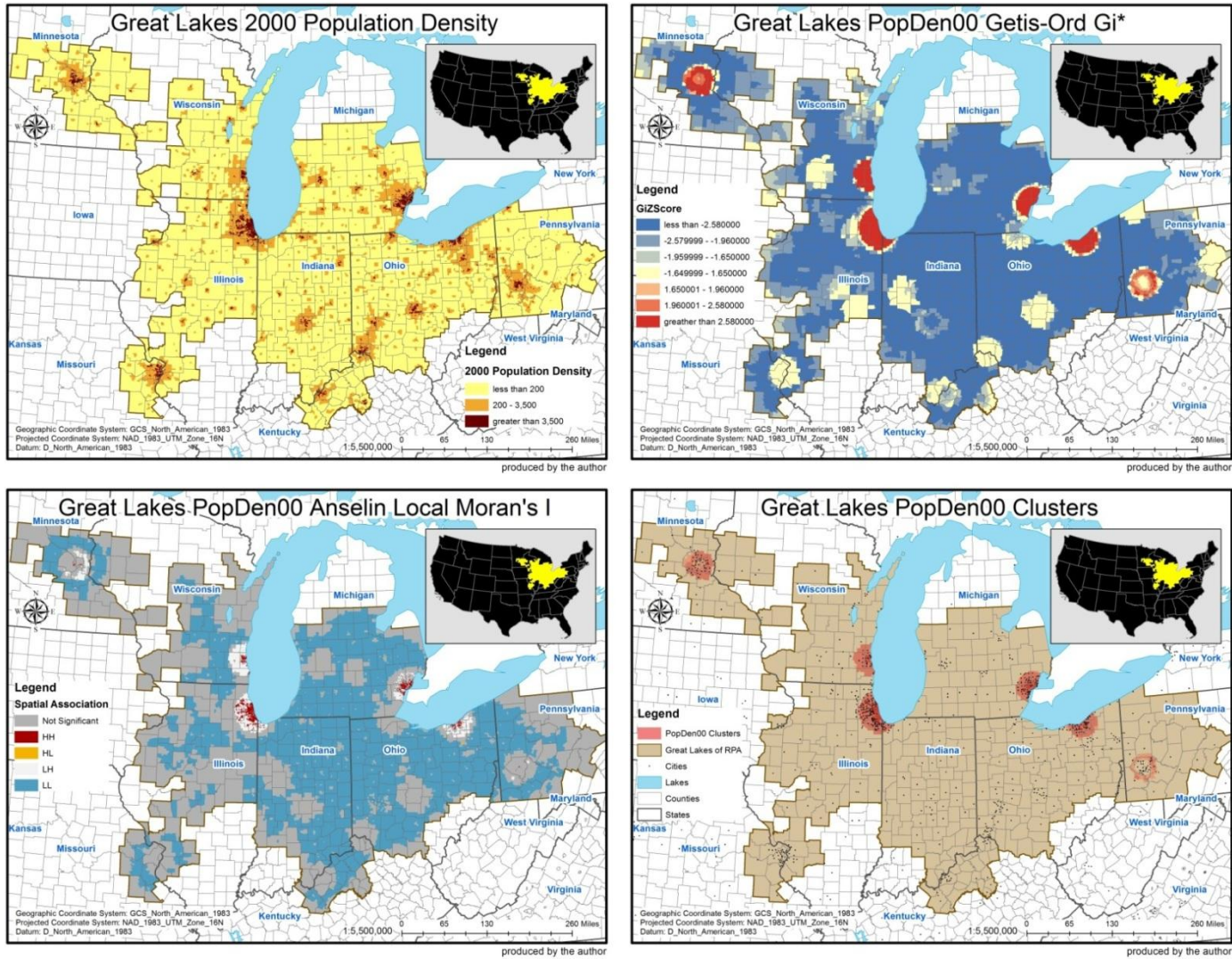


Figure 21 The Great Lakes megaregion local clustering analysis results by 2000 population density

represent such concentration areas in Milwaukee – Chicago including Wisconsin, Illinois, and Indiana; Detroit – Michigan including Michigan and Ohio; Cleveland, Ohio; Pittsburgh, Pennsylvania; Minneapolis, Minnesota; St. Louis including Missouri and Illinois, Indianapolis, Indiana; Louisville, Kentucky; Cincinnati, Ohio; and Columbus, Ohio. High population density areas are centered for these low population density areas.

Table 22 Great Lakes 2000 population density hot spots descriptors

Clustering Areas	Census Tracts	Land Area (sq. mi)	2000 Total Population
	13,394 (100%)	201,369.09 (100%)	53,700,872 (100%)
Chicago	1,672 (12.48%)	1,767.32 (0.88%)	7,059,248 (13.15%)
Detroit	1,037 (7.74%)	1,104.5 (0.55%)	3,542,523 (6.6%)
Cleveland	607 (4.53%)	1,059.1 (0.53%)	1,850,228 (3.45%)
Minneapolis	596 (4.45%)	1,396.52 (0.69%)	2,333,222 (4.34%)
Milwaukee	421 (3.14%)	1,061.66 (0.53%)	1,499,630 (2.79%)
Pittsburgh	137 (1.02%)	866.9 (0.43%)	510,189 (0.95%)
Total	4,470 (33.37%)	7,256.01 (3.6%)	16,795,040 (31.28%)

The statistically significant hot spots at the 0.05 alpha level, as a result of Getis-Ord G_i^* analysis in terms of 2000 population density, represent polycentric clustering (top right of figure). Hot Spots are spatially concentrated in the areas around Chicago including Illinois and Indiana, Detroit, Michigan, Cleveland, Ohio, Minneapolis, Minnesota, Milwaukee, Wisconsin, and the outskirts of Pittsburgh, Pennsylvania. Table 22 shows hot spots descriptors of 2000 population density for Great Lakes. The mean of 2000 population density for hot spot areas is around 7,431.01 in comparison with the

mean value of approximately 4,019.19 for the Great Lakes megaregion. Resulted hot spots, therefore, indicate that the levels of land use per capita are similarly high within the hot spot boundary.

Table 23 Great Lakes 2000 population density HH spatial associations descriptors

Clustering Areas	Census Tracts	Land Area (sq. mi)	2000 Total Population
		13,394 (100%)	201,369.09 (100%)
Chicago	1,185 (8.85%)	489.64 (0.24%)	4,841,563 (9.02%)
Detroit	395 (2.95%)	178.02 (0.09%)	1,406,203 (2.62%)
Cleveland	216 (1.61%)	67.16 (0.03%)	613,426 (1.14%)
Minneapolis	62 (0.46%)	17.23 (0.01%)	215,398 (0.4%)
Milwaukee	216 (1.61%)	70.23 (0.03%)	633,560 (1.18%)
Pittsburgh	32 (0.24%)	5.37 (0.003%)	79,801 (0.15%)
Total	2,106 (15.72%)	827.65 (0.41%)	7,789,951 (14.51%)

The HH spatial association, as a result of Anselin Local Moran's *I* analysis in terms of 2000 population density, represents also polycentric clustering around Chicago, Detroit, Cleveland, Milwaukee, Minneapolis, and Pittsburgh (bottom left of figure). The clustering boundary is smaller and clustering pattern is more fragmented compared with above hot spots analysis result by 2000 population density. Table 23 shows HH spatial associations descriptors of 2000 population density for Texas Triangle. The mean of 2000 population density for HH spatial associations is around 12,837.5 in comparison with the mean value of approximately 4,019.19 for the Great Lakes megaregion. Resulted HH spatial associations, therefore, indicate that a high level of land use per

capita is clustered with other similarly high levels of land use per capita within the resulted areas.

Morphological clustering, as a result of overlapping two analysis results in terms of 2000 population density, has the mostly same clustering boundary as the Getis- Ord G_i^* analysis result (bottom right of the figure). 42 census tracts resulted by HH spatial associations are not included in hot spots analysis result. The 42 census tracts are located in the area around Pittsburgh and Minneapolis. The overlapping of the two clustering analysis results shows that the clustering pattern of 2000 population density is polycentric around Chicago, Detroit, Cleveland, Minneapolis, Milwaukee, and Pittsburgh. The result of overlapping also shows that the concentration of 2000 population density clusters is located repeatedly in the central city areas. Table 24 shows the total extent of 2000 population density clustering descriptors for Great Lakes. The morphological clustering map represents, therefore, that the levels of land use per capita are similarly high and clustered within the clustering boundary. In terms of the clustering by 2000 population density, the Great Lakes megaregion identified by RPA seems to have an exaggerated boundary.

Table 24 Great Lakes 2000 population density clustering descriptors

Clustering Total	Census Tracts	Land Area (sq. mi)	2000 Total Population
		13,394 (100%)	201,369.09 (100%)
2000 population density	4,512 (33.69%)	7,263.68 (3.61%)	16,913,035 (31.49%)

2) Local clustering of 2001 impervious land cover

Figure 22 shows local clustering analysis results produced by using 2001 impervious land cover. The general observation of the distribution of 2001 impervious land cover is that the highest degree of imperviousness in 2001 was likely concentrated in areas where low and high population density areas are located (top left of figure). The highly impervious areas are most likely to be clustered around areas such as Milwaukee – Chicago including Wisconsin, Illinois, and Indiana; Detroit – Oregon including Michigan and Ohio; Cleveland, Ohio; Pittsburgh, Maryland; Minneapolis, Minnesota; St. Louis including Missouri and Illinois, Indianapolis, Indiana; Louisville, Kentucky; Cincinnati, Ohio; and Columbus, Ohio.

The statistically significant hot spots at the 0.05 alpha level, as a result of Getis-Ord G_i^* analysis in terms of 2001 impervious land cover, represent polycentric clustering (top right of figure). Hot spots are spatially concentrated in the areas around Chicago – Milwaukee, Detroit, Pittsburgh, Minneapolis, and the outskirts of Lancaster, Ohio. The clustering around Cleveland is excluded in the result by 2001 impervious land cover compared to the result by 2000 population density. Table 25 shows hot spots descriptors of 2001 impervious land cover for Great Lakes. The mean of 2001 impervious land cover is around 53.74% in comparison with the mean value of approximately 29.38% for the Great Lakes megaregion. Resulted hot spots areas, therefore, indicate that the urbanization levels of built environments are similarly high within the hot spot boundary.

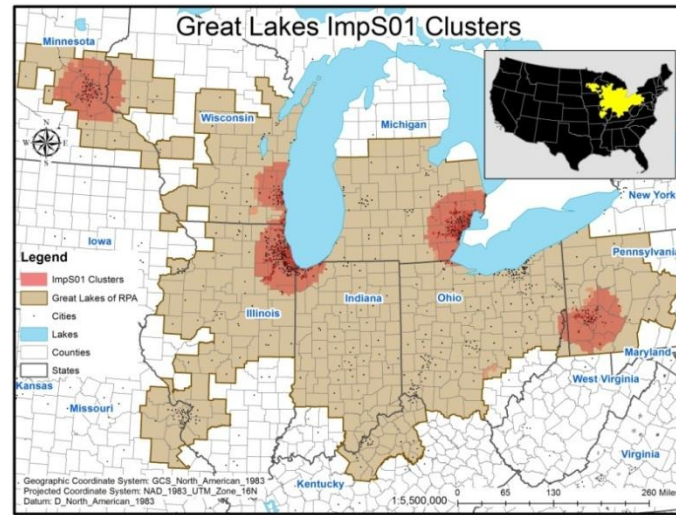
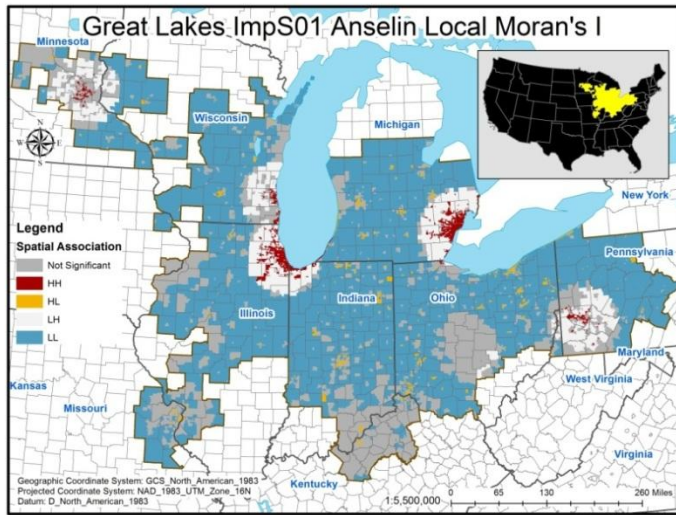
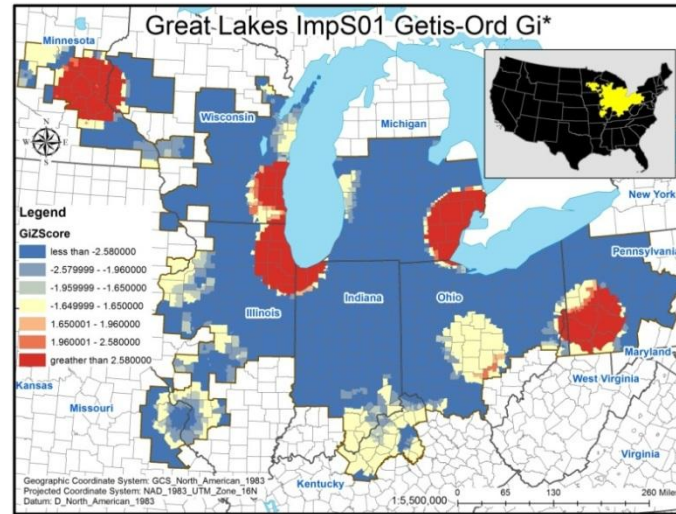


Figure 22 The Great Lakes megaregion local clustering analysis results by 2001 impervious land cover

Table 25 Great Lakes 2001 impervious land cover hot spots descriptors

Clustering Areas	Census Tracts	Land Area (sq. mi)	2000 Total Population
		13,394 (100%)	201,369.09 (100%)
Chicago – Milwaukee	2,497 (18.64%)	7,507.24 (3.73%)	10,683,679 (19.89%)
Detroit	1,470 (10.98%)	4,790.46 (2.38%)	5,093,154 (9.48%)
Minneapolis	748 (5.58%)	5,911.66 (2.94%)	2,998,313 (5.58%)
Pittsburgh	714 (5.33%)	5,160.58 (2.56%)	5,093,154 (9.48%)
Lancaster	4 (0.03%)	192.74 (0.1%)	16,138 (0.03%)
Total	5,433 (40.56%)	23,562.68 (11.7%)	21,207,111 (39.49%)

The HH spatial association, as a result of Anselin Local Moran's *I* analysis in terms of 2001 impervious land cover, represents polycentric clustering located in the areas around Chicago – Milwaukee, Detroit, Cleveland, and Minneapolis (bottom left of figure). Even though the central area of Lancaster also has HH spatial association in terms of 2001 impervious land cover, the clustering only includes 1 census tract. Table 26 shows HH spatial associations descriptors of 2001 impervious land cover for Great Lakes. The mean of 2001 impervious land cover is around 62.88% in comparison with the mean value of approximately 29.38% for the Great Lakes megaregion. Resulted HH spatial associations, therefore, indicate that a high level of urbanization for built environments is clustered with other similarly highly urbanized built environments within the resulted areas.

Table 26 Great Lakes 2001 impervious land cover HH spatial associations descriptors

Clustering Areas	Census Tracts	Land Area (sq. mi)	2000 Total Population
		13,394 (100%)	201,369.09 (100%)
Chicago – Milwaukee	1,484 (11.08%)	1,170.74 (0.58%)	5,534,058 (10.31%)
Detroit	933 (6.97%)	910.53 (0.45%)	3,129,305 (5.83%)
Minneapolis	158 (1.18%)	182.33 (0.09%)	517,075 (0.96%)
Pittsburgh	246 (1.84%)	222.69 (0.11%)	656,569 (1.22%)
Lancaster	1 (0.01%)	0.82 (0.0004%)	3,072 (0.01%)
Total	2,822 (21.07%)	2,487.11 (1.24%)	9,840,079 (18.32%)

Table 27 Great Lakes 2001 impervious land cover clustering descriptors

Clustering Total	Census Tracts	Land Area (sq. mi)	2000 Total Population
		13,394 (100%)	201,369.09 (100%)
2001 impervious land cover	5,444 (40.65%)	23,576.6 (11.71%)	21,234,715 (39.54%)

Morphological clustering, as a result of overlapping two analysis results in terms of 2001 impervious land cover, has the similar clustering boundary with Getis-Ord G_i^* analysis result (bottom right of figure). The overlapping shows that central areas of Chicago and Detroit appear to become morphological cores. The clustering around Minneapolis, Milwaukee, and Pittsburgh also show fragmented core areas. Table 27 shows the total extent of 2001 impervious land cover clustering descriptors for Great Lakes. The morphological clustering map represents, therefore, that the urbanization levels of these built environments are similarly high and clustered within the clustering

boundary. In terms of the clustering by 2001 impervious land cover, the Great Lakes megaregion identified by RPA seems to have an exaggerated boundary.

3) Local clustering of 2000 nighttime light emissions (DMSP-OLS)

Figure 23 shows local clustering analysis results produced by using 2000 nighttime light emissions (DMSP-OLS). The general observation of the distribution of 2000 nighttime light emissions is that the highest degree of nighttime light emissions in 2000 follows both distributions of 2000 population density and 2001 impervious land cover (top left of figure).

The statistically significant hot spots at the 0.05 alpha level, as a result of Getis-Ord G_i^* analysis in terms of 2000 nighttime light emissions, represent polycentric clustering (top right of figure). Hot spots are spatially concentrated in areas around Chicago – Milwaukee, Detroit – Cleveland, Minneapolis, St. Louis, Cincinnati, Indiana, Columbus, Louisville, and the outskirts of Pittsburgh. Table 28 shows hot spots descriptors of 2000 nighttime light emissions for Great Lakes. The mean of 2000 nighttime light emissions is around 56.92% in comparison with the mean value of approximately 50.37% for the Great Lakes megaregion. Resulted hot spots, therefore, indicate that the urban development levels caused by nighttime socio-economic activities are similarly high within the hot spot boundary.

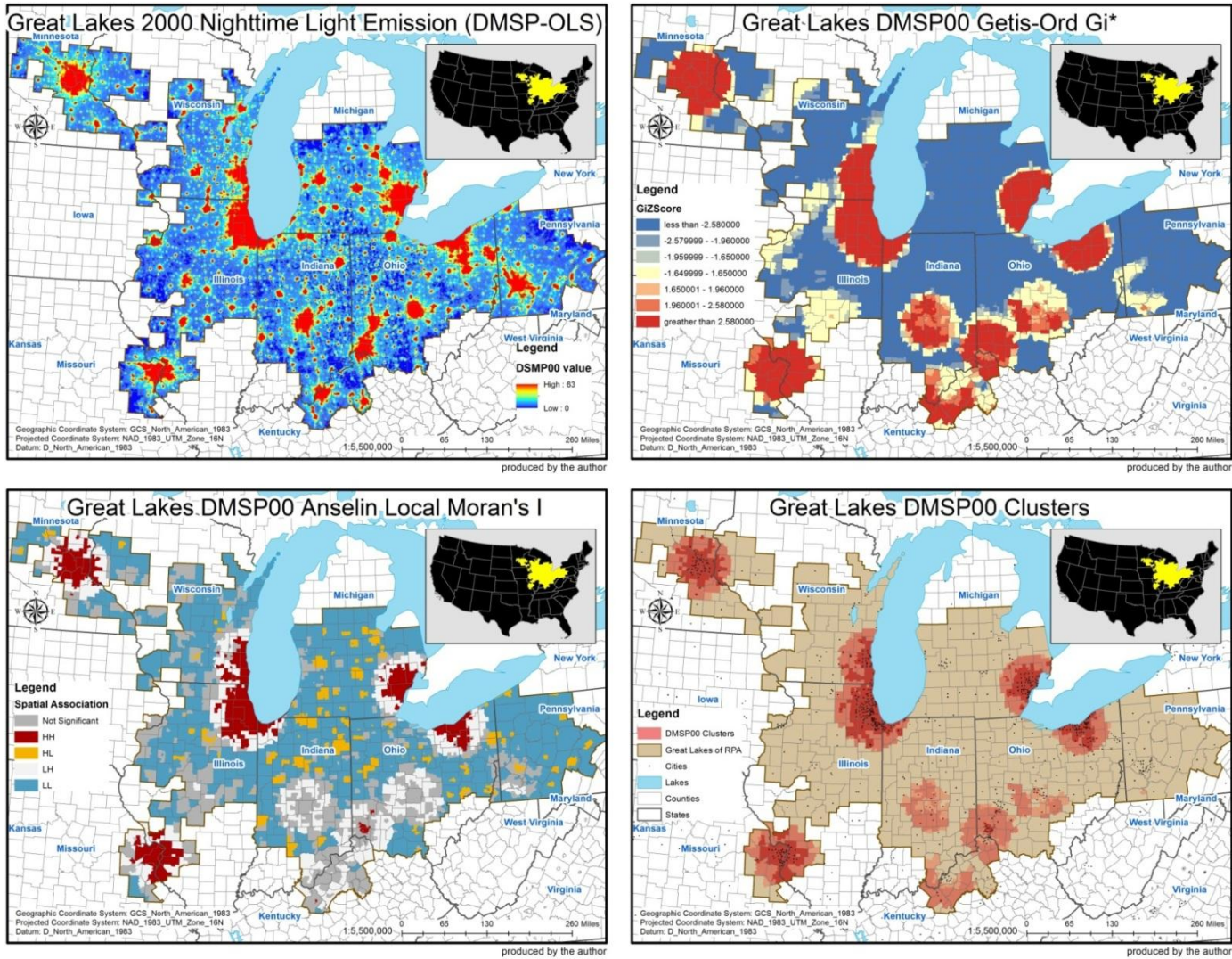


Figure 23 The Great Lakes megaregion local clustering analysis results by 2000 nighttime light emissions

Table 28 Great Lakes 2000 nighttime light emissions hot spots descriptors

Clustering Areas	Census Tracts	Land Area (sq. mi)	2000 Total Population
	13,394 (100%)	201,369.09 (100%)	53,700,872 (100%)
Chicago – Milwaukee	2,593 (19.36%)	10,287.27 (5.11%)	11,133,244 (20.73%)
Detroit – Cleveland	2,307 (17.22%)	8,044.52 (3.99%)	7,880,636 (14.68%)
Minneapolis	757 (5.65%)	6,532.62 (3.24%)	3,045,290 (5.67%)
St. Louis	534 (3.99%)	6,763.15 (3.36%)	2,612,014 (4.86%)
Cincinnati	568 (4.24%)	5,285.61 (2.62%)	2,342,215 (4.36%)
Indiana	323 (2.41%)	4,149.87 (2.06%)	1,548,117 (2.88%)
Columbus	260 (1.94%)	2,711.4 (1.35%)	1,062,182 (1.98%)
Louisville	77 (0.57%)	3,502.66 (1.74%)	401,863 (0.75%)
Pittsburgh	3 (0.02%)	61.85 (0.03%)	14,612 (0.03%)
Total	7,422 (55.41%)	47,338.95 (23.51%)	30,040,153 (55.94%)

The HH spatial association, as a result of Anselin Local Moran's *I* analysis in terms of 2000 nighttime light emissions, represents polycentric clustering around the areas of Chicago – Milwaukee, Detroit, Cleveland, Minneapolis, St. Louis, Cincinnati, and the outskirts of Louisville (bottom left of figure). It is noticeable that the hot spots of Detroit – Cleveland are divided into two separate HH spatial associations. Table 29 shows HH spatial associations descriptors of 2000 nighttime light emissions for Great Lakes. The mean of 2000 nighttime light emissions is around 62.11% in comparison with the mean value of approximately 50.37% for the Great Lakes megaregion. Resulted HH spatial associations, therefore, indicate that a high level of urban development caused by nighttime socio-economic activities is clustered with other similarly high levels of nighttime socio-economic urban activities within the resulted areas.

Table 29 Great Lakes 2000 nighttime light emissions HH spatial associations descriptors

Clustering Areas	Census Tracts	Land Area (sq. mi)	2000 Total Population
		13,394 (100%)	201,369.09 (100%)
Chicago – Milwaukee	2,462 (18.38%)	5,484.87 (2.72%)	10,488,457 (19.53%)
Detroit	1,241 (9.27%)	1,896.35 (0.94%)	4,291,830 (7.99%)
Cleveland	783 (5.85%)	1,462.29 (0.73%)	2,549,924 (4.75%)
Minneapolis	692 (5.17%)	2,917.75 (1.45%)	2,771,979 (5.16%)
St. Louis	480 (3.58%)	3,016.34 (1.5%)	2,336,895 (4.35%)
Cincinnati	109 (0.81%)	206.67 (0.1%)	474,786 (0.88%)
Louisville	4 (0.03%)	12.65 (0.01%)	16,675 (0.03%)
Total	5,771 (43.09%)	14,997.32 (7.45%)	22,930,546 (42.7%)

Morphological clustering, as a result of overlapping two analysis results in terms of 2000 nighttime light emissions, follows the clustering boundary in the result of Getis-Ord G_i^* analysis (bottom right of figure). The extent of 2000 nighttime light emissions clustering for the Great Lakes megaregion, therefore, is identical to the extent of hot spot clustering. The overlapping of the two clustering analysis results shows that the clustering pattern of 2000 nighttime light emissions has four round shape clusterings around Chicago – Milwaukee, Detroit – Cleveland, Minneapolis, and St. Louis. Central areas of the clusterings have morphological concentrations placed by both local clustering spatial analysis results. Other morphological clusterings for the Great Lakes megaregion is located around Cincinnati, which is composed by four distinct but likely connected morphological clustering areas of Cincinnati, Indiana, Columbus, and Louisville. These morphological clusterings are spread in Indiana State, Ohio State, and

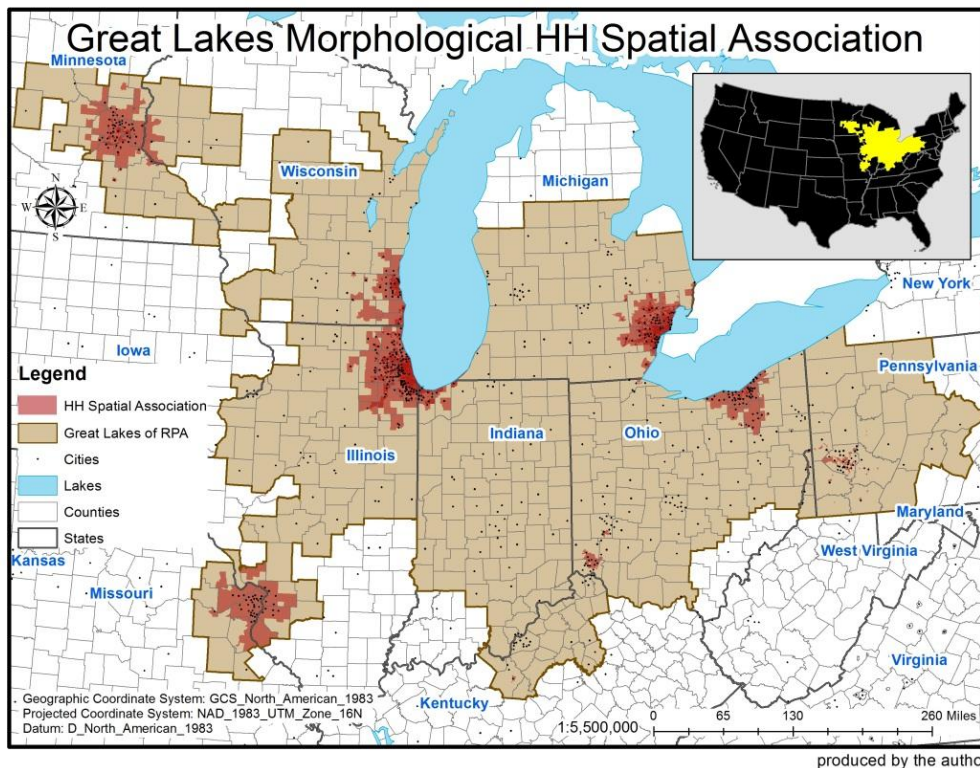
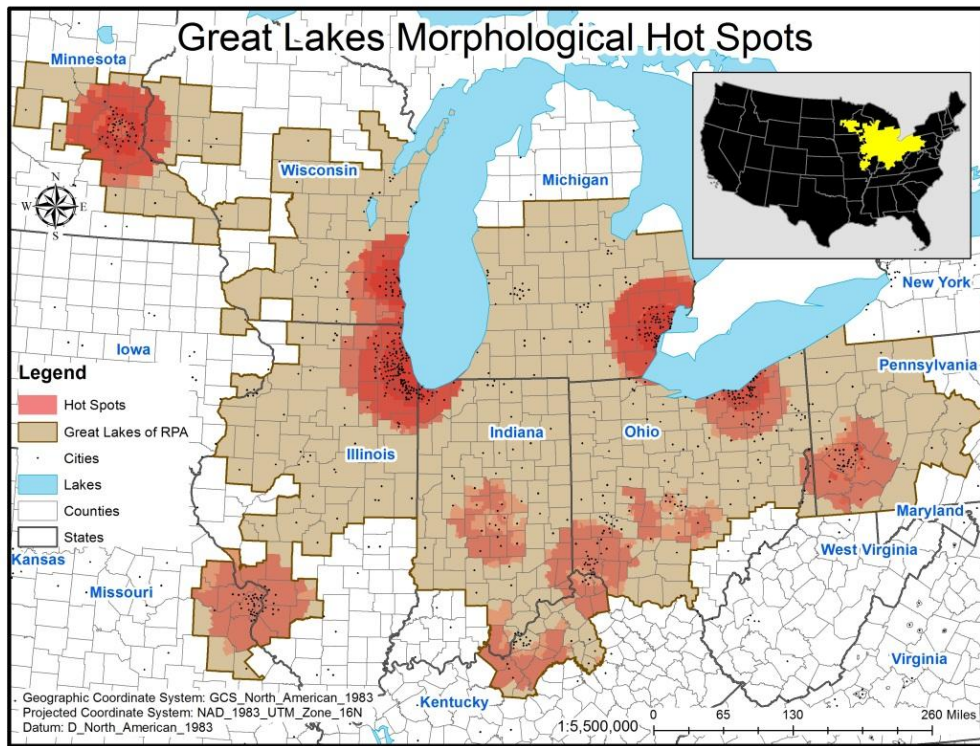


Figure 24 Local clusterings of morphological features in the Great Lakes megaregion

Kentucky State. The clustering around Cincinnati only has morphological concentration among those four clustering areas in the group. The morphological clustering map shows that the levels of urban development caused by nighttime socio-economic activities are similarly high and clustered within the clustering boundary. In terms of the clustering by 2000 nighttime light emissions, the Great Lakes megaregion identified by RPA seems to have an exaggerated boundary.

4) Morphological local clustering

Figure 24 represents results only produced by overlapping every clustering of the Getis-Ord G_i^* hot spots analysis (top of figure) and only by overlapping every HH spatial cluster of the Anselin Local Moran's I spatial cluster and outlier analysis (bottom of figure). As the final representation for Great Lakes megaregion morphological clustering, Figure 25 represents a result produced by overlapping the results separately represented in Figure 24. Table 30 summarizes the Great Lakes megaregion morphological clustering descriptors.

Representing polycentric morphological clustering for the Great Lakes megaregion, the clustering around Chicago – Milwaukee, Detroit, Cleveland, Minneapolis, and St. Louis are highlighted, meaning that the cities and the surrounding areas have an excess of morphological characteristics such as population density, impervious land cover, and nighttime light emissions (see Figure 25). In comparison with above 5 large clustering areas, Pittsburgh and Cincinnati clusterings have relatively weak morphological concentrations. It is noticeable that the clustering areas located in southern area of the

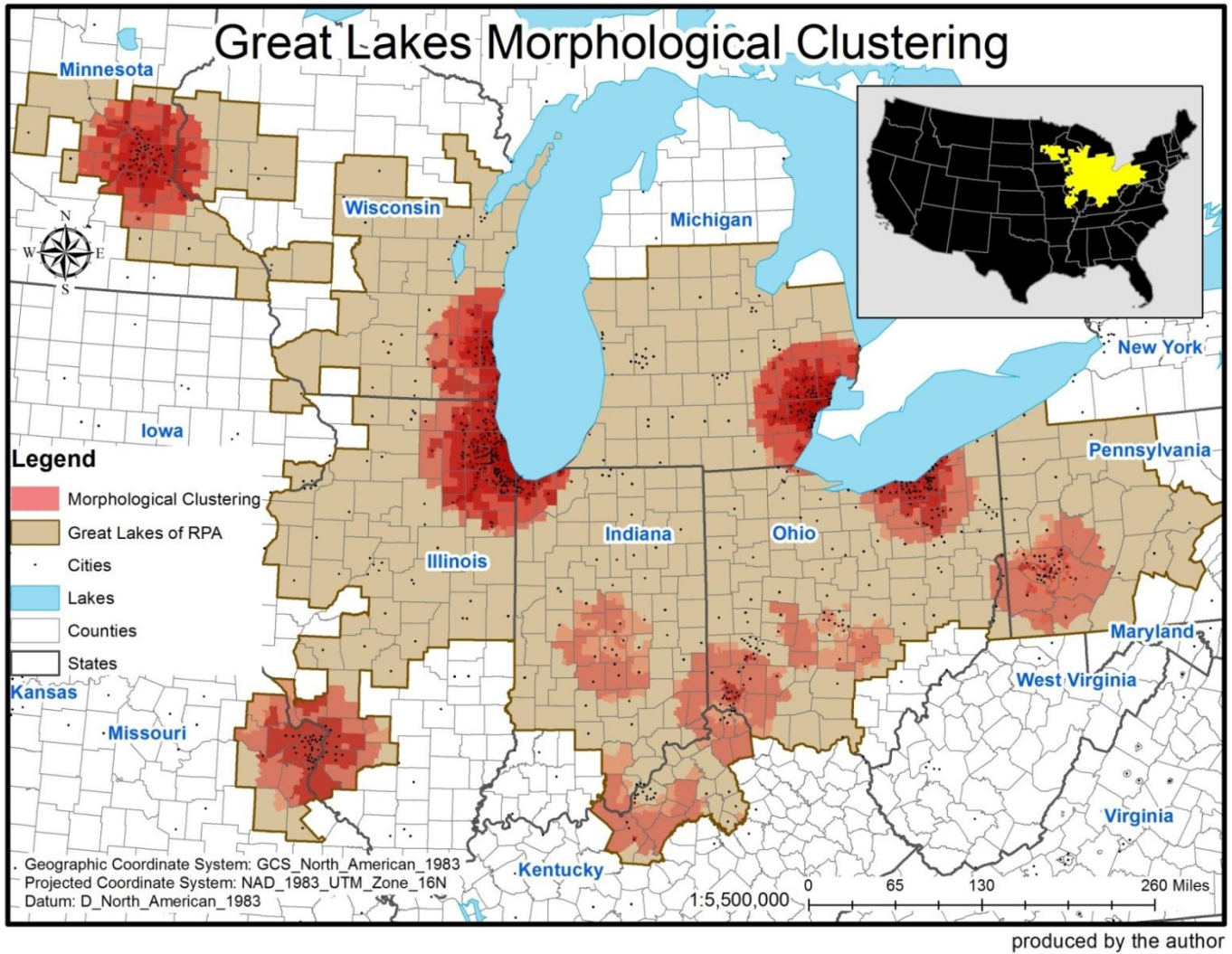


Figure 25 Morphological clusterings of the Great Lakes megaregion

Table 30 The Great Lakes megaregion morphological clusterings descriptors

Data Type	Clustering Area	Analysis	Great Lakes Morphological Clusterings Descriptors		
			Census Tracts	Land Areas (sq. mi)	2000 Total Population
			13,394 (100%)	201,369.09 (100%)	53,700,872 (100%)
PopDen00	Chicago	Hot Spot	1,672 (12.48%)	1,767.32 (0.88%)	7,059,248 (13.15%)
		HH Cluster	1,185 (8.85%)	489.64 (0.24%)	4,841,563 (9.02%)
	Detroit	Hot Spot	1,037 (7.74%)	1,104.5 (0.55%)	3,542,523 (6.6%)
		HH Cluster	395 (2.95%)	178.02 (0.09%)	1,406,203 (2.62%)
	Cleveland	Hot Spot	607 (4.53%)	1,059.1 (0.53%)	1,850,228 (3.45%)
		HH Cluster	216 (1.61%)	67.16 (0.03%)	613,426 (1.14%)
	Minneapolis	Hot Spot	596 (4.45%)	1,396.52 (0.69%)	2,333,222 (4.34%)
		HH Cluster	62 (0.46%)	17.23 (0.01%)	215,398 (0.4%)
	Milwaukee	Hot Spot	421 (3.14%)	1,061.66 (0.53%)	1,499,630 (2.79%)
		HH Cluster	216 (1.61%)	70.23 (0.03%)	633,560 (1.18%)
	Pittsburgh	Hot Spot	137 (1.02%)	866.9 (0.43%)	510,189 (0.95%)
		HH Cluster	32 (0.24%)	5.37 (0.003%)	79,801 (0.15%)
	Subtotal	Hot Spot	4,470 (33.37%)	7,256.01 (3.6%)	16,795,040 (31.28%)
		HH Cluster	2,106 (15.72%)	827.65 (0.41%)	7,789,951 (14.51%)
Clustering Total			4,512 (33.69%)	7,263.68 (3.61%)	16,913,035 (31.49%)
ImpS01	Chicago - Milwaukee	Hot Spot	2,497 (18.64%)	7,507.24 (3.73%)	10,683,679 (19.89%)
		HH Cluster	1,484 (11.08%)	1,170.74 (0.58%)	5,534,058 (10.31%)
	Detroit	Hot Spot	1,470 (10.98%)	4,790.46 (2.38%)	5,093,154 (9.48%)
		HH Cluster	933 (6.97%)	910.53 (0.45%)	3,129,305 (5.83%)
	Minneapolis	Hot Spot	748 (5.58%)	5,911.66 (2.94%)	2,998,313 (5.58%)
		HH Cluster	158 (1.18%)	182.33 (0.09%)	517,075 (0.96%)
	Pittsburgh	Hot Spot	714 (5.33%)	5,160.58 (2.56%)	5,093,154 (9.48%)
		HH Cluster	246 (1.84%)	222.69 (0.11%)	656,569 (1.22%)
	Lancaster	Hot Spot	4 (0.03%)	192.74 (0.1%)	16,138 (0.03%)
		HH Cluster	1 (0.01%)	0.82 (0.0004%)	3,072 (0.01%)
	Subtotal	Hot Spot	5,433 (40.56%)	23,562.68 (11.7%)	21,207,111 (39.49%)
		HH Cluster	2,822 (21.07%)	2,487.11 (1.24%)	9,840,079 (18.32%)

Table 30 continued.

ImpS01	Clustering Total		5,444 (40.65%)	23,576.6 (11.71%)	21,234,715 (39.54%)
DMSP00	Chicago - Milwaukee	Hot Spot	2,593 (19.36%)	10,287.27 (5.11%)	11,133,224 (20.73%)
		HH Cluster	2,462 (18.38%)	5,484.87 (2.72%)	10,488,457 (19.53%)
	Detroit - Cleveland	Hot Spot	2,307 (17.22%)	8,044.52 (3.99%)	7,880,636 (14.68%)
		HH Cluster *	1,241 (9.27%)	1,896.35 (0.94%)	4,291,830 (7.99%)
		HH Cluster **	783 (5.85%)	1,462.69 (0.73%)	2,549,924 (4.75%)
	Minneapolis	Hot Spot	757 (5.65%)	6,532.62 (3.24%)	3,045,290 (5.67%)
		HH Cluster	692 (5.17%)	2,917.75 (1.45%)	2,771,979 (5.16%)
	St. Louis	Hot Spot	534 (3.99%)	6,763.15 (3.36%)	2,612,014 (4.86%)
		HH Cluster	480 (3.58%)	3,016.34 (1.5%)	2,336,895 (4.35%)
	Cincinnati	Hot Spot	568 (4.24%)	5,285.61 (2.62%)	2,342,215 (4.36%)
		HH Cluster	109 (0.81%)	206.67 (0.1%)	474,786 (0.88%)
	Indiana	Hot Spot	323 (2.41%)	4,149.87 (2.06%)	1,548,117 (2.88%)
		HH Cluster	n/a	n/a	n/a
	Columbus	Hot Spot	260 (1.94%)	2,711.40 (1.35%)	1,062,182 (1.98%)
		HH Cluster	n/a	n/a	n/a
	Louisville	Hot Spot	77 (0.57%)	3,502.66 (1.74%)	401,863 (0.75%)
		HH Cluster	4 (0.03%)	12.65 (0.01%)	16,675 (0.03%)
	Pittsburgh	Hot Spot	3 (0.02%)	61.85 (0.03%)	14,612 (0.03%)
		HH Cluster	n/a	n/a	n/a
	Subtotal	Hot Spot	7,422 (55.41%)	47,338.95 (23.51%)	30,040,153 (55.94%)
HH Cluster		5,771 (43.09%)	14,997.32 (7.45%)	22,930,546 (42.7%)	
Clustering Total		7,422 (55.41%)	47,338.95 (23.51%)	30,040,153 (55.94%)	
The Great Lakes Subtotal		Hot Spot	8,211 (61.3%)	53,053.1 (26.35%)	32,735,866 (60.96%)
		HH Cluster	6,056 (45.21%)	15,282.29 (7.59%)	23,708,002 (44.15%)
The Great Lakes Morphological Clusterings Total		8,219 (61.36%)	53,065.24 (26.35%)	32,753,550 (60.99%)	

HH Cluster* - Clustering around Detroit

HH Cluster** - Clustering around Cleveland

Great Lakes megaregion, including Pittsburgh, Cincinnati, Indiana, Columbus, and Louisville, are likely to show smaller extent of morphological clustering compared to the clustering areas located in northern area of the megaregion. This means that the concentration of morphological clustering for the Great Lakes megaregion is driven by the northern part clustering areas. Concerning the megaregion boundary of RPA, the Great Lakes megaregion is not likely considered as an entity that is morphologically interconnected and integrated because of the strong concentration of morphological characteristics in particular areas and because of the strong separation of locations for the morphological clusterings within the megaregion boundary. The total extent of Great Lakes clustering in terms of all morphological features analyzed thus far includes 8,219 census tracts being around 61.36% of the total Great Lakes census tracts; about 53,065.24 square miles equal approximately 26.35% of the total Great Lakes land area; and 32,753,550 total population being around 60.99% of the total population of the Great Lakes megaregion.

The Great Lakes morphological clustering map resulted finally represents the locations where high levels of land uses per capita, urbanized built environment, and nighttime socio-economic urban activities are clustered. The clustering areas of Detroit, Cleveland, and Pittsburgh seem to have morphological connections being physically close. The clustering areas of Cincinnati, Columbus, Lancaster, and Louisville also seem to have morphological connections as well. The clustering areas of Chicago – Milwaukee, Minneapolis, and St. Louis seem to be difficult to consider morphological connections to other clustering areas because of their physically distant locations. The

final map also represents an exaggerated boundary for the Great Lakes megaregion in the morphological observations.

2.4. The Piedmont Atlantic megaregion

1) Local clustering of 2000 population density

Figure 26 shows local clustering analysis results produced by using 2000 population density. Following the threshold of Density-based Sprawl Index, 2000 population density is categorized into three groups: rural areas population density (i.e., less than 200 persons per square mile), low population density areas (i.e., between 200 and 3,500 persons per square mile), and high population density areas (i.e., greater than 3,500 persons per square mile) (top left of figure). The general observation of the distribution of 2000 population density shows that low and high population density areas represent density concentrations around Atlanta, Georgia and Birmingham, Alabama. These density concentrations linearly connected low and high population density areas crossing Greenville, South Carolina, and Charlotte, Greensboro, and Raleigh, North Carolina.

The statistically significant hot spots at the 0.05 alpha level, as a result of Getis-Ord G_i^* analysis in terms of 2000 population density, represent polycentric clustering (top right of figure). Hot spots are spatially concentrated in the areas around Atlanta, Birmingham, Charlotte, and Raleigh – Greensboro. Table 31 shows hot spots descriptors of 2000 population density for Piedmont Atlantic. The mean of 2000 population density is around 2,323.88 in comparison with the mean value of approximately 1,500.21 for the

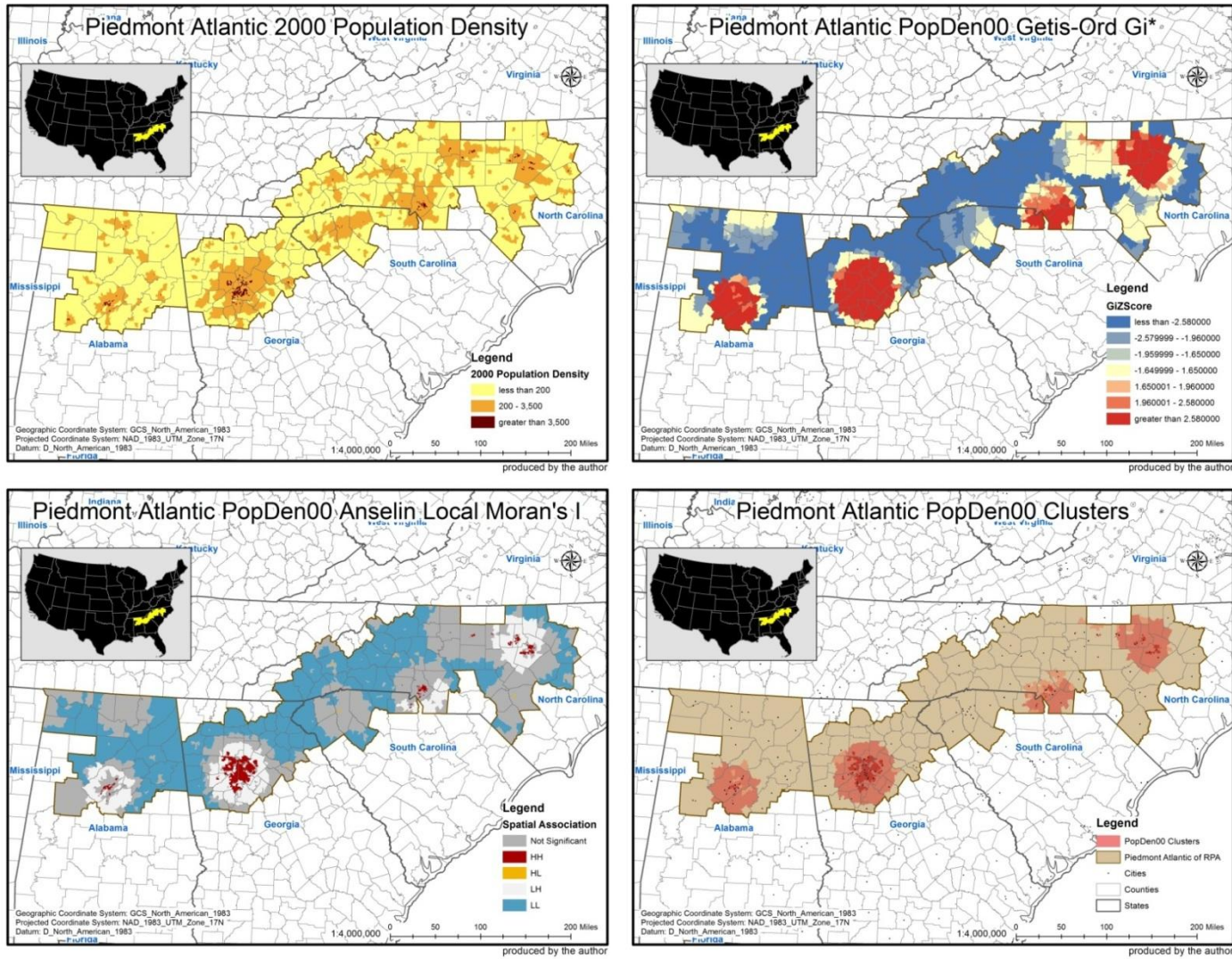


Figure 26 The Piedmont Atlantic megaregion local clustering analysis results by 2000 population density

Piedmont Atlantic megaregion. Resulted hot spots, therefore, indicate that the levels of land use per capita are similarly high within the hot spot boundary.

Table 31 Piedmont Atlantic 2000 population density hot spots descriptors

Clustering Areas	Census Tracts	Land Area (sq. mi)	2000 Total Population
		2,834 (100%)	58,298.75 (100%)
Atlanta	599 (21.14%)	3,741.15 (6.42%)	3,750,432 (25.36%)
Birmingham	187 (6.6%)	2,220.24 (3.81%)	846,677 (5.73%)
Raleigh – Greensboro	211 (7.45%)	2,688.93 (4.61%)	1,162,617 (7.86%)
Charlotte	226 (7.97%)	1,791.45 (3.07%)	1,117,713 (7.56%)
Total	1,223 (43.15%)	10,441.78 (17.91%)	6,877,439 (46.51%)

The HH spatial associations, as a result of Anselin Local Moran's *I* analysis in terms of 2000 population density, also represent polycentric clustering in same areas as the result of hot spots analysis (bottom left of figure). The clustering patterns around the areas, however, are not circular but fragmented. Table 32 shows HH spatial associations descriptors of 2000 population density for Piedmont Atlantic. The mean of 2000 population density is around 3,925.62 in comparison with the mean value of approximately 1,500.21 for the Piedmont Atlantic megaregion. Resulted HH spatial associations, therefore, indicate that a high level of land use per capita is clustered with other similarly high levels of land use per capita within the resulted areas.

Table 32 Piedmont Atlantic 2000 population density HH spatial associations descriptors

Clustering Areas	Census Tracts	Land Area (sq. mi)	2000 Total Population
		2,834 (100%)	58,298.75 (100%)
Atlanta	370 (13.06%)	740.28 (1.27%)	2,164,804 (14.64%)
Birmingham	48 (1.69%)	50.8 (0.09%)	199,452 (1.35%)
Raleigh – Greensboro	97 (3.42%)	117.63 (0.2%)	418,171 (2.83%)
Charlotte	56 (1.98%)	66.62 (0.11%)	251,569 (1.7%)
Total	571 (20.15%)	975.33 (1.67%)	3,033,996 (20.52%)

Morphological clustering, as a result of overlapping two analysis results in terms of 2000 population density, has the mostly same clustering boundary with Getis-Ord G_i^* analysis result (bottom right of figure). 13 census tracts of HH spatial clustering are not included in the result of the Getis-Ord G_i^* analysis, which are located in the area around Greensboro. The overlapping of the two clustering analysis results shows that the clustering pattern of 2000 population density is polycentric around Atlanta, Birmingham, Raleigh – Greensboro, and Charlotte. The clustering pattern of 2000 population density also shows that the concentrations of clusters are repeated in the central city areas, and that the central area of Atlanta has the most concentration of clustering. Table 33 shows the total extent of 2000 population density clustering descriptors for Piedmont Atlantic. The morphological clustering map represents, therefore, that the levels of land use per capita are similarly high and clustered within the clustering boundary. In terms of the clustering by 2000 population density, the Piedmont Atlantic megaregion identified by RPA seems to have an exaggerated boundary.

Table 33 Piedmont Atlantic 2000 population density clustering descriptors

Clustering Total	Census Tracts	Land Area (sq. mi)	2000 Total Population
	2,834 (100%)	58,298.75 (100%)	14,787,483 (100%)
2000 population density	1,236 (33.69%)	10,451.21 (17.93%)	6,921,597 (46.81%)

2) Local clustering of 2001 impervious land cover

Figure 27 shows local clustering analysis results produced by using 2001 impervious land cover. The general observation of the distribution of 2001 impervious land cover is that the highest degree of imperviousness in 2001 was likely to follow the distribution of 2000 population density (top left of figure). The impervious areas are likely to be clustered around Atlanta, Charlotte – Raleigh, and Birmingham.

The statistically significant hot spots at the 0.05 alpha level, as a result of Getis-Ord G_i^* analysis in terms of 2001 impervious land cover, represent polycentric clustering (top right of figure). Hot spots are spatially concentrated in the areas of Atlanta, Raleigh – Greensboro, Greenville, Charlotte, and the outskirts of Birmingham. Table 34 shows hot spots descriptors of 2001 impervious land cover for Piedmont Atlantic. The mean of 2001 impervious land cover is around 44.55% in comparison with the mean value of approximately 14.71% for the Piedmont Atlantic megaregion. Resulted hot spots, therefore, indicate that the urbanization levels of built environments are similarly high within the hot spot boundary.

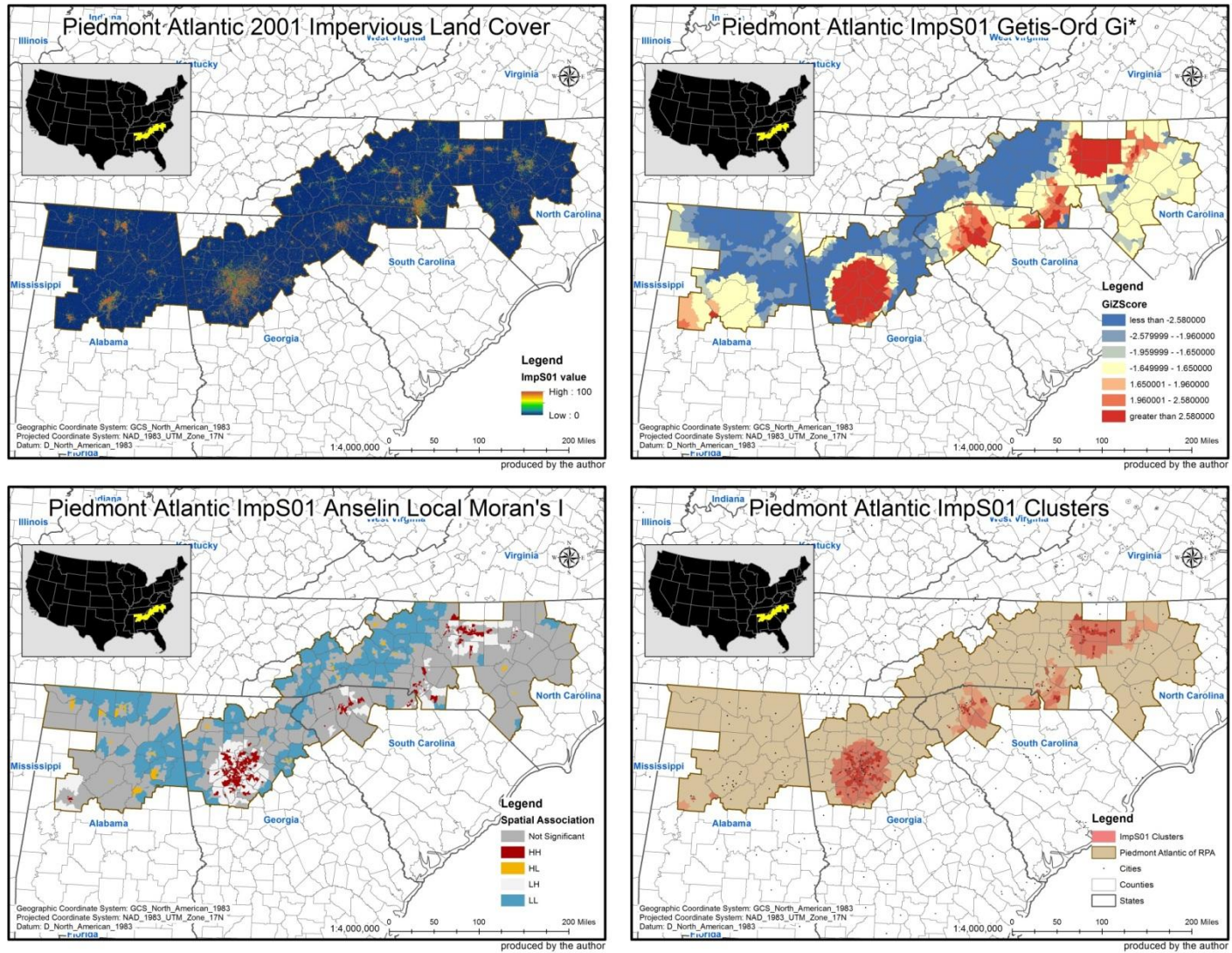


Figure 27 The Piedmont Atlantic megaregion local clustering analysis results by 2001 impervious land cover

Table 34 Piedmont Atlantic 2001 impervious land cover hot spots descriptors

Clustering Areas	Census Tracts	Land Area (sq. mi)	2000 Total Population
		2,834 (100%)	58,298.75 (100%)
Atlanta	591 (20.85%)	3,546.41 (6.08%)	3,697,629 (25.01%)
Raleigh – Greensboro	265 (9.35%)	2,718.64 (4.66%)	1,217,167 (8.23%)
Greenville	122 (4.3%)	1,449.06 (2.49%)	550,979 (3.73%)
Charlotte	76 (2.68%)	1,221.87 (2.1%)	416,369 (2.82%)
Birmingham	2 (0.07%)	155.71 (0.27%)	9,511 (0.06%)
Total	1,056 (37.26%)	9,091.68 (15.59%)	5,891,655 (39.84%)

The HH spatial association, as a result of Anselin Local Moran's *I* analysis in terms of 2001 impervious land cover, also represents polycentric clustering located in the areas around Atlanta, Raleigh – Greensboro, Charlotte, Greenville, and the outskirts of Birmingham (bottom left of figure). Even though the HH spatial clustering of 2001 impervious land cover is located around the same place as the hot spot clustering, the clustering pattern is more fractal and fragmented than the hot spot clustering pattern. Table 35 shows HH spatial associations descriptors of 2001 impervious land cover for Piedmont Atlantic. The mean of 2001 impervious land cover is around 54.06% in comparison with the mean value of approximately 14.71% for the Piedmont Atlantic megaregion. Resulted HH spatial associations, therefore, indicate that a high level of urbanization for built environments is clustered with other similarly highly urbanized built environments within the resulted areas.

Table 35 Piedmont Atlantic 2001 impervious land cover HH spatial associations descriptors

Clustering Areas	Census Tracts	Land Area (sq. mi)	2000 Total Population
		2,834 (100%)	58,298.75 (100%)
Atlanta	284 (10.02%)	846.91 (1.45%)	1,598,555 (10.81%)
Raleigh – Greensboro	89 (3.14%)	311.46 (0.53%)	328,437 (2.22%)
Greenville	40 (1.41%)	125.92 (0.22%)	126,269 (0.85%)
Charlotte	31 (1.09%)	146.43 (0.25%)	107,736 (0.73%)
Birmingham	10 (0.35%)	15.86 (0.03%)	38,877 (0.26%)
Total	454 (16.02%)	1,446.59 (2.48%)	2,199,874 (14.88%)

Morphological clustering, as a result of overlapping two analysis results in terms of 2001 impervious land cover, has the similar clustering boundary with Getis-Ord G_i^* analysis result (bottom right of figure). Greenville's 37 census tracts for HH spatial clustering are not included in the result of hot spots analysis. The overlapping of the two analysis results shows that, compared to the observation of 2000 population density, the clustering around Birmingham area is disappeared and only outskirt areas are left in 2001 impervious land cover hot spots analysis result. It is also noticeable for the appearance of new clustering areas around Greenville in 2001 impervious land cover hot spots analysis result, compared to 2000 population density analysis results. Table 36 shows the total extent of 2001 impervious land cover clustering descriptors for Piedmont Atlantic. The morphological clustering map represents, therefore, that the urbanization levels of these built environments are similarly high and clustered within the clustering boundary. In terms of the clustering by 2001 impervious land cover, the Piedmont Atlantic megaregion identified by RPA seems to have an exaggerated boundary.

Table 36 Piedmont Atlantic 2001 impervious land cover clustering descriptors

Clustering Total	Census Tracts	Land Area (sq. mi)	2000 Total Population
	2,834 (100%)	58,298.75 (100%)	14,787,483 (100%)
2001 impervious land cover	1,093 (38.57%)	9,197.66 (15.78%)	6,012,334 (40.66%)

3) Local clustering of 2000 nighttime light emissions (DMSP-OLS)

Figure 28 shows local clustering analysis results produced by using 2000 nighttime light emissions (DMSP-OLS). The general observation of the distribution of 2000 nighttime light emissions is that the highest degree of nighttime light emissions in 2000 follows both distribution of 2000 low and high population density and 2001 impervious land cover (top left of figure).

The statistically significant hot spots at the 0.05 alpha level, as a result of Getis-Ord G_i^* analysis in terms of 2000 nighttime light emissions, represent polycentric clustering (top right of figure). Hot spots are spatially concentrated in the areas around Atlanta, Raleigh – Greensboro, Charlotte, Birmingham, and the outskirts of Greenville. Compared to the hot spots analysis results of 2000 population density and 2001 impervious land cover, it is noticeable for the strong connection of clustering area around Raleigh – Greensboro. Table 37 shows hot spots descriptors of 2000 nighttime light emissions for Piedmont Atlantic. The mean of 2000 nighttime light emissions is around 56.86% in comparison with the mean value of approximately 44.83% for the Piedmont Atlantic megaregion. Resulted hot spots, therefore, indicate that the urban development levels caused by nighttime socio-economic activities are similarly high within the hot spot boundary.

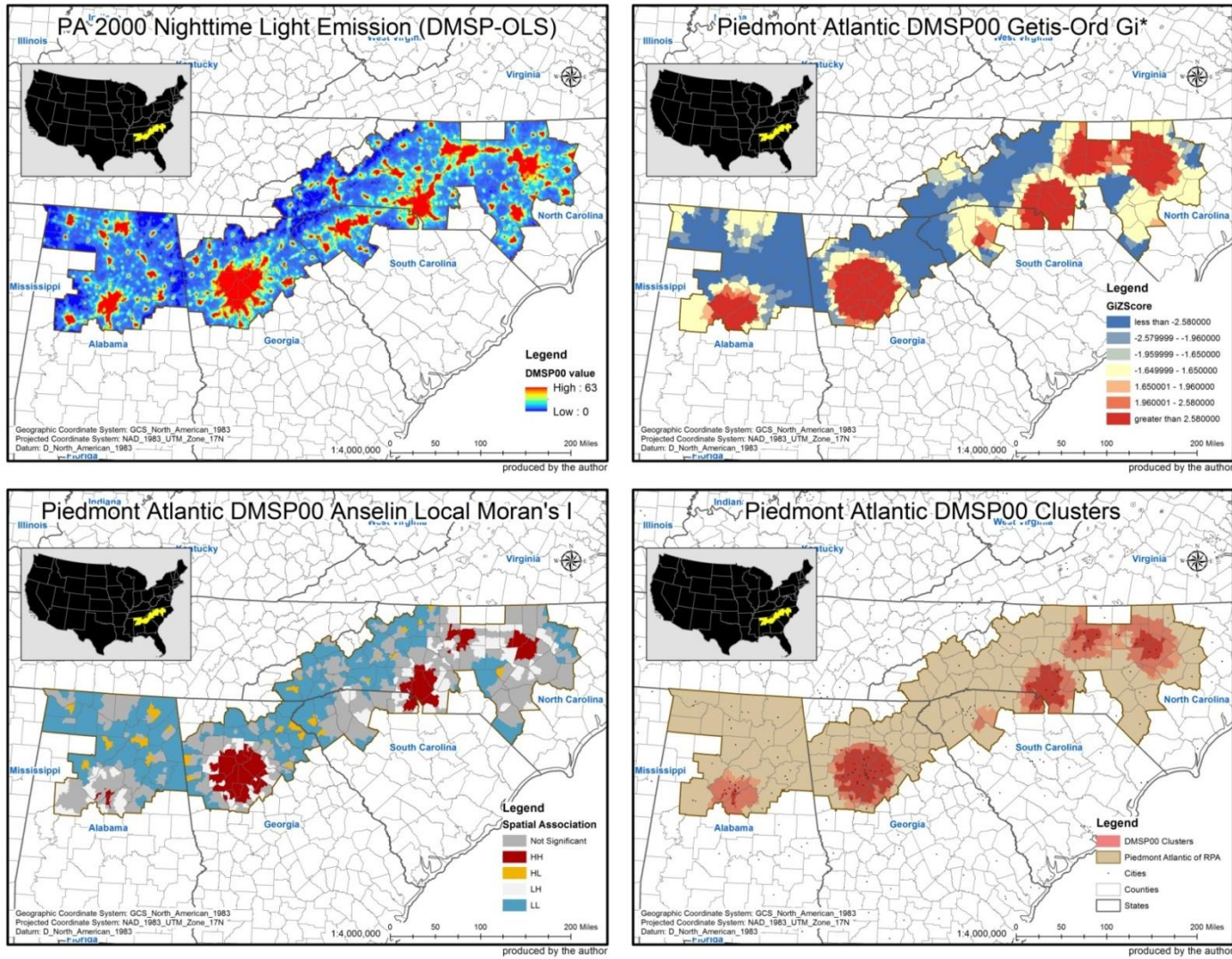


Figure 28 The Piedmont Atlantic megaregion local clustering analysis results by 2000 nighttime light emissions

Table 37 Piedmont Atlantic 2000 nighttime light emissions hot spots descriptors

Clustering Areas	Census Tracts	Land Area (sq. mi)	2000 Total Population
		2,834 (100%)	58,298.75 (100%)
Atlanta	610 (21.52%)	4,127.57 (7.08%)	3,821,179 (25.84%)
Raleigh – Greensboro	436 (15.38%)	5,404.73 (9.27%)	2,255,609 (15.25%)
Charlotte	273 (9.63%)	2,740.73 (4.7%)	1,404,769 (9.5%)
Birmingham	176 (6.21%)	1,831.97 (3.14%)	783,816 (5.3%)
Greenville	10 (0.35%)	484.59 (0.83%)	75,424 (0.51%)
Total	1,505 (53.11%)	14,589.59 (25.03%)	8,340,797 (56.4%)

The HH spatial association, as a result of Anselin Local Moran's *I* analysis in terms of 2000 nighttime light emissions, represents polycentric clustering around Atlanta, Charlotte, Raleigh, Greensboro, and the outskirts of Birmingham (bottom left of figure). It is noticeable, compared to the hot spot clustering result, for the disconnection of Raleigh – Greensboro clustering areas. Table 38 shows HH spatial associations descriptors of 2000 nighttime light emissions for Piedmont Atlantic. The mean of 2000 nighttime light emissions is around 61.76% in comparison with the mean value of approximately 44.83% for the Piedmont Atlantic megaregion. Resulted HH spatial associations, therefore, indicate that a high level of urban development caused by nighttime socio-economic activities is clustered with other similarly high levels of nighttime socio-economic urban activities within the resulted areas.

Table 38 Piedmont Atlantic 2000 nighttime light emissions HH spatial associations descriptors

Clustering Areas	Census Tracts	Land Area (sq. mi)	2000 Total Population
		2,834 (100%)	58,298.75 (100%)
Atlanta	552 (19.48%)	2,605.66 (4.47%)	3,452,219 (23.35%)
Raleigh	153 (5.4%)	666.86 (1.14%)	784,421 (5.3%)
Greensboro	140 (4.94%)	449.46 (0.77%)	555,520 (3.76%)
Charlotte	230 (8.12%)	1,284.6 (2.2%)	1,162,374 (7.86%)
Birmingham	29 (1.02%)	109.76 (0.19%)	137,717 (0.93%)
Total	1,104 (38.96%)	5,116.35 (8.78%)	6,092,251 (41.2%)

Morphological clustering, as a result of overlapping two analysis results in terms of 2000 nighttime light emissions, follows the clustering boundary in the result of Getis-Ord G_i^* analysis (bottom right of figure). The extent of the 2000 nighttime light emissions clustering of the Piedmont Atlantic megaregion, therefore, is identical to the extent of hot spot clustering. The overlapping of the two clustering analysis results shows that the clustering pattern of 2000 nighttime light emissions has four round shape clustering areas around Atlanta, Raleigh – Greensboro, Charlotte, and Birmingham. Another clustering is located in the outskirts of Greenville. The clustering areas around Atlanta, Raleigh – Greensboro, and Charlotte have the concentration of nighttime light emissions in central areas. The interconnection between clustering areas around Raleigh and Greensboro is likely clustered to one area. The morphological clustering map represents, therefore, that the levels of urban development caused by nighttime socio-economic activities are similarly high and clustered within the clustering boundary. In terms of the clustering by

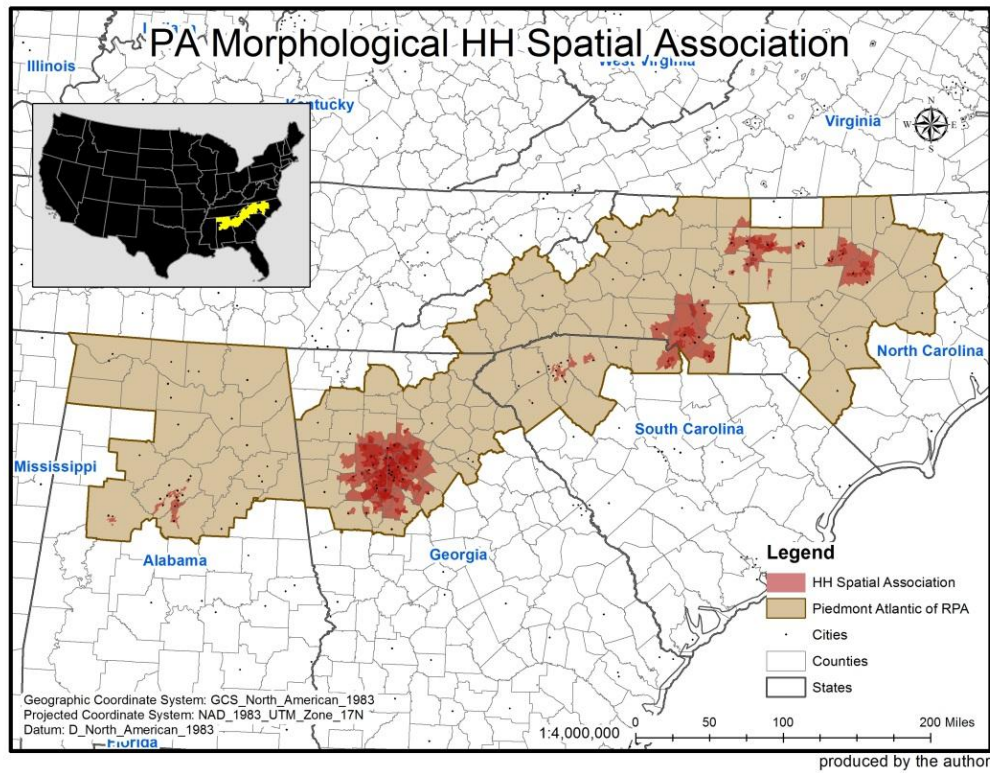
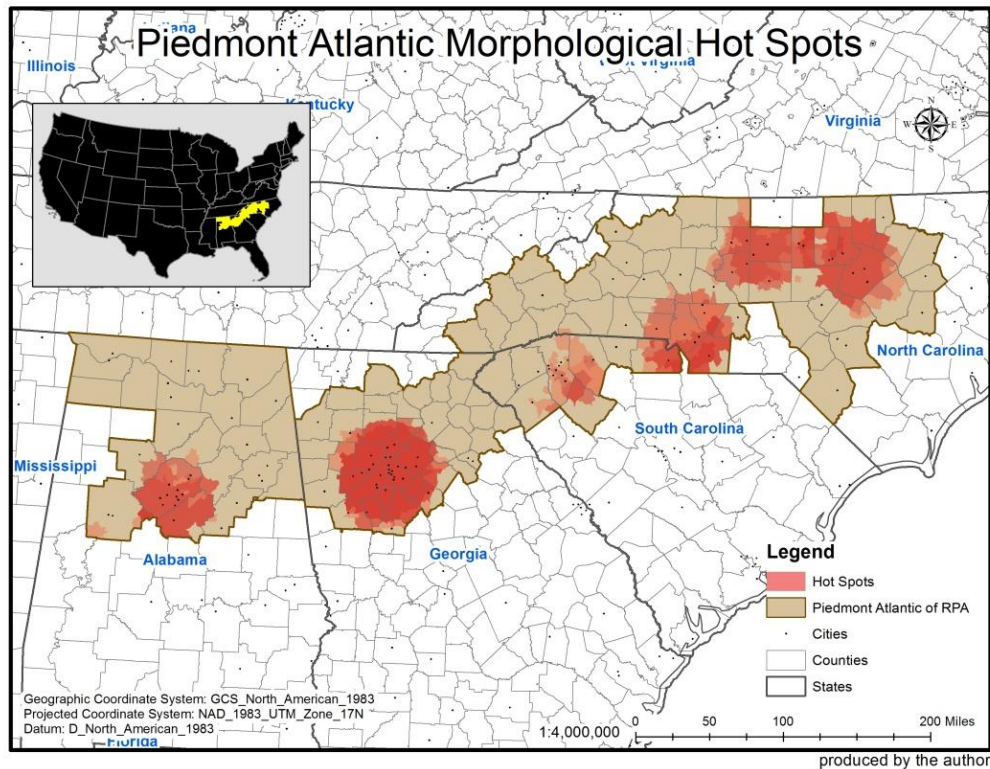


Figure 29 Local clusterings of morphological features in the Piedmont Atlantic megaregion

2000 nighttime light emissions, the Piedmont Atlantic megaregion identified by RPA seems to have an exaggerated boundary.

4) Morphological local clustering

Figure 29 represents results only produced by overlapping every clustering of the Getis-Ord G_i^* hot spots analysis (top of figure) and only by overlapping every HH spatial cluster of the Anselin Local Moran's I spatial cluster and outlier analysis (bottom of figure). As the final representation for the Piedmont Atlantic megaregion morphological clustering, Figure 30 represents a result produced by overlapping the results separately represented in Figure 29. Table 9 summarizes the Piedmont Atlantic megaregion morphological clustering descriptors.

Representing polycentric morphological clustering for the Piedmont Atlantic megaregion, the clusterings around Atlanta, Raleigh – Greensboro, Charlotte, and Birmingham are highlighted, meaning that the cities and the surrounding areas have an excess of morphological characteristics such as population density, impervious land cover, and nighttime light emissions (see Figure 30). The Atlanta clustering is the strongest among morphological clusterings for the Piedmont Atlantic megaregion. The clustering interconnection between Raleigh and Greensboro is obvious to be regarded as one clustering region. The Charlotte clustering may be connected to the Raleigh – Greensboro clustering areas within near future. The Atlanta and Raleigh – Greensboro – Charlotte clustering areas, however, are not likely connected because of being physically distant. This means that morphological characteristics are spatially concentrated in the

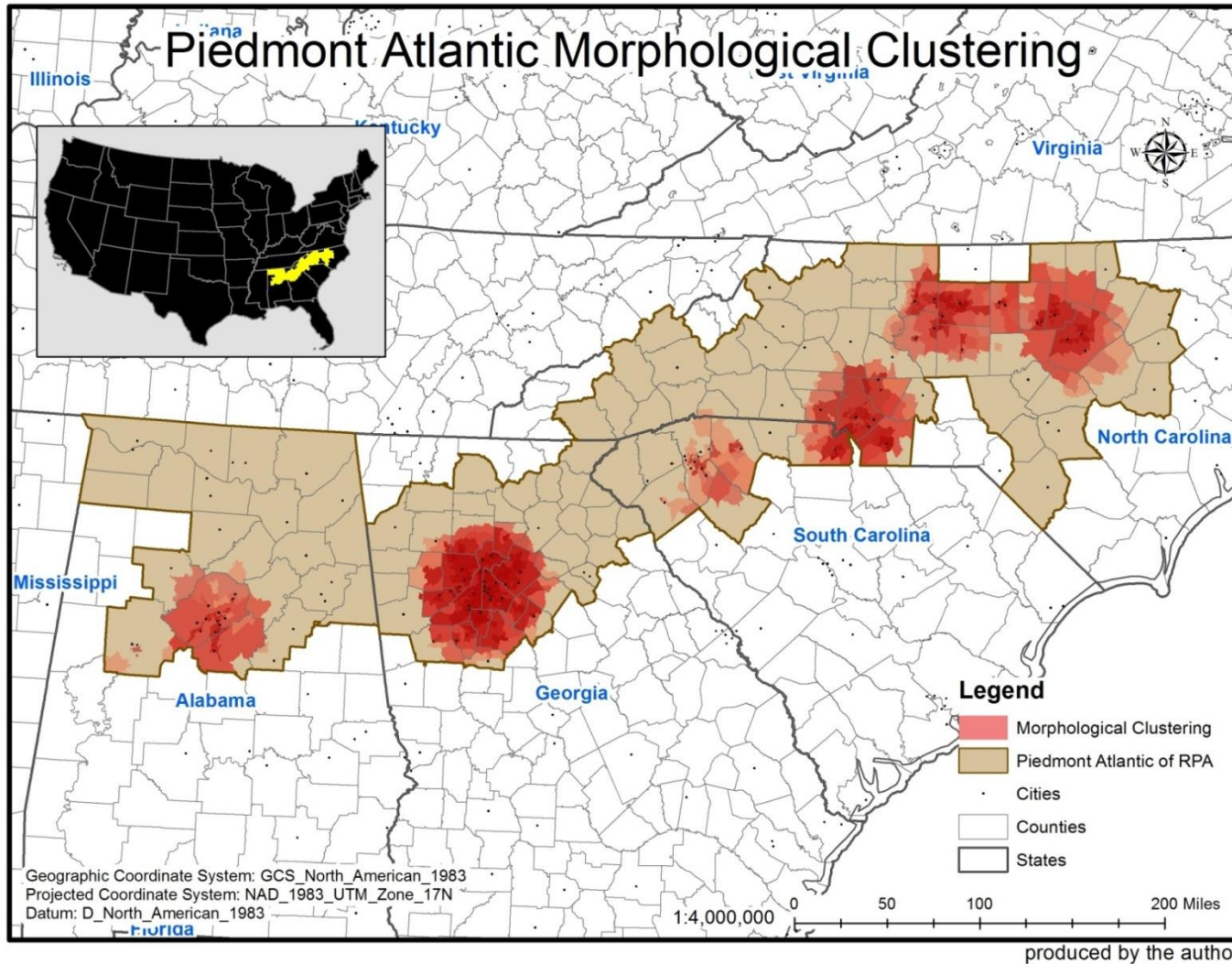


Figure 30 Morphological clusterings of the Piedmont Atlantic megaregion

Table 39 The Piedmont Atlantic megaregion morphological clusterings descriptors

Data Type	Clustering Area	Analysis	Piedmont Atlantic Morphological Clusterings Descriptors		
			Census Tracts	Land Areas (sq. mi)	2000 Total Population
			2,834 (100%)	58,298.75 (100%)	14,787,483 (100%)
PopDen00	Atlanta	Hot Spot	599 (21.14%)	3,741.15 (6.42%)	3,750,432 (25.36%)
		HH Cluster	370 (13.06%)	740.28 (1.27%)	2,164,804 (14.64%)
	Birmingham	Hot Spot	187 (6.6%)	2,220.24 (3.81%)	846,677 (5.73%)
		HH Cluster	48 (1.69%)	50.8 (0.09%)	199,452 (1.35%)
	Raleigh - Greensboro	Hot Spot	211 (7.45%)	2,688.93 (4.61%)	1,162,617 (7.86%)
		HH Cluster	97 (3.42%)	117.63 (0.2%)	418,171 (2.83%)
	Charlotte	Hot Spot	226 (7.97%)	1,791.45 (3.07%)	1,117,713 (7.56%)
		HH Cluster	56 (1.98%)	66.62 (0.11%)	251,569 (1.7%)
	Subtotal	Hot Spot	1,223 (43.15%)	10,441.78 (17.91%)	6,877,439 (46.51%)
		HH Cluster	571 (20.15%)	975.33 (1.67%)	3,033,996 (20.52%)
Clustering Total			1,236 (43.61%)	10,451.21 (17.93%)	6,921,597 (46.81%)
ImpS01	Atlanta	Hot Spot	591 (20.85%)	3,546.41 (6.08%)	3,697,629 (25.01%)
		HH Cluster	284 (10.02%)	846.91 (1.45%)	1,598,555 (10.81%)
	Raleigh - Greensboro	Hot Spot	265 (9.35%)	2,718.64 (4.66%)	1,217,167 (8.23%)
		HH Cluster	89 (3.14%)	311.46 (0.53%)	328,437 (2.22%)
	Charlotte	Hot Spot	76 (2.68%)	1,221.87 (2.1%)	416,369 (2.82%)
		HH Cluster	31 (1.09%)	146.43 (0.25%)	107,736 (0.73%)
	Greenville	Hot Spot	122 (4.3%)	1,449.06 (2.49%)	550,979 (3.73%)
		HH Cluster	40 (1.41%)	125.92 (0.22%)	126,269 (0.85%)
	Birmingham	Hot Spot	2 (0.07%)	155.71 (0.27%)	9,511 (0.06%)
		HH Cluster	10 (0.35%)	15.86 (0.03%)	38,877 (0.26%)
Subtotal	Hot Spot	1,056 (37.26%)	9,091.68 (15.59%)	5,891,655 (39.84%)	
	HH Cluster	454 (16.02%)	1,446.59 (2.48%)	2,199,874 (14.88%)	
Clustering Total			1,093 (38.57%)	9,197.66 (15.78%)	6,012,334 (40.66%)

Table 39 continued.

DMSP00	Atlanta	Hot Spot	610 (21.52%)	4,127.57 (7.08%)	3,821,179 (25.84%)
		HH Cluster	552 (19.48%)	2,605.66 (4.47%)	3,452,219 (23.35%)
	Raleigh - Greensboro	Hot Spot	436 (15.38%)	5,404.73 (9.27%)	2,255,609 (15.25%)
		HH Cluster *	153 (5.40%)	666.86 (1.14%)	784,421 (5.3%)
		HH Cluster **	140 (4.94%)	449.46 (0.77%)	555,520 (3.76%)
	Charlotte	Hot Spot	273 (9.63%)	2,740.73 (4.7%)	1,404,769 (9.5%)
		HH Cluster	230 (8.12%)	1,284.6 (2.2%)	1,162,374 (7.86%)
	Birmingham	Hot Spot	176 (6.21%)	1,831.97 (3.14%)	783,816 (5.3%)
		HH Cluster	29 (1.02%)	109.76 (0.19%)	137,717 (0.93%)
	Greenville	Hot Spot	10 (0.35%)	484.59 (0.83%)	75,424 (0.51%)
		HH Cluster	n/a	n/a	n/a
	Subtotal	Hot Spot	1,505 (53.11%)	14,589.59 (25.03%)	8,340,797 (56.4%)
		HH Cluster	1,104 (38.96%)	5,116.35 (8.78%)	6,092,251 (41.2%)
Clustering Total		1,505 (53.11%)	14,589.59 (25.03%)	8,340,797 (56.4%)	
The Piedmont Atlantic Subtotal	Hot Spot	1,647 (58.12%)	16,524.65 (28.34%)	8,986,532 (60.77%)	
	HH Cluster	1,217 (42.94%)	5,486.36 (9.41%)	6,529,514 (44.16%)	
The Piedmont Atlantic Morphological Clustering Total		1,660 (58.57%)	16,546.31 (28.38%)	9,034,885 (61.1%)	

HH Cluster* - Clustering around Raleigh

HH Cluster** - Clustering around Greensboro

Raleigh – Greensboro – Charlotte clustering areas apart from the Atlanta clustering area, even though they are located in the same megaregion. Concerning the megaregion boundary of RPA, therefore, the Piedmont Atlantic megaregion boundary is not likely to fit the morphological clustering and connection. It may be recommendable to consider being one region for the Raleigh – Greensboro – Charlotte clustering areas, in terms of morphological connection and integration. The total extent of Piedmont Atlantic clustering in terms of all morphological features analyzed thus far includes 1,660 census tracts being around 58.57% of the total Piedmont Atlantic census tracts; about 16,546.31 square miles equal approximately 28.38% of the total Piedmont Atlantic land area; and 9,034,885 total population being around 61.1% of the total population of the Piedmont Atlantic megaregion.

The Piedmont Atlantic morphological clustering map resulted finally represents the locations where high levels of land uses per capita, urbanized built environment, and nighttime socio-economic urban activities are clustered. The clustering areas of Raleigh – Greensboro, Charlotte, and Greenville seem to have morphological connections being physically close. The clustering areas of Atlanta and Birmingham, however, seem to be difficult to consider morphological connections with other clustering areas because of their physically distant locations. The final map also represents an exaggerated boundary for the Piedmont Atlantic megaregion in the morphological observations.

2.5. The Florida megaregion

1) Local clustering of 2000 population density

Figure 31 shows local clustering analysis results produced by using 2000 population density. Following the threshold of Density-based Sprawl Index, 2000 population density is categorized into three groups: rural areas population density (i.e., less than 200 persons per square mile), low population density areas (i.e., between 200 and 3,500 persons per square mile), and high population density areas (i.e., greater than 3,500 persons per square mile) (top left of figure). The general observation of the distribution of 2000 population density is that low and high population density are concentrated around Miami – West Palm Beach, Tampa, Orlando, Jacksonville, Key West, Daytona Beach, Melbourne, and Cape Coral.

Table 40 Florida 2000 population density hot spots descriptors

Clustering Areas	Census Tracts	Land Area (sq. mi)	2000 Total Population
	2,889 (100%)	36,401.4 (100%)	14,619,179 (100%)
Miami	732 (25.34%)	2,952.74 (8.11%)	4,319,273 (29.55%)
Tampa	159 (5.5%)	166.35 (0.46%)	680,049 (4.65%)
Total	891 (30.84%)	3,119.09 (8.57%)	4,999,322 (34.2%)

The statistically significant hot spots at the 0.05 alpha level, as a result of Getis-Ord G_i^* analysis in terms of 2000 population density, represent dual-centric clustering (top right of figure). Hot spots are spatially concentrated in the areas around Miami and the outskirts of Tampa. Table 40 shows hot spot descriptors of 2000 population density for Florida. The

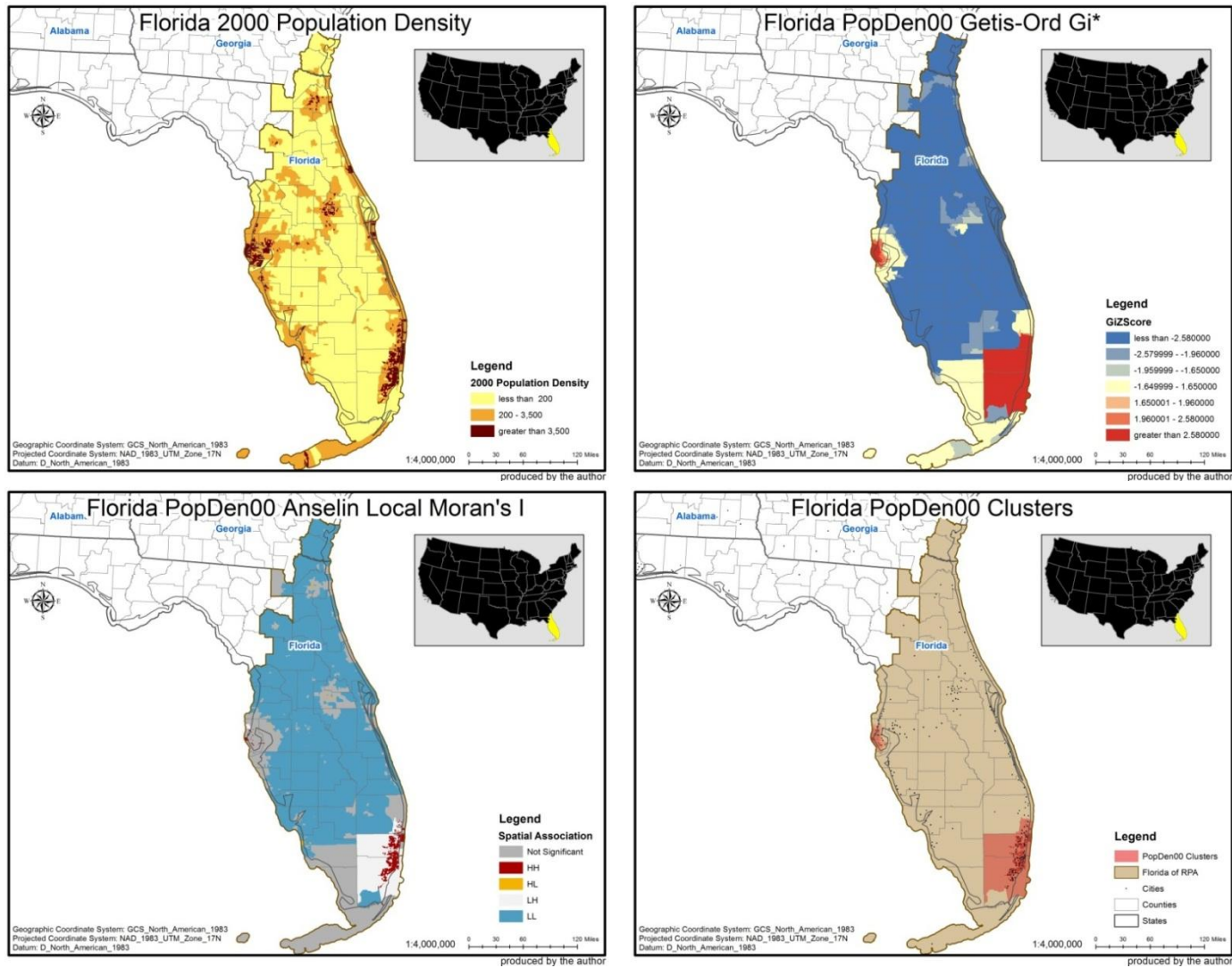


Figure 31 The Florida megaregion local clustering analysis results by 2000 population density

mean of 2000 population density is around 6,337 in comparison with the mean value of approximately 3,525.82 for the Florida megaregion. Resulted hot spots, therefore, indicate that the levels of land use per capita are similarly high within the hot spot boundary.

Table 41 Florida 2000 population density HH spatial association descriptors

Clustering Areas	Census Tracts	Land Area (sq. mi)	2000 Total Population
		2,889 (100%)	36,401.4 (100%)
Miami	509 (17.62%)	432.51 (1.19%)	3,157,810 (21.6%)
Tampa	14 (0.48%)	7.99 (0.02%)	57,172 (4.65%)
Total	523 (18.1%)	440.5 (1.21%)	3,214,982 (21.99%)

The HH spatial association, as a result of Anselin Local Moran's *I* analysis in terms of 2000 population density, also represents dual-centric clustering located in the same areas as result of hot spots analysis (bottom left of figure). The patterns HH spatial associations, however, are fractal and fragmented. Table 41 shows HH spatial associations descriptors of 2000 population density for Florida. The mean of 2000 population density is around 8,565.45 in comparison with the mean value of approximately 3,525.82 for the Florida megaregion. Resulted HH clustering areas, therefore, indicate that a high level of land use per capita is clustered with other similarly high levels of land use per capita within the resulted areas.

Morphological clustering, as a result of overlapping two analysis results in terms of 2000 population density, has the mostly same clustering boundary with Getis-Ord G_i^* analysis result (bottom right of figure). Only 1 census tract of HH spatial clustering is

not included in the result of Getis-Ord G_i^* analysis, which is located in the outskirts area of Tampa. The overlapping of the two clustering analysis results shows that the clustering pattern of 2000 population density is dual-centric around Miami and Tampa. The clustering pattern of 2000 population density also shows that the concentrations of clusters are repeated in coastal areas. Table 42 shows the total extent of 2000 population density clustering descriptors for Florida. The morphological clustering map represents, therefore, that the levels of land use per capita are similarly high and clustered within the clustering boundary. In terms of the clustering by 2000 population density, the Florida megaregion identified by RPA seems to have an exaggerated boundary.

Table 42 Florida 2000 population density clustering descriptors

Clustering Total	Census Tracts	Land Area (sq. mi)	2000 Total Population
	2,889 (100%)	36,401.4 (100%)	14,619,179 (100%)
2000 population density	892 (30.88%)	3,119.52 (8.57%)	5,003,343 (34.22%)

2) Local clustering of 2001 impervious land cover

Figure 32 shows local clustering analysis results produced by using 2001 impervious land cover. The general observation of the distribution of 2001 impervious land cover is that the highest degree of imperviousness in 2001 follows the spatial distribution of low and high population density (top left of figure). The impervious areas are likely clustered following coastal area such as Miami and Tampa.

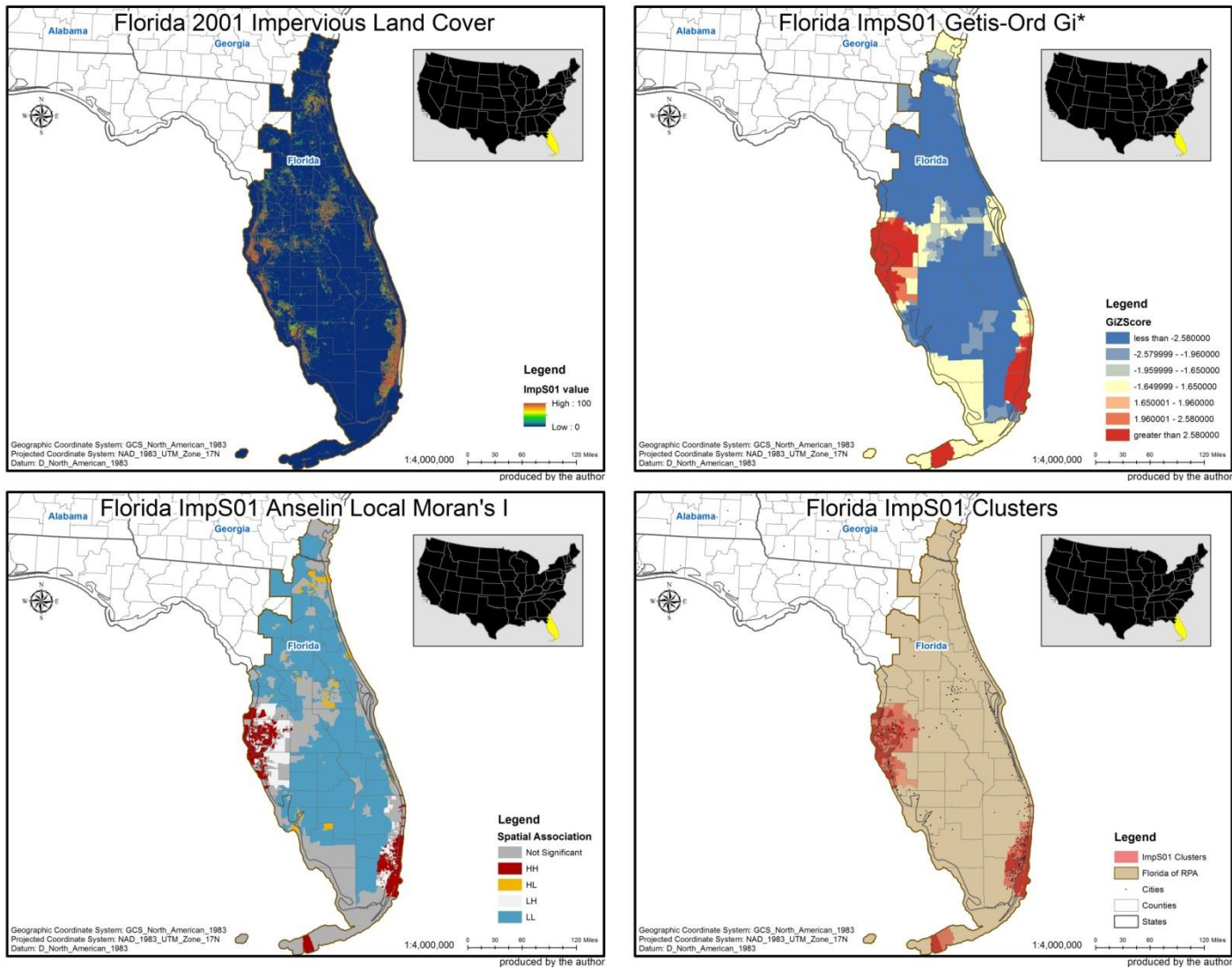


Figure 32 The Florida megaregion local clustering analysis results by 2001 impervious land cover

The statistically significant hot spots at the 0.05 alpha level, as a result of Getis-Ord G_i^* analysis in terms of 2001 impervious land cover, represent tri-centric clustering (top right of figure). Hot spots are spatially concentrated in the areas around Miami, Tampa, and Key West. Table 43 shows hot spots descriptors of 2001 impervious land cover for Florida. The mean of 2001 impervious land cover is around 49.55% in comparison with the mean value of approximately 23.96% for the Florida megaregion. Resulted hot spots, therefore, indicate that the urbanization levels of built environments are similarly high within the hot spot boundary.

Table 43 Florida 2001 impervious land cover hot spots descriptors

Clustering Areas	Census Tracts	Land Area (sq. mi)	2000 Total Population
		2,889 (100%)	36,401.4 (100%)
Miami	702 (24.3%)	1,042.45 (2.86%)	4,133,651 (28.28%)
Tampa	631 (21.84%)	2,347.83 (6.45%)	2,711,976 (18.55%)
Key West	11 (0.38%)	46.97 (0.13%)	39,054 (0.27%)
Total	1,344 (46.52%)	3,437.25 (9.44%)	6,884,681 (47.09%)

The HH spatial association, as a result of Anselin Local Moran's I analysis in terms of 2001 impervious land cover, also represents polycentric clustering located around the same areas with the result of hot spots analysis (bottom left of figure). They are spatially clustered around Miami, Tampa, and Key West. The clustering pattern, however, appears to be more fractal and fragmented than the hot spots clustering pattern. Table 44 shows HH spatial associations descriptors of 2001 impervious land cover for

Florida. The mean of 2001 impervious land cover is around 56.75% in comparison with the mean value of approximately 23.96% for the Florida megaregion. Resulted HH spatial associations, therefore, indicate that a high level of urbanization for built environments is clustered with other similarly highly urbanized built environments within the resulted areas.

Table 44 Florida 2001 impervious land cover HH spatial associations descriptors

Clustering Areas	Census Tracts	Land Area (sq. mi)	2000 Total Population
		2,889 (100%)	36,401.4 (100%)
Miami	328 (11.35%)	445.47 (1.22%)	1,939,408 (13.27%)
Tampa	328 (11.35%)	635.83 (1.75%)	1,415,178 (9.68%)
Key West	9 (0.31%)	13.93 (0.04%)	32,466 (0.22%)
Total	665 (23.02%)	1,095.24 (3.01%)	3,387,052 (23.17%)

Morphological clustering, as a result of overlapping two analysis results in terms of 2001 impervious land cover, has the similar clustering boundary with Getis-Ord G_i^* analysis result (bottom right of figure). Only 19 census tracts primarily located around Miami HH spatial associations are not included in the hot spots clustering areas. The overlapping observation shows that the clustering concentrations follow coastal line. Table 45 shows the total extent of 2001 impervious land cover clustering descriptors for Florida. The morphological clustering map represents, therefore, that the urbanization levels of these built environments are similarly high and clustered within the clustering boundary. In terms of the clustering by 2001 impervious land cover, the Florida

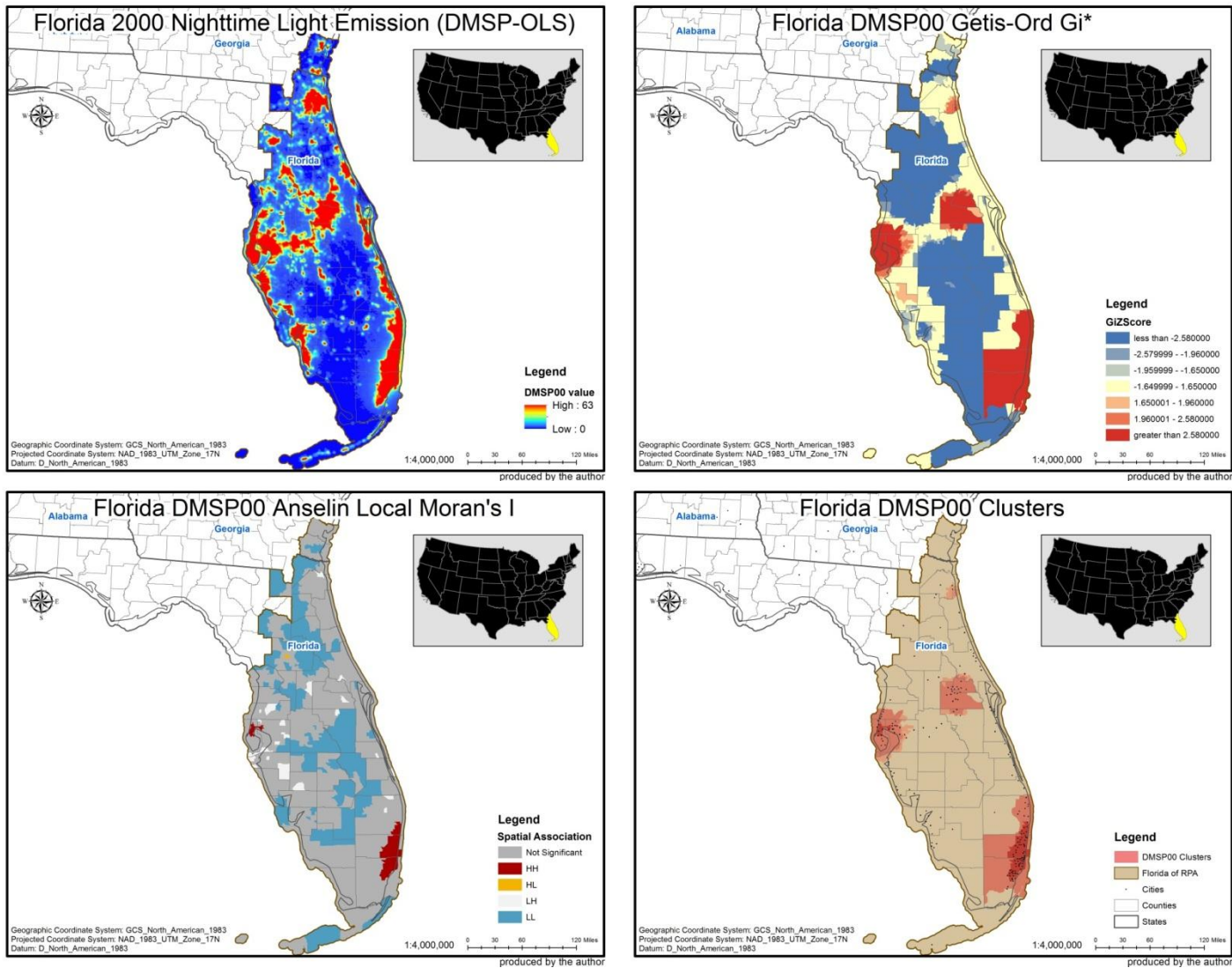


Figure 33 The Florida megaregion local clustering analysis results by 2000 nighttime light emissions

megaregion identified by RPA seems to have an exaggerated boundary.

Table 45 Florida 2001 impervious land cover clustering descriptors

Clustering Total	Census Tracts	Land Area (sq. mi)	2000 Total Population
	2,889 (100%)	36,401.4 (100%)	14,619,179 (100%)
2001 impervious land cover	1,363 (47.18%)	3,457.65 (9.5%)	6,941,227 (47.48%)

3) Local clustering of 2000 nighttime light emissions (DMSP-OLS)

Figure 33 shows local clustering analysis results produced by using 2000 nighttime light emissions (DMSP-OLS). The general observation of the distribution of 2000 nighttime light emissions is that the highest degree of nighttime light emissions in 2000 follows both distributions of 2000 population density and the 2001 impervious land cover (top left of figure).

The statistically significant hot spots at the 0.05 alpha level, as a result of Getis-Ord G_i^* analysis in terms of 2000 nighttime light emissions, represent polycentric clustering (top right of figure). Hot spots are spatially concentrated in the areas around Miami, Tampa, Orlando, and Jacksonville Beach. Compared to above local clustering analysis results for the Florida megaregion, it is noticeable that the Orlando clustering areas is resulted by 2000 nighttime light emissions. Table 46 shows hot spots descriptors of 2000 nighttime light emissions for Florida. The mean of 2000 nighttime light emissions is around 62.1% in comparison with the mean value of approximately 53.3% for the Florida megaregion. Resulted hot spots, therefore, indicate that the urban

development levels caused by nighttime socio-economic activities are similarly high within the hot spot boundary.

Table 46 Florida 2000 nighttime light emissions hot spots descriptors

Clustering Areas	Census Tracts	Land Area (sq. mi)	2000 Total Population
		2,889 (100%)	36,401.4 (100%)
Miami	879 (30.43%)	3,273.53 (8.99%)	4,946,647 (33.84%)
Tampa	468 (16.2%)	1,098.18 (3.02%)	2,033,423 (13.91%)
Orlando	296 (10.25%)	1,394.5 (3.83%)	1,441,904 (9.86%)
Jacksonville Beach	18 (0.62%)	142.29 (0.39%)	138,891 (0.95%)
Total	1,661 (57.49%)	5,908.5 (16.23%)	8,560,865 (58.56%)

The HH spatial association, as a result of Anselin Local Moran's *I* analysis in terms of 2000 nighttime light emissions, represents dual-centric clustering around Miami and Tampa (bottom left of figure). The Orlando clustering is disappeared in this HH spatial clustering analysis result. Table 47 shows HH spatial associations descriptors of 2000 nighttime light emissions for Florida. The mean of 2000 nighttime light emissions is around 62.97% in comparison with the mean value of approximately 53.3% for the Florida megaregion. Resulted HH spatial associations, therefore, indicate that a high level of urban development caused by nighttime socio-economic activities is clustered with other similarly high levels of nighttime socio-economic urban activities within the resulted areas.

Table 47 Florida 2000 nighttime light emissions HH spatial associations descriptors

Clustering Areas	Census Tracts	Land Area (sq. mi)	2000 Total Population
		2,889 (100%)	36,401.4 (100%)
Miami	647 (22.4%)	777.34 (2.14%)	3,802,835 (26.01%)
Tampa	67 (2.32%)	88.6 (0.24%)	329,566 (2.25%)
Total	714 (24.71%)	865.93 (2.38%)	4,132,401 (28.27%)

Morphological clustering, as a result of overlapping two analysis results in terms of 2000 nighttime light emissions, follows the clustering boundary resulted by Getis-Ord G_i^* analysis (bottom right of figure). The extent of 2000 nighttime light emissions clustering for the Florida megaregion, therefore, is identical to the extent of hot spot clustering. The overlapping of the two clustering analysis results shows that the clustering pattern of 2000 nighttime light emissions has three clustering concentrations in the areas around Miami, Tampa, and Orlando. The morphological clustering map represents, therefore, that the levels of urban development caused by nighttime socio-economic activities are similarly high and clustered within the clustering boundary. In terms of the clustering by 2000 nighttime light emissions, the Florida megaregion identified by RPA seems to have an exaggerated boundary.

4) Morphological local clustering

Figure 34 represents a result only produced by overlapping every clustering of the Getis-Ord G_i^* hot spots analysis (top of figure) and only by the Anselin Local Moran's I spatial cluster and outlier analysis (bottom of figure). As the final representation for the

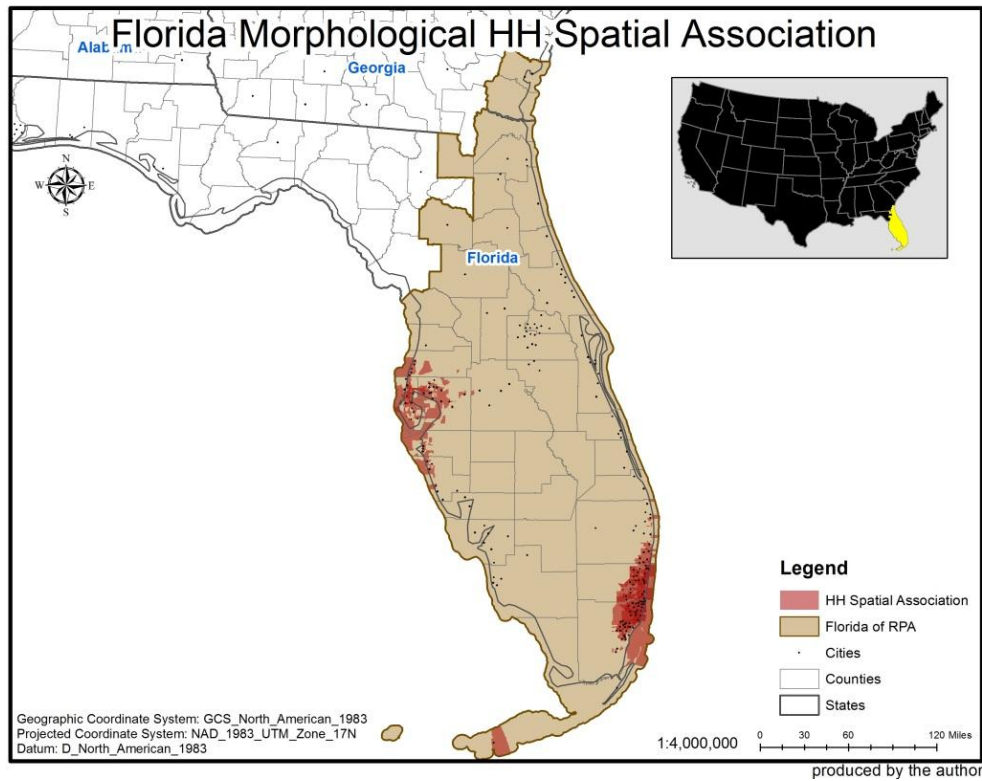
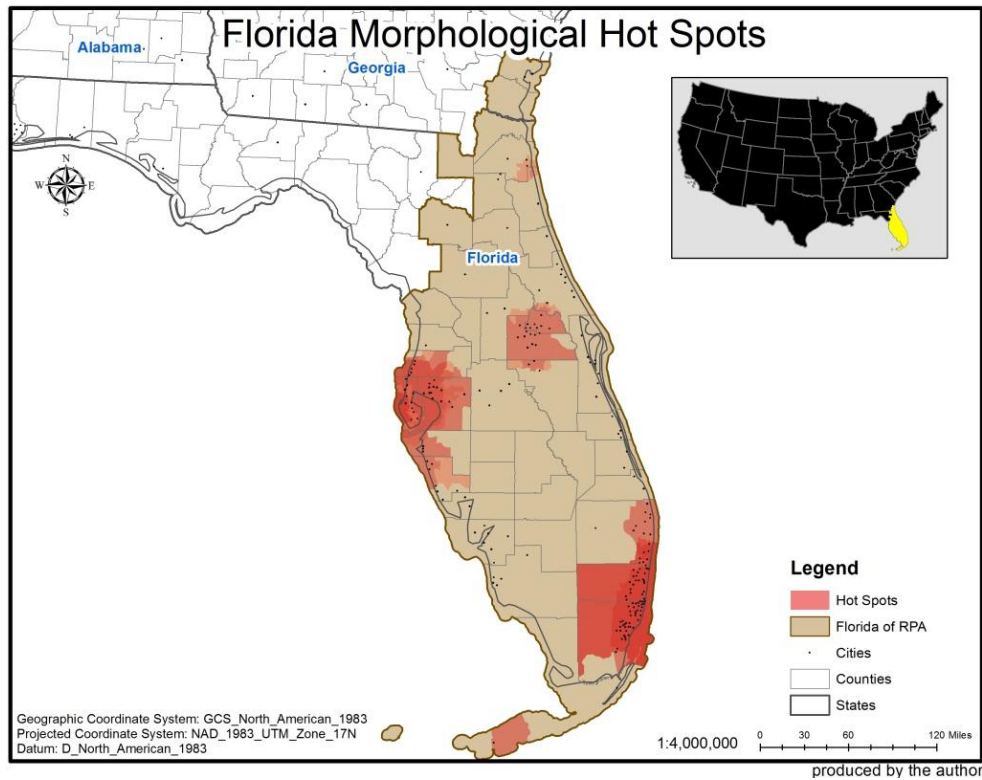


Figure 34 Local clusterings of morphological features in the Florida megaregion

Florida megaregion morphological clustering, Figure 35 represents a result produced by overlapping the results separately represented in Figure 34. Table 48 summarizes the Florida megaregion morphological clustering descriptors.

Representing polycentric morphological clustering for the Florida megaregion, the clustering around Miami and around Tampa are dominantly highlighted, meaning that the cities and the surrounding areas have an excess of morphological characteristics such as population density, impervious land cover, and nighttime light emissions (see Figure 35). The Orlando clustering may be connected morphologically to the Tampa clustering because of being physical close. The Tampa clustering, however, seems to be difficult to be connected morphologically to the Miami clustering because of being physically distant. Concerning the megaregion boundary of RPA, therefore, the Florida megaregion boundary is not likely to fit the morphological clustering and connection. The total extent of Florida clustering in terms of all morphological features analyzed thus far includes 1,837 census tracts being around 63.59% of the total Florida census tracts; about 7,306.87 square miles equal approximately 20.07% of the total Florida land area; and 9,283,626 total population sharing around 62.5% of the total population of the Florida megaregion.

The Florida morphological clustering map resulted finally represents the locations where high levels of land uses per capita, urbanized built environment, and nighttime socio-economic urban activities are clustered. The clusterings around Tampa and Orlando seem to have morphological interconnections because of being physically close. The Miami clustering, however, seems to be difficult to be connected morphologically to

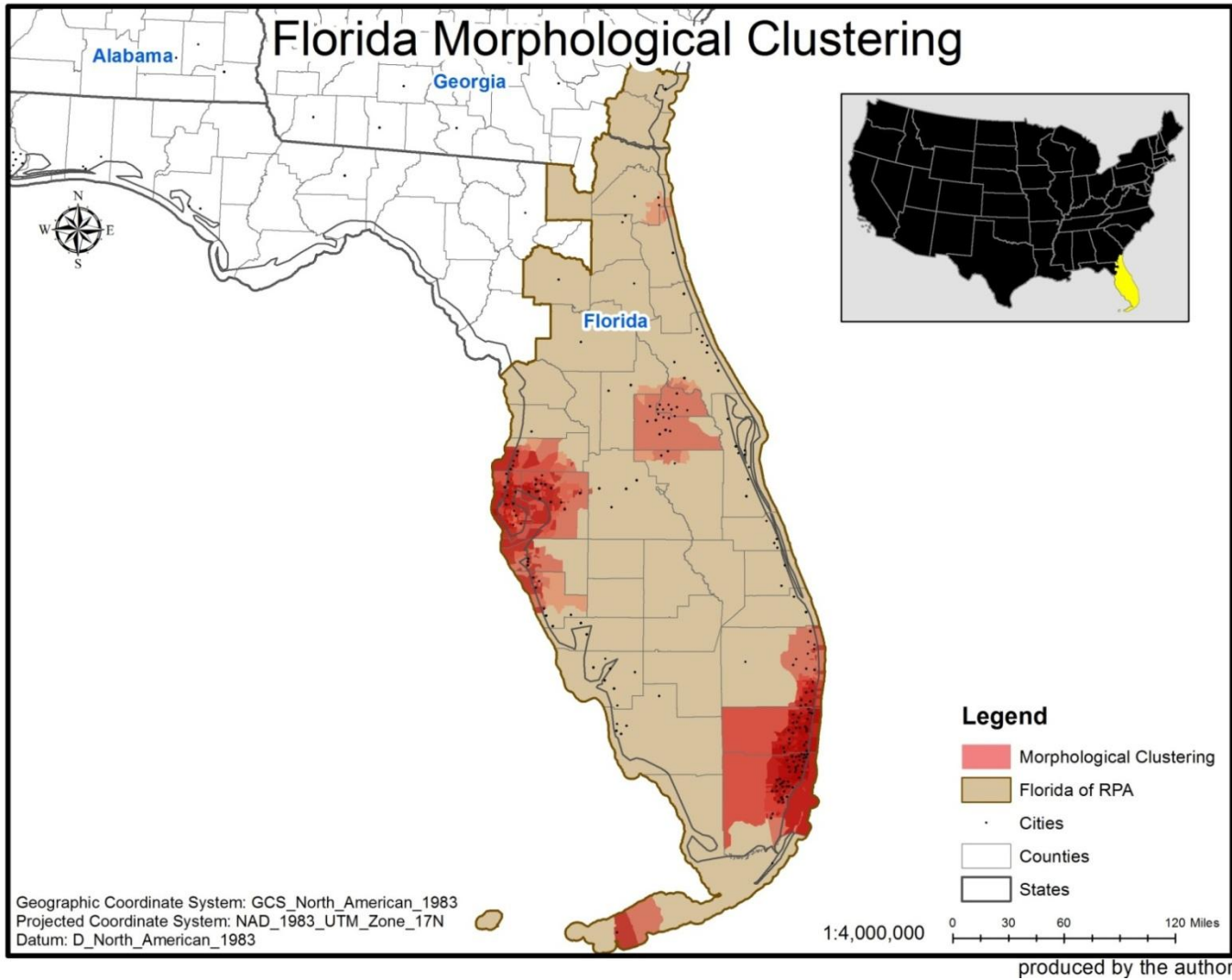


Figure 35 Morphological clusterings of the Florida megaregion

Table 48 The Florida megaregion morphological clusterings descriptors

Data Type	Clustering Area	Analysis	Florida Morphological Clusterings Descriptors		
			Census Tracts	Land Areas (sq. mi)	2000 Total Population
			2,889 (100%)	36,401.4 (100%)	14,619,179 (100%)
PopDen00	Miami	Hot Spot	732 (25.34%)	2,952.74 (8.11%)	4,319,273 (29.55%)
		HH Cluster	509 (17.62%)	432.51 (1.19%)	3,157,810 (21.6%)
	Tampa	Hot Spot	159 (5.5%)	166.35 (0.46%)	680,049 (4.65%)
		HH Cluster	14 (0.48%)	7.99 (0.02%)	57,172 (0.39%)
	Subtotal	Hot Spot	891 (30.84%)	3,119.09 (8.57%)	4,999,322 (34.2%)
		HH Cluster	523 (18.1%)	440.5 (1.21%)	3,214,982 (21.99%)
Clustering Total			892 (30.88%)	3,119.52 (8.57%)	5,003,343 (34.22%)
ImpS01	Miami	Hot Spot	702 (24.3%)	1,042.45 (2.86%)	4,133,651 (28.28%)
		HH Cluster	328 (11.35%)	445.47 (1.22%)	1,939,408 (13.27%)
	Tampa	Hot Spot	631 (21.84%)	2,347.83 (6.45%)	2,711,976 (18.55%)
		HH Cluster	328 (11.35%)	635.83 (1.75%)	1,415,178 (9.68%)
	Key West	Hot Spot	11 (0.38%)	46.97 (0.13%)	39,054 (0.27%)
		HH Cluster	9 (0.31%)	13.93 (0.04%)	32,466 (0.22%)
	Subtotal	Hot Spot	1,344 (46.52%)	3,437.25 (9.44%)	6,884,681 (47.09%)
		HH Cluster	665 (23.02%)	1,095.24 (3.01%)	3,387,052 (23.17%)
Clustering Total			1,363 (47.18%)	3,457.65 (9.5%)	6,941,227 (47.48%)
DMSP00	Miami	Hot Spot	879 (30.43%)	3,273.53 (8.99%)	4,946,647 (33.84%)
		HH Cluster	647 (22.4%)	777.34 (2.14%)	3,802,835 (26.01%)
	Tampa	Hot Spot	468 (16.2%)	1,098.18 (3.02%)	2,033,423 (13.91%)
		HH Cluster	67 (2.32%)	88.6 (0.24%)	329,566 (2.25%)
	Orlando	Hot Spot	296 (10.25%)	1,394.5 (3.83%)	1,441,904 (9.86%)
		HH Cluster	n/a	n/a	n/a
	Jacksonville Beach	Hot Spot	18 (0.62%)	142.29 (0.39%)	138,891 (0.95%)
		HH Cluster	n/a	n/a	n/a

Table 48 continued.

DMSP00	Subtotal	Hot Spot	1,661 (57.49%)	5,908.5 (16.23%)	8,560,865 (58.56%)
		HH Cluster	714 (24.71%)	865.93 (2.38%)	4,132,401 (28.27%)
	Clustering Total		1,661 (57.49%)	5,908.5 (16.23%)	8,560,865 (58.56%)
The Florida Subtotal		Hot Spot	1,836 (63.55%)	7,299.9 (20.05%)	9,282,802 (63.5%)
		HH Cluster	1,064 (36.83%)	1,591.32 (4.37%)	5,660,777 (38.72%)
The Florida Morphological Clustering Total			1,837 (63.59%)	7,306.87 (20.07%)	9,283,626 (63.5%)

other clusterings because of being physically distant. The final map also represents an exaggerated boundary for the Florida megaregion in the morphological observations.

2.6. The Gulf Coast megaregion

1) Local clustering of 2000 population density

Figure 36 shows local clustering analysis results produced by using 2000 population density. Following the threshold of Density-based Sprawl Index, 2000 population density is categorized into three groups: rural areas population density (i.e., less than 200 persons per square mile), low population density areas (i.e., between 200 and 3,500 persons per square mile), and high population density areas (i.e., greater than 3,500 persons per square mile) (top left of figure). The general observation of the distribution of 2000 population density is that low and high population density are concentrated around Houston – Galveston, Beaumont – Port Arthur, Corpus Christi, McAllen – Brownsville, Texas; Lake Charles, Lafayette, Baton Rouge, New Orleans, Louisiana; Biloxi, Mississippi; Mobile, Alabama; and Pensacola, Florida.

The statistically significant hot spots at the 0.05 alpha level, as a result of Getis-Ord G_i^* analysis in terms of 2000 population density, represent dual-centric clustering (top right of figure). Hot spots are spatially concentrated in the areas around Houston – Galveston and New Orleans. Even though clustering around the outskirts of Brownville is also resulted, it includes only 1 census tract in the clustering. Table 49 shows hot spot descriptors of 2000 population density for Gulf Coast. The mean of 2000 population density is around 5,468.19 in comparison with the mean value of approximately 3,166.12

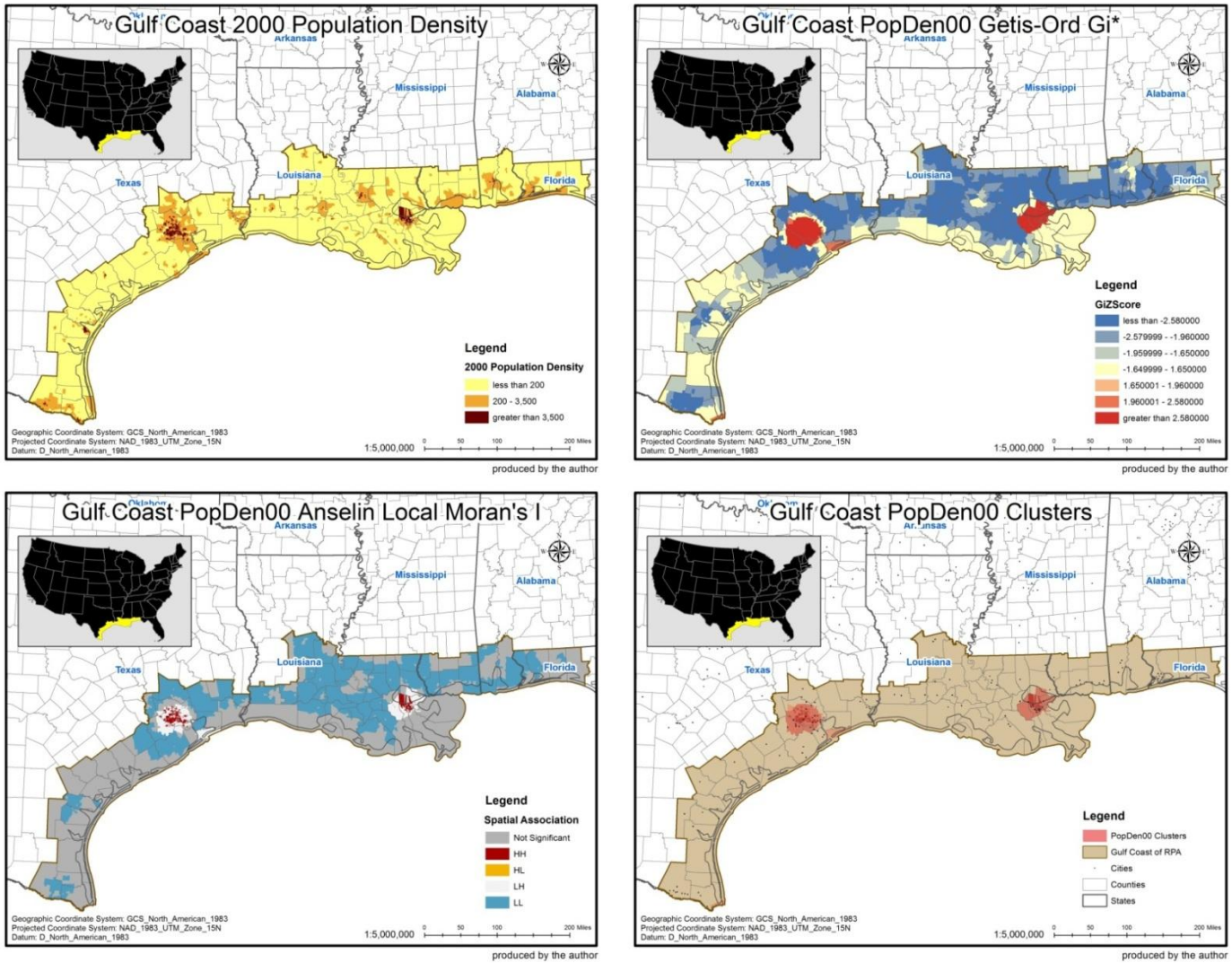


Figure 36 The Gulf Coast megaregion local clustering analysis results by 2000 population density

for the Gulf Coast megaregion. Resulted hot spots, therefore, indicate that the levels of land use per capita are similarly high within the hot spot boundary.

Table 49 Gulf Coast 2000 population density hot spots descriptors

Clustering Areas	Census Tracts	Land Area (sq. mi)	2000 Total Population
		2,494 (100%)	56,650.56 (100%)
Houston – Galveston	647 (25.94%)	1,708.51 (3.02%)	3,417,502 (29.19%)
New Orleans	337 (13.51%)	718.29 (1.27%)	1,069,147 (9.13%)
Total	985 (39.49%)	2,476.85 (4.37%)	4,490,936 (38.36%)

The HH spatial association, as a result of Anselin Local Moran's *I* analysis in terms of 2000 population density, also represents dual-centric clustering (bottom left of figure). The HH spatial association of 2000 population density, compared to the hot spot clustering, the spatial concentration is in Houston excluding Galveston. The clustering extent of New Orleans is also smaller than the hot spot clustering. The clustering around the outskirts of Brownsville includes only 6 census tracts. Table 50 shows HH spatial associations descriptors of 2000 population density for Gulf Coast. The mean of 2000 population density is around 7,815.99 in comparison with the mean value of approximately 3,166.12 for the Gulf Coast megaregion. Resulted HH spatial associations, therefore, indicate that a high level of land use per capita is clustered with other similarly high levels of land use per capita within the resulted areas.

Table 50 Gulf Coast 2000 population density HH spatial associations descriptors

Clustering Areas	Census Tracts	Land Area (sq. mi)	2000 Total Population
		2,494 (100%)	56,650.56 (100%)
Houston	329 (13.19%)	299.42 (0.53%)	1,877,426 (16.03%)
New Orleans	262 (10.51%)	113.84 (0.2%)	824,690 (7.04%)
Total	597 (23.94%)	415.31 (0.73%)	2,723,257 (23.26%)

Morphological clustering, as a result of overlapping two analysis results in terms of 2000 population density, has the same clustering boundary with Getis-Ord G_i^* analysis result, except the Brownsville clustering (bottom right of figure). Only 6 census tracts of Brownsville are not included in the hot spots analysis result, but included in the HH spatial clustering analysis result. The overlapping of the two clustering analysis results shows that the clustering pattern of 2000 population density is dual-centric around Houston – Galveston and New Orleans. The clustering pattern of 2000 population density also shows that the concentrations of clusters are duplicated in the central Houston and Miami areas. Table 51 shows the total extent of 2000 population density clustering descriptors for Gulf Coast. The morphological clustering map represents, therefore, that the levels of land use per capita are similarly high and clustered within the clustering boundary. In terms of the clustering by 2000 population density, the Gulf Coast megaregion identified by RPA seems to have an exaggerated boundary.

Table 51 Gulf Coast 2000 population density clustering descriptors

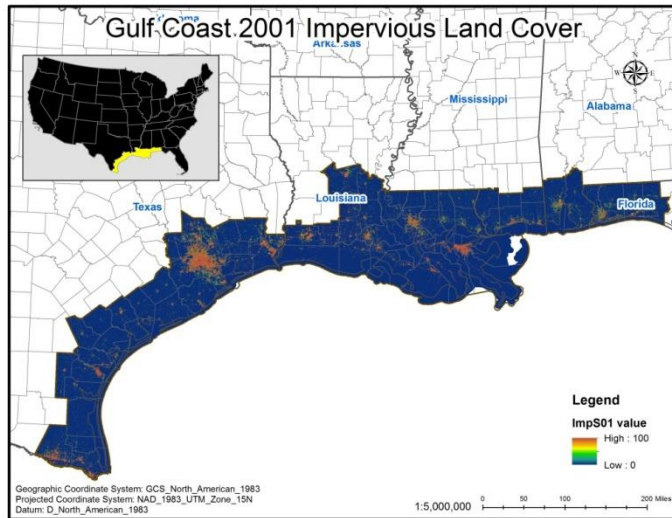
Clustering Total	Census Tracts	Land Area (sq. mi)	2000 Total Population
	2,494 (100%)	56,650.56 (100%)	11,708,826 (100%)
2000 population density	991 (39.74%)	2,478.9 (4.38%)	4,512,077 (38.54%)

2) Local clustering of 2001 impervious land cover

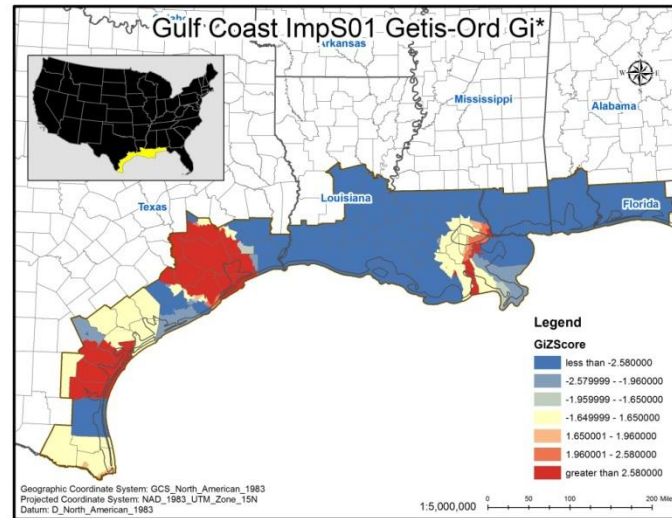
Figure 37 shows local clustering analysis results produced by using 2001 impervious land cover. The general observation of the distribution of 2001 impervious land cover is that the highest degree of imperviousness in 2001 follows the spatial distribution of 2000 low and high population density (top left of figure). The dominant concentration of 2000 impervious land cover is located around Houston.

The statistically significant hot spots at the 0.05 alpha level, as a result of Getis-Ord G_i^* analysis in terms of 2001 impervious land cover, represent tri-centric clustering (top right of figure). Hot spots are spatially concentrated in the areas around Houston – Galveston, Corpus Christi, and Miami. Table 52 shows hot spots descriptors of 2001 impervious land cover for Gulf Coast. The mean of 2001 impervious land cover is around 55.57% in comparison with the mean value of approximately 28.05% for the Gulf Coast megaregion. Resulted hot spots, therefore, indicate that the urbanization levels of built environments are similarly high within the hot spot boundary.

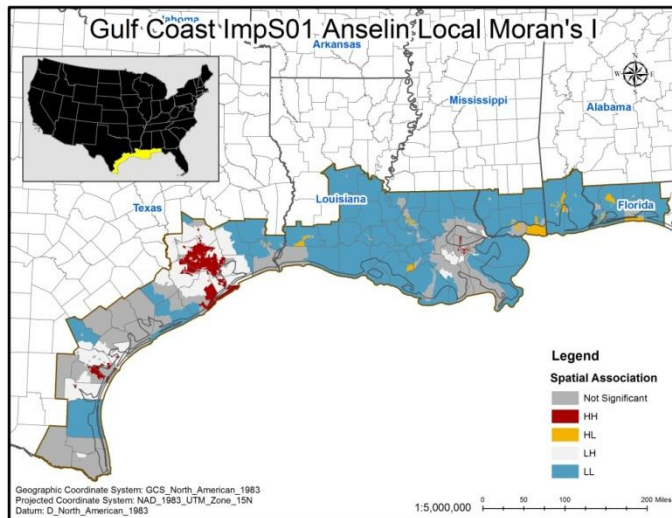
The HH spatial association, as a result of Anselin Local Moran's I analysis in terms of 2001 impervious land cover, also represents polycentric clustering located around the same areas with the result of hot spots analysis (bottom left of figure). The clustering pattern, however, appears to be more fractal and fragmented than the hot spot



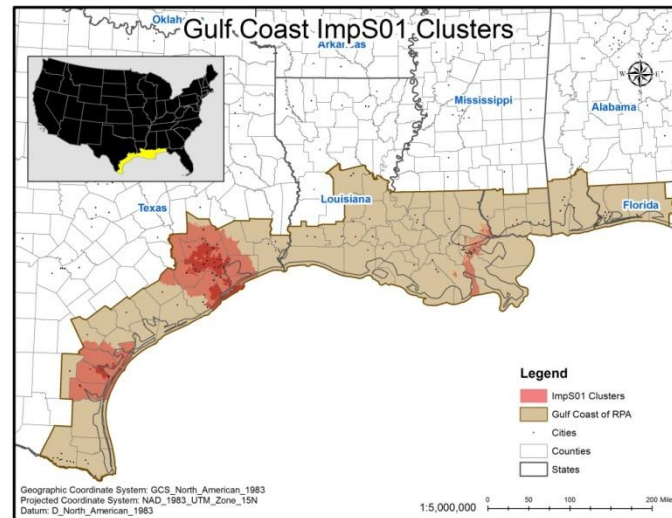
produced by the author



produced by the author



produced by the author



produced by the author

Figure 37 The Gulf Coast megaregion local clustering analysis results by 2001 impervious land cover

Table 52 Gulf Coast 2001 impervious land cover hot spots descriptors

Clustering Areas	Census Tracts	Land Area (sq. mi)	2000 Total Population
		2,494 (100%)	56,650.56 (100%)
Houston – Galveston	858 (34.4%)	6,338.03 (11.19%)	4,530,868 (38.7%)
Corpus Christi	90 (3.61%)	3,102.24 (5.32%)	440,325 (3.76%)
New Orleans	203 (8.14%)	626.68 (1.11%)	679,736 (5.81%)
Total	1,151 (46.15%)	9,976.95 (17.61%)	5,650,929 (48.26%)

clustering pattern. Table 53 shows HH spatial associations descriptors of 2001 impervious land cover for Gulf Coast. The mean of 2001 impervious land cover is around 61.68% in comparison with the mean value of approximately 28.05% for the Gulf Coast megaregion. Resulted HH spatial associations, therefore, indicate that a high level of urbanization for built environments is clustered with other similarly highly urbanized built environments within the resulted areas.

Table 53 Gulf Coast 2001 impervious land cover HH spatial associations descriptors

Clustering Areas	Census Tracts	Land Area (sq. mi)	2000 Total Population
		2,494 (100%)	56,650.56 (100%)
Houston – Galveston	633 (25.38%)	1,490.04 (2.63%)	3,373,323 (28.81%)
Corpus Christi	58 (2.33%)	179.76 (0.32%)	293,565 (2.51%)
New Orleans	57 (2.29%)	27.1 (0.05%)	129,371 (1.1%)
Total	752 (30.15%)	1,699.29 (3%)	3,806,260 (32.51%)

Morphological clustering, as a result of overlapping two analysis results in terms of 2001 impervious land cover, has the similar clustering boundary to Getis-Ord G_i^* analysis result (bottom right of figure). Only 20 census tracts of New Orleans clustering resulted by HH spatial clustering are not included in the hot spots areas. The overlapping observation represents that the clustering concentration is dominantly repeated in Houston – Galveston and Corpus Christi. Table 54 shows the total extent of 2001 impervious land cover clustering descriptors for Gulf Coast. The morphological clustering map represents, therefore, that the urbanization levels of these built environments are similarly high and clustered within the clustering boundary. In terms of the clustering by 2001 impervious land cover, the Gulf Coast megaregion identified by RPA seems to have an exaggerated boundary.

Table 54 Gulf Coast 2001 impervious land cover clustering descriptors

Clustering Total	Census Tracts	Land Area (sq. mi)	2000 Total Population
	2,494 (100%)	56,650.56 (100%)	11,708,826 (100%)
2001 impervious land cover	1,171 (46.95%)	9,990.06 (17.63%)	5,712,512 (48.79%)

3) Local clustering of 2000 nighttime light emissions (DMSP-OLS)

Figure 38 shows local clustering analysis results produced by using 2000 nighttime light emissions (DMSP-OLS). The general observation of the distribution of 2000 nighttime light emissions is that the highest degree of nighttime light emissions in 2000 follows both distributions of 2000 low and high population density and 2001 impervious land cover (top left of figure).

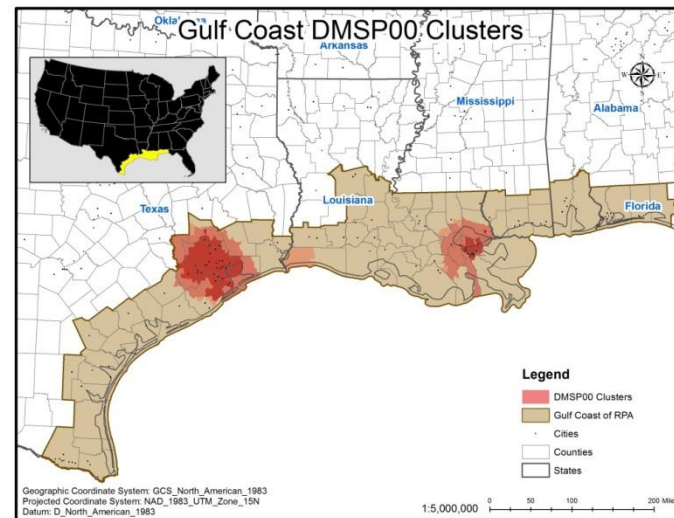
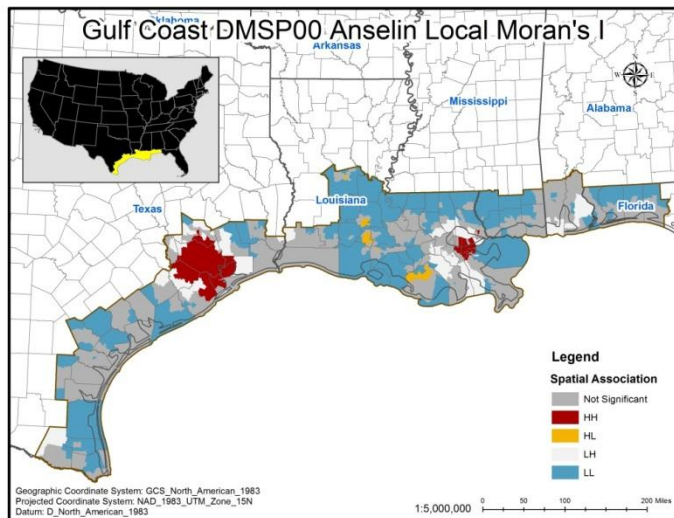
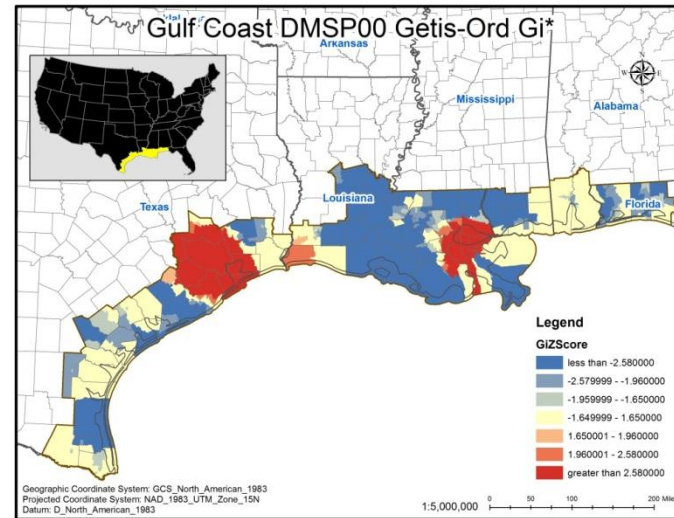
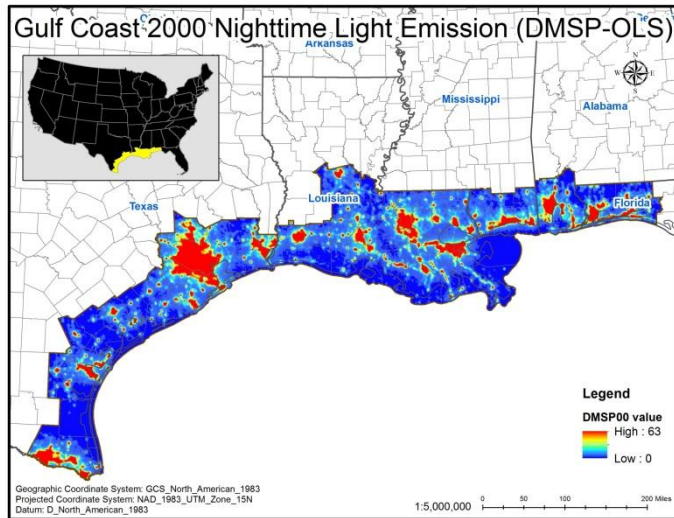


Figure 38 The Gulf Coast megaregion local clustering analysis results by 2000 nighttime light emissions

The statistically significant hot spots at the 0.05 alpha level, as a result of Getis-Ord G_i^* analysis in terms of 2000 nighttime light emissions, represent polycentric clustering (top right of figure). Hot spots are spatially concentrated in the areas around Houston – Galveston and Miami. Compared to above clustering analysis results for the Gulf Coast megaregion, it is noticeable that the clustering around the outskirts of Beaumont is resulted by 2000 nighttime light emissions. Table 55 shows hot spots descriptors of 2000 nighttime light emissions for Great Lakes. The mean of 2000 nighttime light emissions is around 59.65% in comparison with the mean value of approximately 49.32% for the Gulf Coast megaregion. Resulted hot spots, therefore, indicate that the urban development levels caused by nighttime socio-economic activities are similarly high within the hot spot boundary.

Table 55 Gulf Coast 2000 nighttime light emissions hot spots descriptors

Clustering Areas	Census Tracts	Land Area (sq. mi)	2000 Total Population
	2,494 (100%)	56,650.56 (100%)	11,708,826 (100%)
Houston – Galveston	857 (34.36%)	6,563.5 (11.59%)	4,521,273 (38.61%)
New Orleans	389 (15.6%)	2,165.25 (3.82%)	1,324,520 (11.31%)
Total	1,246 (49.96%)	8,728.75 (15.41%)	5,845,793 (49.93%)

The HH spatial association, as a result of Anselin Local Moran's I analysis in terms of 2000 nighttime light emissions, represents dual-centric clustering around Houston – Galveston and New Orleans (bottom left of figure). The clustering around the outskirts of Beaumont is disappeared in the HH spatial clustering analysis result. Table

56 shows HH spatial associations descriptors of 2000 nighttime light emissions for Gulf Coast. The mean of 2000 nighttime light emissions is around 62.42% in comparison with the mean value of approximately 49.32% for the Gulf Coast megaregion. Resulted HH spatial associations, therefore, indicate that a high level of urban development caused by nighttime socio-economic activities is clustered with other similarly high levels of nighttime socio-economic urban activities within the resulted areas.

Table 56 Gulf Coast 2000 nighttime light emissions HH spatial associations descriptors

Clustering Areas	Census Tracts	Land Area (sq. mi)	2000 Total Population
		2,494 (100%)	56,650.56 (100%)
Houston – Galveston	785 (31.48%)	3,049.52 (5.38%)	4,183,762 (35.73%)
New Orleans	307 (12.31%)	272 (0.48%)	944,254 (8.06%)
Total	1,092 (43.79%)	3,321.52 (5.86%)	5,128,016 (43.8%)

Morphological clustering, as a result of overlapping two analysis results in terms of 2000 nighttime light emissions, follows the clustering boundary in the result of Getis-Ord G_i^* analysis (bottom right of figure). The extent of 2000 nighttime light emissions clustering of the Gulf Coast megaregion, therefore, is identical to the extent of hot spot clustering. The overlapping of the two clustering analysis results represents that the clustering pattern of 2000 nighttime light emissions has two clustering concentrations in the areas around Houston – Galveston and New Orleans. The morphological clustering map represents, therefore, that the levels of urban development caused by nighttime socio-economic activities are similarly high and clustered within the clustering boundary.

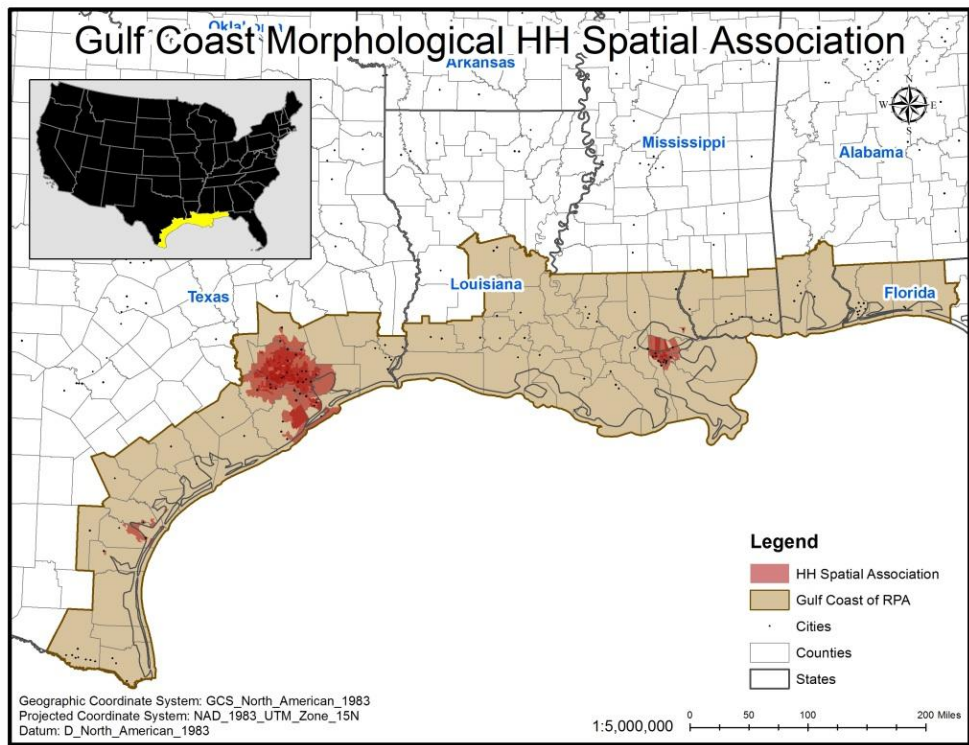
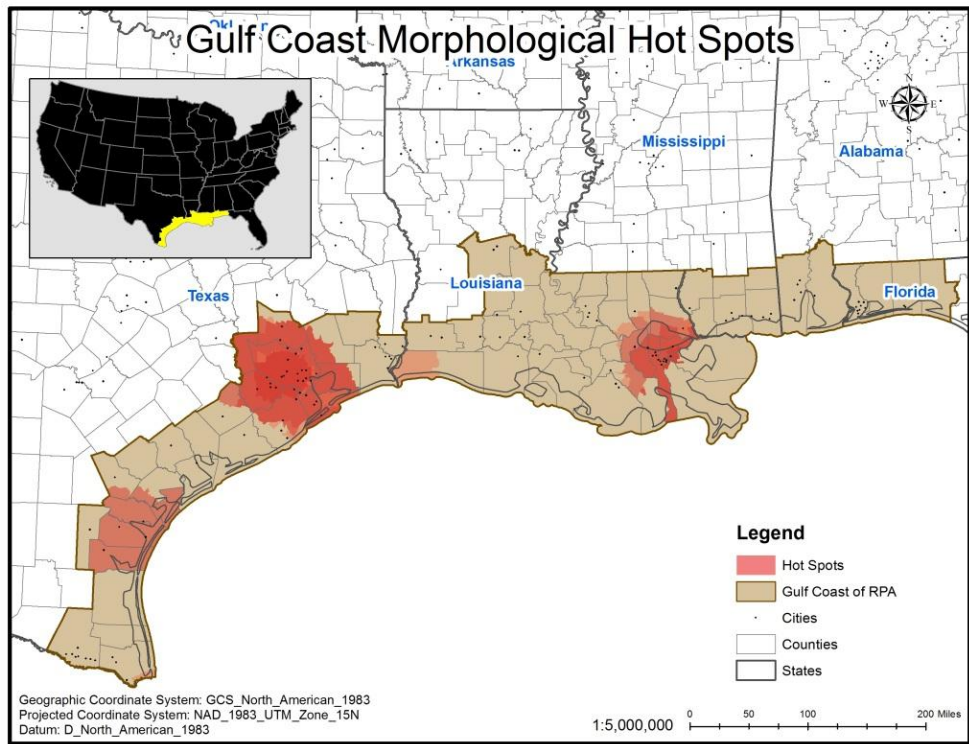


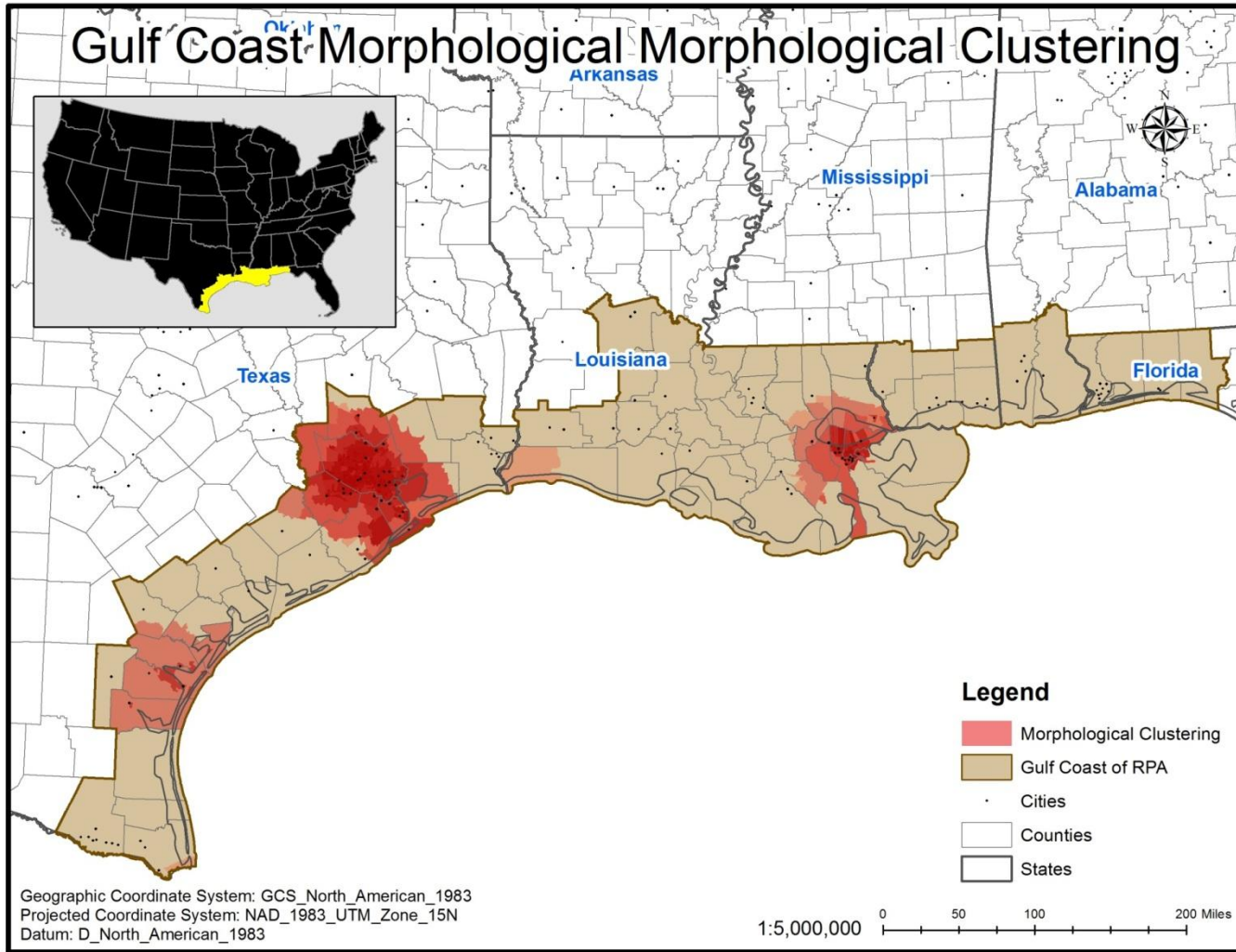
Figure 39 Local clustering of morphological features in the Gulf Coast megaregion

In terms of the clustering by 2000 nighttime light emissions, the Gulf Coast megaregion identified by RPA seems to have an exaggerated boundary.

4) Morphological local clustering

Figure 39 represents results only produced by overlapping every clustering of the Getis-Ord G_i^* hot spots analysis (top of figure) and only by overlapping every HH spatial cluster of the Anselin Local Moran's I spatial cluster and outlier analysis (bottom of figure). As the final representation for the Gulf Coast megaregion morphological clustering, Figure 40 represents a result produced by overlapping the results separately represented in Figure 39. Table 57 summarizes the Gulf Coast megaregion morphological clustering descriptors.

Representing polycentric morphological clustering for the Gulf Coast megaregion, the clusterings around Houston – Galveston and New Orleans are dominantly highlighted, meaning that the cities and the surrounding areas have an excess of morphological characteristics such as population density, impervious land cover, and nighttime light emissions (see Figure 40). The Corpus Christi clustering also has the morphological concentration such as impervious land cover, meaning that the area has an excess of urbanization feature (i.e., impervious land cover). The morphological interconnection between Houston – Galveston and New Orleans clustering seems to be problematic because of being physically distant. It may be also problematic to expect the morphological interconnection between Houston – Galveston and Corpus Christi clusterings. Concerning the megaregion boundary of RPA, therefore, the Gulf Coast



produced by the author

Figure 40 Morphological clusterings of the Gulf Coast megaregion

Table 57 The Gulf Coast megaregion morphological clusterings descriptors

Data Type	Clustering Area	Analysis	Gulf Coast Morphological Clusterings Descriptors			
			Census Tracts	Land Areas (sq. mi)	2000 Total Population	
			2,494 (100%)	56,650.56 (100%)	11,708,826 (100%)	
PopDen00	Houston - Galveston	Hot Spot	647 (25.94%)	1,708.51 (3.02%)	3,417,502 (29.19%)	
		HH Cluster*	329 (13.19%)	299.42 (0.53%)	1,877,426 (16.03%)	
	New Orleans	Hot Spot	337 (13.51%)	718.29 (1.27%)	1,069,147 (9.13%)	
		HH Cluster	262 (10.51%)	113.84 (0.2%)	824,690 (7.04%)	
	Brownsville	Hot Spot	1 (0.04%)	50.05 (0.09%)	4,287 (0.04%)	
		HH Cluster	6 (0.24%)	2.06 (0.004%)	21,141 (0.18%)	
	Subtotal	Hot Spot	985 (39.49%)	2,476.85 (4.37%)	4,490,936 (38.36%)	
		HH Cluster	597 (23.94%)	415.31 (0.73%)	2,723,257 (23.26%)	
	Clustering Total			991 (39.74%)	2,478.9 (4.38%)	4,512,077 (38.54%)
	ImpS01	Houston - Galveston	Hot Spot	858 (34.4%)	6,338.03 (11.19%)	4,530,868 (38.7%)
HH Cluster			633 (25.38%)	1,490.04 (2.63%)	3,373,323 (28.81%)	
Corpus Christi		Hot Spot	90 (3.61%)	3,012.24 (5.32%)	440,325 (3.76%)	
		HH Cluster	58 (2.33%)	179.76 (0.32%)	293,565 (2.51%)	
New Orleans		Hot Spot	203 (8.14%)	626.68 (1.11%)	679,736 (5.81%)	
		HH Cluster	57 (2.29%)	27.1 (0.05%)	129,371 (1.1%)	
Brownsville		Hot Spot	n/a	n/a	n/a	
		HH Cluster	4 (0.16%)	2.39 (0.004%)	10,001 (0.09%)	
Subtotal		Hot Spot	1,151 (46.15%)	9,976.95 (17.61%)	5,650,929 (48.26%)	
		HH Cluster	752 (30.15%)	1,699.29 (3%)	3,806,260 (32.51%)	
Clustering Total			1,171 (46.95%)	9,990.06 (17.63%)	5,712,512 (48.79%)	
DMSP00	Houston - Galveston	Hot Spot	857 (34.36%)	6,563.5 (11.59%)	4,521,273 (38.61%)	
		HH Cluster	785 (31.48%)	3,049.52 (5.38%)	4,183,762 (35.73%)	
	New Orleans	Hot Spot	389 (15.6%)	2,165.25 (3.82%)	1,324,520 (11.31%)	
		HH Cluster	307 (12.31%)	272 (0.48%)	944,254 (8.06%)	

Table 57 continued.

DMSP00	Subtotal	Hot Spot	1,246 (49.96%)	8,728.75 (15.41%)	5,845,793 (49.93%)
		HH Cluster	1,092 (43.79%)	3,321.52 (5.86%)	5,128,016 (43.8%)
	Clustering Total		1,246 (49.96%)	8,728.75 (15.41%)	5,845,793 (49.93%)
The Gulf Coast Subtotal	Hot Spot	1,341 (53.77%)	12,131.03 (21.41%)	6,310,789 (53.9%)	
	HH Cluster	1,179 (47.27%)	3,571.48 (6.3%)	5,524,918 (47.19%)	
The Gulf Coast Morphological Clustering Total		1,350 (54.13%)	12,135.24 (21.42%)	6,339,282 (54.14%)	

HH Cluster* - Clustering around Houston

megaregion boundary is not likely to fit the morphological clustering and connection. It is rather likely to expect a separate region for New Orleans clustering area from the Houston – Galveston clustering area. The total extent of Gulf Coast clustering in terms of all morphological features analyzed thus far includes 1,350 census tracts being around 54.13% of the total Gulf Coast census tracts; about 12,135.24 square miles equal approximately 21.42% of the total Gulf Coast land area; and 6,339,282 total population being around 54.14% of the total population of the Gulf Coast megaregion.

The Gulf Coast morphological clustering map resulted finally represents the locations where high levels of land uses per capita, urbanized built environment, and nighttime socio-economic urban activities are clustered. The clusterings around Houston – Galveston, New Orleans, and Corpus Christi seem to be difficult to be interconnected morphologically because of being physically distant. The final map also represents an exaggerated boundary for the Gulf Coast megaregion in the morphological observations.

2.7. The Front Range megaregion

1) Local clustering of 2000 population density

Figure 41 shows local clustering analysis results produced by using 2000 population density. Following the threshold of Density-based Sprawl Index, 2000 population density is categorized into three groups: rural areas population density (i.e., less than 200 persons per square mile), low population density areas (i.e., between 200 and 3,500 persons per square mile), and high population density areas (i.e., greater than 3,500 persons per square mile) (top left of figure). The general observation of the

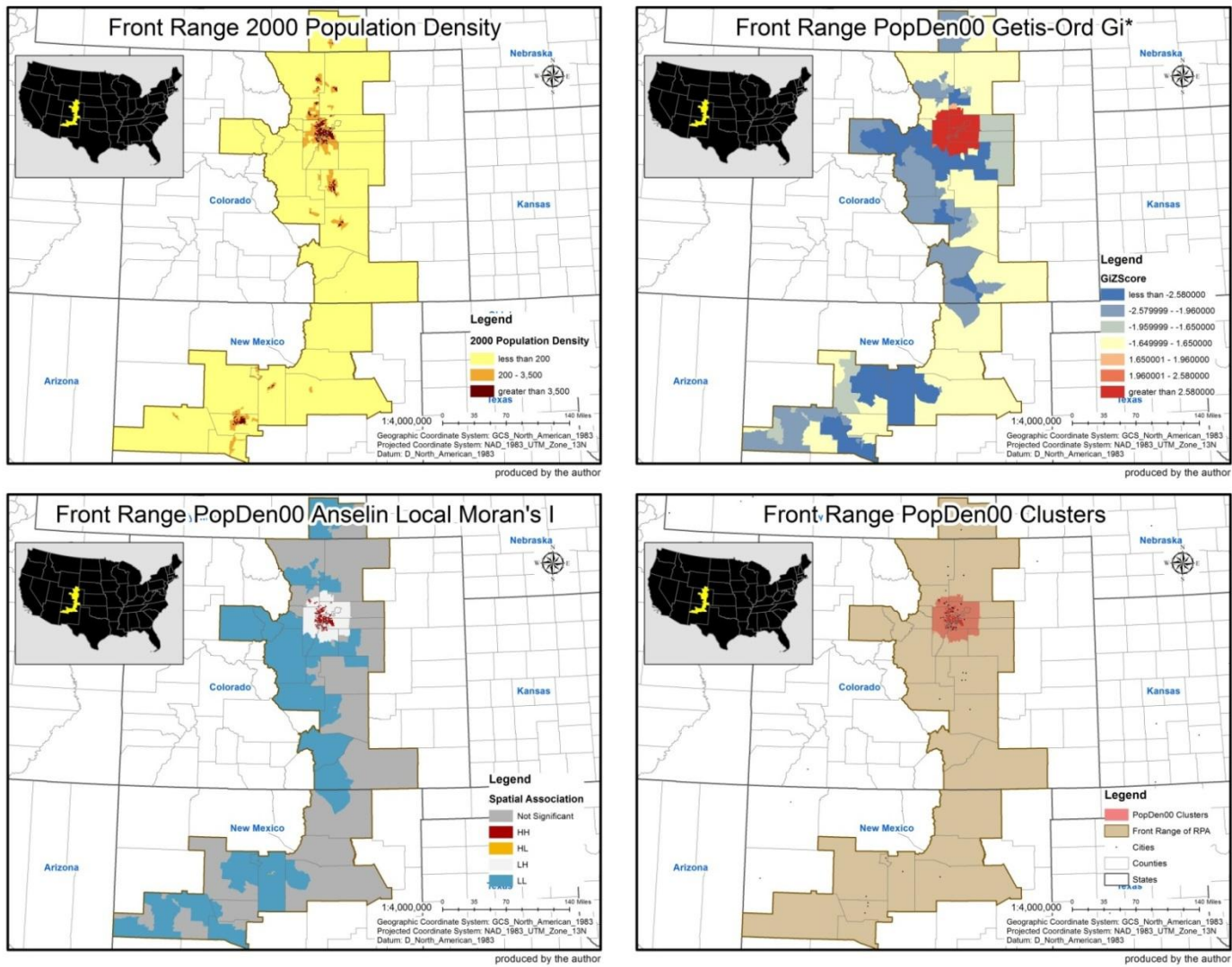


Figure 41 The Front Range megaregion local clustering analysis results by 2000 population density

distribution of 2000 population density is that low and high population density are concentrated in the areas around Denver, Colorado Springs, Cheyenne, Fort Collins, Canon, and Pueblo, Colorado; and Albuquerque, New Mexico.

The statistically significant hot spots at the 0.05 alpha level, as a result of Getis-Ord G_i^* analysis in terms of 2000 population density, represent monocentric clustering (top right of figure). Hot spots are spatially concentrated in the areas around Denver. Table 58 shows hot spot descriptors of 2000 population density for Front Range. The mean of 2000 population density is around 4,659.5 in comparison with the mean value of approximately 3,484.95 for the Front Range megaregion. Resulted hot spots, therefore, indicate that the levels of land use per capita are similarly high within the hot spot boundary.

Table 58 Front Range 2000 population density hot spots descriptors

Clustering Areas	Census Tracts	Land Area (sq. mi)	2000 Total Population
		1,163 (100%)	56,502.07 (100%)
Denver	554 (47.64%)	2,184 (3.87%)	2,286,376 (48.52%)

The HH spatial association, as a result of Anselin Local Moran's I analysis in terms of 2000 population density, also represents monocentric clustering (bottom left of figure). The morphological extent of Denver clustering by the HH spatial clustering analysis is smaller than the extent resulted by the hot spots analysis. Resulted the clustering pattern of HH spatial associations is more fractal and fragmented. Table 59 shows HH spatial associations descriptors of 2000 population density for Front Range.

The mean of 2000 population density is around 6,824.8 in comparison with the mean value of approximately 3,484.95 for the Front Range megaregion. Resulted HH spatial associations, therefore, indicate that a high level of land use per capita is clustered with other similarly high levels of land use per capita within the resulted areas.

Table 59 Front Range 2000 population density HH spatial associations descriptors

Clustering Areas	Census Tracts	Land Area (sq. mi)	2000 Total Population
		1,163 (100%)	56,502.07 (100%)
Denver	310 (26.66%)	220.46 (0.39%)	1,372,050 (29.12%)

Morphological clustering, as a result of overlapping two analysis results in terms of 2000 population density, has the same clustering boundary as Getis-Ord G_i^* analysis result (bottom right of figure). The extent of 2000 population density clustering of the Front Range megaregion, therefore, is identical to the extent of hot spot clustering. The overlapping of the two clustering analysis results shows that the clustering pattern of 2000 population density has the concentration in the areas of Denver. The morphological clustering map represents, therefore, that the levels of land use per capita are similarly high and clustered within the clustering boundary. In terms of the clustering by 2000 population density, the Front Range megaregion identified by RPA seems to have an exaggerated boundary.

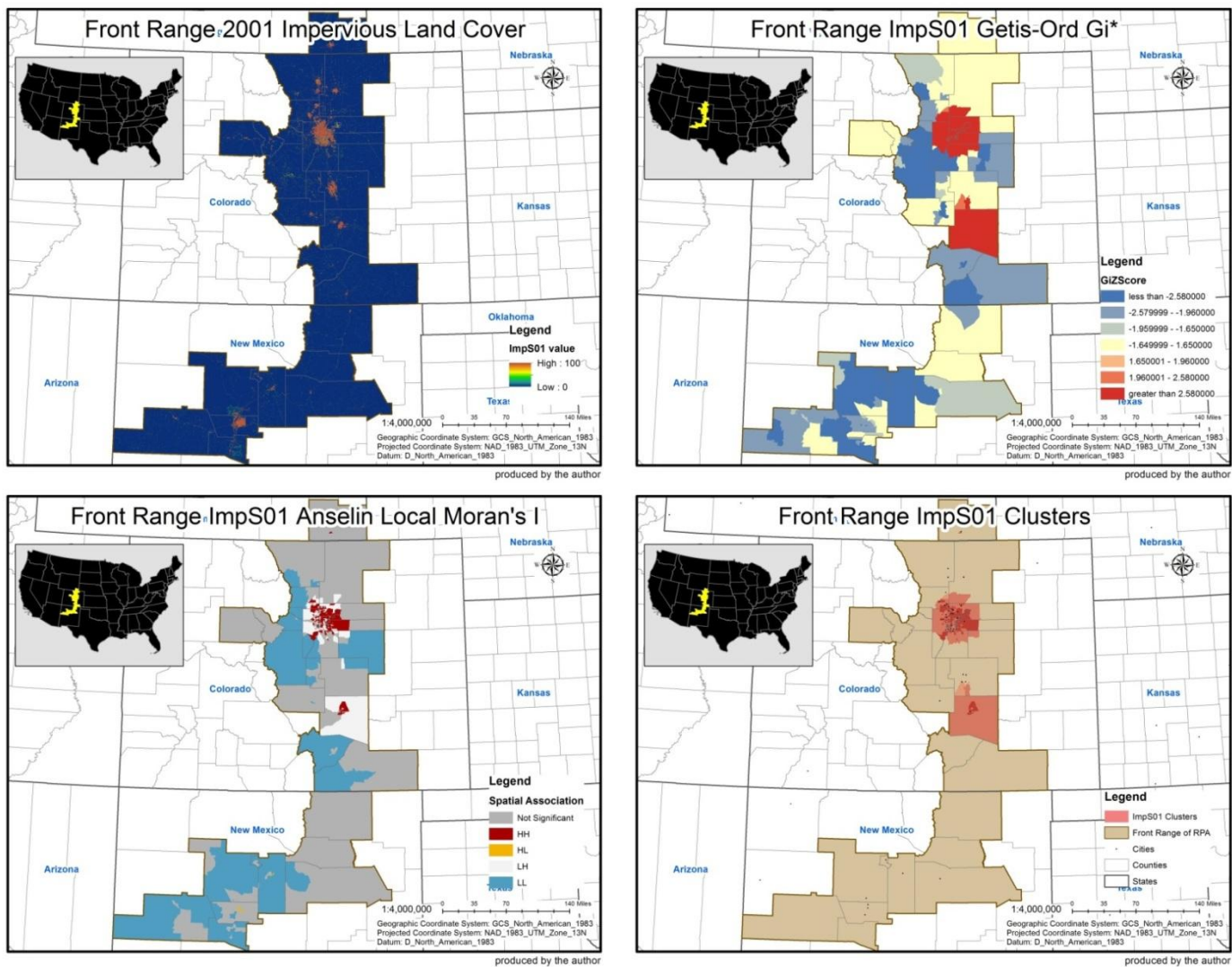


Figure 42 The Front Range megaregion local clustering analysis results by 2001 impervious land cover

2) Local clustering of 2001 impervious land cover

Figure 42 shows local clustering analysis results produced by using 2001 impervious land cover. The general observation of the distribution of 2001 impervious land cover is that the highest degree of imperviousness in 2001 follows the distribution of 2000 low and high population density (top left of figure). The most noticeable concentrations of 2000 impervious land cover are located around Denver, Colorado Springs, and Albuquerque.

The statistically significant hot spots at the 0.05 alpha level, as a result of Getis-Ord G_i^* analysis in terms of 2001 impervious land cover, represent dual-centric clustering (top right of figure). Hot spots are spatially concentrated in the areas of Denver and Pueblo. Table 60 shows hot spots descriptors of 2001 impervious land cover for Front Range. The mean of 2001 impervious land cover is around 47.35% in comparison with the mean value of approximately 23.96% for the Front Range megaregion. Resulted hot spots, therefore, indicate that the urbanization levels of built environments are similarly high within the hot spot boundary.

Table 60 Front Range 2001 impervious land cover hot spots descriptors

Clustering Areas	Census Tracts	Land Area (sq. mi)	2000 Total Population
	1,163 (100%)	56,502.07 (100%)	4,711,921 (100%)
Denver	558 (47.98%)	2,328.17 (4.12%)	2,308,560 (48.99%)
Pueblo	53 (4.56%)	2,589.15 (4.58%)	159,657 (3.39%)
Total	611 (52.54%)	4,917.32 (8.7%)	2,468,217 (52.38%)

The HH spatial association, as a result of Anselin Local Moran's *I* analysis in terms of 2001 impervious land cover, also represents dual-centric clustering located around the same areas with the result of hot spots analysis (bottom left of figure). Even though the Cheyenne clustering is resulted, it includes only 2 census tracts. The clustering patterns of HH spatial associations are more fractal and fragmented and the extents of clusterings are smaller than the hot spots. Table 61 shows HH spatial associations descriptors of 2001 impervious land cover for Front Range. The mean of 2001 impervious land cover is around 53.66% in comparison with the mean value of approximately 23.96% for the Front Range megaregion. Resulted HH spatial associations, therefore, indicate that a high level of urbanization for built environments is clustered with other similarly highly urbanized built environments within the resulted areas.

Table 61 Front Range 2001 impervious land cover HH spatial associations descriptors

Clustering Areas	Census Tracts	Land Area (sq. mi)	2000 Total Population
		1,163 (100%)	56,502.07 (100%)
Denver	270 (23.22%)	780.1 (1.38%)	1,124,095 (23.86%)
Pueblo	27 (2.32%)	95.15 (0.17%)	76,791 (1.63%)
Cheyenne	2 (0.17%)	5.09 (0.01%)	8,170 (0.17%)
Total	299 (25.71%)	880.34 (1.56%)	1,209,056 (25.66%)

Morphological clustering, as a result of overlapping two analysis results in terms of 2001 impervious land cover, has the similar clustering boundary to Getis-Ord G_i^*

analysis result, except the clustering boundary of Cheyenne (bottom right of figure). The overlapping observation represents that the clusterings are dominantly concentrated in Denver and Pueblo. It is noticeable, compared to the morphological clustering of 2000 population density, for the appearance of a new clustering around Pueblo. Table 62 shows the total extent of 2001 impervious land cover clustering descriptors for Front Range. The morphological clustering map represents, therefore, that the urbanization levels of these built environments are similarly high and clustered within the clustering boundary. In terms of the clustering by 2001 impervious land cover, the Front Range megaregion identified by RPA seems to have an exaggerated boundary.

Table 62 Front Range 2001 impervious land cover clustering descriptors

Clustering Total	Census Tracts	Land Area (sq. mi)	2000 Total Population
		1,163 (100%)	56,502.07 (100%)
2001 impervious land cover	613 (52.71%)	4,922.41 (8.71%)	2,476,387 (52.56%)

3) Local clustering of 2000 nighttime light emissions (DMSP-OLS)

Figure 43 shows local clustering analyses results produced by using 2000 nighttime light emissions (DMSP-OLS). The general observation of the distribution of 2000 nighttime light emissions is that the highest degree of nighttime light emissions in 2000 follows both distributions of 2000 low and high population density and 2001 impervious land cover (top left of figure). It is noticeable, however, for the expansion of high degree of nighttime light emissions from Denver to other areas.

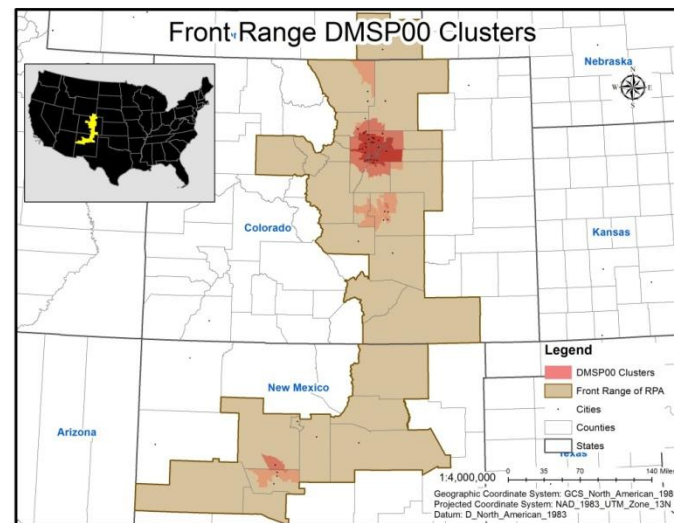
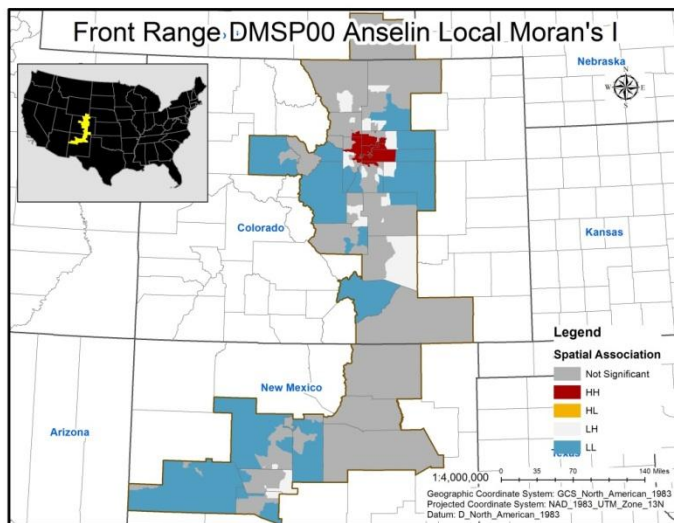
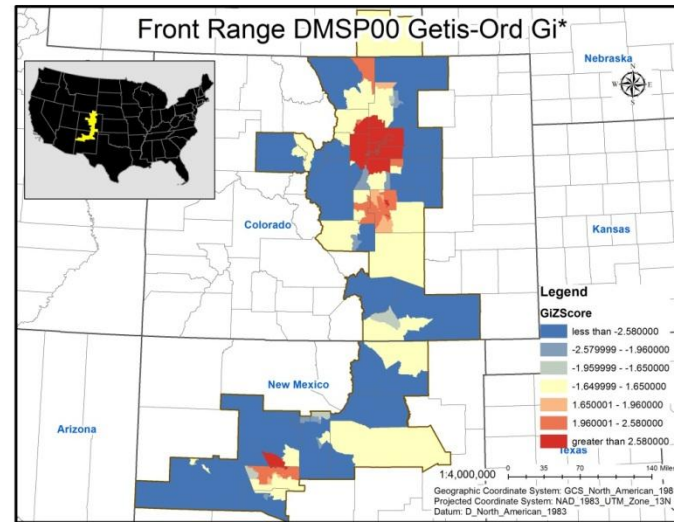
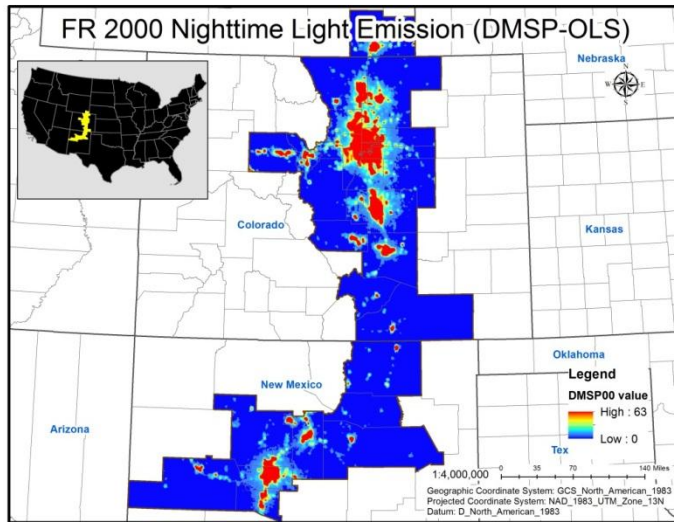


Figure 43 The Front Range megaregion local clustering analysis results by 2000 nighttime light emissions

The statistically significant hot spots at the 0.05 alpha level, as a result of Getis-Ord G_i^* analysis in terms of 2000 nighttime light emissions, represent polycentric clustering (top right of figure). Hot spots are spatially concentrated in the areas around Denver, Colorado Springs, Albuquerque, and Fort Collins. Compared to above clustering analysis results for the Front Range megaregion, it is noticeable for the new clustering areas such as Colorado Springs and Fort Collins. Table 63 shows hot spots descriptors of 2000 nighttime light emissions for Great Lakes. The mean of 2000 nighttime light emissions is around 59.91% in comparison with the mean value of approximately 51.16% for the Front Range megaregion. Resulted hot spots, therefore, indicate that the urban development levels caused by nighttime socio-economic activities are similarly high within the hot spot boundary.

Table 63 Front Range 2000 nighttime light emissions hot spots descriptors

Clustering Areas	Census Tracts	Land Area (sq. mi)	2000 Total Population
		1,163 (100%)	56,502.07 (100%)
Denver	558 (47.98%)	2,267.93 (4.01%)	2,307,320 (48.97%)
Colorado Springs	106 (9.11%)	834.42 (1.48%)	467,469 (9.92%)
Albuquerque	105 (9.03%)	714.42 (1.26%)	417,399 (8.86%)
Fort Collins	1 (0.09%)	401.13 (0.71%)	10,754 (0.23%)
Total	770 (66.21%)	4,217.9 (7.47%)	3,202,942 (67.98%)

The HH spatial association, as a result of Anselin Local Moran's I analysis in terms of 2000 nighttime light emissions, represents monocentric clustering around Denver (bottom left of figure). Table 64 shows HH spatial associations descriptors of

2000 nighttime light emissions for Gulf Coast. The mean of 2000 nighttime light emissions is around 62.62% in comparison with the mean value of approximately 51.16% for the Front Range megaregion. Resulted HH clustering areas, therefore, indicate that a high level of urban development caused by nighttime socio-economic activities is clustered with other similarly high levels of nighttime socio-economic urban activities within the resulted areas.

Table 64 Front Range 2000 nighttime light emissions HH spatial associations descriptors

Clustering Areas	Census Tracts	Land Area (sq. mi)	2000 Total Population
		1,163 (100%)	56,502.07 (100%)
Denver	482 (41.44%)	978.93 (1.73%)	2,000,186 (42.45%)

Morphological clustering, as a result of overlapping two analysis results in terms of 2000 nighttime light emissions, follows the clustering boundary in the result of Getis-Ord G_i^* analysis (bottom right of figure). The extent of 2000 nighttime light emissions clustering of the Front Range megaregion, therefore, is identical to the extent of hot spot clustering. The overlapping of the two clustering analysis results shows that the clustering pattern of 2000 nighttime light emissions has one large clustering concentration in the areas around Denver, additionally small apart clustering around Albuquerque area. The new clusterings of Colorado Springs and Fort Collins are also noticeable. The morphological clustering map represents, therefore, that the levels of urban development caused by nighttime socio-economic activities are similarly high and clustered within the clustering boundary. In terms of the clustering by 2000 nighttime

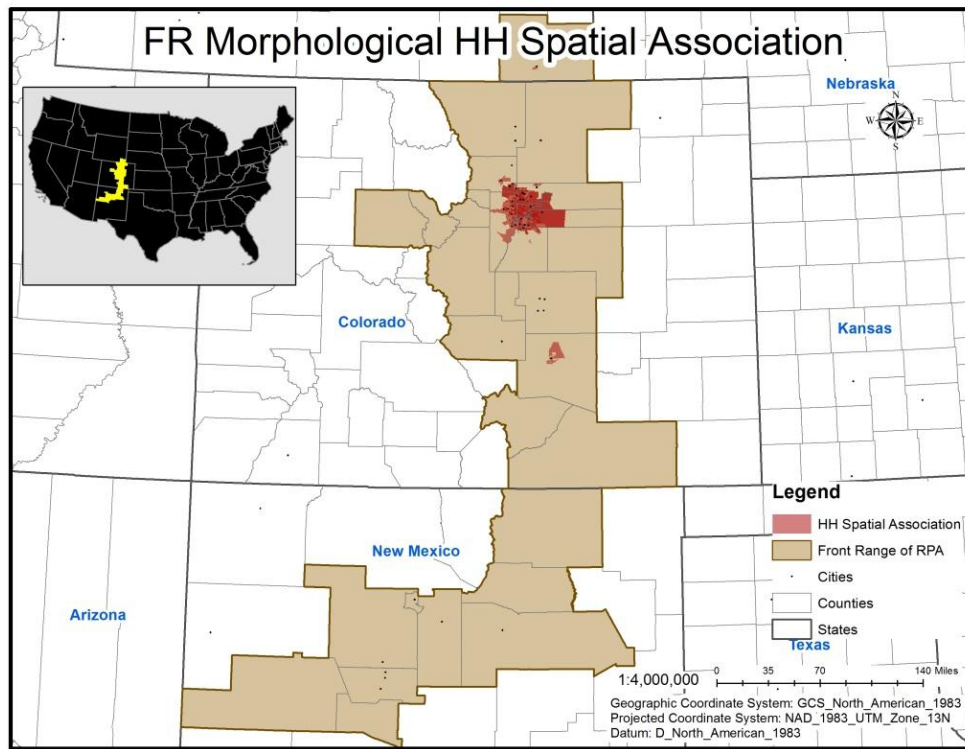
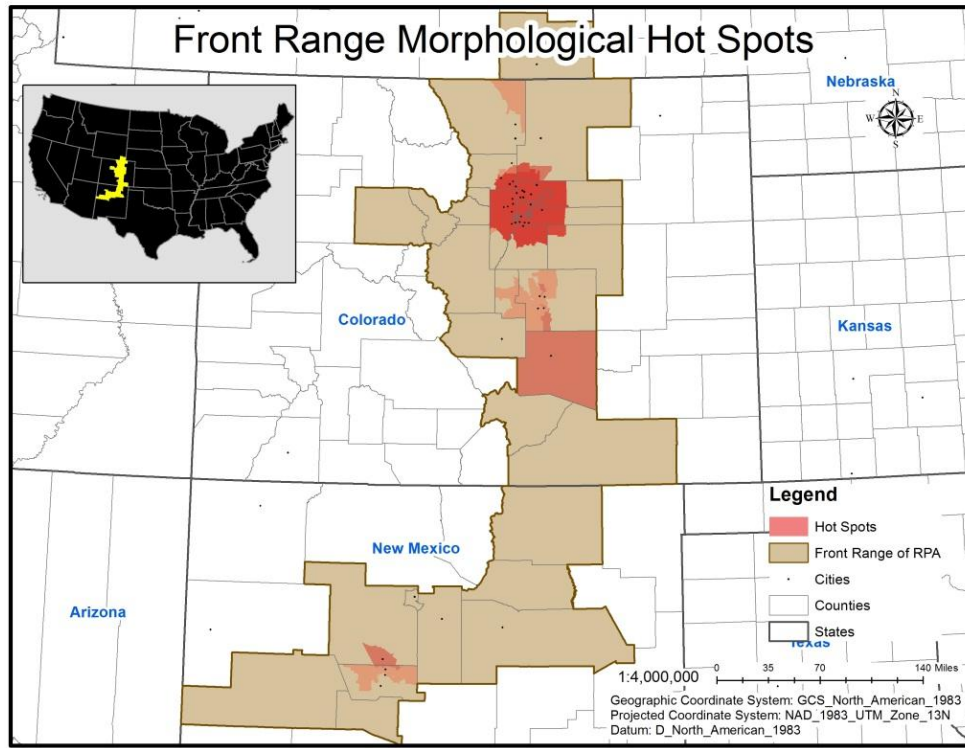


Figure 44 Local clusterings of morphological features in the Front Range megaregion

light emissions, the Front Range megaregion identified by RPA seems to have an exaggerated boundary.

4) Morphological local clustering

Figure 44 represents results only produced by overlapping every clustering of the Getis-Ord G_i^* hot spots analysis (top of figure) and only by overlapping every HH spatial cluster of the Anselin Local Moran's I spatial cluster and outlier analysis (bottom of figure). As the final representation for the Front Range megaregion morphological clustering, Figure 45 represents a result produced by overlapping the results separately represented in Figure 44. Table 65 summarizes the Front Range megaregion morphological clustering descriptors.

Representing polycentric morphological clustering for the Front Range megaregion, the clustering around Denver is primarily highlighted, meaning that the city and the surrounding areas have the most excess of morphological characteristics such as population density, impervious land cover, and nighttime light emissions (see Figure 45). The clusterings around Colorado Spring and Pueblo are interconnected in the final morphological clustering representation. Taking account the physically close distance between the clusterings of Denver and Colorado Springs – Pueblo, they may be considered as a group of morphological clustering. Denver clustering, however, obviously has the dominant concentration of morphological characteristics to Colorado Springs – Pueblo clustering. It may be considerable, therefore, attaching Colorado Springs – Pueblo clustering to Denver clustering area than referring to the separate

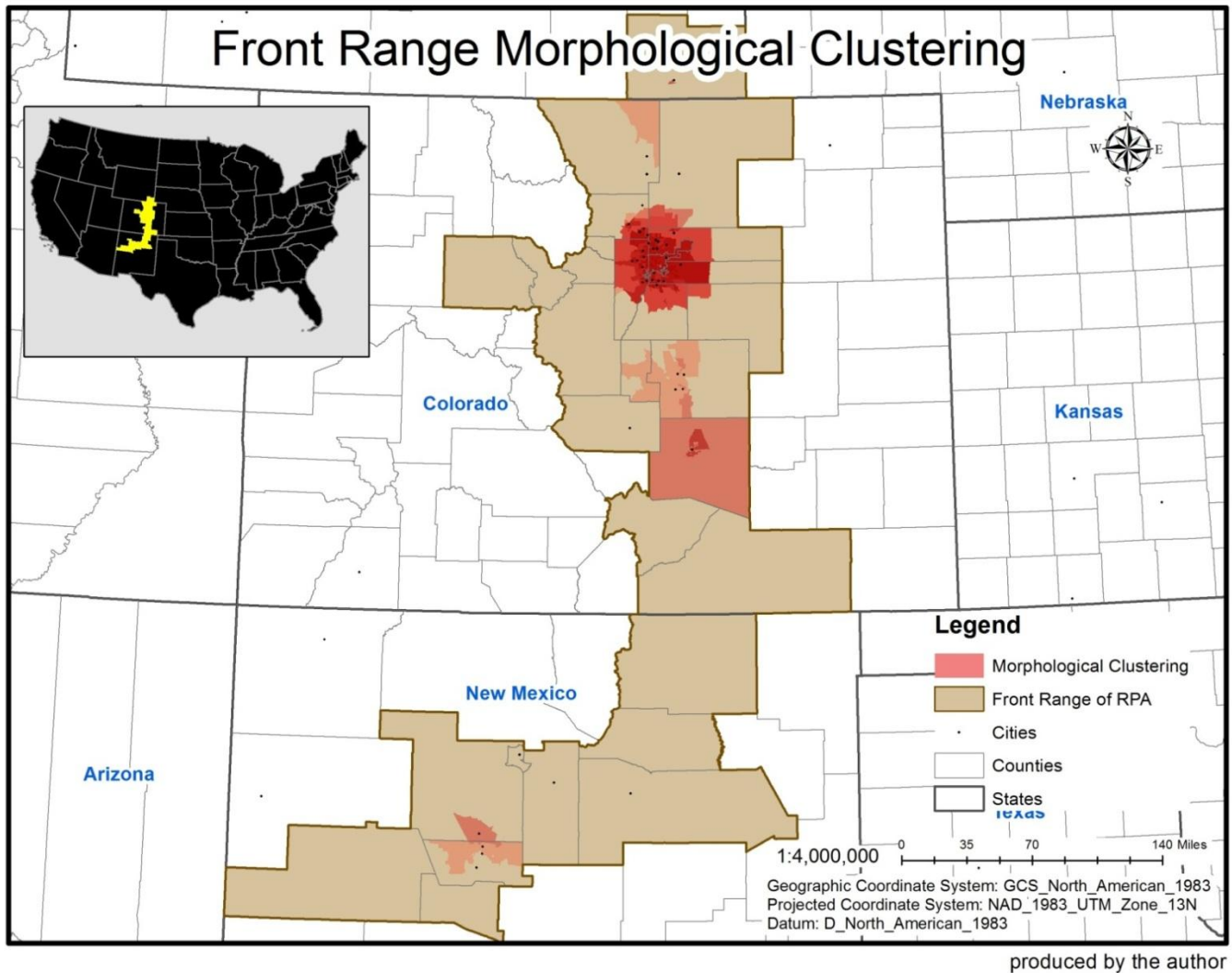


Figure 45 Morphological clusterings of the Front Range megaregion

Table 65 The Front Range megaregion morphological clusterings descriptors

Data Type	Clustering Area	Analysis	Front Range Morphological Clusterings Descriptors		
			Census Tracts	Land Areas (sq. mi)	2000 Total Population
			1,163 (100%)	56,502.07 (100%)	4,711,921 (100%)
PopDen00	Denver	Hot Spot	554 (47.64%)	2,184.75 (3.87%)	2,286,376 (48.52%)
		HH Cluster	310 (26.66%)	220.46 (0.39%)	1,372,050 (29.12%)
	Clustering Total		554 (47.64%)	2,184.75 (3.87%)	2,286,376 (48.52%)
ImpS01	Denver	Hot Spot	558 (47.98%)	2,328.17 (4.12%)	2,308,560 (48.99%)
		HH Cluster	270 (23.22%)	780.1 (1.38%)	1,124,095 (23.86%)
	Pueblo	Hot Spot	53 (4.56%)	2,589.15 (4.58%)	159,657 (3.39%)
		HH Cluster	27 (2.32%)	95.15 (0.17%)	76,791 (1.63%)
	Cheyenne	Hot Spot	n/a	n/a	n/a
		HH Cluster	2 (0.17%)	5.09 (0.01%)	8,170 (0.17%)
	Subtotal	Hot Spot	611 (52.54%)	4,917.32 (8.7%)	2,468,217 (52.38%)
		HH Cluster	299 (25.71%)	880.34 (1.56%)	1,209,056 (25.66%)
	Clustering Total		613 (52.71%)	4,922.41 (8.71%)	2,476,387 (52.56%)
	DMSP00	Denver	Hot Spot	558 (47.98%)	2,267.93 (4.01%)
HH Cluster			482 (41.44%)	978.93 (1.73%)	2,000,186 (42.45%)
Colorado Springs		Hot Spot	106 (9.11%)	834.42 (1.48%)	467,469 (9.92%)
		HH Cluster	n/a	n/a	n/a
Albuquerque		Hot Spot	105 (9.03%)	714.42 (1.26%)	417,399 (8.86%)
		HH Cluster	n/a	n/a	n/a
Fort Collins		Hot Spot	1 (0.09%)	401.13 (0.71%)	10,754 (0.23%)
		HH Cluster	n/a	n/a	n/a
Subtotal		Hot Spot	770 (66.21%)	4,217.9 (7.47%)	3,202,942 (67.98%)
		HH Cluster	482 (41.44%)	978.93 (1.73%)	2,000,186 (42.45%)
Clustering Total		770 (66.21%)	4,217.9 (7.47%)	3,202,942 (67.98%)	
The Front Range Subtotal		Hot Spot	826 (71.02%)	6,901.87 (12.22%)	3,375,394 (71.64%)
		HH Cluster	530 (45.57%)	1,177.83 (2.08%)	2,169,724 (46.05%)
The Front Range Morphological Clustering Total			828 (71.2%)	6,906.96 (12.22%)	3,383,564 (71.81%)

clustering. Concerning the megaregion boundary of RPA, therefore, the Front Range megaregion boundary is not likely to fit the morphological clustering and connection. It is more likely to separate Denver clustering from Albuquerque clustering. The total extent of Front Range clustering in terms of all morphological features analyzed thus far includes 828 census tracts being around 71.2% of the total Front Range census tracts; about 6,906.96 square miles equal approximately 12.22% of the total Front Range land area; and 3,383,564 total population being around 71.81% of the total population of the Front Range megaregion.

The Front Range morphological clustering map resulted finally represents the locations where high levels of land uses per capita, urbanized built environment, and nighttime socio-economic urban activities are clustered. The clustering areas of Denver and Colorado Springs – Pueblo seem to have morphological interconnections because of being physically close. The clustering area of Albuquerque, however, seems to be difficult to consider morphological connections to other clustering areas because of being physically distant. The final map also represents an exaggerated boundary for the Front Range megaregion in the morphological observations.

2.8. The Arizona Sun Corridor megaregion

1) Local clustering of 2000 population density

Figure 46 shows local clustering analysis results produced by using 2000 population density. Following the threshold of Density-based Sprawl Index, 2000 population density is categorized into three groups: rural areas population density (i.e.,

less than 200 persons per square mile), low population density areas (i.e., between 200 and 3,500 persons per square mile), and high population density areas (i.e., greater than 3,500 persons per square mile) (top left of figure). The general observation of the distribution of 2000 population density is that the low and high population density are concentrated around Phoenix, Tucson, Casa Grande, Prescott, Sierra Vista, Douglas, Nogales, and Green Valley.

The statistically significant hot spots at the 0.05 alpha level, as a result of Getis-Ord G_i^* analysis in terms of 2000 population density, represent monocentric clustering around Phoenix (top right of figure). Table 66 shows hot spot descriptors of 2000 population density for Arizona Sun Corridor. The mean of 2000 population density is around 4,671.82 in comparison with the mean value of approximately 3,851.06 for the Arizona Sun Corridor megaregion. Resulted hot spots, therefore, indicate that the levels of land use per capita are similarly high within the hot spot boundary.

Table 66 Arizona Sun Corridor 2000 population density hot spots descriptors

Clustering Areas	Census Tracts	Land Area (sq. mi)	2000 Total Population
		971 (100%)	48,659.42 (100%)
Phoenix	664 (68.38%)	2,596.93 (5.34%)	3,088,564 (68.57%)

The HH spatial association, as a result of Anselin Local Moran's I analysis in terms of 2000 population density, also represents monocentric clustering around Phoenix (bottom left of figure). The HH spatial association of 2000 population density, compared to the hot spot clustering, the extent of HH spatial associations is smaller and

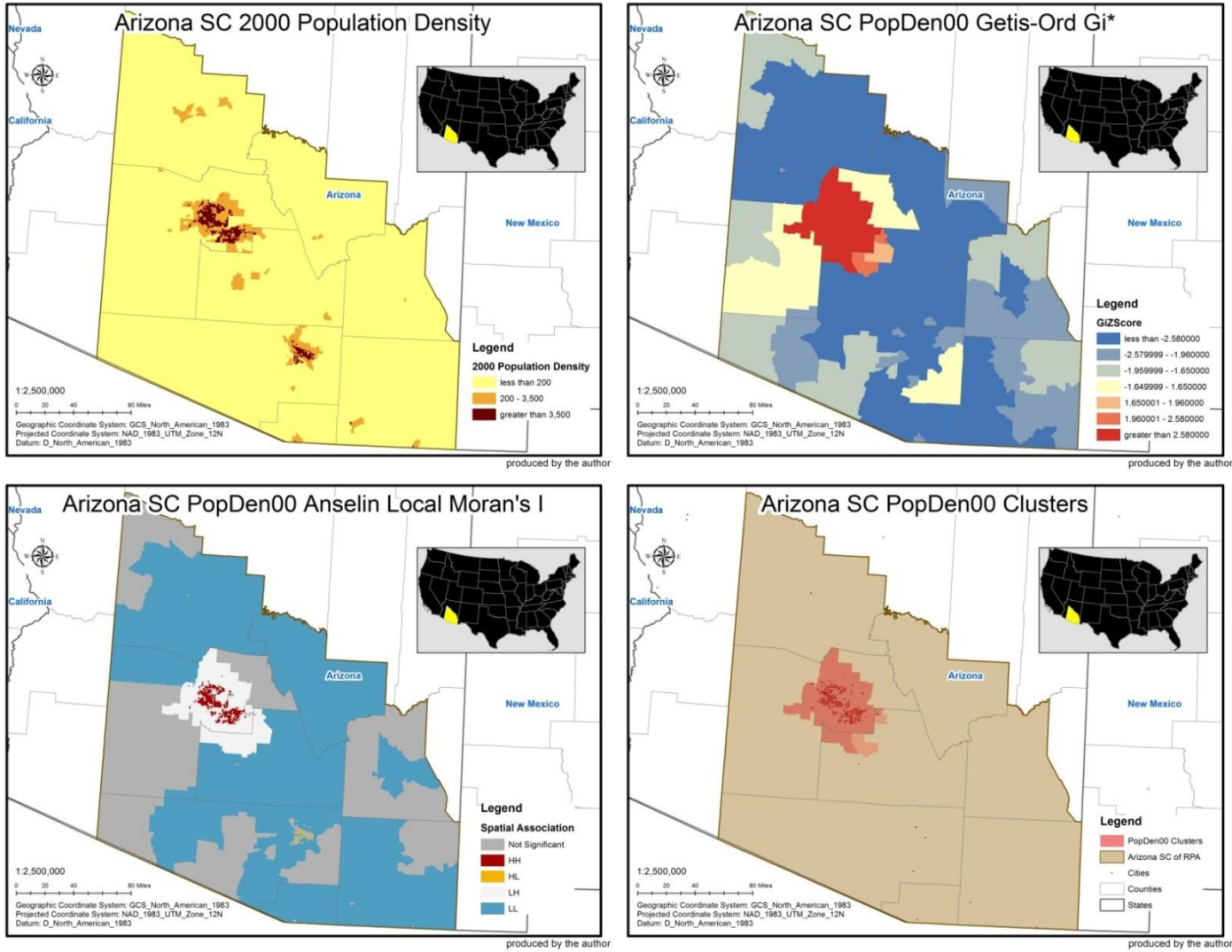


Figure 46 The Arizona Sun Corridor megaregion local clustering analysis results by 2000 population density

the pattern is more fractal and fragmented. Table 67 shows HH spatial associations descriptors of 2000 population density for Arizona Sun Corridor. The mean of 2000 population density is around 7,048.03 in comparison with the mean value of approximately 3,851.06 for the Arizona Sun Corridor megaregion. Resulted HH spatial associations, therefore, indicate that a high level of land use per capita is clustered with other similarly high levels of land use per capita within the resulted areas.

Table 67 Arizona Sun Corridor 2000 population density HH spatial associations descriptors

Clustering Areas	Census Tracts	Land Area (sq. mi)	2000 Total Population
		971 (100%)	48,659.42 (100%)
Phoenix	338 (34.81%)	271.56 (0.56%)	1,780,036 (39.52%)

The morphological clustering, as a result of overlapping two analysis results in terms of 2000 population density, follows the clustering boundary in the result of Getis-Ord G_i^* analysis (bottom right of figure). The extent of 2000 population density clustering of the Arizona Sun Corridor megaregion, therefore, is identical to the extent of hot spot clustering. The overlapping of the two clustering analysis results shows that the clustering pattern of 2000 population density has monocentric clustering around Phoenix area. The morphological clustering map represents, therefore, that the levels of land use per capita are similarly high and clustered within the clustering boundary. In terms of the clustering by 2000 population density, the Arizona Sun Corridor megaregion identified by RPA seems to have an exaggerated boundary.

2) Local clustering of 2001 impervious land cover

Figure 47 shows local clustering analysis results produced by using 2001 impervious land cover. The general observation of the distribution of 2001 impervious land cover is that the highest degree of imperviousness in 2001 follows the distribution of 2000 low and high population density, highlighting the concentration around Phoenix area and Tucson area (top left of figure).

The statistically significant hot spots at the 0.05 alpha level, as a result of Getis-Ord G_i^* analysis in terms of 2001 impervious land cover, represent monocentric clustering around the Phoenix area (top right of figure). Table 68 shows hot spots descriptors of 2001 impervious land cover for Front Range. The mean of 2001 impervious land cover is around 51.85% in comparison with the mean value of approximately 32.49% for the Arizona Sun Corridor megaregion. Resulted hot spots, therefore, indicate that the urbanization levels of these built environments are similarly high within the hot spot boundary.

Table 68 Arizona Sun Corridor 2001 impervious land cover hot spots descriptors

Clustering Areas	Census Tracts	Land Area (sq. mi)	2000 Total Population
	971 (100%)	48,659.42 (100%)	4,504,099 (100%)
Phoenix	664 (68.38%)	2,791.17 (5.74%)	3,087,687 (68.55%)

The HH spatial association, as a result of Anselin Local Moran's I analysis in terms of 2001 impervious land cover, also represents monocentric clustering located

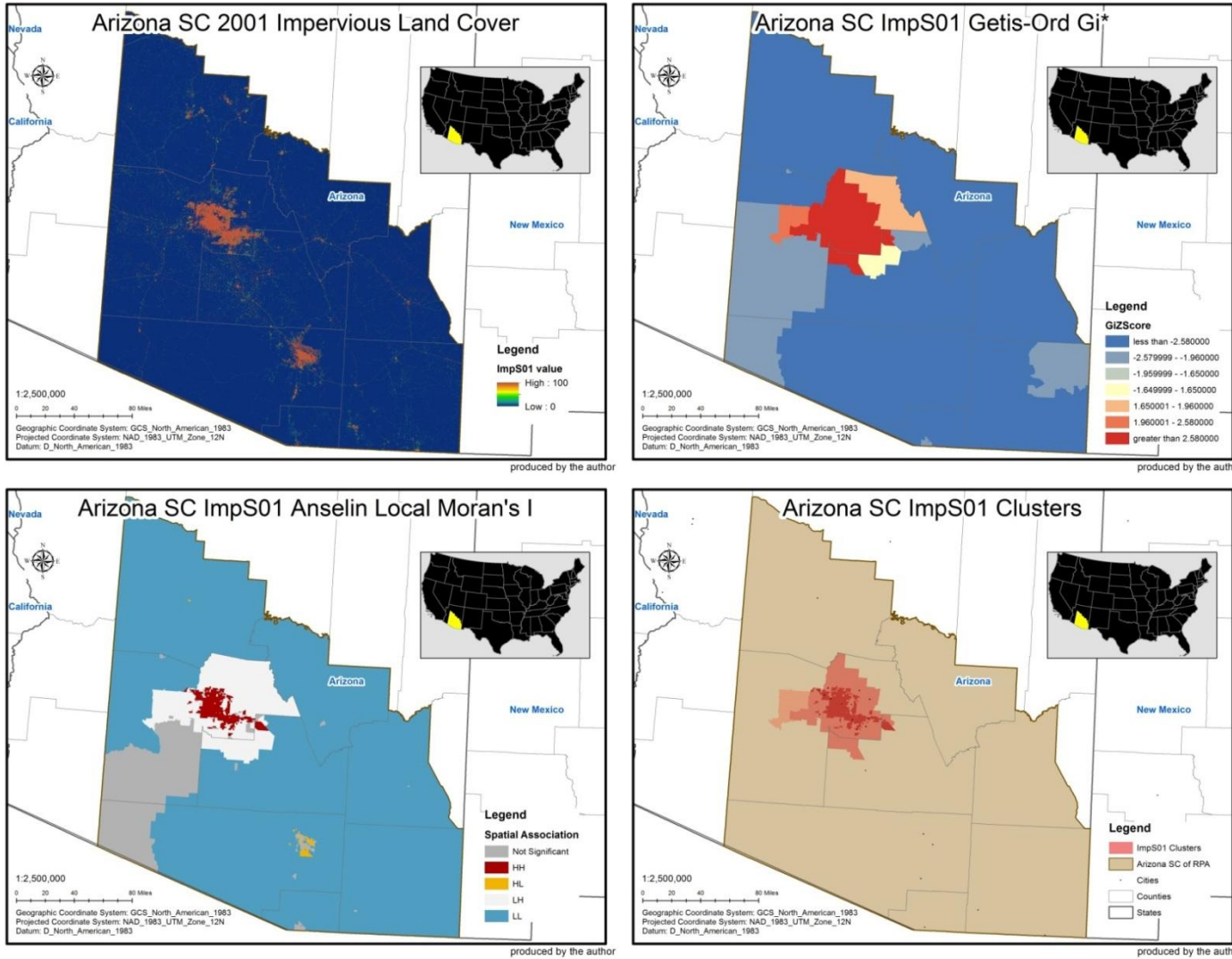


Figure 47 The Arizona Sun Corridor megaregion local clustering analysis results by 2001 impervious land cover

around the same areas with the result of hot spots analysis, although the extent of clustering is smaller (bottom left of figure). Table 69 shows shows HH spatial associations descriptors of 2001 impervious land cover for Arizona Sun Corridor. The mean of 2001 impervious land cover is around 55.88% in comparison with the mean value of approximately 32.49% for the Arizona Sun Corridor megaregion. Resulted HH spatial associations, therefore, indicate that a high level of urbanization for built environments is clustered with other similarly highly urbanized built environments within the resulted areas.

Table 69 Arizona Sun Corridor 2001 impervious land cover HH spatial associations descriptors

Clustering Areas	Census Tracts	Land Area (sq. mi)	2000 Total Population
		971 (100%)	48,659.42 (100%)
Phoenix	430 (44.28%)	539.7 (1.11%)	2,029,409 (45.06%)

Morphological clustering, as a result of overlapping two analysis results in terms of 2001 impervious land cover, has the same clustering boundary with Getis-Ord G_i^* analysis result (bottom right of figure). The extent of 2001 impervious land cover clustering of the Arizona Sun Corridor megaregion, therefore, is identical to the extent of hot spot clustering. The overlapping of the two clustering analysis results shows that the clustering pattern of 2001 impervious land cover also has monocentric clustering around Phoenix area. The morphological clustering map represents, therefore, that the urbanization levels of these built environments are similarly high and clustered within

the clustering boundary. In terms of the clustering by 2001 impervious land cover, the Arizona Sun Corridor megaregion identified by RPA seems to have an exaggerated boundary.

3) Local clustering of 2000 nighttime light emissions (DMSP-OLS)

Figure 48 shows local clustering analysis results produced by using 2000 nighttime light emissions (DMSP-OLS). The general observation of the distribution of 2000 nighttime light emissions is that the highest degree of nighttime light emissions in 2000 follows both distributions of 2000 low and high population density and 2001 impervious land cover (top left of figure).

Table 70 Arizona Sun Corridor 2000 nighttime light emissions hot spots descriptors

Clustering Areas	Census Tracts	Land Area (sq. mi)	2000 Total Population
		971 (100%)	48,659.42 (100%)
Phoenix	667 (68.69%)	4,258.35 (8.75%)	3,103,484 (68.9%)

The statistically significant hot spots at the 0.05 alpha level, as a result of Getis-Ord G_i^* analysis in terms of 2000 nighttime light emissions, represent monocentric clustering around Phoenix area (top right of figure). Table 70 shows hot spots descriptors of 2000 nighttime light emissions for Great Lakes. The mean of 2000 nighttime light emissions is around 61.49% in comparison with the mean value of approximately 53.92% for the Arizona Sun Corridor megaregion. Resulted hot spots, therefore, indicate that the urban development levels caused by nighttime socio-economic

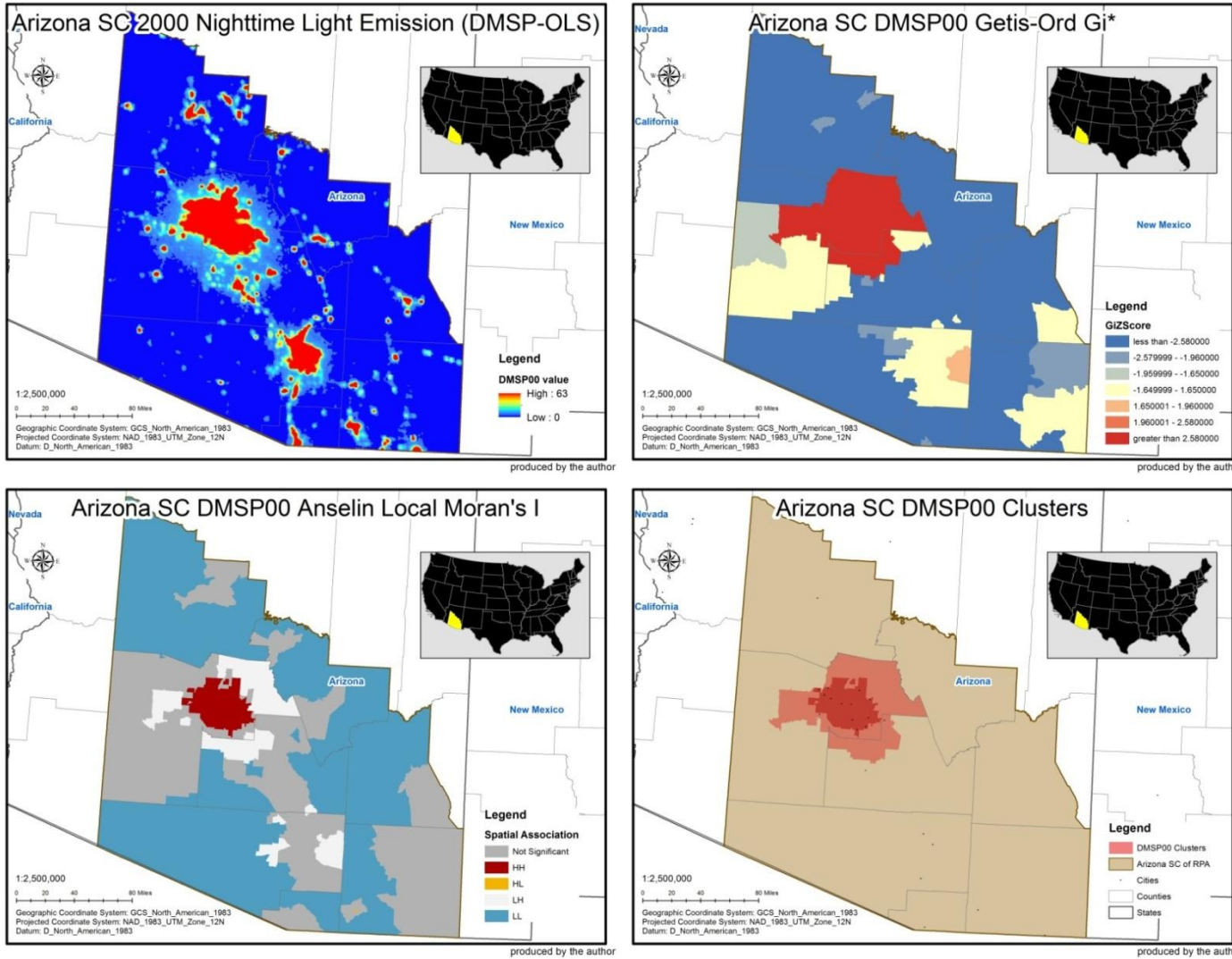


Figure 48 The Arizona Sun Corridor megaregion local clustering analysis results by 2000 nighttime light emissions

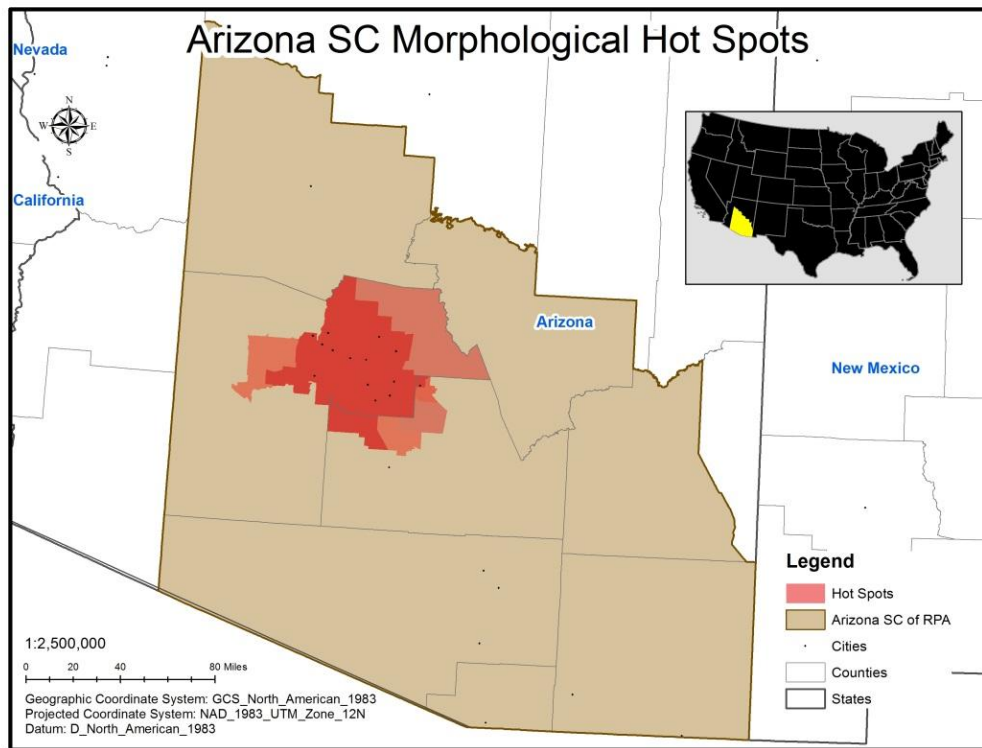
activities are similarly high within the hot spot boundary.

The HH spatial association, as a result of Anselin Local Moran's *I* analysis in terms of 2000 nighttime light emissions, represents monocentric clustering around Phoenix area (bottom left of figure). Table 71 shows HH spatial associations descriptors of 2000 nighttime light emissions for Gulf Coast. The mean of 2000 nighttime light emissions is around 62.86% in comparison with the mean value of approximately 53.92% for the Arizona Sun Corridor megaregion. Resulted HH spatial associations, therefore, indicate that a high level of urban development caused by nighttime socio-economic activities is clustered with other similarly high levels of nighttime socio-economic urban activities within the resulted areas.

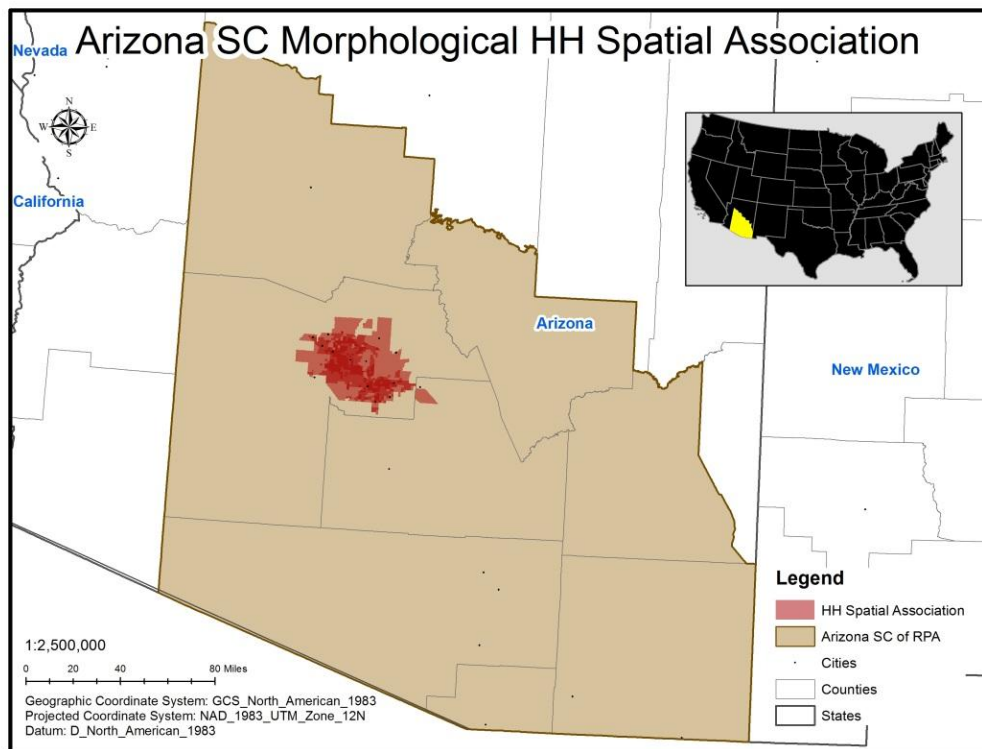
Table 71 Arizona Sun Corridor 2000 nighttime light emissions HH spatial associations descriptors

Clustering Areas	Census Tracts	Land Area (sq. mi)	2000 Total Population
		971 (100%)	48,659.42 (100%)
Phoenix	611 (62.92%)	1,153.32 (2.37%)	2,865,563 (63.62%)

Morphological clustering, as a result of overlapping two analysis results in terms of 2000 nighttime light emissions, follows the clustering boundary in the result of Getis-Ord G_i^* analysis (bottom right of the figure). The extent of 2000 nighttime light emissions clustering of the Arizona Sun Corridor megaregion, therefore, is identical to the extent of hot spot clustering. The overlapping of the two clustering analysis results shows that the clustering pattern of 2000 nighttime light emissions has monocentric



produced by the author



produced by the author

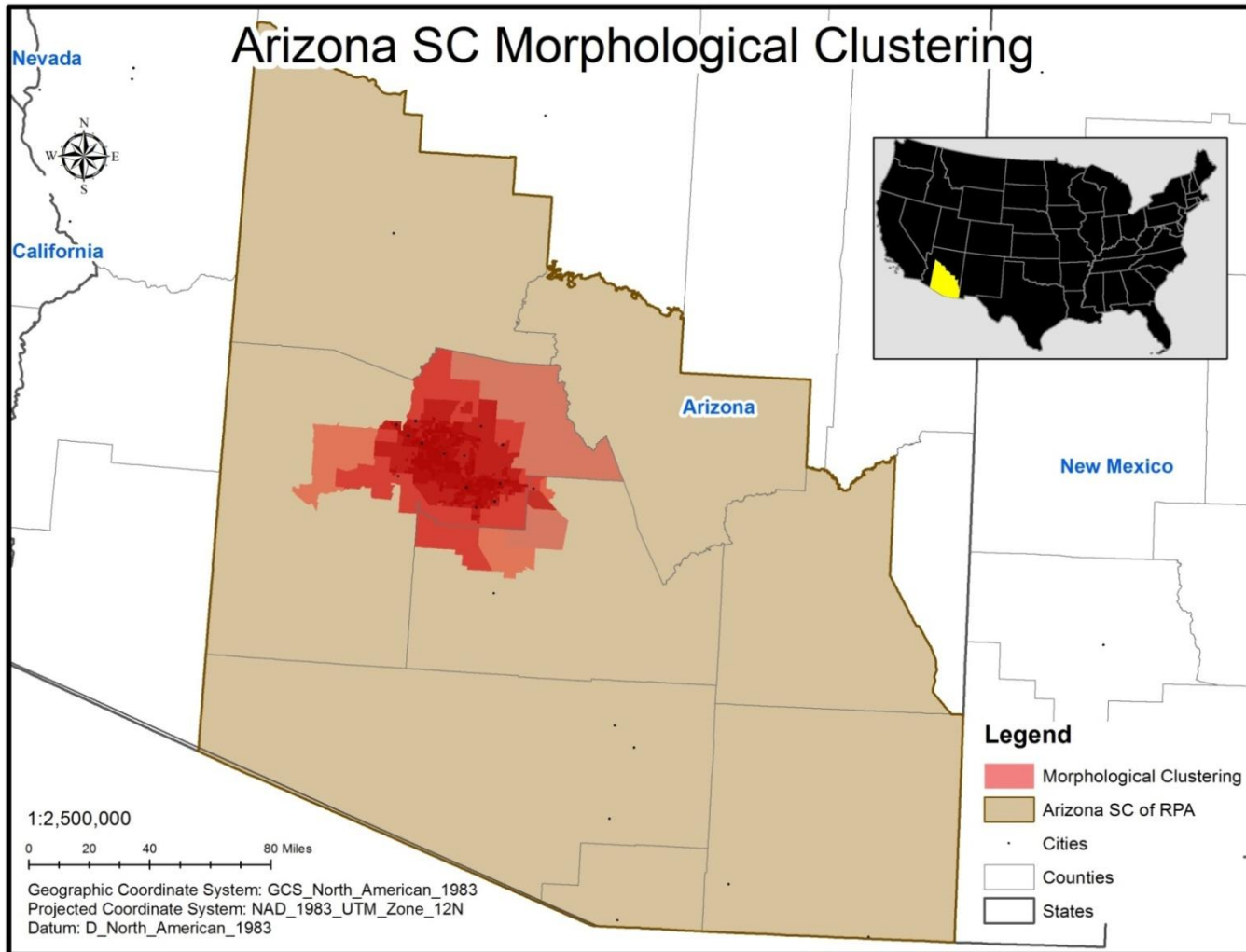
Figure 49 Local clusterings of morphological features in the Arizona Sun Corridor megaregion

clustering in the Phoenix areas. The morphological clustering map represents, therefore, that the levels of urban development caused by nighttime socio-economic activities are similarly high and clustered within the clustering boundary. In terms of the clustering by 2000 nighttime light emissions, the Arizona Sun Corridor megaregion identified by RPA seems to have an exaggerated boundary.

4) Morphological local clustering

Figure 49 represents results only produced by overlapping every clustering of the Getis-Ord G_i^* hot spots analysis (top of figure) and only by overlapping every HH spatial cluster of the Anselin Local Moran's I spatial cluster and outlier analysis (bottom of figure). As the final representation for the Arizona Sun Corridor megaregion morphological clustering, Figure 50 represents a result produced by overlapping the results separately represented in Figure 49. Table 72 summarizes the Arizona Sun Corridor megaregion morphological clustering descriptors.

Representing monocentric morphological clustering for the Arizona Sun Corridor megaregion, the clustering around Phoenix is highlighted, meaning that the city and the surrounding areas have an excess of morphological characteristics such as population density, impervious land cover, and nighttime light emissions (see Figure 50). Concerning the megaregion boundary of RPA, therefore, Arizona Sun Corridor is not likely delineated by the RPA's boundary in terms of morphological clustering pattern. It is more likely to consider a large metropolitan area where has morphological clustering in Phoenix. The total extent of Arizona Sun Corridor clustering in terms of all



produced by the author

Figure 50 Morphological clusterings of the Arizona Sun Corridor megaregion

Table 72 The Arizona Sun Corridor megaregion morphological clusterings descriptors

Data Type	Clustering Area	Analysis	Arizona Sun Corridor Morphological Clusterings Descriptors		
			Census Tracts	Land Areas (sq. mi)	2000 Total Population
			971 (100%)	48,659.42 (100%)	4,504,099 (100%)
PopDen00	Phoenix	Hot Spot	664 (68.38%)	2,596.93 (5.34%)	3,088,564 (68.57%)
		HH Cluster	338 (34.81%)	271.56 (0.56%)	1,780,036 (39.52%)
	Clustering Total		664 (68.38%)	2,596.93 (5.34%)	3,088,564 (68.57%)
ImpS01	Phoenix	Hot Spot	664 (68.38%)	2,791.17 (5.74%)	3,087,687 (68.55%)
		HH Cluster	430 (44.28%)	539.7 (1.11%)	2,029,409 (45.06%)
	Clustering Total		664 (68.38%)	2,791.17 (5.74%)	3,087,687 (68.55%)
DMSP00	Phoenix	Hot Spot	667 (68.69%)	4,258.35 (8.75%)	3,103,484 (68.9%)
		HH Cluster	611 (62.92%)	1,153.32 (2.37%)	2,865,563 (63.62%)
	Clustering Total		667 (68.69%)	4,258.35 (8.75%)	3,103,484 (68.9%)
The Arizona Sun Corridor Subtotal		Hot Spot	667 (68.69%)	4,258.35 (8.75%)	3,103,484 (68.9%)
		HH Cluster	617 (63.54%)	1,207.18 (2.48%)	2,894,543 (64.26%)
The Arizona Sun Corridor Morphological Clustering Total			667 (68.69%)	4,258.35 (8.75%)	3,103,484 (68.9%)

morphological features analyzed thus far is identical to the extent of clustering resulted from the 2000 nighttime light emissions hot spots analysis. This means that the nighttime light emissions clusterings, in case of the Arizona Sun Corridor megaregion, dominates the morphological clustering boundary and extent.

The Arizona Sun Corridor morphological clustering map resulted finally represents the locations which high levels of land uses per capita, urbanized built environments, and nighttime socio-economic urban activities are clustered. The clustering area of Phoenix seems not to be available to consider morphological connections with other clustering areas for the monocentric clustering in the region. The final map also represents an exaggerated boundary for the Arizona Sun Corridor megaregion in the morphological observations.

2.9. The Northern California megaregion

1) Local clustering of 2000 population density

Figure 51 shows local clustering analysis results produced by using 2000 population density. Following the threshold of Density-based Sprawl Index, population density 2000 is categorized into three groups: rural areas population density (i.e., less than 200 persons per square mile), low population density areas (i.e., between 200 and 3,500 persons per square mile), and high population density areas (i.e., greater than 3,500 persons per square mile) (top left of figure). The general observation of the distribution of 2000 population density is that the low and high population density are concentrated around San Francisco – San Jose, Santa Cruz, Sacramento, Yuba, Stockton

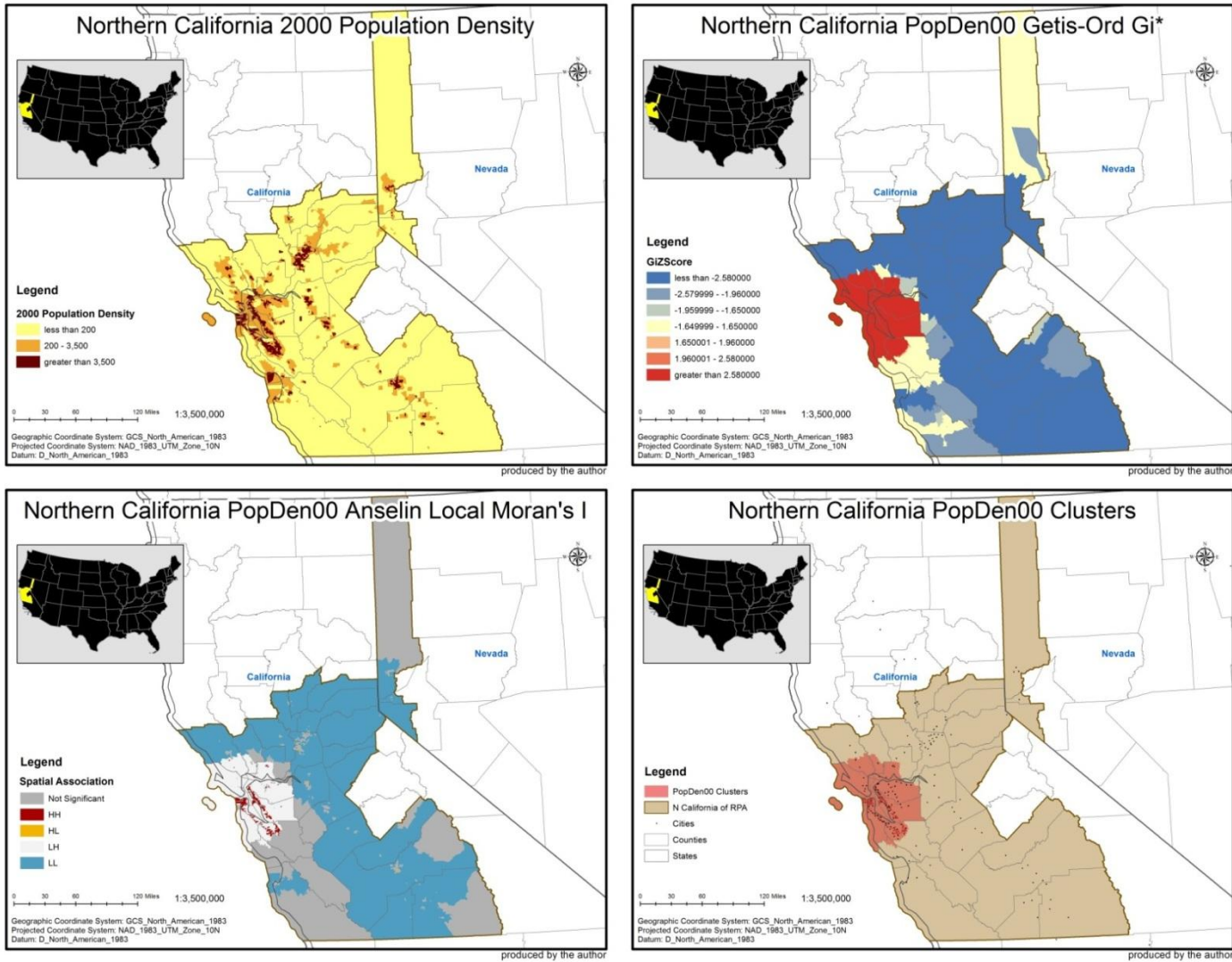


Figure 51 The Northern California megaregion local clustering analysis results by 2000 population density

– Merced, Madera – Porterville, and Reno of Nevada.

The statistically significant hot spots at the 0.05 alpha level, as a result of Getis-Ord G_i^* analysis in terms of 2000 population density, represent monocentric clustering around San Francisco – San Jose area (top right of figure). Table 72 shows hot spot descriptors of 2000 population density for Northern California. The mean of 2000 population density is around 10,435.33 in comparison with the mean value of approximately 6,951.76 for the Northern California megaregion. Resulted hot spots, therefore, indicate that the levels of land use per capita are similarly high within the hot spot boundary.

Table 73 Northern California 2000 population density hot spots descriptors

Clustering Areas	Census Tracts	Land Area (sq. mi)	2000 Total Population
		2,637 (100%)	47,216.26 (100%)
San Francisco – San Jose	1,267 (48.05%)	3,595.05 (7.61%)	6,041,259 (47.67%)

The HH spatial association, as a result of Anselin Local Moran's I analysis in terms of 2000 population density, also represents monocentric clustering around San Francisco – San Jose area (bottom left of figure). It is noticeable that the clustering pattern of HH spatial association analysis seems to represent the direction and connection of morphological clustering with the fractal and fragmented form within the boundary of morphological clustering. Table 74 shows HH spatial associations descriptors of 2000 population density for Northern California. The mean of 2000 population density is around 18,138.16 in comparison with the mean value of

approximately 6,951.76 for the Northern California megaregion. Resulted HH spatial associations, therefore, indicate that a high level of land use per capita is clustered with other similarly high levels of land use per capita within the resulted areas.

Table 74 Northern California 2000 population density HH spatial associations descriptors

Clustering Areas	Census Tracts	Land Area (sq. mi)	2000 Total Population
		2,637 (100%)	47,216.26 (100%)
San Francisco – San Jose	573 (21.73%)	200.39 (0.42%)	2,776,383 (21.91%)

Morphological clustering, as a result of overlapping two analysis results in terms of 2000 population density, has the same clustering boundary with Getis-Ord G_i^* analysis result (bottom right of figure). The extent of 2000 population density clustering of the Northern California megaregion, therefore, is identical to the extent of hot spot clustering. The overlapping of the two clustering analysis results shows that the clustering of 2000 population density has a pattern connecting San Francisco to San Jose. The morphological clustering map represents, therefore, that the levels of land use per capita are similarly high and clustered within the clustering boundary. In terms of the clustering by 2000 population density, the Northern California megaregion identified by RPA seems to have an exaggerated boundary.

2) Local clustering of 2001 impervious land cover

Figure 52 shows local clustering analyses results produced by using 2001 impervious land cover. The general observation of the distribution of 2001 impervious land cover is that the highest degree of imperviousness in 2001 follows the distribution of 2000 low and high population density (top left of figure).

The statistically significant hot spots at the 0.05 alpha level, as a result of Getis-Ord G_i^* analysis in terms of 2001 impervious land cover, represent monocentric clustering around San Francisco – San Jose area (top right of figure). Compared to the clustering pattern of 2000 population density hot spots analysis, it is noticeable for the expanded clustering boundary to northern area such as Santa Rosa. Table 75 shows hot spots descriptors of 2001 impervious land cover for Northern California. The mean of 2001 impervious land cover is around 58.5% in comparison with the mean value of approximately 37.95% for the Northern California megaregion. Resulted hot spots, therefore, indicate that the urbanization levels of these built environments are similarly high within the hot spot boundary.

Table 75 Northern California 2001 impervious land cover hot spots descriptors

Clustering Areas	Census Tracts	Land Area (sq. mi)	2000 Total Population
	2,637 (100%)	47,216.26 (100%)	12,672,400 (100%)
San Francisco – San Jose	1,436 (54.46%)	5,686.47 (12.04%)	6,906,795 (54.5%)

The HH spatial association, as a result of Anselin Local Moran's I analysis in terms of 2001 impervious land cover, also represents monocentric clustering around

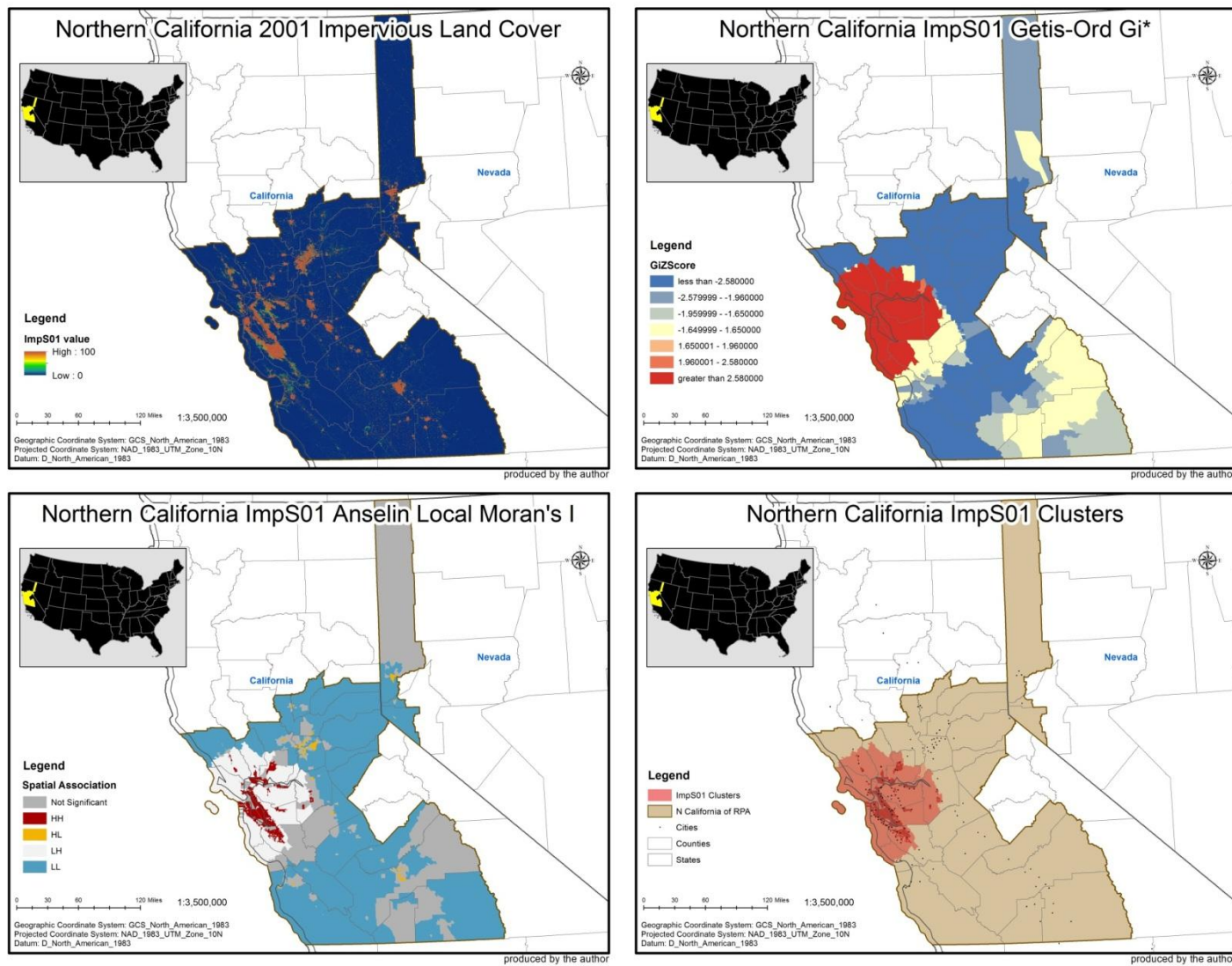


Figure 52 The Northern California megaregion local clustering analysis results by 2001 impervious land cover

San Francisco – San Jose area (bottom left of figure). The clustering pattern of 2001 impervious land cover HH spatial associations also represents morphological interconnections between cities such as San Francisco – San Jose with the fractal and fragmented form. Table 76 shows HH spatial associations descriptors of 2001 impervious land cover for Northern California. The mean of 2001 impervious land cover is around 67.2% in comparison with the mean value of approximately 37.95% for the Northern California megaregion. Resulted HH spatial associations, therefore, indicate that a high level of urbanization for built environments is clustered with other similarly highly urbanized built environments within the resulted areas.

Table 76 Northern California 2001 impervious land cover HH spatial associations descriptors

Clustering Areas	Census Tracts	Land Area (sq. mi)	2000 Total Population
		2,637 (100%)	47,216.26 (100%)
San Francisco – San Jose	758 (28.74%)	643.01 (1.36%)	3,627,760 (28.63%)

Morphological clustering, as a result of overlapping two analysis results in terms of 2001 impervious land cover, has the similar clustering boundary to Getis-Ord G_i^* analysis result, except 1 census tract located in the outskirts of Stockton (bottom right of figure). The overlapping observation represents that the clustering concentration primarily highlights the morphological interconnection between San Francisco and San Jose in terms of 2001 impervious land cover. Table 77 shows the total extent of 2001 impervious land cover clustering descriptors for Northern California. The

morphological clustering map represents, therefore, that the urbanization levels of these built environments are similarly high and clustered within the clustering boundary. In terms of the clustering by 2001 impervious land cover, the Northern California megaregion identified by RPA seems to have an exaggerated boundary.

Table 77 Northern California 2001 impervious land cover clustering descriptors

Clustering Total	Census Tracts	Land Area (sq. mi)	2000 Total Population
	2,637 (100%)	47,216.26 (100%)	12,672,400 (100%)
2001 impervious land cover	1,437 (54.49%)	5,687.18 (12.04%)	6,911,361 (54.54%)

3) Local clustering of 2000 nighttime light emissions (DMSP-OLS)

Figure 53 shows local clustering analysis results produced by using 2000 nighttime light emissions (DMSP-OLS). The general observation of the distribution of 2000 nighttime light emissions is that the highest degree of nighttime light emissions in 2000 follows both distributions of 2000 low and high population density and 2001 impervious land cover (top left of figure). It is noticeable, however, for the expanded clustering pattern around San Francisco – San Jose area and clearer connections of nighttime light emissions in eastern California cities than the distribution of population density.

The statistically significant hot spots at the 0.05 alpha level, as a result of Getis-Ord G_i^* analysis in terms of 2000 nighttime light emissions, represent monocentric clustering around San Francisco – San Jose area (top right of figure). The hot spot clustering area in terms of nighttime light emissions, compared to other data source hot spot clustering area, is more expanded reaching Sacramento area. Table 78 shows hot

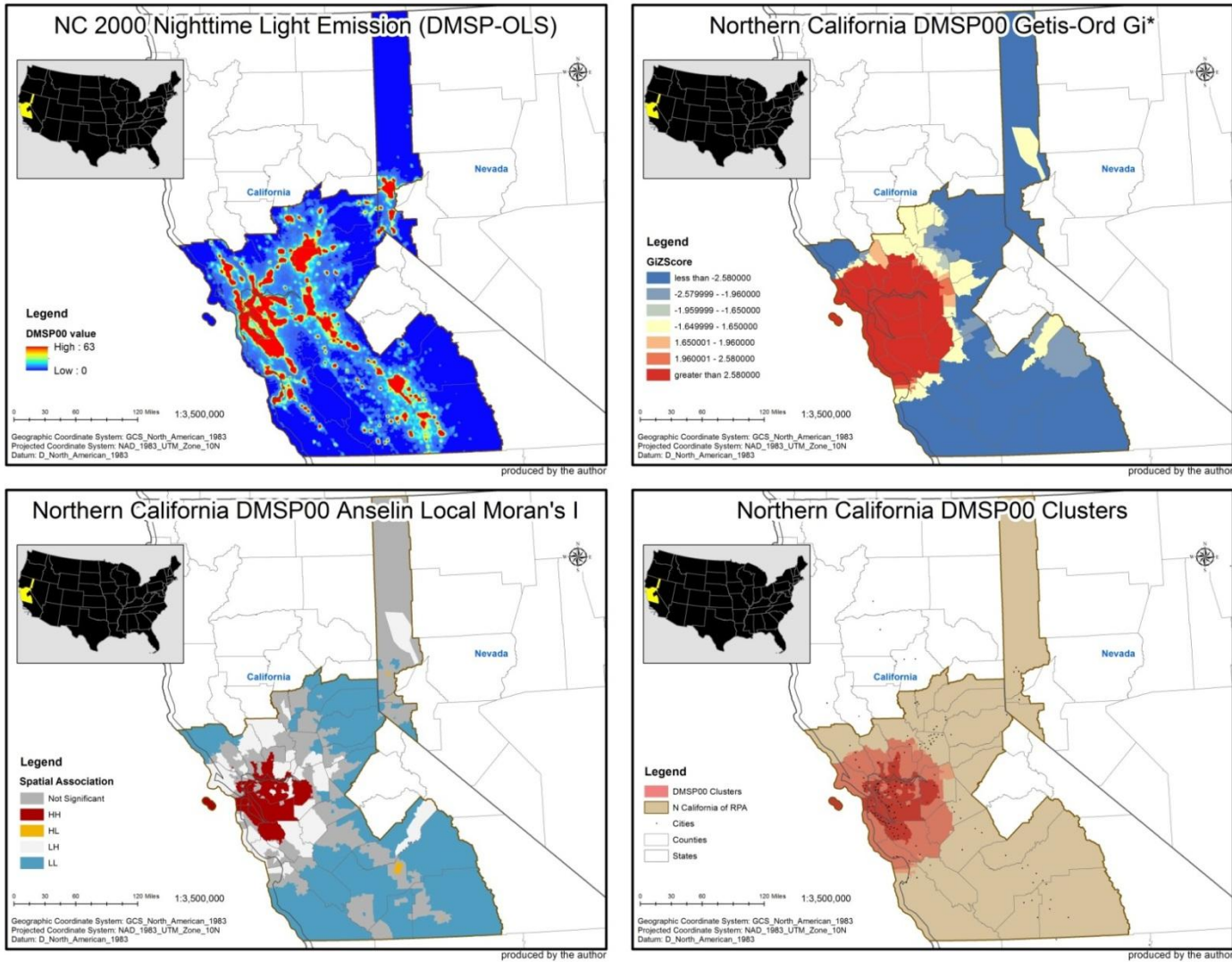


Figure 53 The Northern California megaregion local clustering analysis results by 2000 nighttime light emissions

spots descriptors of 2000 nighttime light emissions for Northern California. The mean of 2000 nighttime light emissions is around 59.47% in comparison with the mean value of approximately 52.57% for the Northern California megaregion. Resulted hot spots, therefore, indicate that the urban development levels caused by nighttime socio-economic activities are similarly high within the hot spot boundary.

Table 78 Northern California 2000 nighttime light emissions hot spots descriptors

Clustering Total	Census Tracts	Land Area (sq. mi)	2000 Total Population
	2,637 (100%)	47,216.26 (100%)	12,672,400 (100%)
San Francisco – San Jose	1,597 (60.56%)	8,361.91 (17.71%)	7,654,558 (60.4%)

The HH spatial association, as a result of Anselin Local Moran's *I* analysis in terms of 2000 nighttime light emissions, represents monocentric clustering around San Francisco – San Jose area (bottom left of figure). Even though the clustering pattern of HH spatial association of nighttime light emissions is still fractal and fragmented, the clustering pattern is closer to the hot spot clustering pattern of nighttime light emissions than other HH spatial association clustering patterns. Table 79 shows HH spatial associations descriptors of 2000 nighttime light emissions for Gulf Coast. The mean of 2000 nighttime light emissions is around 62.31% in comparison with the mean value of approximately 52.57% for the Northern California megaregion. Resulted HH spatial associations, therefore, indicate that a high level of urban development caused by nighttime socio-economic activities is clustered with other similarly high levels of nighttime socio-economic urban activities within the resulted areas.

Table 79 Northern California 2000 nighttime light emissions HH spatial associations descriptors

Clustering Total	Census Tracts	Land Area (sq. mi)	2000 Total Population
		2,637 (100%)	47,216.26 (100%)
San Francisco – San Jose	1,300 (49.3%)	2,568.5 (5.44%)	6,214,642 (49.04%)

Morphological clustering, as a result of overlapping two analysis results in terms of 2000 nighttime light emissions, follows the clustering boundary in the result of Getis-Ord G_i^* analysis (bottom right of figure). The extent of 2000 nighttime light emissions clustering of the Northern California megaregion, therefore, is identical to the extent of hot spot clustering. The overlapping of the two clustering analysis results shows that the clustering pattern of 2000 nighttime light emissions has one large clustering concentration in the areas around San Francisco – San Jose. The morphological clustering map represents, therefore, that the levels of urban development caused by nighttime socio-economic activities are similarly high and clustered within the clustering boundary. In terms of the clustering by 2000 nighttime light emissions, the Northern California megaregion identified by RPA seems to have an exaggerated boundary.

4) Morphological local clustering

Figure 54 represents results only produced by overlapping every clustering of the Getis-Ord G_i^* hot spots analysis (top of figure) and only by overlapping every HH spatial cluster of the Anselin Local Moran's I spatial cluster and outlier analysis (bottom of figure). As the final representation for the Northern California megaregion

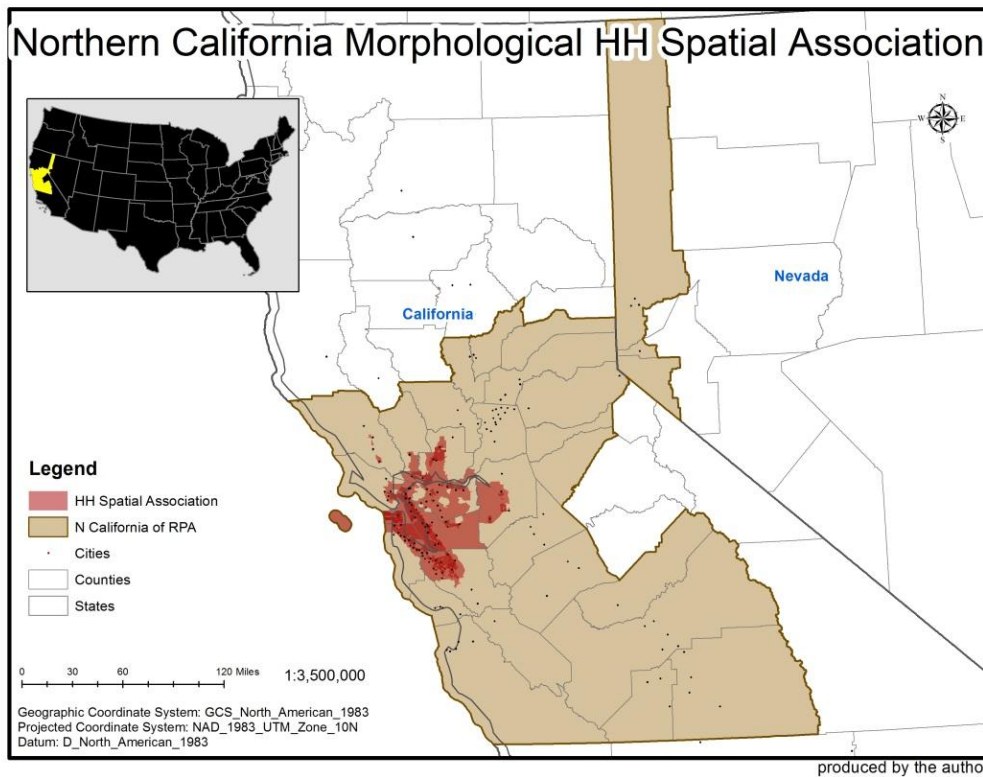
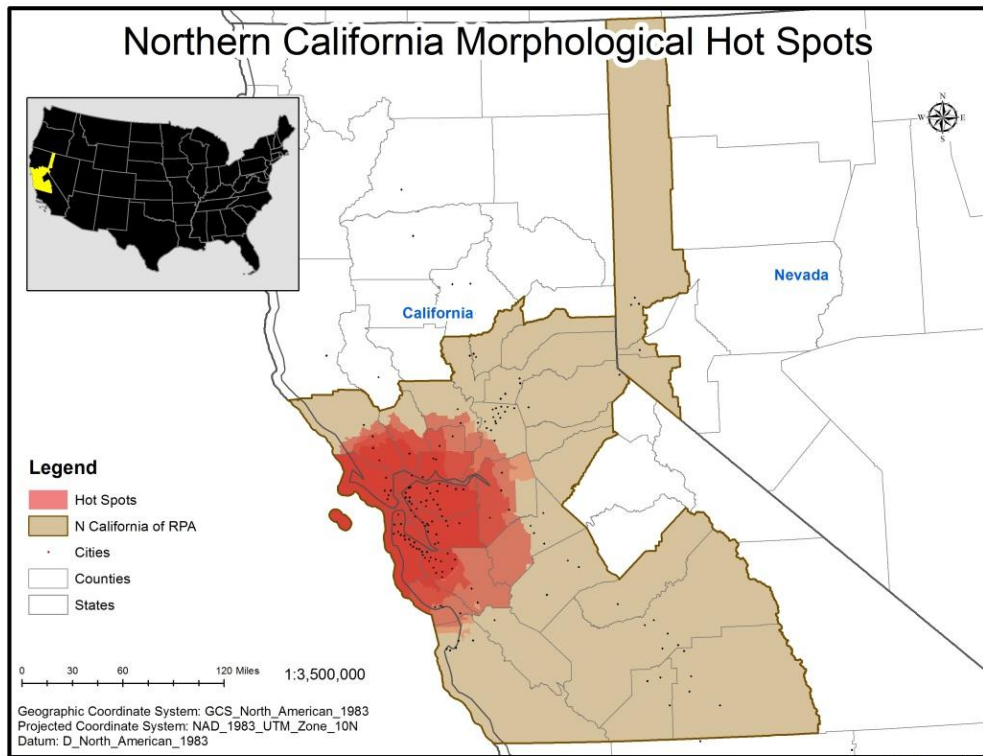


Figure 54 Local clusterings of morphological features in the Northern California megaregion

morphological clustering, Figure 55 represents a result produced by overlapping the results separately represented in Figure 54. Table 80 summarizes the Northern California megaregion morphological clustering descriptors.

Representing monocentric morphological clustering for the Northern California megaregion, the clustering around San Francisco – San Jose is primarily highlighted, meaning that the city and the surrounding areas have an excess of morphological characteristics such as population density, impervious land cover, and nighttime light emissions (see Figure 55). Concerning the megaregion boundary of RPA, therefore, the Northern California megaregion boundary is not likely to fit the morphological clustering and connection. It is more likely to consider as a large metropolitan or megapolitan area around San Francisco – San Jose clustering. The total extent of Northern California clustering in terms of all morphological features analyzed thus far includes 1,607 census tracts being around 60.94% of the total Northern California census tracts; about 8,577.84 square miles equal approximately 18.17% of the total Northern California land area; and 7,714,088 total population being around 60.87% of the total population of the Northern California megaregion.

The Northern California morphological clustering map resulted finally represents the locations where high levels of land uses per capita, urbanized built environment, and nighttime socio-economic urban activities are clustered. The clustering area of San Francisco – San Jose seems to be difficult to consider morphological interconnections with other clustering areas because of being monocentric. The final map also represents an exaggerated boundary for the Northern California megaregion in the morphological observations.

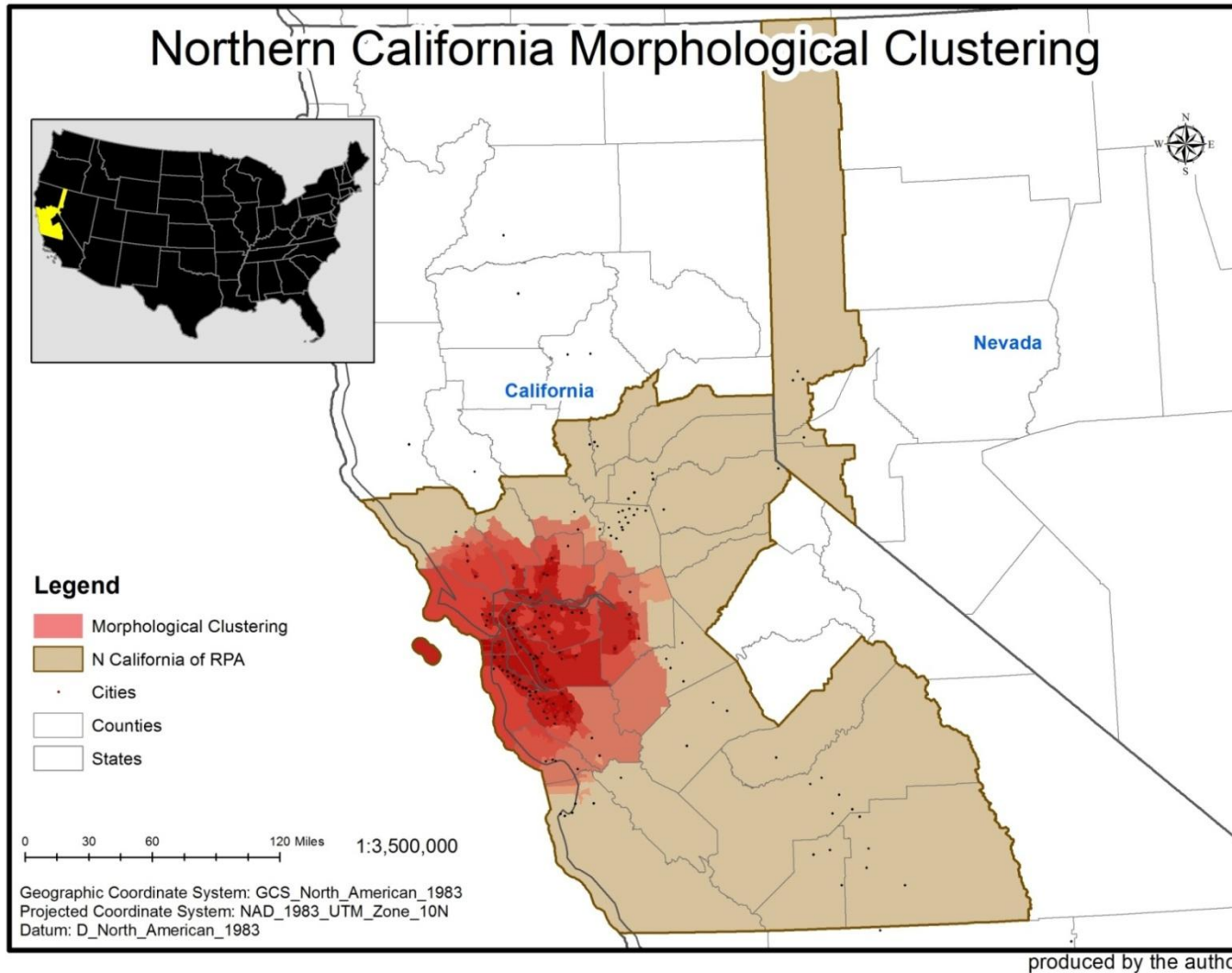


Figure 55 Morphological clusterings of the Northern California megaregion

Table 80 The Northern California megaregion morphological clusterings descriptors

Data Type	Clustering Area	Analysis	Northern California Morphological Clustering Descriptors		
			Census Tracts	Land Areas (sq. mi)	2000 Total Population
			2,637 (100%)	47,216.26 (100%)	12,672,400 (100%)
PopDen00	San Francisco - San Jose	Hot Spot	1,267 (48.05%)	3,595.05 (7.61%)	6,041,259 (47.67%)
		HH Cluster	573 (21.73%)	200.39 (0.42%)	2,776,383 (21.91%)
	Clustering Total		1,267 (48.05%)	3,595.05 (7.61%)	6,041,259 (47.67%)
ImpS01	San Francisco - San Jose	Hot Spot	1,436 (54.46%)	5,686.47 (12.04%)	6,906,795 (54.5%)
		HH Cluster	758 (28.74%)	643.01 (1.36%)	3,627,760 (28.63%)
	Clustering Total		1,437 (54.49%)	5,687.18 (12.04%)	6,911,361 (54.54%)
DMSP00	San Francisco - San Jose	Hot Spot	1,597 (60.56%)	8,361.91 (17.71%)	7,654,558 (60.4%)
		HH Cluster	1,300 (49.3%)	2,568.5 (5.44%)	6,214,642 (49.04%)
	Clustering Total		1,597 (60.56%)	8,361.91 (17.71%)	7,654,558 (60.4%)
The Northern California Subtotal		Hot Spot	1,607 (60.94%)	8,577.84 (18.17%)	7,714,088 (60.87%)
		HH Cluster	1,318 (49.98%)	2,616.74 (5.54%)	6,305,277 (49.76%)
The Northern California Morphological Clustering Total			1,607 (60.94%)	8,577.84 (18.17%)	7,714,088 (60.87%)

2.10. The Southern California megaregion

1) Local clustering of the 2000 population density

Figure 56 shows local clustering analysis results produced by using 2000 population density. Following the threshold of Density-based Sprawl Index, 2000 population density is categorized into three groups: rural areas population density (i.e., less than 200 persons per square mile), low population density areas (i.e., between 200 and 3,500 persons per square mile), and high population density areas (i.e., greater than 3,500 persons per square mile) (top left of figure). The general observation of the distribution of 2000 population density is that the low and high population density are concentrated around Los Angeles – San Diego, California and Las Vegas, Nevada.

The statistically significant hot spots at the 0.05 alpha level, as a result of Getis-Ord G_i^* analysis in terms of 2000 population density, represent monocentric clustering around Los Angeles area (top right of figure). Table 81 shows hot spot descriptors of 2000 population density for Southern California. The mean of 2000 population density is around 11,703.42 in comparison with the mean value of approximately 8,788.43 for the Southern California megaregion. Resulted hot spots, therefore, indicate that the levels of land use per capita are similarly high within the hot spot boundary.

Table 81 Southern California 2000 population density hot spots descriptors

Clustering Areas	Census Tracts	Land Area (sq. mi)	2000 Total Population
		4,578 (100%)	61,132.61 (100%)
Los Angeles	2,585 (56.47%)	3,495.7 (5.72%)	12,350,780 (56.74%)

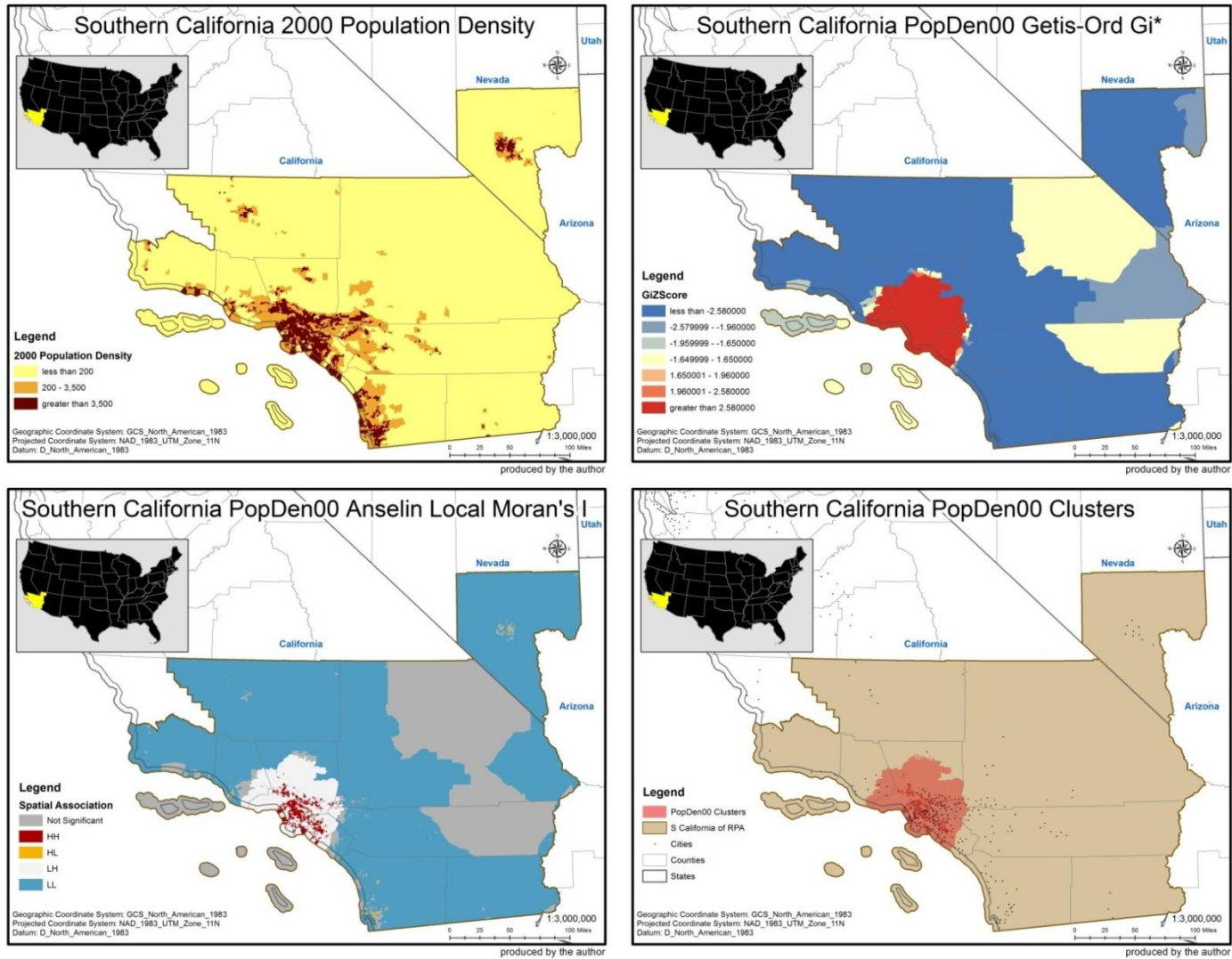


Figure 56 The Southern California megaregion local clustering analysis results by 2000 population density

The HH spatial association, as a result of Anselin Local Moran's *I* analysis in terms of 2000 population density, also represents monocentric clustering around Los Angeles area (bottom left of figure). Table 82 shows HH spatial associations descriptors of 2000 population density for Southern California. The mean of 2000 population density is around 18,552.18 in comparison with the mean value of approximately 8,788.43 for the Southern California megaregion. Resulted HH spatial associations, therefore, indicate that a high level of land use per capita is clustered with other similarly high levels of land use per capita within the resulted areas.

Table 82 Southern California 2000 population density HH spatial associations descriptors

Clustering Areas	Census Tracts	Land Area (sq. mi)	2000 Total Population
		4,578 (100%)	61,132.61 (100%)
Los Angeles	1,246 (27.22%)	419.88 (0.69%)	0.69 (29.4%)

Morphological clustering, as a result of overlapping two analysis results in terms of 2000 population density, follows the clustering boundary in the result of Getis-Ord G_i^* analysis (bottom right of figure). The extent of 2000 population density clustering of the Southern California megaregion, therefore, is identical to the extent of hot spot clustering. The overlapping of the two clustering analysis results shows that the clustering pattern of 2000 population density has monocentric clustering concentration on the areas around Los Angeles. The morphological clustering map represents, therefore, that the levels of land use per capita are similarly high and clustered within the

clustering boundary. In terms of the clustering by 2000 population density, the Southern California megaregion identified by RPA seems to have an exaggerated boundary.

2) Local clustering of 2001 impervious land cover

Figure 57 shows local clustering analysis results produced by using 2001 impervious land cover. The general observation of the distribution of 2001 impervious land cover is that the highest degree of imperviousness in 2001 follows the distribution of 2000 low and high population density (top left of figure).

Table 83 Southern California 2001 impervious land cover hot spots descriptors

Clustering Areas	Census Tracts	Land Area (sq. mi)	2000 Total Population
	4,578 (100%)	61,132.61 (100%)	21,766,596 (100%)
Los Angeles	2,550 (55.7%)	3,121.95 (5.11%)	12,154,026 (55.84%)
San Diego	486 (10.62%)	1,308.58 (2.14%)	2,181,804 (10.02%)
Las Vegas	332 (7.25%)	5,297.32 (8.67%)	1,350,005 (6.2%)
Total	3,368 (73.57%)	9,727.85 (15.91%)	15,685,835 (72.06%)

The statistically significant hot spots at the 0.05 alpha level, as a result of Getis-Ord G_i^* analysis in terms of 2001 impervious land cover, represent tri-centric clustering (top right of figure). Hot spots are spatially concentrated in the areas around Los Angeles, San Diego, and Las Vegas. Even though the Los Angeles and San Diego clustering areas are spatially separated, it is likely to consider the clusterings as one area because of being physically close. Table 83 shows hot spots descriptors of 2001

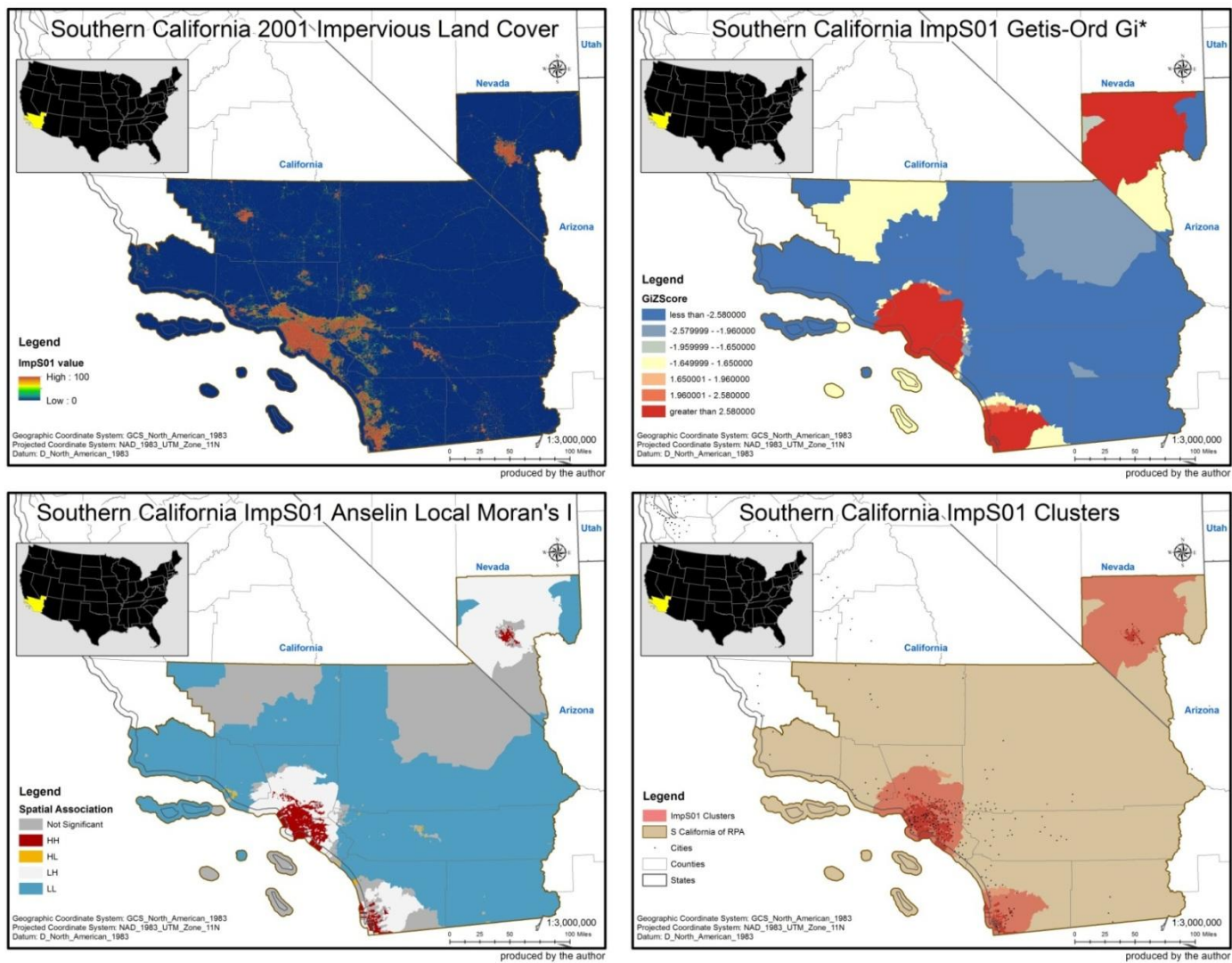


Figure 57 The Southern California megaregion local clustering analysis results by 2001 impervious land cover

impervious land cover for Southern California. The mean of 2001 impervious land cover is around 61.14% in comparison with the mean value of approximately 46.1% for the Southern California megaregion. Resulted hot spots, therefore, indicate that the urbanization levels of these built environments are similarly high within the hot spot boundary.

Table 84 Southern California 2001 impervious land cover HH spatial associations descriptors

Clustering Areas	Census Tracts	Land Area (sq. mi)	2000 Total Population
		4,578 (100%)	61,132.61 (100%)
Los Angeles	1,495 (32.66%)	720.43 (1.18%)	7,198,501 (33.07%)
San Diego	203 (4.43%)	134.14 (0.22%)	893,220 (4.1%)
Las Vegas	118 (2.58%)	89.65 (0.15%)	507,344 (2.33%)
Total	1,816 (39.67%)	944.22 (1.54%)	8,599,065 (39.51%)

The HH spatial association, as a result of Anselin Local Moran's *I* analysis in terms of 2001 impervious land cover, also represents tri-centric clustering located around the same areas with the result of hot spots analysis (bottom left of figure). The HH spatial clustering result, however, represents core areas for such hot spots clusterings as Los Angeles, San Diego, and Las Vegas with the fractal and fragmented clustering pattern. Table 84 shows HH spatial associations descriptors of 2001 impervious land cover for Southern California. The mean of 2001 impervious land cover is around 69.79% in comparison with the mean value of approximately 46.1% for the Southern California megaregion. Resulted HH spatial associations, therefore, indicate that a high level of

urbanization for these built environments is clustered with other similarly highly urbanized built environments within the resulted areas.

The morphological clustering, as a result of overlapping two analysis results in terms of 2001 impervious land cover, follows the clustering boundary in the result of Getis-Ord G_i^* analysis (bottom right of figure). The extent of 2001 impervious land cover clustering of the Southern California megaregion, therefore, is identical to the extent of hot spot clustering. The overlapping of the two clustering analysis results shows that the clustering pattern of 2001 impervious land cover has three round shape clustering areas around Los Angeles, San Diego, and Las Vegas. The morphological clustering map represents, therefore, that the urbanization levels of these built environments are similarly high and clustered within the clustering boundary. In terms of the clustering by 2001 impervious land cover, the Southern California megaregion identified by RPA seems to have an exaggerated boundary.

3) Local clustering of 2000 nighttime light emissions (DMSP-OLS)

Figure 58 shows local clustering analysis results produced by using 2000 nighttime light emissions (DMSP-OLS). The general observation of the distribution of 2000 nighttime light emissions is that the highest degree of nighttime light emissions in 2000 follows both distributions of 2000 low and high population density and 2001 impervious land cover (top left of figure). It is noticeable, however, for the expansion of high degree of nighttime light emissions from the area around Los Angeles to other surrounding areas so that there seems to exist the clustering flow of nighttime light

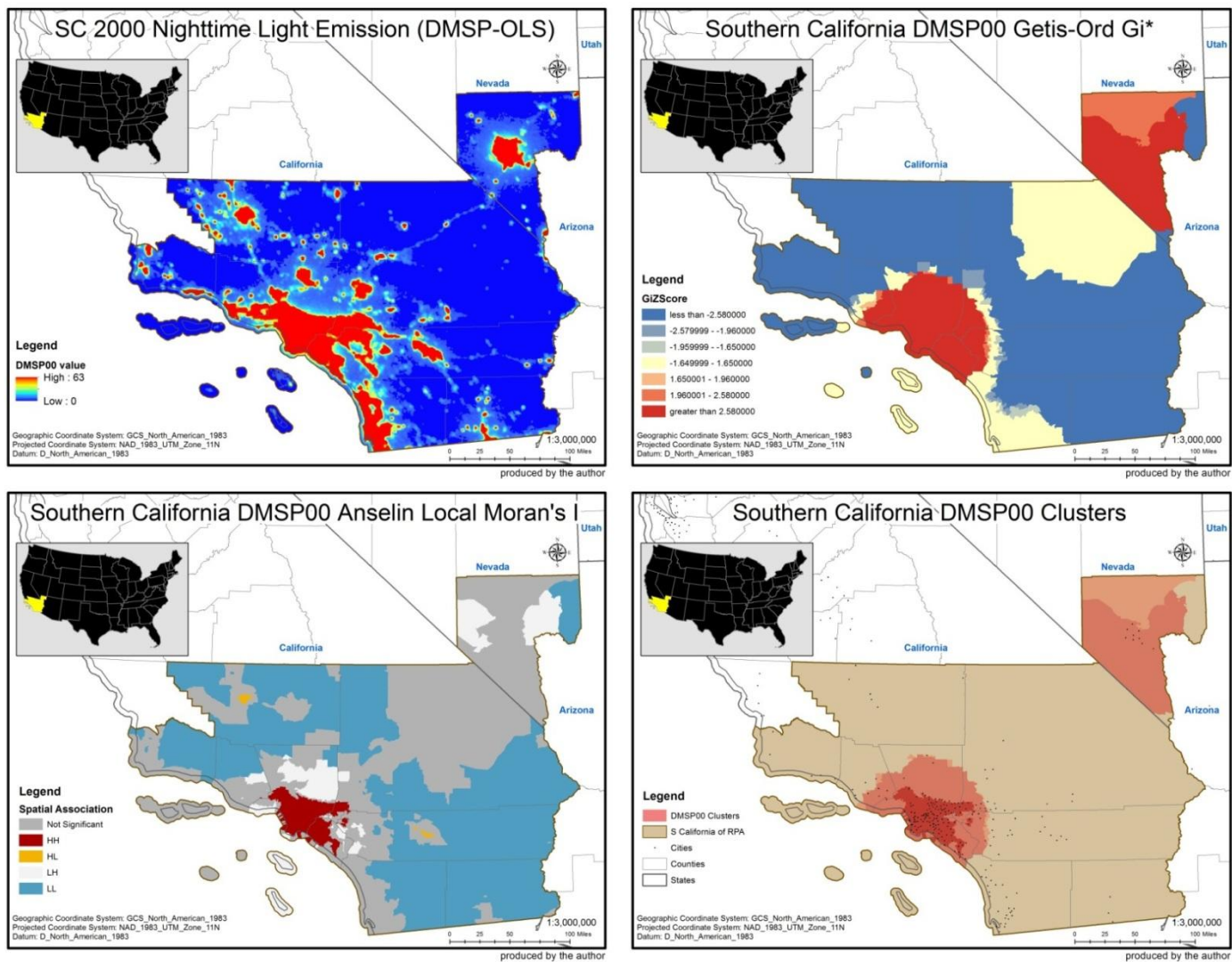


Figure 58 The Southern California megaregion local clustering analysis results by 2000 nighttime light emissions

emissions from Los Angeles to San Diego.

The statistically significant hot spots at the 0.05 alpha level, as a result of Getis-Ord G_i^* analysis in terms of 2000 nighttime light emissions, represent dual-centric clustering (top right of figure). Hot spots are spatially concentrated in the areas around Los Angeles and Las Vegas. Compared to the hot spot clustering analysis result in terms of 2001 impervious land cover, it is noticeable for the disappearance of San Diego clustering. Table 85 shows hot spots descriptors of 2000 nighttime light emissions for Southern California. The mean of 2000 nighttime light emissions is around 61.87% in comparison with the mean value of approximately 58.08% for the Southern California megaregion. Resulted hot spots, therefore, indicate that the urban development levels caused by nighttime socio-economic activities are similarly high within the hot spot boundary.

Table 85 Southern California 2000 nighttime light emissions hot spots descriptors

Clustering Areas	Census Tracts	Land Area (sq. mi)	2000 Total Population
	4,578 (100%)	61,132.61 (100%)	21,766,596 (100%)
Los Angeles	2,932 (64.05%)	5,250.08 (8.59%)	14,208,062 (65.27%)
Las Vegas	334 (7.3%)	6,907.32 (11.3%)	1,355,724 (6.23%)
Total	3,266 (71.34%)	12,157.4 (19.89%)	15,563,786 (71.5%)

The HH spatial association, as a result of Anselin Local Moran's I analysis in terms of 2000 nighttime light emissions, represents monocentric clustering around areas of Los Angeles (bottom left of figure). It is noticeable for the disappearance of the Las

Vegas clustering, compared to the hot spot clustering analysis result in terms of the same data source. Table 86 shows HH spatial associations descriptors of 2000 nighttime light emissions for Southern California. The mean of 2000 nighttime light emissions is around 62.95% in comparison with the mean value of approximately 58.08% for the Southern California megaregion. Resulted HH spatial associations, therefore, indicate that a high level of urban development caused by nighttime socio-economic activities is clustered with other similarly high levels of nighttime socio-economic urban activities within the resulted areas.

Table 86 Southern California 2000 nighttime light emissions HH spatial associations descriptors

Clustering Areas	Census Tracts	Land Area (sq. mi)	2000 Total Population
		4,578 (100%)	61,132.61 (100%)
Los Angeles	2,387 (52.14%)	1,585.59 (2.59%)	11,599,164 (53.29%)

Morphological clustering, as a result of overlapping two analysis results in terms of 2000 nighttime light emissions, follows the clustering boundary in the result of Getis-Ord G_i^* analysis (bottom right of figure). The extent of 2000 nighttime light emissions clustering for the Southern California megaregion, therefore, is identical to the extent of hot spot clustering. The overlapping of the two clustering analysis results shows that the clustering pattern of 2000 nighttime light emissions has two large clustering in the areas around Los Angeles and Las Vegas. The concentration in the central area of clustering by two local clustering analyses is only placed on the Los Angeles clustering area. The

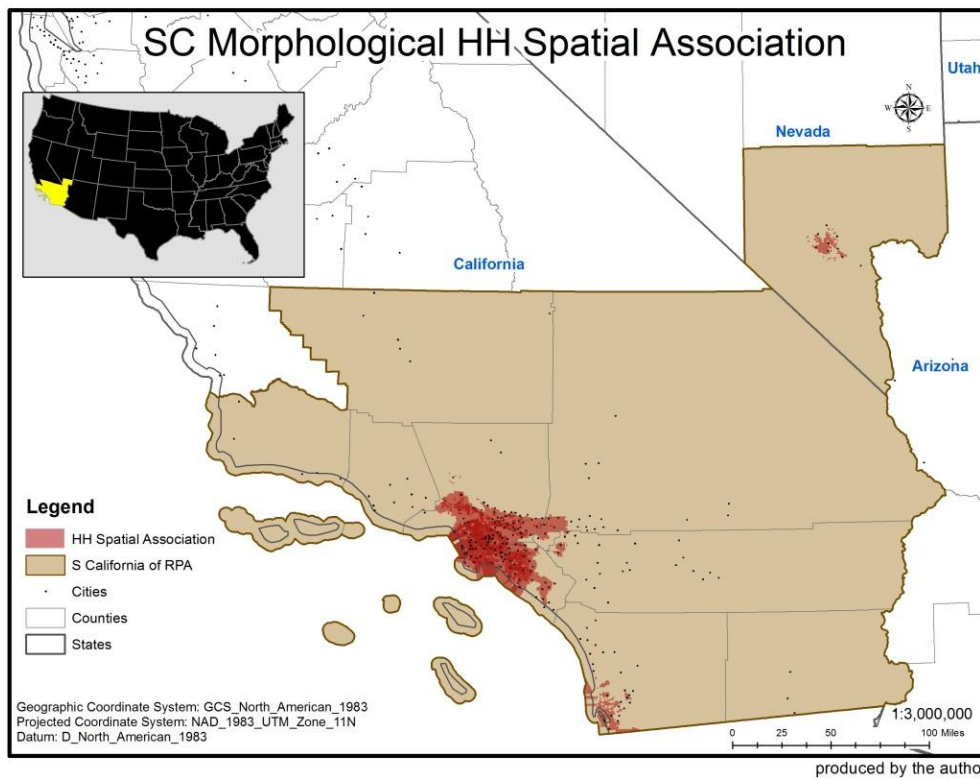
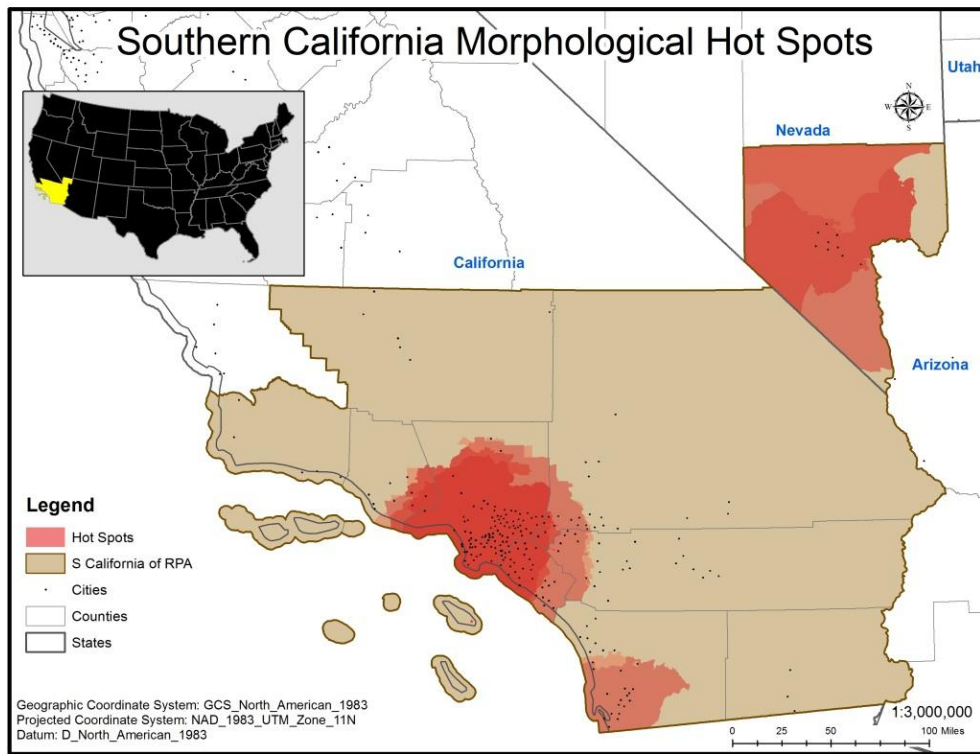


Figure 59 Local clusterings of morphological features in the Southern California megaregion

morphological clustering map represents, therefore, that the levels of urban development caused by nighttime socio-economic activities are similarly high and clustered within the clustering boundary. In terms of the clustering by 2000 nighttime light emissions, the Southern California megaregion identified by RPA seems to have an exaggerated boundary.

4) Morphological local clustering

Figure 59 represents results only produced by overlapping every clustering of the Getis-Ord G_i^* hot spots analysis (top of figure) and only by overlapping every HH spatial cluster of the Anselin Local Moran's I spatial cluster and outlier analysis (bottom of the figure). As the final representation for the Southern California megaregion morphological clustering, Figure 60 represents a result produced by overlapping the results separately represented in Figure 59. Table 87 summarizes the Southern California megaregion morphological clustering descriptors.

Representing polycentric morphological clustering for the Southern California megaregion, the Los Angeles clustering is primarily highlighted, meaning that the city and the surrounding areas have an excess of morphological characteristics such as population density, impervious land cover, and nighttime light emissions (see Figure 60). The Las Vegas clustering is highlighted as the concentration of impervious land cover and nighttime light emissions in the area. The San Diego clustering is also highlighted as the concentration of impervious land cover in the area. The clusterings around Los Angeles and San Diego are likely to have morphological interconnections because of

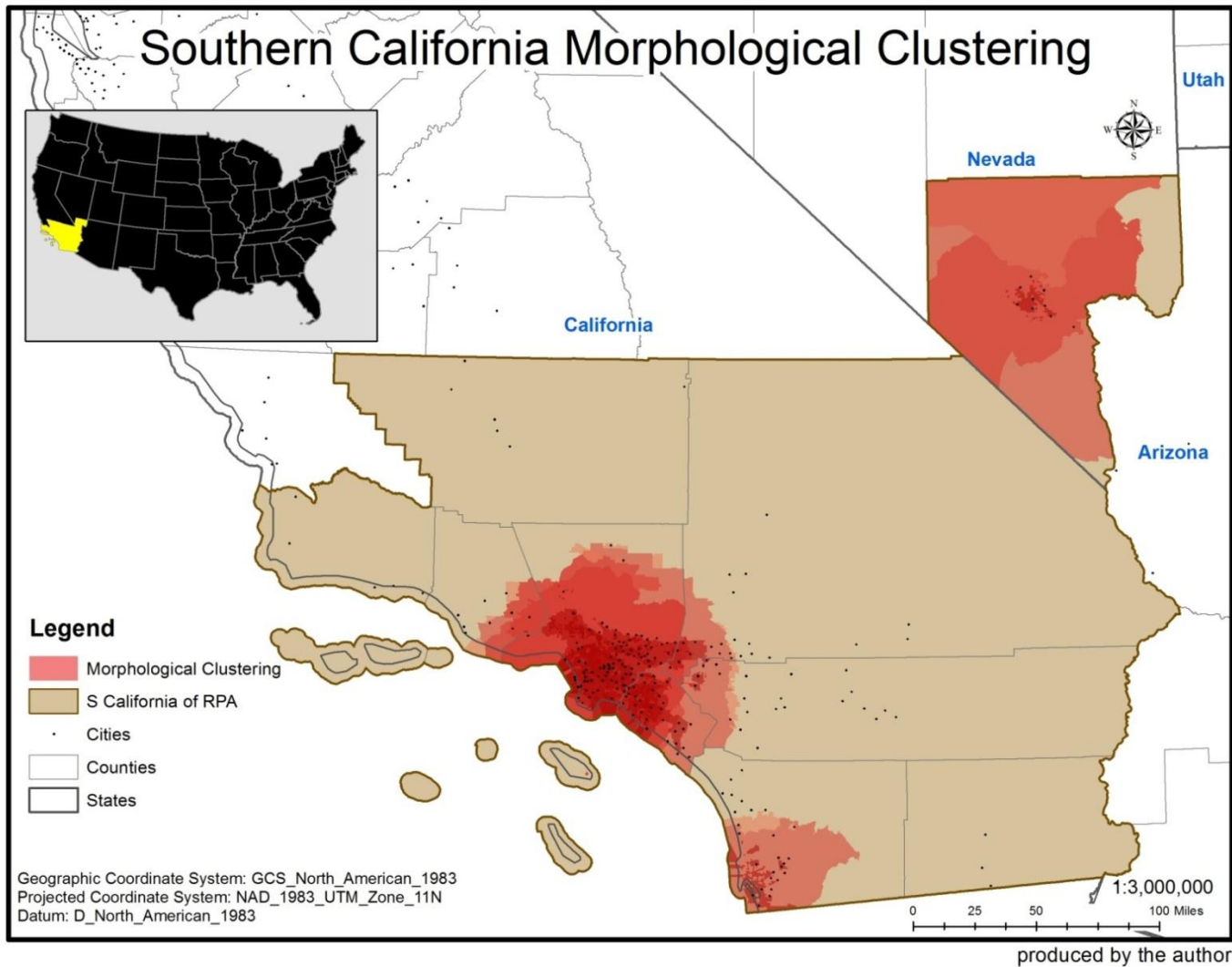


Figure 60 Morphological clusterings of the Southern California megaregion

Table 87 The Southern California megaregion morphological clusterings descriptors

Data Type	Clustering Area	Analysis	Southern California Morphological Clusterings Descriptors		
			Census Tracts	Land Areas (sq. mi)	2000 Total Population
			4,578 (100%)	61,132.61 (100%)	21,766,596 (100%)
PopDen00	Los Angeles	Hot Spot	2,585 (56.47%)	3,495.7 (5.72%)	12,350,780 (56.74%)
		HH Cluster	1,246 (27.22%)	419.88 (0.69%)	6,398,764 (29.4%)
	Clustering Total		2,585 (56.47%)	3,495.7 (5.72%)	12,350,780 (56.74%)
ImpS01	Los Angeles	Hot Spot	2,550 (55.7%)	3,121.95 (5.11%)	12,154,026 (55.84%)
		HH Cluster	1,495 (32.66%)	720.43 (1.18%)	7,198,501 (33.07%)
	San Diego	Hot Spot	486 (10.62%)	1,308.58 (2.14%)	2,181,804 (10.02%)
		HH Cluster	203 (4.43%)	134.14 (0.22%)	893,220 (4.10%)
	Las Vegas	Hot Spot	332 (7.25%)	5,297.32 (8.67%)	1,350,005 (6.2%)
		HH Cluster	118 (2.58%)	89.65 (0.15%)	507,344 (2.33%)
	Subtotal	Hot Spot	3,368 (73.57%)	9,727.85 (15.91%)	15,685,835 (72.06%)
		HH Cluster	1,816 (39.67%)	944.22 (1.54%)	8,599,065 (39.51%)
Clustering Total		3,368 (73.57%)	9,727.85 (15.91%)	15,685,835 (72.06%)	
DMSP00	Los Angeles	Hot Spot	2,932 (64.05%)	5,250.08 (8.59%)	14,208,062 (65.27%)
		HH Cluster	2,387 (52.14%)	1,585.59 (2.59%)	11,599,164 (53.29%)
	Las Vegas	Hot Spot	334 (7.3%)	6,907.32 (11.3%)	1,355,724 (6.23%)
		HH Cluster	n/a	n/a	n/a
	Subtotal	Hot Spot	3,266 (71.34%)	12,157.4 (19.89%)	15,563,786 (71.5%)
		HH Cluster	2,387 (52.14%)	1,585.59 (2.59%)	11,599,164 (53.29%)
Clustering Total		3,266 (71.34%)	12,157.4 (19.89%)	15,563,786 (71.5%)	
The Southern California Subtotal		Hot Spot	3,752 (81.96%)	13,465.98 (22.03%)	17,745,590 (81.53%)
		HH Cluster	2,742 (59.9%)	1,827.18 (2.99%)	13,147,491 (60.4%)
The Southern California Morphological Clustering Total			3,752 (81.96%)	13,465.98 (22.03%)	17,745,590 (81.53%)

being physically close. The Las Vegas clustering, however, is not likely to consider the morphological clustering connection because of being physically distant. Concerning the megaregion boundary of RPA, therefore, the Southern California megaregion boundary is not likely to fit the morphological clustering and connection. It is more likely to consider a separate region for Los Angeles – San Diego clustering area from Las Vegas clustering area. The total extent of Southern California clustering in terms of all morphological features analyzed thus far includes 3,752 census tracts being around 81.96% of the total Southern California census tracts; about 13,465.98 square miles equal approximately 22.03% of the total Southern California land area; and 17,745,590 total population being around 81.53% of the total population of the Southern California megaregion.

The Southern California morphological clustering map resulted finally represents the locations where high levels of land uses per capita, urbanized built environment, and nighttime socio-economic urban activities are clustered. The clustering areas of Los Angeles and San Diego seem to have morphological interconnections because of being physically close. The clustering area of Las Vegas, however, seems to be difficult to consider morphological connections to other clustering areas because of being physically distant. The final map also represents an exaggerated boundary for the Southern California megaregion in the morphological observations.

2.11. The Cascadia megaregion

1) Local clustering of 2000 population density

Figure 61 shows local clustering analysis results produced by using 2000 population

density. Following the threshold of Density-based Sprawl Index, 2000 population density is categorized into three groups: rural areas population density (i.e., less than 200 persons per square miles), low population density areas (i.e., between 200 and 3,500 persons per square miles), and high population density areas (i.e., greater than 3,500 persons per square miles) (top left of figure). The general observation of the distribution of 2000 population density is that the low and high population density are concentrated around Seattle, Washington and Portland, Oregon. Small clusterings around Salem, Albany, and Eugene is also noticeable.

The statistically significant hot spots at the 0.05 alpha level, as a result of Getis-Ord G_i^* analysis in terms of 2000 population density, represent dual-centric clustering around Seattle and Portland (top right of figure). Table 88 shows hot spot descriptors of 2000 population density for Cascadia. The mean of 2000 population density is around 4,352.32 in comparison with the mean value of approximately 3,315.06 for the Cascadia megaregion. Resulted hot spots, therefore, indicate that the levels of land use per capita are similarly high within the hot spot boundary.

Table 88 Cascadia 2000 population density hot spots descriptors

Clustering Areas	Census Tracts	Land Area (sq. mi)	2000 Total Population
		1,619 (100%)	46,848.31 (100%)
Seattle	594 (36.69%)	2,137.09 (4.56%)	2,721,403 (36.86%)
Portland	406 (25.08%)	2,469.93 (5.27%)	1,856,252 (25.14%)
Total	1,000 (61.77%)	4,607.01 (9.83%)	4,511,655 (62.01%)

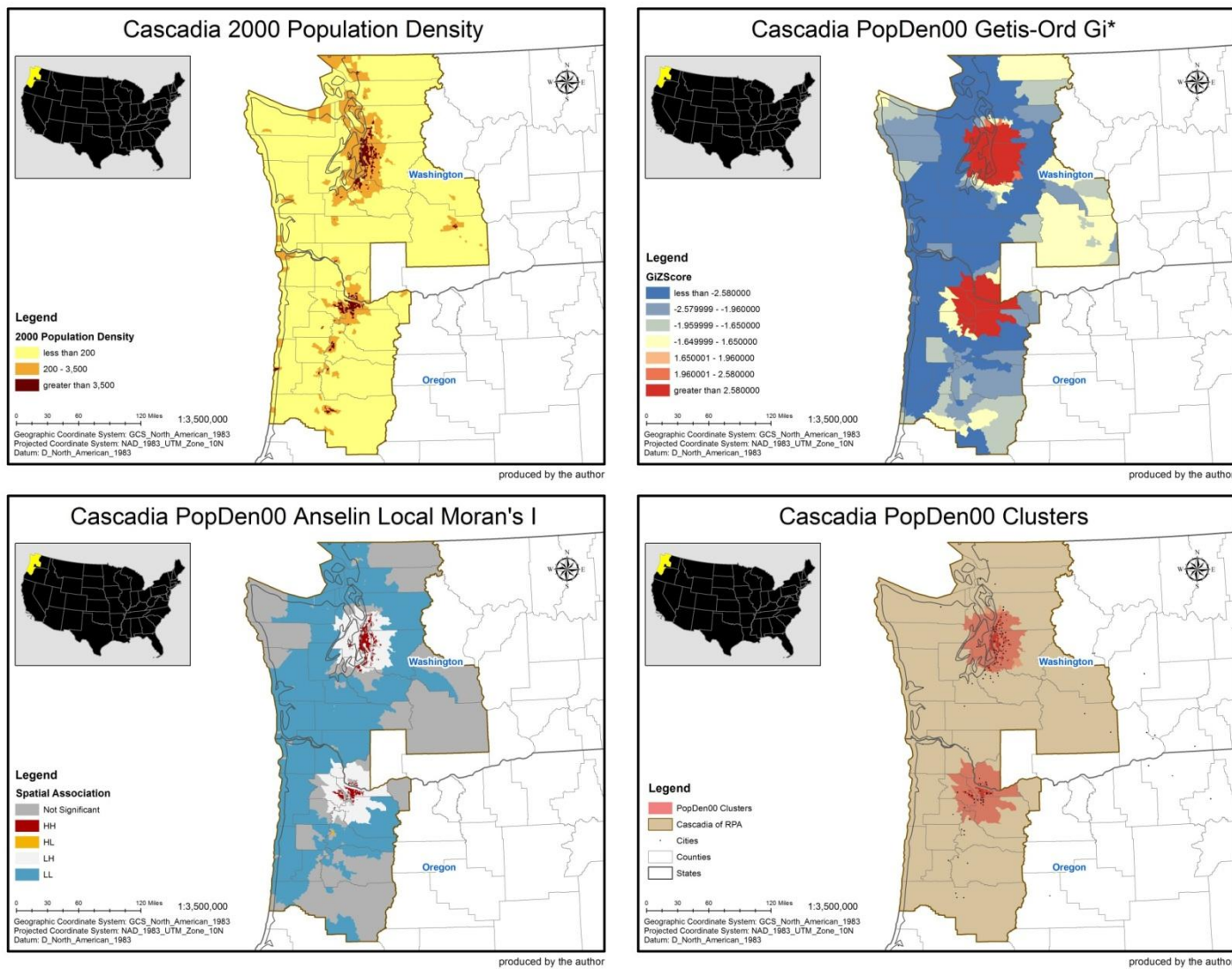


Figure 61 The Cascadia megaregion local clustering analysis results by 2000 population density

The HH spatial association, as a result of Anselin Local Moran's *I* analysis in terms of 2000 population density, also represents dual-centric clustering around Seattle and Portland (bottom left of figure). When the HH spatial clustering pattern of 2000 population density is compared to the hot spot clustering pattern, it is more fractal and fragmented, representing core areas of clustering concentration. Table 89 shows HH spatial associations descriptors of 2000 population density for Cascadia. The mean of 2000 population density is around 7,349.6 in comparison with the mean value of approximately 3,315.06 for the Cascadia megaregion. Resulted HH spatial associations, therefore, indicate that a high level of land use per capita is clustered with other similarly high levels of land use per capita within the resulted areas.

Table 89 Cascadia 2000 population density HH spatial associations descriptors

Clustering Areas	Census Tracts	Land Area (sq. mi)	2000 Total Population
		1,619 (100%)	46,848.31 (100%)
Seattle	262 (16.18%)	199.17 (0.43%)	1,255,031 (17%)
Portland	171 (10.56%)	122.96 (0.26%)	774,264 (10.49%)
Total	433 (26.74%)	322.13 (0.69%)	2,029,295 (27.49%)

Morphological clustering, as a result of overlapping two analysis results in terms of 2000 population density, has the same clustering boundary with Getis-Ord G_i^* analysis result (bottom right of figure). The extent of 2000 population density clustering of the Cascadia megaregion, therefore, is identical to the extent of hot spot clustering. The overlapping of the two clustering analysis results shows that the clustering pattern of

2000 population density has two large clustering concentrations in the areas around Seattle and Portland. The morphological clustering map represents, therefore, that the levels of land use per capita are similarly high and clustered within the clustering boundary. In terms of the clustering by 2000 population density, the Cascadia megaregion identified by RPA seems to have an exaggerated boundary.

2) Local clustering of 2001 impervious land cover

Figure 62 shows local clustering analysis results produced by using 2001 impervious land cover. The general observation of the distribution of 2001 impervious land cover is that most high degree of imperviousness in 2001 follows the distribution of 2000 low and high population density (top left of figure).

Table 90 Cascadia 2001 impervious land cover hot spots descriptors

Clustering Areas	Census Tracts	Land Area (sq. mi)	2000 Total Population
		1,619 (100%)	46,848.31 (100%)
Seattle	567 (35.02%)	1,941.16 (4.14%)	2,591,841 (35.11%)
Portland	406 (25.08%)	2,469.93 (5.27%)	1,856,252 (25.14%)
Total	973 (60.1%)	4,411.08 (9.42%)	4,448,093 (60.25%)

The statistically significant hot spots at the 0.05 alpha level, as a result of Getis-Ord G_i^* analysis in terms of 2001 impervious land cover, represent dual-centric clustering around Seattle and Portland (top right of figure). Table 90 shows hot spots descriptors of 2001 impervious land cover for Cascadia. The mean of 2001 impervious

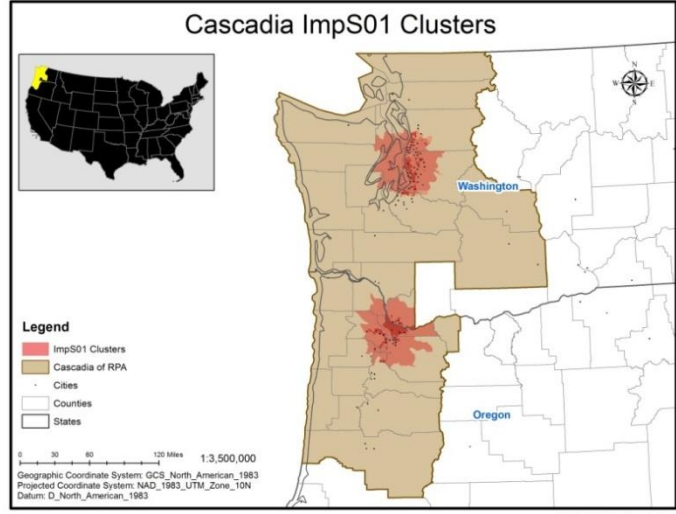
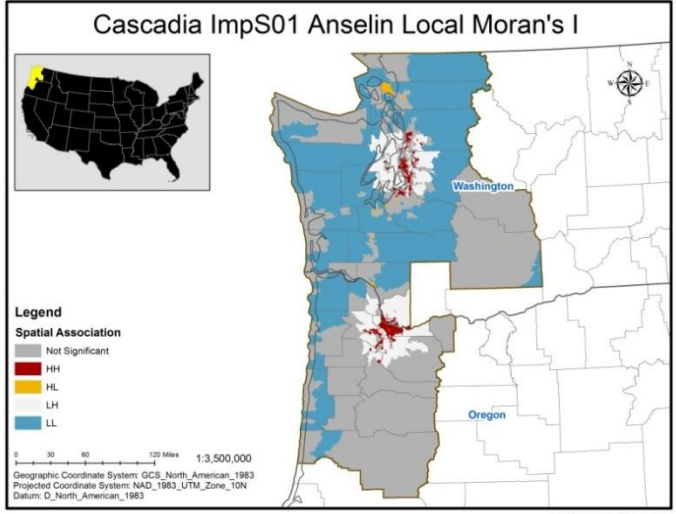
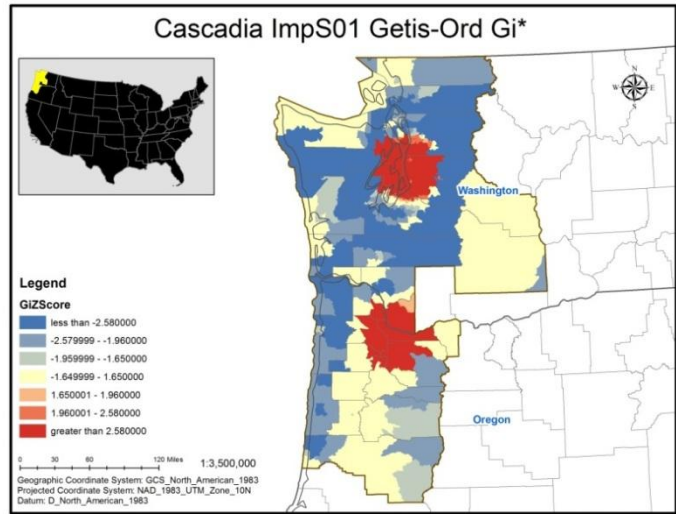
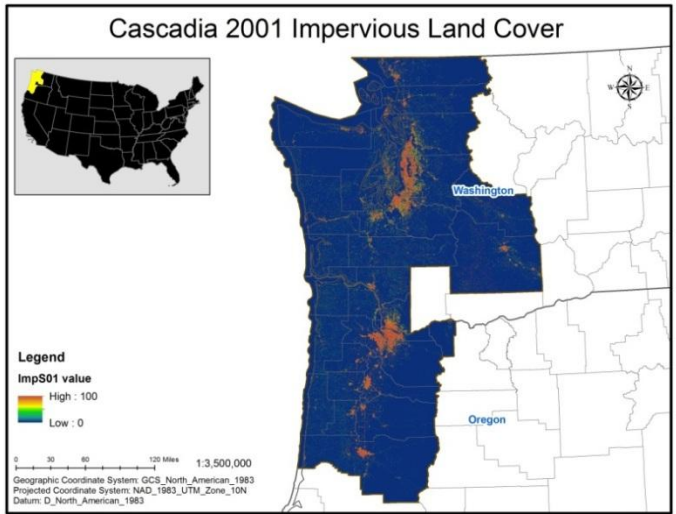


Figure 62 The Cascadia Megaregion local clustering analysis results by 2001 impervious land cover

land cover is around 50.78% in comparison with the mean value of approximately 28.42% for the Cascadia megaregion. Resulted hot spots, therefore, indicate that the urbanization levels of built environments are similarly high within the hot spot boundary. The HH spatial association, as a result of Anselin Local Moran's *I* analysis in terms of 2001 impervious land cover, also represents dual-centric clustering around Seattle and Portland (bottom left of figure). The clustering pattern, however, seems more fractal and fragmented compared to the hot spot clustering pattern. Table 91 shows HH spatial associations descriptors of 2001 impervious land cover for Cascadia. The mean of 2001 impervious land cover is around 62.4% in comparison with the mean value of approximately 28.42% for the Cascadia megaregion. Resulted HH spatial associations, therefore, indicate that a high level of urbanization for these built environments is clustered with other similarly highly urbanized built environments within the resulted areas.

Table 91 Cascadia 2001 impervious land cover HH spatial associations descriptors

Clustering Areas	Census Tracts	Land Area (sq. mi)	2000 Total Population
		1,619 (100%)	46,848.31 (100%)
Seattle	151 (9.33%)	181.89 (0.39%)	657,175 (8.9%)
Portland	204 (12.6%)	268.22 (0.57%)	849,657 (11.51%)
Total	355 (21.93%)	450.11 (0.96%)	1,506,832 (20.41%)

Morphological clustering, as a result of overlapping two analysis results in terms of 2001 impervious land cover, has the similar clustering boundary to Getis-Ord G_i^*

analysis result (bottom right of figure). Only 1 census tract of HH spatial clustering analysis result that is located in the outskirts of Seattle area is not included in the hot spot clustering areas. The overlapping observation represents that the clustering concentration is primarily located in Seattle and Portland. Table 92 shows the total extent of 2001 impervious land cover clustering descriptors for Cascadia. The morphological clustering map represents, therefore, that the urbanization levels of these built environments are similarly high and clustered within the clustering boundary. In terms of the clustering by 2001 impervious land cover, the Cascadia megaregion identified by RPA seems to have an exaggerated boundary.

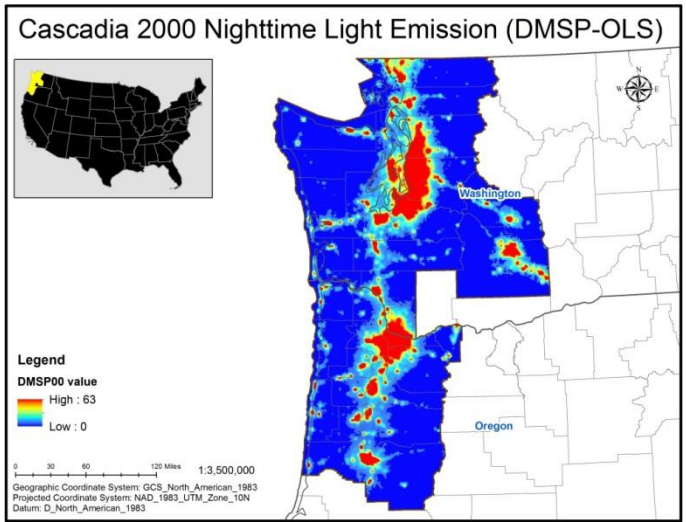
Table 92 Cascadia 2001 impervious land cover clustering descriptors

Clustering Total	Census Tracts	Land Area (sq. mi)	2000 Total Population
		1,619 (100%)	46,848.31 (100%)
2001 impervious land cover	974 (60.16%)	4,413.76 (9.42%)	4,450,689 (60.29%)

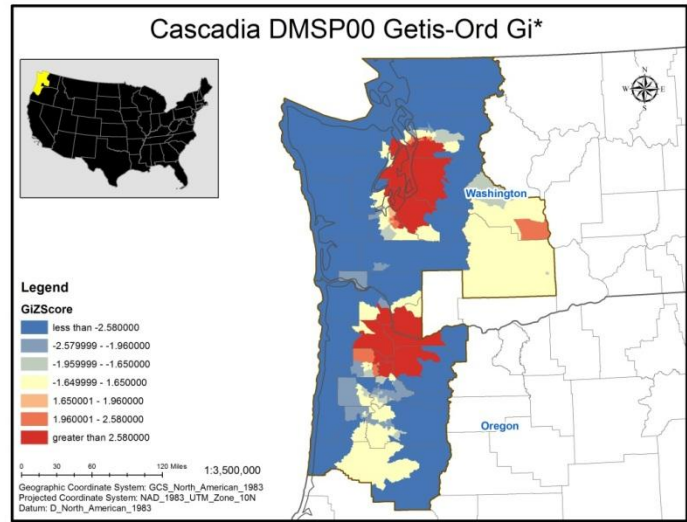
3) Local clustering of 2000 nighttime light emissions (DMSP-OLS)

Figure 63 shows local clustering analysis results produced by using 2000 nighttime light emissions (DMSP-OLS). The general observation of the distribution of 2000 nighttime light emissions is that the highest degree of nighttime light emissions in 2000 follows both distributions of 2000 low and high population density and 2001 impervious land cover (top left of figure).

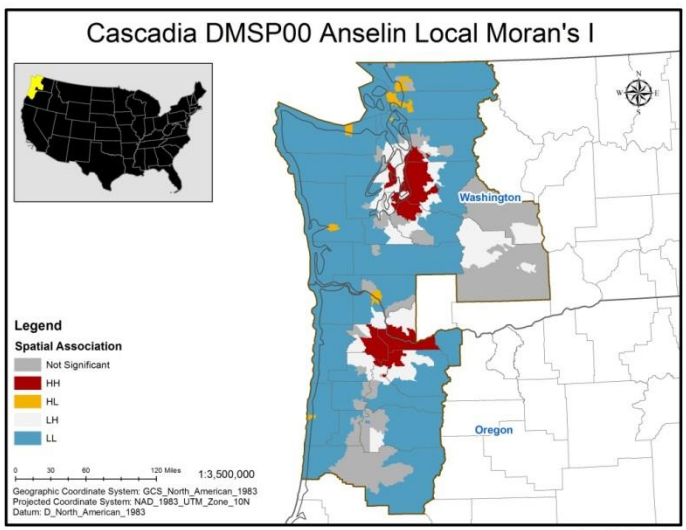
The statistically significant hot spots at the 0.05 alpha level, as a result of Getis-Ord G_i^* analysis in terms of 2000 nighttime light emissions, represent polycentric



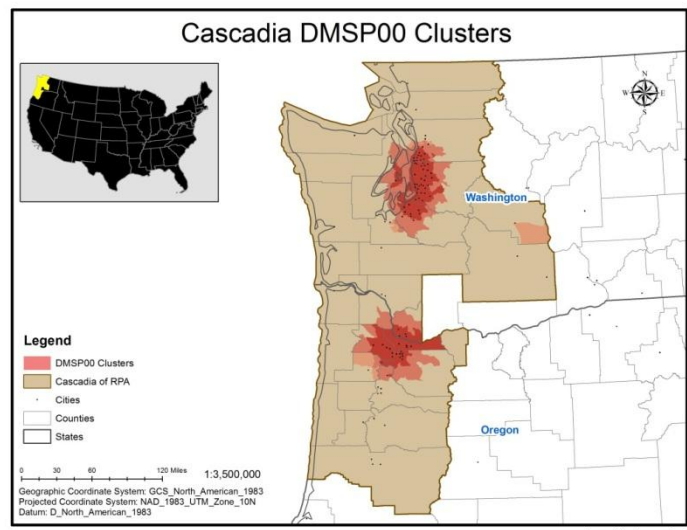
produced by the author



produced by the author



produced by the author



produced by the author

Figure 63 The Cascadia megaregion local clustering analysis results by 2000 nighttime light emissions

clustering (top right of figure). Hot spots are spatially concentrated in the areas around Seattle and Portland. It is noticeable for the appearance of hot spot clustering in the outskirts of Ellensburg, Washington. Table 93 shows hot spots descriptors of 2000 nighttime light emissions for Cascadia. The mean of 2000 nighttime light emissions is around 55% in comparison with the mean value of approximately 47.26% for the Cascadia megaregion. Resulted hot spots, therefore, indicate that the urban development levels caused by nighttime socio-economic activities are similarly high within the hot spot boundary.

Table 93 Cascadia 2000 nighttime light emissions hot spots descriptors

Clustering Areas	Census Tracts	Land Area (sq. mi)	2000 Total Population
		1,619 (100%)	46,848.31 (100%)
Seattle	693 (42.8%)	2,652.01 (5.66%)	3,180,292 (43.08%)
Portland	411 (25.39%)	2,913.67 (6.22%)	1,879,196 (25.46%)
Ellensburg	3 (0.19%)	418.89 (0.89%)	10,425 (0.14%)
Total	1,107 (68.38%)	5,984.57 (12.77%)	5,069,913 (68.68%)

The HH spatial association, as a result of Anselin Local Moran's *I* analysis in terms of 2000 nighttime light emissions, represents dual-centric clustering around areas of Seattle and Portland (bottom left of figure). The clustering around the outskirts of Ellensburg is disappeared in the HH spatial clustering analysis result. Table 94 shows HH spatial associations descriptors of 2000 nighttime light emissions for Cascadia. The mean of 2000 nighttime light emissions is around 61.8% in comparison with the mean

value of approximately 47.26% for the Cascadia megaregion. Resulted HH spatial associations, therefore, indicate that a high level of urban development caused by nighttime socio-economic activities is clustered with other similarly high levels of nighttime socio-economic urban activities within the resulted areas.

Table 94 Cascadia 2000 nighttime light emissions HH spatial associations descriptors

Clustering Areas	Census Tracts	Land Area (sq. mi)	2000 Total Population
		1,619 (100%)	46,848.31 (100%)
Seattle	582 (35.95%)	1,127.54 (2.41%)	2,711,487 (36.73%)
Portland	368 (22.73%)	1,271.08 (2.71%)	1,669,463 (22.61%)
Total	950 (58.68%)	2,398.63 (5.12%)	4,380,950 (59.34%)

Morphological clustering, as a result of overlapping two analysis results in terms of 2000 nighttime light emissions, follows the clustering boundary in the result of Getis-Ord G_i^* analysis (bottom right of figure). The extent of 2000 nighttime light emissions clustering of the Cascadia megaregion, therefore, is identical to the extent of hot spot clustering. The overlapping of the two clustering analysis results shows that the clustering pattern of 2000 nighttime light emissions has two large clustering concentrations in the areas around Seattle and Portland. The clustering around the outskirts of Ellensburg is also noticeable. The morphological clustering map represents, therefore, that the levels of urban development caused by nighttime socio-economic activities are similarly high and clustered within the clustering boundary. In terms of the clustering by 2000 nighttime light emissions, the Cascadia megaregion identified by

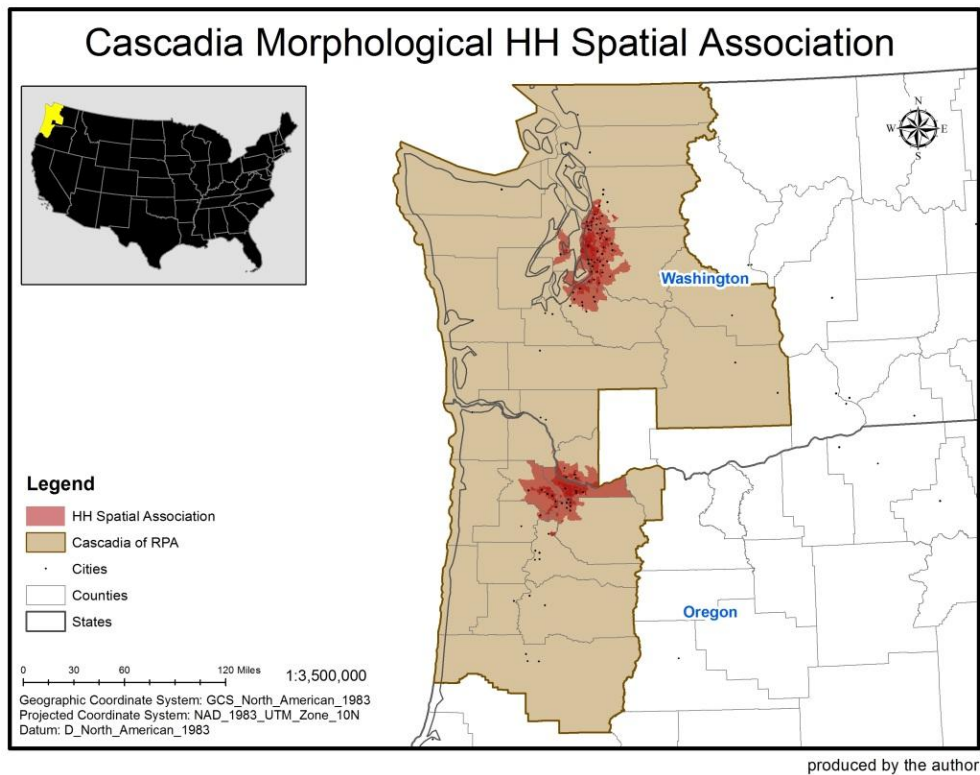
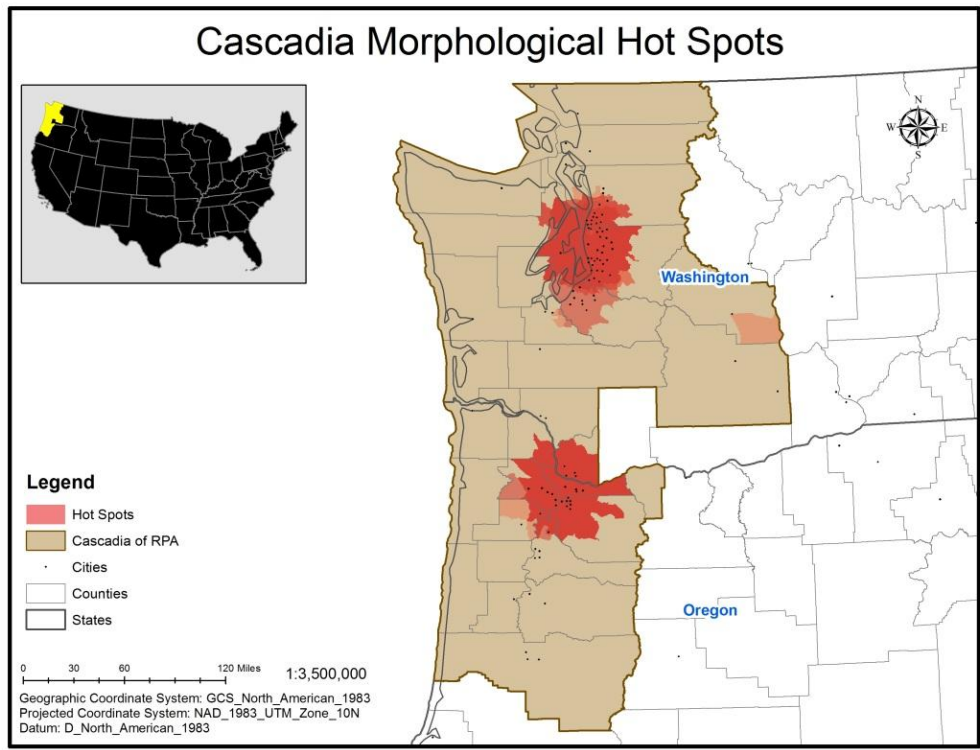


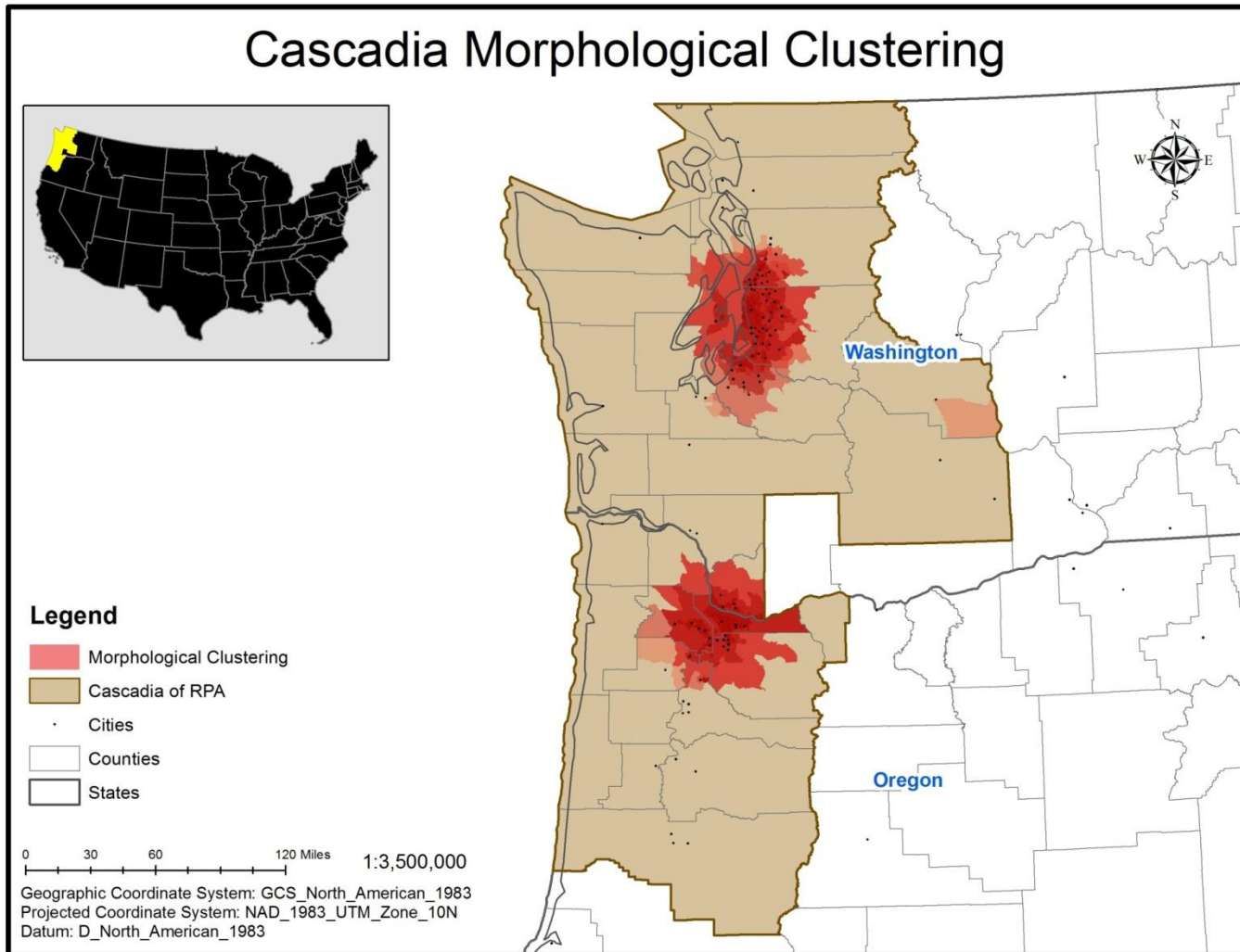
Figure 64 Local clusterings of morphological features in the Cascadia megaregion

RPA seems to have an exaggerated boundary.

4) Morphological local clustering

Figure 64 represents results only produced by overlapping every clustering of the Getis-Ord G_i^* hot spots analysis (top of figure) and only by overlapping every HH spatial cluster of the Anselin Local Moran's I spatial cluster and outlier analysis (bottom of figure). As the final representation for the Cascadia megaregion morphological clustering, Figure 65 represents a result produced by overlapping the results separately represented in Figure 64. Table 95 summarizes the Cascadia megaregion morphological clustering descriptors.

Representing polycentric morphological clustering for the Cascadia megaregion, the clustering around Seattle and around Portland are primarily highlighted, meaning that the cities and the surrounding areas have an excess of morphological characteristics such as population density, impervious land cover, and nighttime light emissions (see Figure 65). The outskirts of Ellensburg also have an excess of nighttime light emissions in the hot spot clustering analysis result. Without any small clustering areas to bridge the two morphological clustering areas, the areas are likely separated. Concerning megaregions boundaries of RPA, therefore, the Cascadia megaregion boundary is not likely to fit the morphological clustering and connection. It is more likely, rather, to consider as a separate region for Seattle clustering area from the region for Portland clustering area. The total extent of Cascadia clustering in terms of all morphological features analyzed thus far includes 1,114 census tracts being around 68.81% of the total



produced by the author

Figure 65 Morphological clusterings of the Cascadia megaregion

Table 95 The Cascadia megaregion morphological clusterings descriptors

Data Type	Clustering Area	Analysis	Cascadia Morphological Clusterings Descriptors		
			Census Tracts	Land Areas (sq. mi)	2000 Total Population
			1,619 (100%)	46,848.31 (100%)	7,382,192 (100%)
PopDen00	Seattle	Hot Spot	594 (36.69%)	2,137.09 (4.56%)	2,721,403 (36.86%)
		HH Cluster	262 (16.18%)	199.17 (0.43%)	1,255,031 (17%)
	Portland	Hot Spot	406 (25.08%)	2,469.93 (5.27%)	1,856,252 (25.14%)
		HH Cluster	171 (10.56%)	122.96 (0.26%)	774,264 (10.49%)
	Subtotal	Hot Spot	1,000 (61.77%)	4,607.01 (9.83%)	4,577,655 (62.01%)
		HH Cluster	433 (26.74%)	322.13 (0.69%)	2,029,295 (27.49%)
	Clustering Total		1,000 (61.77%)	4,607.01 (9.83%)	4,577,655 (62.01%)
ImpS01	Seattle	Hot Spot	567 (35.02%)	1,941.16 (4.14%)	2,591,841 (35.11%)
		HH Cluster	151 (9.33%)	181.89 (0.39%)	657,175 (8.9%)
	Portland	Hot Spot	406 (25.08%)	2,469.93 (5.27%)	1,856,252 (25.14%)
		HH Cluster	204 (12.6%)	268.22 (0.57%)	849,657 (11.51%)
	Subtotal	Hot Spot	973 (60.1%)	4,411.08 (9.42%)	4,448,093 (60.25%)
		HH Cluster	355 (21.93%)	450.11 (0.96%)	1,506,832 (20.41%)
	Clustering Total		974 (60.16%)	4,413.76 (9.42%)	4,450,689 (60.29%)
DMSP00	Seattle	Hot Spot	693 (42.8%)	2,652.01 (5.66%)	3,180,292 (43.08%)
		HH Cluster	582 (35.95%)	1,127.54 (2.41%)	2,711,487 (36.73%)
	Portland	Hot Spot	411 (25.39%)	2,913.67 (6.22%)	1,879,196 (25.46%)
		HH Cluster	368 (22.73%)	1,271.08 (2.71%)	1,669,463 (22.61%)
	Ellensburg	Hot Spot	3 (0.19%)	418.89 (0.89%)	10,425 (0.14%)
		HH Cluster	n/a	n/a	n/a
	Subtotal	Hot Spot	1,107 (68.38%)	5,984.57 (12.77%)	5,069,913 (68.68%)
HH Cluster		950 (58.68%)	2,398.63 (5.12%)	4,380,950 (59.34%)	
Clustering Total		1,107 (68.38%)	5,984.57 (12.77%)	5,069,913 (68.68%)	
The Cascadia Subtotal		Hot Spot	1,114 (68.81%)	6,134.91 (13.1%)	5,094,144 (69.01%)
		HH Cluster	959 (59.23%)	2,406.94 (5.14%)	4,414,358 (59.8%)
The Cascadia Morphological Clustering Total		1,114 (68.81%)	6,134.91 (13.1%)	5,094,144 (69.01%)	

Cascadia census tracts; about 6,134.91 square miles equal approximately 13.1% of the total Cascadia land area; and 5,094,144 total population being around 69.01% of the total population of the Cascadia megaregion.

The Cascadia morphological clustering map resulted finally represents the locations where high levels of land uses per capita, urbanized built environment, and nighttime socio-economic urban activities are clustered. The clustering areas of Seattle and Portland seem to have morphological interconnections because of being physically close. The final map, however, represents an exaggerated boundary for the Cascadia megaregion in the morphological observations.

3. Results summary for research hypotheses

3.1. Spatial patterns of the 11 U.S. megaregions

The first research sub-question for this study asked what spatial patterns of morphological characteristics of U.S. megaregions represent concerning variations of morphological characteristics spatial distribution. This study has observed three spatial patterns such as density-based sprawl, spatial scattering, and spatial clustering based on morphological characteristics such as 2000 total population, 2000 population density, 2001 impervious land cover, and 2000 nighttime light emissions.

Results of the density-based sprawl index (DSI) have indicated that the pattern of land use per capita has varied among U.S. megaregions. In 2000, ranging from around 22 DSI to around 78 DSI, the DSI distinguished low level population sprawl megaregions – Northern and Southern California, Arizona Sun Corridor, Front Range,

and Northeast – from high level population sprawl megaregions – Piedmont Atlantic, Gulf Coast, Great Lakes, Florida, Texas Triangle, and Cascadia.

The results of the spatial scattering pattern index (SPI) have indicated that the 11 U.S. megaregions share a common spatial scattering pattern of morphological characteristics that are not evenly scattered but unevenly concentrated in fewer areas within the corresponding megaregion boundary. However, the Piedmont Atlantic megaregion has shown exceptionally high scattering in terms of both the 2000 total population and 2000 population density as exceeding the 2 standard deviation range from the mean SPI value. It means that, except for the Piedmont Atlantic megaregion, morphological characteristics of U.S. megaregions show consistent spatial scattering patterns that are not evenly scattered but spatially concentrated on fewer areas within the boundaries of the megaregions.

The spatial clustering pattern index (CPI) has indicated that the spatial clustering pattern of all U.S. megaregions morphological characteristics have statistically significant spatial clustering (see Appendix B). There is variation, however, in the extent of spatial clustering of morphological characteristics. 2000 population density distinguished loosely clustered spatial pattern megaregions such as the Front Range and Arizona Sun Corridor from a closely clustered spatial pattern megaregion such as the Northeast. 2001 impervious land cover also differentiates loosely clustered spatial pattern megaregions such as Cascadia and Front Range from a closely clustered spatial pattern megaregion such as Northeast. The 2000 nighttime light emissions makes a distinction between loosely clustered spatial pattern megaregions such as the Southern

California and the Northern California and closely clustered spatial pattern megaregions such as the Northeast and the Texas Triangle.

Based on the density-based sprawl pattern index, therefore, this study was able to reject the null hypothesis and accept the first research hypothesis that spatial patterns of morphological characteristics of the U.S. megaregions may not represent a common spatial structure. Based on the spatial scattering pattern index, this study has rejected the null hypothesis and accepted the first research hypothesis for the exceptionally high level of scattering spatial patterns in the Piedmont Atlantic megaregion in terms of both 2000 total population and 2000 population density. Based on the spatial clustering pattern index, this study failed to reject the null hypothesis for the statistically significant spatial clustering pattern in the 11 U.S. megaregions, even though they represent various extents of morphological clustering. The failure to reject the null hypothesis in the spatial clustering index, however, should be considered with local scale clustering analysis because the spatial clustering pattern index that is a global statistic cannot identify the location of morphological clustering, nor does it quantify how spatial association varies from one region to another. The spatial clustering pattern index is still useful, however, to determine whether or not a spatial association exists (Jacquez, 2008).

3.2. Spatial associations of the 11 U.S. megaregions

The second research sub-question for this study asked what spatial associations of morphological characteristics of the U.S. megaregions represent concerning spatial interconnections of morphological characteristics within the boundaries of U.S.

megaregions. This study has examined two types of spatial association analysis, the Getis-Ord G_i^* hot spot and the Anselin Local Moran's I cluster and outlier based on morphological characteristics such as 2000 population density, 2001 impervious land cover, and 2000 nighttime light emissions.

The two spatial analysis model results and mapping results for the U.S. megaregions show that the hot spots analysis model generates a broader range of spatial boundary for morphological clustering than the cluster and outlier analysis model does. The cluster and outlier analysis model has rather pointed out core areas of each morphological clustering. The cluster and outlier analysis model has not generated core clustering areas in some cases of morphological clustering even though the hot spots analysis model has pointed out morphological clustering in the same areas. The inconsistency in representing spatial clustering between the two local spatial clustering analysis models has occurred in the Northeast megaregion (Williamstown clustering area in terms of 2001 impervious land cover); the Texas Triangle megaregion (San Antonio clustering area and Georgetown – San Marcos clustering area in terms of 2000 nighttime light emissions); the Great Lakes megaregion (Indiana clustering area, Columbus clustering area, and Pittsburgh clustering area in terms of 2000 nighttime light emissions); the Piedmont Atlantic megaregion (Greenville clustering area in terms of 2000 nighttime light emissions); the Florida megaregion (Orland clustering area and Jacksonville Beach clustering area in terms of 2000 nighttime light emissions); the Front Range megaregion (Colorado Springs clustering area, Albuquerque clustering area, and Fort Collins clustering area in terms of 2000 nighttime light emissions); the Southern

California megaregion (Las Vegas clustering area in terms of 2000 nighttime light emissions); and the Cascadia megaregion (Ellensburg clustering area in terms of 2000 nighttime light emissions).

As a summary of the 11 U.S. megaregions morphological clustering, this study has examined where local scale spatial clustering areas are located within the boundaries of the megaregions. Two types of spatial clustering patterns were observed in mapping results that show monocentric morphological clustering megaregions and polycentric morphological clustering megaregions. The monocentric morphological clustering megaregions are the Arizona Sun Corridor and Northern California. This means that spatial interconnections of spatial clustering of morphological characteristics within boundaries of the US megaregions cannot exist because of the absence of other spatial clusterings to connect with. The polycentric morphological clustering megaregions are the Northeast, the Texas Triangle, the Great Lakes, the Piedmont Atlantic, the Florida, the Gulf Coast, the Front Range, the Southern California, and the Cascadia. In the polycentric morphological clustering megaregions, except for the Northeast megaregion, however, it is difficult to consider spatial interconnections between spatial clustering areas because of physically distant clustering locations.

Based on mapping results of two spatial association analysis models, therefore, this study was able to reject the null hypothesis and accept the second research hypothesis stating that spatial association of morphological characteristics of the U.S. megaregions may not be spatially interconnected within the boundaries of the U.S. megaregions.

3.3. Morphological characteristics of the 11 U.S. megaregions

This study has examined spatial patterns and spatial associations of morphological characteristics, having two research sub-questions for each spatial attribute. The spatial patterns of morphological characteristics of the U.S. megaregions have shown inconsistent spatial patterns in various population density sprawl levels and the diverse spatial scattering extent of morphological characteristics. This means that the 11 U.S. megaregions have inconsistent morphological spatial patterns such as population density sprawl and spatial scattering. This contrasts with the 11 U.S. megaregions consistent functional relationships such as the interconnected economic structure across jurisdictional boundaries.

The spatial clustering pattern has been resulted to be statistically significant for all the 11 U.S. megaregions, meaning a consistent spatial clustering pattern for the 11 U.S. megaregions unlike inconsistent population density sprawl and spatial scattering spatial patterns. It was necessary to examine local scale clustering pattern analysis for the global scale measurement characteristics of the spatial clustering pattern analysis model. Compensating for the limitation of the global scale measurement, the local scale spatial association of morphological characteristics of U.S. megaregions was examined.

The result demonstrated inconsistent local scale spatial clustering patterns. 2 U.S. megaregions represented a monocentric morphological clustering pattern and the other 9 U.S. megaregions have demonstrated a polycentric morphological clustering pattern. Concerning the spatial interconnection between morphological clustering areas within megaregions boundaries, the spatially faraway clustering locations within the boundaries

of the U.S. megaregions were observed. It means for the monocentric morphological clustering megaregions that spatial interconnection of morphological characteristics primarily occurs within each morphological clustering boundary which is unable to have interconnection of morphological characteristics between morphological clustering areas. It also means for the polycentric morphological clustering megaregions that spatial interconnection of morphological characteristics occurs within the boundary of each morphological clustering with few opportunities for morphological characteristics interconnecting between morphological clustering areas which are spatially distant.

Table 96 and Figure 66 represent a summary of the morphological clustering and proportional extent of morphological clustering of the 11 U.S. megaregions, respectively. In the table and figure, the clustering extent has been proportionally observed in terms of morphological elements such as the number of census tracts, the amount of land area, and total population according to morphological characteristics such as 2000 population density, 2001 impervious land cover, and 2000 nighttime light emissions. The proportional extent of morphological clustering in terms of morphological elements indicates how much morphological characteristics account for each morphological element. Figure 66 shows that proportional extents of morphological clustering by census tracts and by 2000 total population are almost identical. Contrasted to the high proportions for the census tracts and 2000 total population, the figure also represents that the proportional extent of morphological clustering in terms of land area is obviously low.

Table 96 A summary of morphological clustering extent of the 11 U.S. megaregions

Megaregions	Morphological Elements	Morphological Characteristics			
		Total Clustering	PopDen00	ImpS01	DMSP00
Northeast	Census Tracts	73.16%	31.62%	41.12%	70.92%
	Land Area	28.47%	3.24%	8.57%	26.38%
	2000 Total Population	72.33%	29.71%	40.31%	69.91%
Texas Triangle	Census Tracts	73.56%	65.82%	52.83%	69.35%
	Land Area	22.72%	14.26%	10.58%	21.13%
	2000 Total Population	76.01%	68.56%	54.64%	71.59%
Great Lakes	Census Tracts	61.36%	33.69%	40.65%	55.41%
	Land Area	26.35%	3.61%	11.71%	23.51%
	2000 Total Population	60.99%	31.49%	39.54%	55.94%
Piedmont Atlantic	Census Tracts	58.57%	43.61%	38.57%	53.11%
	Land Area	28.38%	17.93%	15.78%	25.03%
	2000 Total Population	61.10%	46.81%	40.66%	56.40%
Florida	Census Tracts	63.59%	30.88%	47.18%	57.49%
	Land Area	20.07%	8.57%	9.50%	16.23%
	2000 Total Population	63.50%	34.22%	47.48%	58.56%
Gulf Coast	Census Tracts	54.13%	39.74%	46.95%	49.96%
	Land Area	21.42%	4.38%	17.63%	15.41%
	2000 Total Population	54.14%	38.54%	48.79%	49.93%
Front Range	Census Tracts	71.20%	47.64%	52.71%	66.21%
	Land Area	12.22%	3.87%	8.71%	7.47%
	2000 Total Population	71.81%	48.52%	52.56%	67.98%
Arizona Sun Corridor	Census Tracts	68.69%	68.38%	68.38%	68.69%
	Land Area	8.75%	5.34%	5.74%	8.75%
	2000 Total Population	68.90%	68.57%	68.55%	68.90%
Northern California	Census Tracts	60.94%	48.05%	54.49%	60.56%
	Land Area	18.17%	7.61%	12.04%	17.71%
	2000 Total Population	60.87%	47.67%	54.54%	60.40%
Southern California	Census Tracts	81.96%	56.47%	73.57%	71.34%
	Land Area	22.03%	5.72%	15.91%	19.89%
	2000 Total Population	81.53%	56.74%	72.06%	71.50%
Cascadia	Census Tracts	68.81%	61.77%	60.16%	68.38%
	Land Area	13.10%	9.83%	9.42%	12.77%
	2000 Total Population	69.01%	62.01%	60.29%	68.68%
Mean of the 11 U.S. Megaregions	Census Tracts	66.91%	47.97%	52.42%	62.86%
	Land Area	20.15%	7.67%	11.42%	17.66%
	2000 Total Population	67.29%	48.44%	52.67%	63.62%

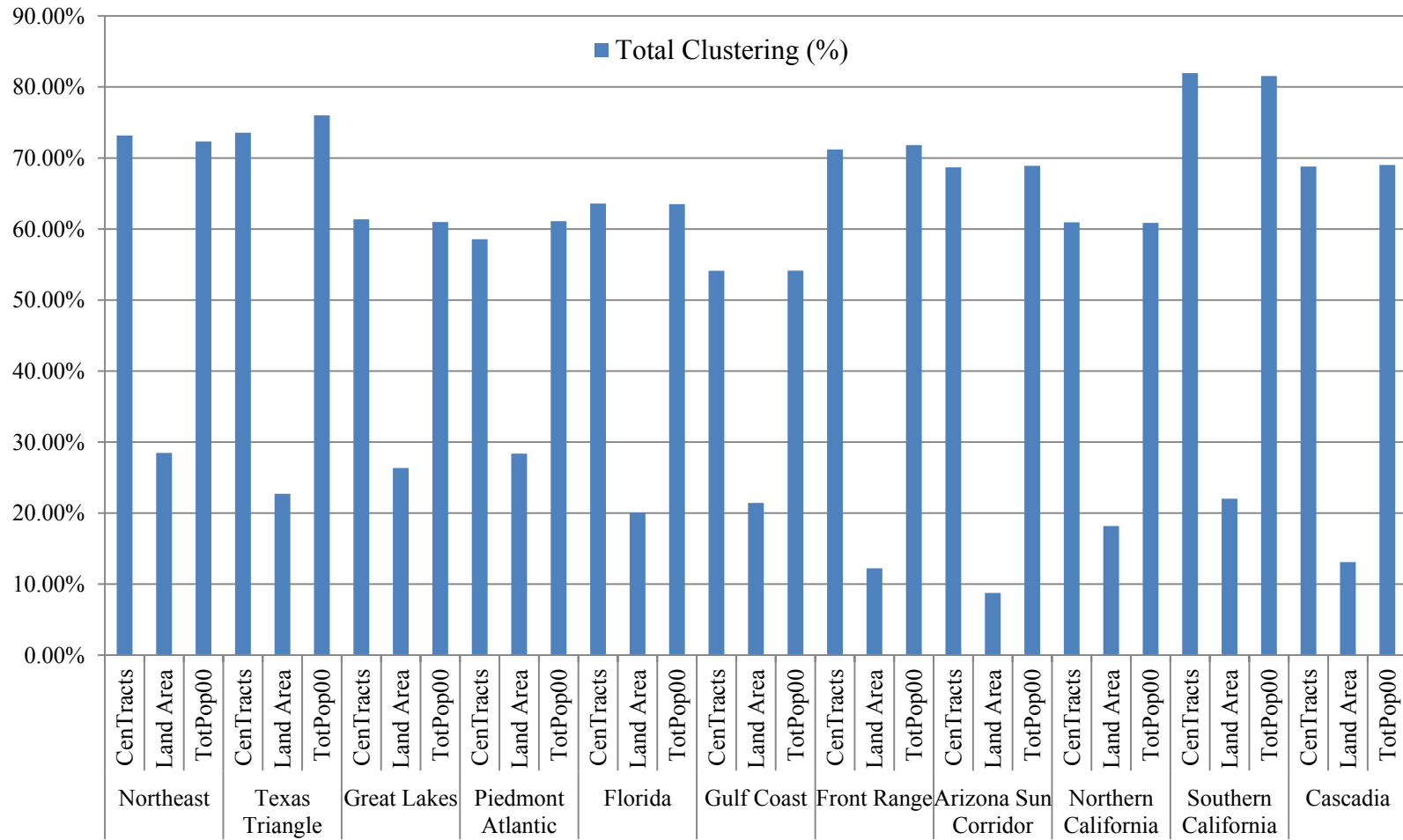


Figure 66 Proportional extents of morphological clusterings in terms of morphological elements of the 11 U.S. megaregions

The 11 U.S. megaregions morphological clustering areas comprise about 66.91% mean of the total census tracts of the megaregions, around 20.15% mean of the total land areas of the megaregions, and approximately 67.29% mean of 2000 total population of the megaregions. It means, in terms of mean values, that the 11 U.S. megaregions morphological clustering areas are spatially concentrated, consuming only about 20.15% of the total land areas of the megaregions and including around 67.29% of the 2000 total population of the megaregions in the morphological clustering areas. The 11 U.S. megaregions morphological clustering areas also represent an excess of morphological characteristics such as 2000 population density, 2001 impervious land cover, and 2000 nighttime light emissions in the clustering areas. This means that the morphological clustering areas are in excess of the effective land consumption per capita, urbanized built environment, the urban development that primarily consists of socio-economic activity.

Figure 67 illustrates the spatial clustering distribution of morphological characteristics of the 11 U.S. megaregions. Taking into account the results of spatial patterns analysis, the spatial clustering distribution in the figure supports the inconsistent spatial distribution patterns of morphological characteristics of the U.S. megaregions. Especially in the case of the Piedmont Atlantic megaregion, the exceptionally high scattering spatial pattern is visualized. The figure demonstrates the definite presence of morphological clustering for every U.S. megaregion and explains the result of global scale spatial clustering pattern analysis that has resulted in statistically significant clustering for every U.S. megaregion. It does not mean for the 11 U.S. megaregions,

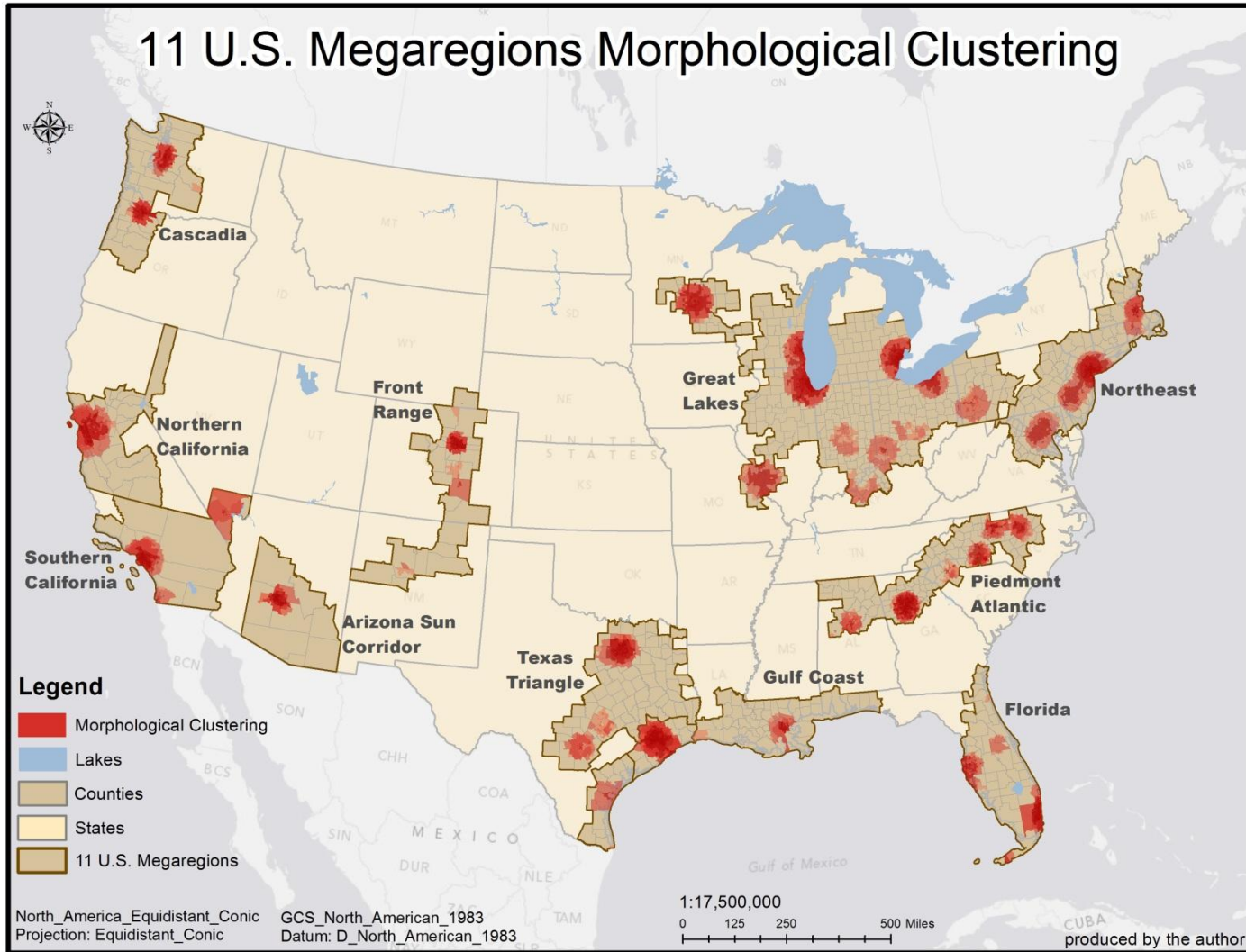


Figure 67 The 11 U.S. megaregions morphological clusterings

however, to have a consistent spatial clustering pattern. It demonstrates, rather, that spatial clustering patterns of morphological characteristics are located in major cities including surrounding cities and areas in each clustering boundary, inconsistently representing monocentric or polycentric clustering patterns for each megaregion. The extent of morphological clustering in terms of each morphological characteristic is also diverse in each megaregion. The figure of the 11 U.S. megaregions morphological clustering, therefore, compensates for the limitation of a global scale spatial clustering pattern measurement and as such, supports the inconsistent spatial clustering patterns of the 11 U.S. megaregions.

The primary research question for this study asked what the morphological characteristics of the U.S. megaregions represent, concerning their current geographic boundaries. Based on the results of spatial patterns analysis and spatial association examinations in terms of morphological characteristics in 2000, this study determined that the morphological characteristics of the U.S. megaregions are spatially distinct from the current boundaries of the 11 U.S. megaregions as visualized in the above figure. Both local scale spatial clustering distribution and clustering boundaries represent diverse spatial patterns and locations of spatial clustering within each U.S. megaregion. Each spatial clustering also delineates a boundary of excessive morphological characteristics. Physically distant and spatially disconnected morphological clustering areas within a megaregion boundary provide few opportunities for interconnections between the clustering areas within the megaregion boundary. This means that interconnection of morphological characteristics within a megaregion boundary is not

likely to expand contrasted to the functional interconnection and integration that has been considered promising in contemporary megaregion research. This study, therefore, has rejected the null hypothesis and accepted the primary research hypothesis that U.S. megaregions spatially examined by morphological characteristics may not be equal to current representation of U.S. megaregions.

CHAPTER V

CONCLUSION

1. Summary

This study has examined the morphological characteristics of U.S. megaregions to identify the megaregion scale of morphological characteristics in comparison with the current U.S. megaregions. In the past the U.S. megaregions seemed to be identified in terms of functional relationships. The identification of a region, however, should be performed not only by the functional relationships of regional components but also by the morphological characteristics of the region. For that reason, this study has hypothesized that the current U.S. megaregions may not correspond to the U.S. megaregions which are identified by the morphological characteristics.

The theoretical and empirical megaregion studies were reviewed as the first step. The concept of megaregion originated from Gottmann (1961) and was expanded to the 11 U.S. megaregions (RPA, 2006). The megaregions explored and examined by contemporary studies showed distinct characteristics from traditional urban and metropolitan areas. The review for the theoretical studies has recognized that megaregions share a polycentric urban structure and dominant economic entities. The review for the empirical studies also found that both the functional interconnection-integration and the economically-oriented polycentric structure of megaregions were primarily examined. The reviews discovered that perspectives of contemporary megaregion research have been biased, focusing on megaregional functional

relationships and related economic advantages. The contemporary megaregion studies have also limited consideration of megaregional morphological characteristics.

Extending consideration of urban morphology to the megaregion scale, this study examined megaregional morphology which represents the built environment, megaregional form, and the megaregional fabric that consists of the space in which human beings are able to move from one place to another within the megaregion boundary. This study characterized the megaregional morphology based on 2000 total population, 2000 population density, 2001 impervious land cover, and 2000 nighttime light emissions that are practicable at the megaregion scale observation. Contrasted to a county level measurement unit which is popular in contemporary megaregion research, the morphological characteristics have been examined at a census tract level as relatively homogeneous units with respect to population characteristics, economic status, and living conditions at the time they were established (Poston, 2010).

The global scale morphological characteristics examination of population density-based sprawl index, spatial scattering pattern index, and spatial clustering pattern index were conducted to determine whether the 11 U.S. megaregions share a consistent pattern in spatial distributions of morphological characteristics within each megaregion boundary. There were limitations in the global scale examinations in determining the extent of morphological clusters and spatial delineation of excess of morphological characteristics. Compensating for the limitations, the local scale morphological characteristics analysis models such as Getis-Ord G_i^* hot spots analysis and Anselin Local Moran's I cluster and outlier analysis were used to determine whether the 11 U.S.

megaregions morphological clustering shares a consistent spatial association of morphological characteristics within each megaregion boundary.

The 11 U.S. megaregions morphological characteristics have so many different spatial patterns in terms of population density sprawl, spatial scattering, and spatial clustering that it is problematic to argue that they share common spatial patterns of morphological characteristics with each other. Morphological characteristics of the 11 U.S. megaregions also showed many distant spatial clustering locations within a megaregion boundary when the clustering pattern is polycentric that it is problematic to argue that they contain spatially close interconnections between morphological clustering areas. This is in contrast to the functional interconnections that have been considered as promising megaregion characteristics in contemporary megaregion studies.

Both the inconsistent spatial patterns and spatially distant clustering locations of morphological characteristics of the 11 U.S. megaregions represent distinct depictions of the megaregions in terms of morphological characteristics, contrasted to current U.S. megaregions topographic boundaries. The disagreement between morphological representation and functional identification of the current 11 U.S. megaregions is expanded when the analysis results are overlapped and visualized on a map. The 11 U.S. megaregions morphological clustering map has demonstrated that both local scale spatial clustering distribution and clustering boundaries are spatially limited within each U.S. megaregion boundary. The map has also visualized topographic boundaries of excess of morphological characteristics, meaning that the current spatial definition of the 11 U.S. megaregions is not likely to fit the morphological identification of the megaregions.

2. Conclusions

Initiated in the U.S. northeastern seaboard area, the U.S. megaregions have theoretically and empirically been focused on for their distinctive functional relationships in the traditional roles of metropolitan areas in urban and regional planning fields. The Regional Plan Association (2006), among many contemporary megaregion studies, has identified the 11 U.S. megaregions based on many practicable urban elements that primarily highlight megaregional characteristics which are functionally interconnected and integrated. Most other megaregion research has focused on polycentric urban structures and dominant economic entities. Their empirical examinations have identified the functional interconnection-integration and economically-oriented polycentric structures. Concerning the limited perspective of functional relationships of the U.S. megaregions and delineated geographic boundaries, this study has identified the morphological characteristics of the megaregions.

Examination of morphological characteristics in terms of global scale spatial patterns and local scale spatial clustering has recognized that the U.S. megaregions do not share common patterns of morphological spatial distribution or provide close interconnection for spatial morphological clustering areas within a corresponding megaregion boundary. The boundaries of morphological clustering areas distinct from those of current megaregions have also identified that each megaregion determined to be functionally interconnected does not appear to be a region which has interconnections between morphological clustering areas within the current megaregion boundary.

Urban areas which do not share common urban environments, structures, and fabrics are not likely to be recognized as a region morphologically integrated. It does not mean, however, that functional interconnections are not there. A relationship between functional interconnection and morphological concentration for each U.S. megaregion has not yet been identified. This study has concluded that previous spatial patterns and clustering of morphological characteristics of the 11 U.S. megaregions do not identify the current 11 U.S. megaregions.

3. Limitations and further research

This study has focused on the morphological characteristics of U.S. megaregions; it has, however, limitations in conceptualizing more efficient morphological characteristics of the U.S. megaregions. It is difficult to define a megaregion scale morphology compared to traditional morphological studies that included micro scale urban environments such as parcels, buildings, streets, monuments, and open spaces. A megaregion scale morphology may present coarser observations than traditional scales. At the same time the megaregion scale morphology needs to be observed at finer resolutions in order to provide a homogeneous measurement unit. If other data sets are available on a megaregion-wide scale and provide a practical method for a census tract level measurement at the same time in addition to impervious land cover and nighttime light emissions used in this study, the morphological examination of the 11 U.S. megaregions can more accurately determine the identification of megaregions in terms of morphological characteristics.

This study predicts better research results than current cross-sectional morphology data observation when the 2010 census data is added. This study was conducted between 2010 and 2011 so the 2010 census data was not available to produce the time series comparison observation. When the 2010 census data is added with the 2010 morphological data sets, this study may determine whether or not the morphological spatial patterns and clustering areas have changed. If they have changed, growth or shrinking could be observed. Finding new morphological clustering areas will contribute as well.

This study has identified spatially distant morphological clustering locations within a megaregion boundary. However, this study has limitations in examining transportation networks that interconnect the morphological clustering areas within each megaregion boundary. If a high-speed rail system, for example, had been installed to connect the morphological clustering areas within a megaregion boundary, the interconnection between distant morphological clustering areas can be expanded. If a high-speed rail system is taken into account a megaregion boundary can be meaningless for interconnections of functional roles and morphological characteristics of urban areas that go beyond the megaregion boundary. This study, therefore, calls for further consideration of transportation network systems that would promote functional and morphological interconnections not only inside a megaregion boundary but also outside the boundary.

The limited identification of relationships between megaregional function and megaregional morphology is another weakness of this study. Even though this study has

reviewed morphological clustering areas for the 11 U.S. megaregions, this study is limited in correlating the morphological spatial patterns and clustering results to interconnected functional relationships of megaregions. The functional relationships and morphological characteristics of megaregions, however, should be studied separately for their distinct empirical dimensions from each other. With a complete identification of each characteristic, the relationship between two megaregional features may be able to be defined.

Last, this study has limitations in observing social and economic contrasts based on morphological characteristics which may exist not only inside morphological clustering areas but also outside the clustering areas. When the social and economic contrast between inside and outside the morphological clustering areas is identified, it may promote other studies and policies to resolve the issue.

4. Urban and regional planning implications

A concept of megaregion initiated from the observation of metropolitan areas that had an interconnected morphology. Many studies examined and defined the interconnections of a new urban morphology as functional relationships. The functional relationships between metropolitan areas are influential for economic development to cross jurisdictional boundaries of current metropolitan areas. When the concept of megaregion reflects the constellation of functional relations, the 11 U.S. megaregions can be considered to contain the mega-power to lead future urban and regional development of the U.S. The professionals who guide the megaregions, however,

should not forget to look at the new urban topology with morphological perspectives. The morphological observations of the U.S. megaregions, for example, can contribute to megaregion governance. Because of the inherently ambiguous jurisdictional boundaries of the megaregions, it is difficult for the current governance institutions to take care of the new urban morphology (Wheeler, 2009). With the power of morphological clustering for future development based on population density, the urbanized built environment, and extended socio-economic activities, it may be easier to determine how new institutions can be developed and how much governance power needs to be developed.

Beyond the morphological observations for the 11 U.S. megaregions, the results of this study can be related to the conceptualization of megaregional sprawl. Concerning land use patterns, spatial scattering and spatial clustering has been proposed to measure urban sprawl (Galster et al., 2001). It seems to be difficult to determine whether a megaregion has been sprawled or not based only on the dimensions. Local scale spatial clustering analysis seems to be helpful by representing population concentrations. When the total population of a megaregion and the population of morphological clustering areas are compared, and when total land areas of the clustering areas are considered, then megaregion scale sprawl can be determined. In the results of this study, the Great Lakes megaregion, Gulf Coast megaregion, and Piedmont Atlantic megaregion seem to have sprawl. The megaregions have shown relatively small differences between the extent of total clustering areas by 2000 total population and the extent of total clustering land area.

Interconnection of human activities over a megaregional scale requires a high degree of mobility within the boundaries of megaregions (Wheeler, 2009). The popular focus of megaregion research on the transportation infrastructure has been observable in urban and regional planning. The Regional Plan Association recently published high speed rail system studies (Hagler & Todorovich, 2009; Todorovich & Hagler, 2011) which encourage high speed rail to connect main metropolitan areas and determine places to connect under the concept of megaregion. Assuming a high degree of mobility for megaregions, this study encourages inserting observations of morphological characteristics of megaregions into transportation planning. Remembering that urban morphology reflects the built environment for human activities, it is reasonable to take into account morphological characteristics in megaregion scale transportation planning. Identification of morphological characteristics observed by population density, urbanized built environment, and extended nighttime socio-economic activities can help megaregion scale transportation planners determine where routes of high speed rails should be installed and the volume of transportation expected to take care of integrated human activities within a megaregion.

For the environmental planning professions, morphological clustering results may provide a clue. The Regional Plan Association recently posted research results to propose the improvement of water quality using landscape conservation initiatives (Torrens, 2011). Concerning the issues of natural resources and urban environments, the results of this study may be applied to environmental planning. Morphological clustering stands for excess urban environments and social activities in the areas. The

clustering areas, therefore, may produce higher levels of pollution than other areas of the megaregions. The clustering areas may also consume higher levels of natural resources, including water, than other areas. When morphological clustering is considered, environmental planning can be more effective and successful than environmental planning without morphological observations.

Finally, but most important, this study may promote reconsideration of megaregions boundaries. Keeping in mind the importance of functional relationships for each megaregion, this study asks urban and regional planning researchers to take into account morphological characteristics of megaregions to be a sustainable new urban morphology (Bright, 2007).

REFERENCES

- Allen, D. W.** (2009). *GIS tutorial II: Spatial analysis workbook* (1 ed.). California: ESRI Press.
- Amin, A.** (2002). Spatialities of globalisation. *Environment and Planning A*, 34, 385-399.
- Anselin, L.** (1995). Local indicators of spatial association—LISA. *Geographical Analysis*, 27(2), 93-115.
- Arnold, C. L., Jr., & Gibbons, C. J.** (1996). Impervious surface coverage: The emergence of a key environmental indicator. *Journal of the American Planning Association*, 62(2), 243.
- Banerjee, T.** (2009). Megaregions or megasprawls? In C. L. Ross (Ed.), *Megaregions: Planning for global competitiveness* (pp. 83-106). Washington, DC: Island Press.
- Bright, E.** (2007). Viewpoint: Megs? Maybe not. *Planning*, 73(4), 46.
- Carbonell, A., & Yaro, R. D.** (2005). American spatial development and the new megalopolis. *Land Lines*, 17(2), 1-4.
- Contant, C. K., & de Nie, K. L.** (2009). Scale matters: Rethinking planning approaches across jurisdictional and sectoral boundaries. In C. L. Ross (Ed.), *Megaregions: Planning for global competitiveness* (pp. 11-17). Washington, DC: Island Press.
- Cowell, M.** (2010). Polycentric regions: Comparing complementarity and institutional governance in the San Francisco Bay Area, the Randstad and Emilia-Romagna. *Urban Studies*, 47(5), 945-965.
- Cutsinger, J., Galster, G., Wolman, H., Hanson, R., & Towns, D.** (2005). Verifying the multi-dimensional nature of metropolitan land use: Advancing the understanding and measurement of sprawl. *Journal of Urban Affairs*, 27(3), 235-259.
- Davoudi, S.** (2008). Conceptions of the city-region: A critical review. *Urban Design and Planning*, 161(2), 51-60.
- de Vries, J., & Priemus, H.** (2003). Megacorridors in north-west Europe: Issues for transnational spatial governance. *Journal of Transport Geography*, 11(3), 225-233.

- Dewar, M., & Epstein, D.** (2007). Planning for “Megaregions” in the United States. *Journal of Planning Literature*, 22(2), 108-124.
- Ewing, R., Pendall, R., & Chen, D.** (2002). *Measuring sprawl and its impact*. Washington, D.C.: Smart Growth America.
- Fainstein, N., & Fainstein, S. S.** (2009). Social equity and the challenge of distressed places. In C. L. Ross (Ed.), *Megaregions: Planning for global competitiveness* (pp. 191-215). Washington, DC: Island Press.
- Feser, E., & Hewings, G.** (2007). *U.S. regional economic fragmentation & integration: Selected empirical evidence and implications*. Paper presented at the The Healdsburg Research Seminar on Megaregions.
- Florida, R., Gulden, T., & Mellander, C.** (2008). The rise of the mega-region. *Cambridge Journal of Regions, Economy and Society*, 1(3), 459-476.
- Frenkel, A., & Ashkenazi, M.** (2008). Measuring urban sprawl: How can we deal with it? *Environment and Planning B: Planning and Design*, 35, 56-79.
- Galster, G., Hanson, R., Ratcliffe, M. R., Wolman, H., Coleman, S., & Freihage, J.** (2001). Wrestling sprawl to the ground: Defining and measuring an elusive concept. *Housing Policy Debate*, 2(4), 681-717.
- Getis, A., & Ord, J. K.** (1992). The analysis of spatial association by use of distance statistics. *Geographical Analysis*, 24(3), 189-206.
- Glaeser, E. L.** (2007). *Do regional economies need regional coordination?* , Harvard University - John F. Kennedy School of Government, Cambridge. (2131)
- Glaeser, E. L., & Kahn, M. E.** (2004). Sprawl and urban growth. In J. V. Henderson & T. Jacques-François (Eds.), *Handbook of regional and urban economics* (Vol. Volume 4, pp. 2481-2527). Amsterdam: Elsevier.
- Gottmann, J.** (1961). *Megalopolis: The urbanized northeastern seaboard of the United States*. New York: Twentieth Century Fund.
- Green, N.** (2007). Functional polycentricity: A formal definition in terms of social network analysis. *Urban Studies*, 44(11), 2077-2103.
- Hagler, Y.** (2009). Defining U.S. megaregions. *America 2050*, 1-8.
- Hagler, Y., & Todorovich, P.** (2009). Where high-speed rail works best. *America 2050*, 1-12.

- Hall, P.** (2007). Urban land, housing, and transportation: The global challenge. *Global Urban Development*, 3(1), 1-11.
- Hoyler, M.**, Kloosterman, R. C., & Sokol, M. (2008). Polycentric puzzles – Emerging mega-city regions seen through the lens of advanced producer services. *Regional Studies*, 42(8), 1055 - 1064.
- Imhoff, M. L.**, Lawrence, W. T., Stutzer, D. C., & Elvidge, C. D. (1997). A technique for using composite DMSP/OLS “City Lights” satellite data to map urban area. *Remote Sensing of Environment*, 61(3), 361-370.
- Jacquez, G. M.** (2008). Spatial cluster analysis. In J. P. Wilson & A. S. Fotheringham (Eds.), *The handbook of geographic information science* (pp. 395-416). Oxford, UK: Blackwell Publishing Ltd.
- Jacquez, G. M.** (2009). Cluster morphology analysis. *Spatial and spatio-temporal epidemiology*, 1(1), 19-29.
- Jiang, B.**, & Claramunt, C. (2002). Integration of space syntax into GIS: New perspectives for urban morphology. *Transactions in GIS*, 6(3), 295-309.
- Knaap, G.-J.**, Song, Y., Ewing, R., & Clifton, K. (2005). Seeing the elephant: Multi-disciplinary measures of urban sprawl. *National Center for Smart Growth Research and Education in University of Maryland*, 1-46.
- Lang, R. E.** (2003). Open spaces, bounded places: Does the American West's arid landscape yield dense metropolitan growth? *Housing Policy Debate*, 13(4), 755-778.
- Lang, R. E.**, & Dhavale, D. (2005). Beyond megalopolis: Exploring America’s new “Megapolitan” geography. *Census Report Series*, 5, 1-35.
- Lang, R. E.**, & Knox, P. K. (2009). The new metropolis: Rethinking megalopolis. *Regional Studies*, 43(6), 789 - 802.
- Lang, R. E.**, & Nelson, A. C. (2007). *Beyond the metropolex: Examining commuter patterns at the "Megapolitan" scale*. Lincoln Institute of Land Policy.
- Lang, R. E.**, & Nelson, A. C. (2009). Megapolitan America: Defining and applying a new geography. In C. L. Ross (Ed.), *Megaregions: Planning for global competitiveness* (pp. 107-126). Washington, DC: Island Press.
- Levy, A.** (1999). Urban morphology and the problem of the modern urban fabric: Some questions for research. *Urban Morphology*, 3(2), 79-85.

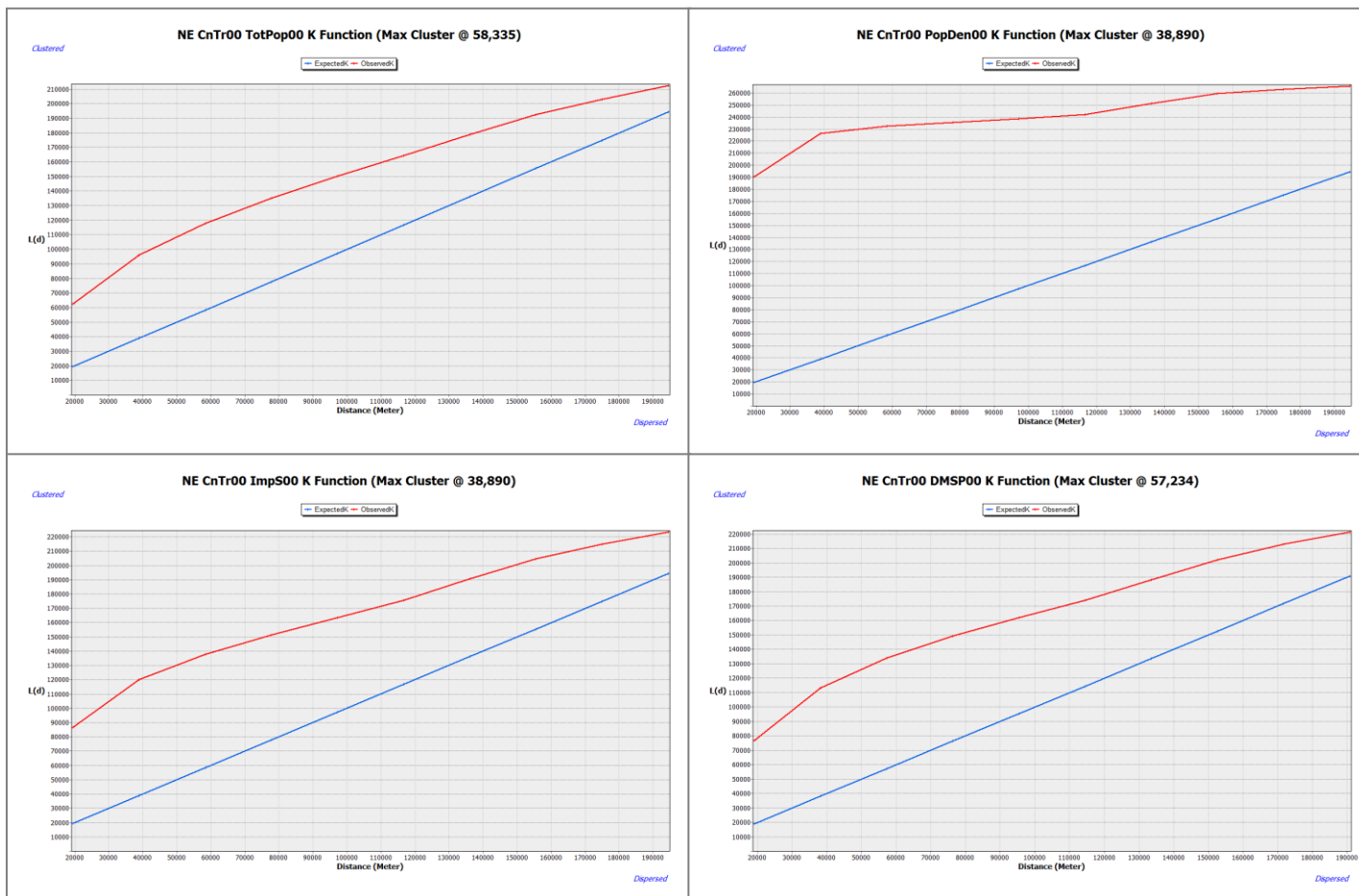
- Lopez, R., & Hynes, H. P.** (2003). Sprawl in the 1990s. *Urban Affairs Review*, 38(3), 325-355.
- Malpezzi, S., & Guo, W. K.** (2001). *Measuring "Sprawl:" Alternative measures of urban form in U.S. metropolitan areas*. The Center for Urban Land Economics Research, The University of Wisconsin. Madison, WI.
- Meijers, E. J.** (2008). Measuring polycentricity and its promises. *European Planning Studies*, 16(9), 1313-1323.
- Meijers, E. J., & Burger, M. J.** (2009). *Urban spatial structure and labor productivity in U.S. metropolitan areas*. Paper presented at the 2009 Regional Studies Association, Leuven, Belgium.
- Moran, P. A. P.** (1950). Notes on continuous stochastic phenomena. *Biometrika*, 37(1/2), 17-23.
- Neuman, M., & Hull, A.** (2009). The futures of the city region. *Regional Studies*, 43(6), 777 - 787.
- Ord, J. K., & Getis, A.** (1995). Local spatial autocorrelation statistics: Distributional issues and an application. *Geographical Analysis*, 27(4), 286-306.
- Pain, K.** (2006). Policy challenges of functional polycentricity in a global mega-city region: South East England. *Built Environment*, 32(2), 194-205.
- Parr, J.** (2005). Perspectives on the city-region. *Regional Studies*, 39(5), 555 - 566.
- Poston, D.** (2010). *SOCI 633: Demographic methods*. Class note. Sociology. Texas A&M University. College Station.
- Priemus, H., & Hall, P.** (2004). Multifunctional urban planning of mega-city-regions. *Built Environment*, 30(4), 338-349.
- Regional Plan Association.** (2006). *America 2050: A prospectus*. Paper presented at the The Healdsburg Research Seminar on Megaregions, New York.
- Regional Plan Association.** (2008). *America 2050: An infrastructure vision for 21st century America* (pp. 1-24). New York, NY: Regional Plan Association.
- Rodrigue, J. P.** (2004). Freight, gateways and mega-urban regions: The logistical integration of the BostWash corridor. *Tijdschrift voor economische en sociale geografie*, 95(2), 147-161.
- Rodríguez-Pose, A.** (2008). The rise of the "City-region" concept and its development policy implications. *European Planning Studies*, 16(8), 1025 - 1046.

- Ross, C. L.** (2008). Megaregions: Literature review of the implications for U.S. infrastructure investment and transportation planning (pp. 1-95). Atlanta: Center for Quality Growth and Regional Development, Georgia Institute of Technology.
- Ross, C. L.** (2009a). Introduction. In C. L. Ross (Ed.), *Megaregions: Planning for global competitiveness* (pp. 1-8). Washington, D.C.: Island Press.
- Ross, C. L.** (2009b). *Megaregions: Planning for global competitiveness*. Washington, D.C.: Island Press.
- Ross, C. L., & Woo, M.** (2009). Identifying megaregions in the United States: Implications for infrastructure investment. In C. L. Ross (Ed.), *Megaregions: Planning for global competitiveness* (pp. 53-80). Washington, D.C.: Island Press.
- Sargent, C. S.** (1972). Toward a dynamic model of urban morphology. *Economic Geography*, 48(4), 357-374.
- Scott, L. M., & Janikas, M. V.** (2010). Spatial statistics in ArcGIS. In M. M. Fischer & A. Getis (Eds.), *Handbook of applied spatial analysis: Software tools, methods and applications* (pp. 27 - 41). Verlag Berlin Heidelberg: Springer.
- Sokol, M., Van Egeraat, C., & Williams, B.** (2008). Revisiting the 'Informational City': Space of flows, polycentricity and the geography of knowledge-intensive business services in the emerging global city-region of Dublin. *Regional Studies*, 42(8), 1133 - 1146.
- Taylor, P. J., Evans, D. M., & Pain, K.** (2008). Application of the interlocking network model to mega-city-regions: Measuring polycentricity within and beyond city-regions. *Regional Studies*, 42(8), 1079 - 1093.
- Todorovich, P.** (2009). America's emerging megaregions and implications for a national growth strategy. *The International Journal of Public Sector Management*, 22(3), 221.
- Todorovich, P., & Hagler, Y.** (2011). *High speed rail in America*. New York: Regional Plan Association.
- Torrens, P. M.** (2008). A toolkit for measuring sprawl. *Applied Spatial Analysis and Policy*, 1(1), 5-36.
- Torrens, P. M.** (2011). Tracing the river's path, landscape initiatives protect water resources across jurisdictions Retrieved 12/05, 2011, from <http://www.america2050.org/2011/05/following-the-river-whenever-it-may-lead-landscape-initiatives-protect-water-resources-across-jurisd.html#more>

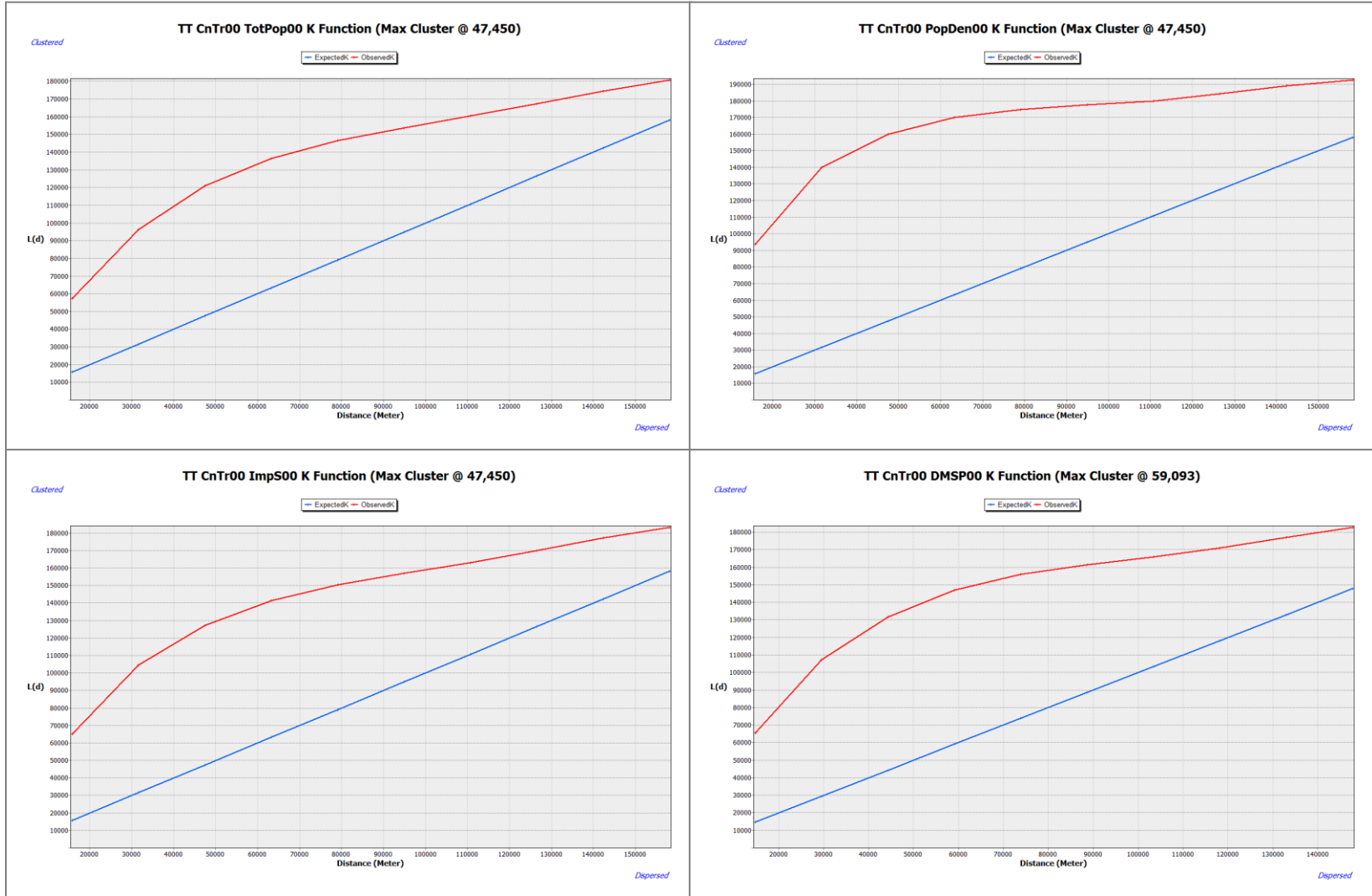
- Torrems, P. M., & Alberti, M.** (2000). *Measuring sprawl*. Paper presented at the Association of Collegiate Schools of Planning Conference, Atlanta, GA.
- Tsai, Y.-H.** (2005). Quantifying urban form: Compactness versus 'Sprawl'. *Urban Studies*, 42(1), 141-161.
- Turok, I.** (2009). Limits to the mega-city region: Conflicting local and regional needs. *Regional Studies*, 43(6), 845 - 862.
- Vicino, T. J., Hanlon, B., & Short, J. R.** (2007). Megalopolis 50 years on: The transformation of a city region. *International Journal of Urban and Regional Research*, 31(2), 344-367.
- Wheeler, S.** (2009). Regions, megaregions, and sustainability. *Regional Studies*, 43(6), 863-876.
- Whitehand, J. W. R., & Morton, N. J.** (2004). Urban morphology and planning: The case of fringe belts. *Cities*, 21(4), 275-289. doi: DOI: 10.1016/j.cities.2004.04.001
- Wolman, H., Galster, G., Hanson, R., Ratcliffe, M., Furdell, K., & Sarzynski, A.** (2005). The fundamental challenge in measuring sprawl: Which land should be considered? *The Professional Geographer*, 57(1), 94-105.
- Yaro, R. D., & Carbonell, A.** (2007). Reinventing megalopolis: The Northeast megaregion. In J. Barnett (Ed.), *Smart growth in a changing world* (pp. 77-93). Chicago, Illinois & Washington, D.C.: American Planning Association.
- Zhang, C., Luo, L., Xu, W., & Ledwith, V.** (2008). Use of local Moran's I and GIS to identify pollution hotspots of Pb in urban soils of Galway, Ireland. *Science of The Total Environment*, 398(1-3), 212-221.
- Zhang, M., & Chen, B.** (2009). Future travel demand and its implications for transportation infrastructure investments in the Texas Triangle (pp. 50). Austin, Texas: Center for Transportation Research, University of Texas at Austin.
- Zhang, M., Steiner, F., & Butler, K.** (2007). *Connecting the Texas Triangle: Economic integration and transportation coordination*. Paper presented at the The Healdsburg Research Seminar on Megaregions.

APPENDIX A

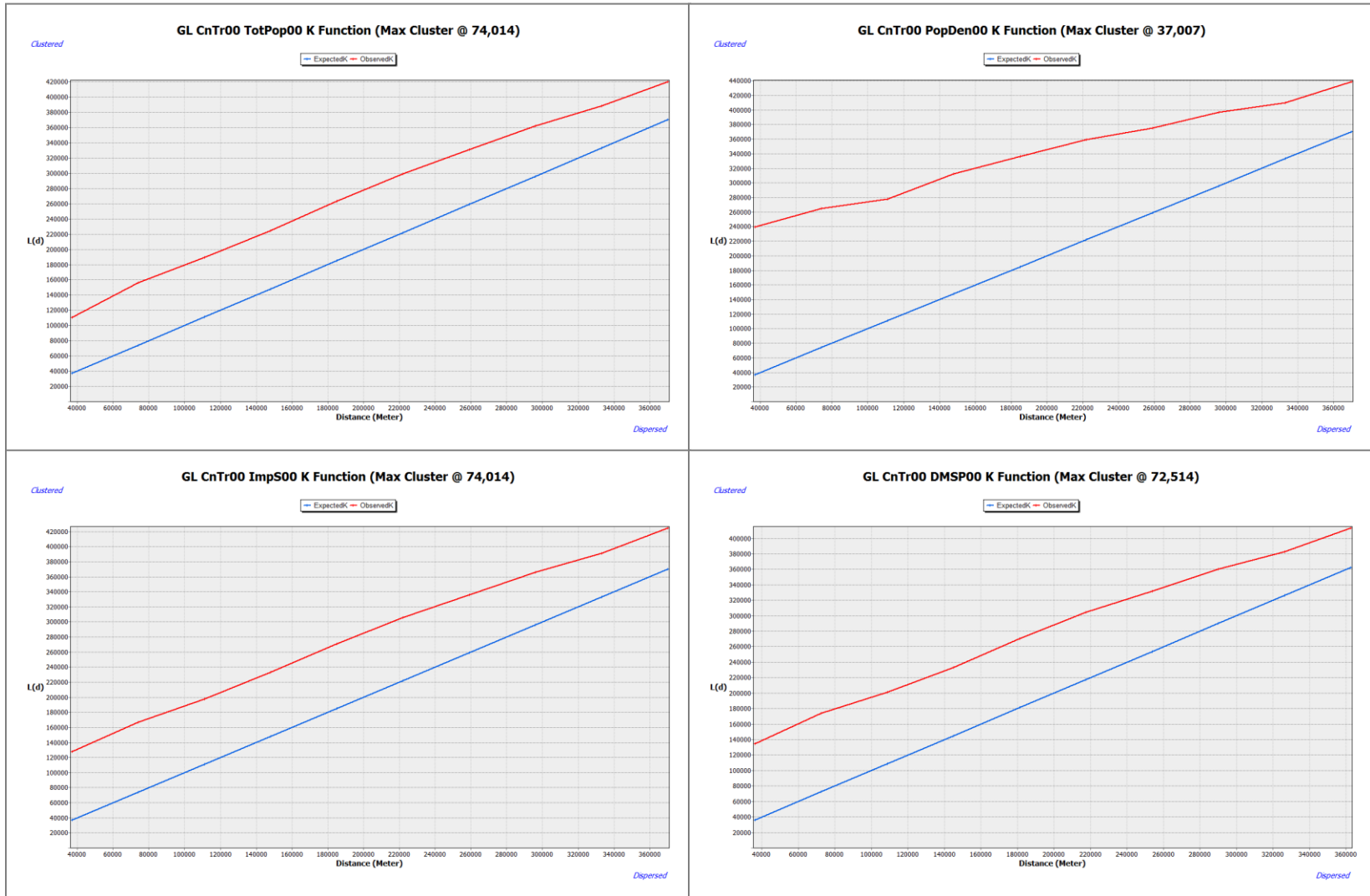
A.1. Ripley's K function results for the Northeast megaregion



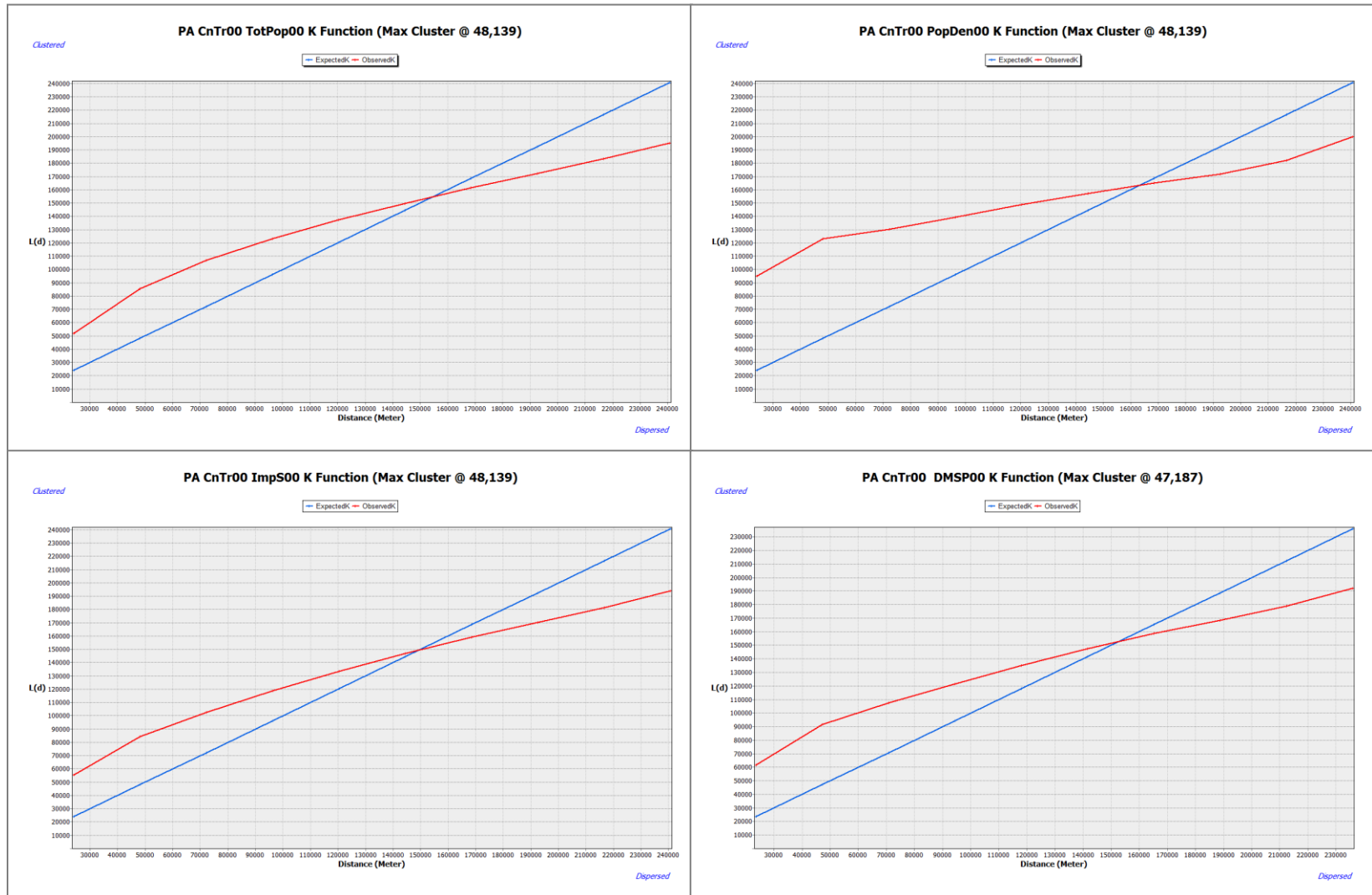
A.2. Ripley's K function results for the Texas Triangle megaregion



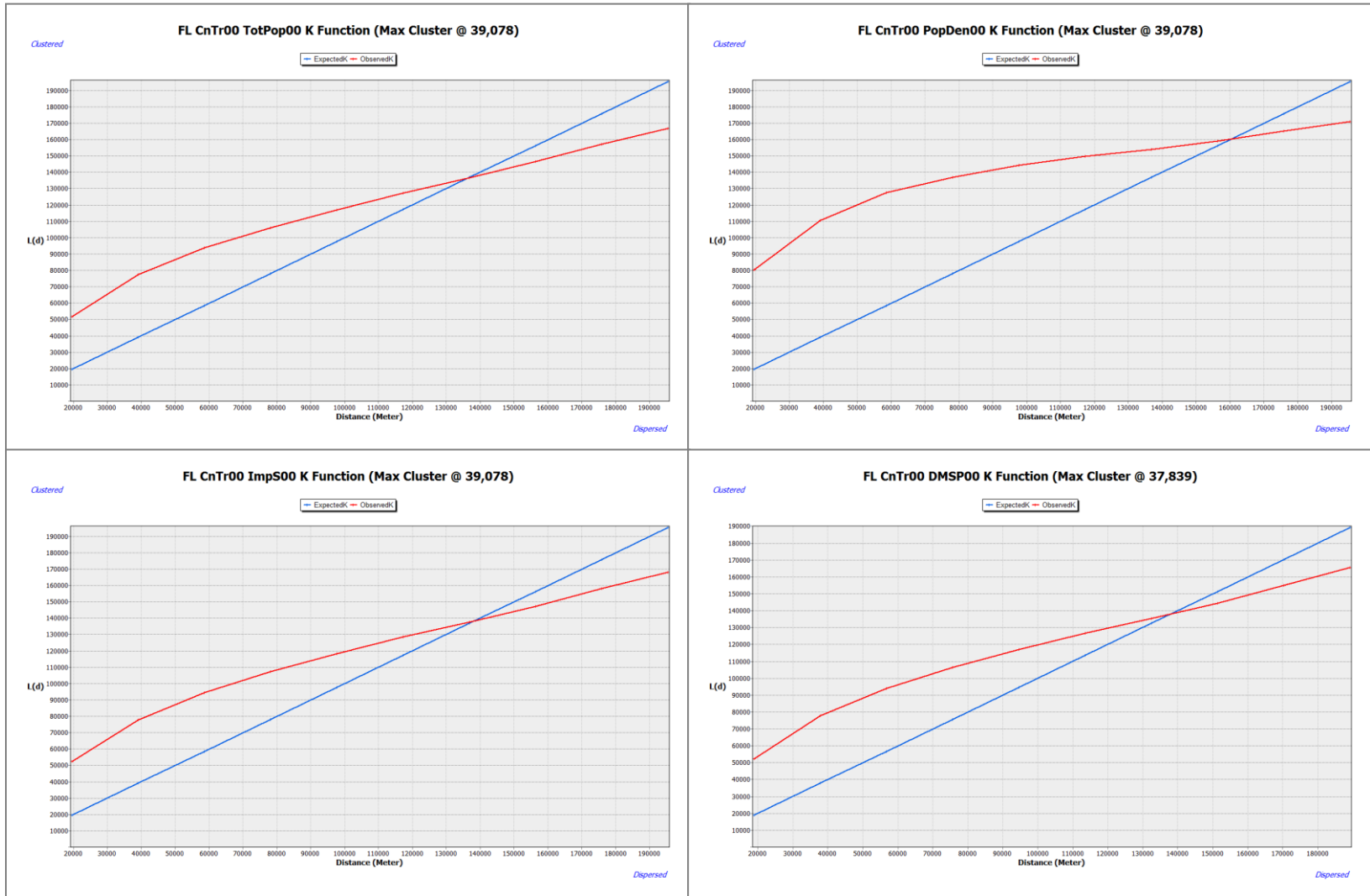
A.3. Ripley's K function results for the Great Lakes megaregion



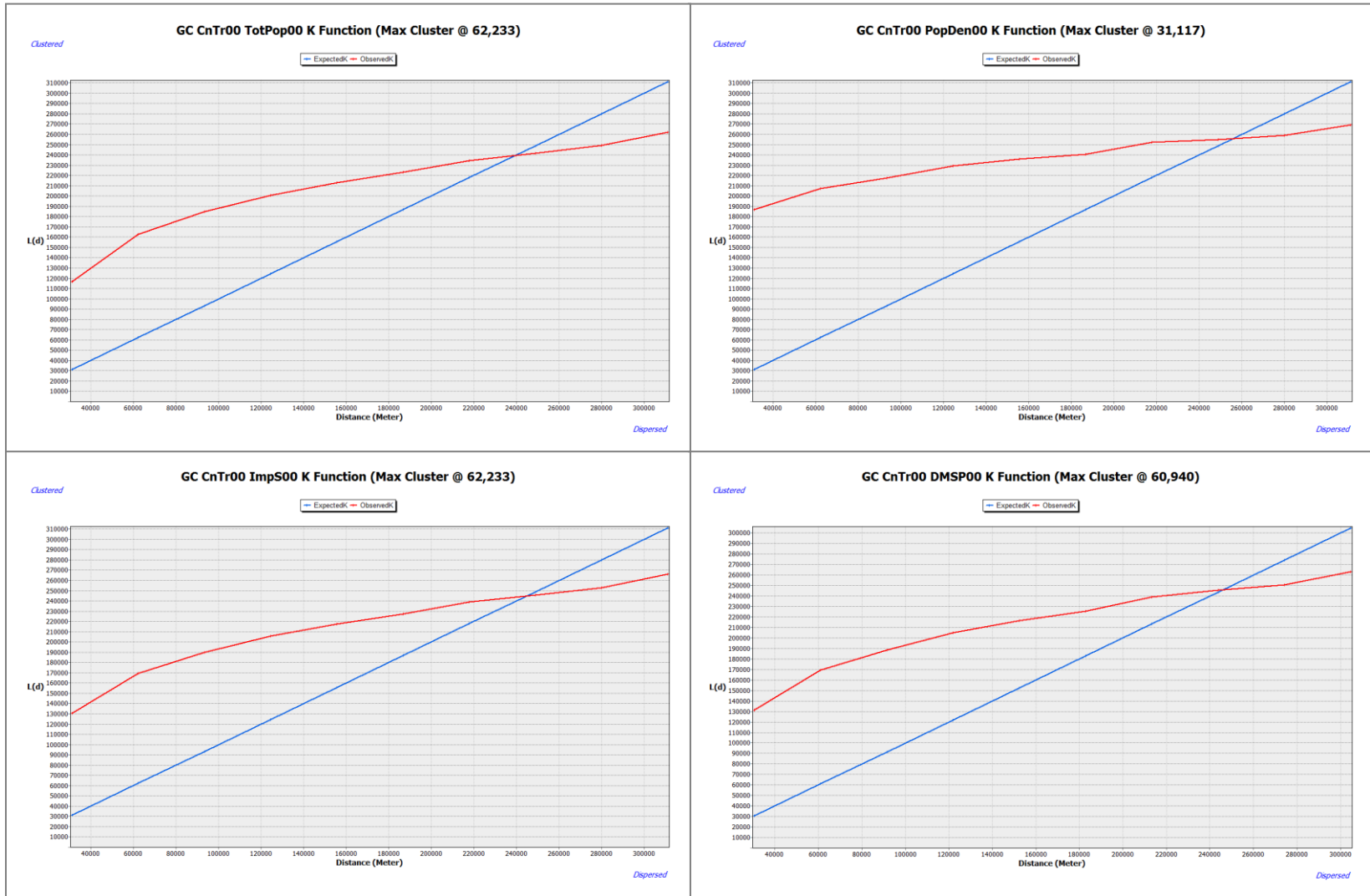
A.4. Ripley's K function results for the Piedmont Atlantic megaregion



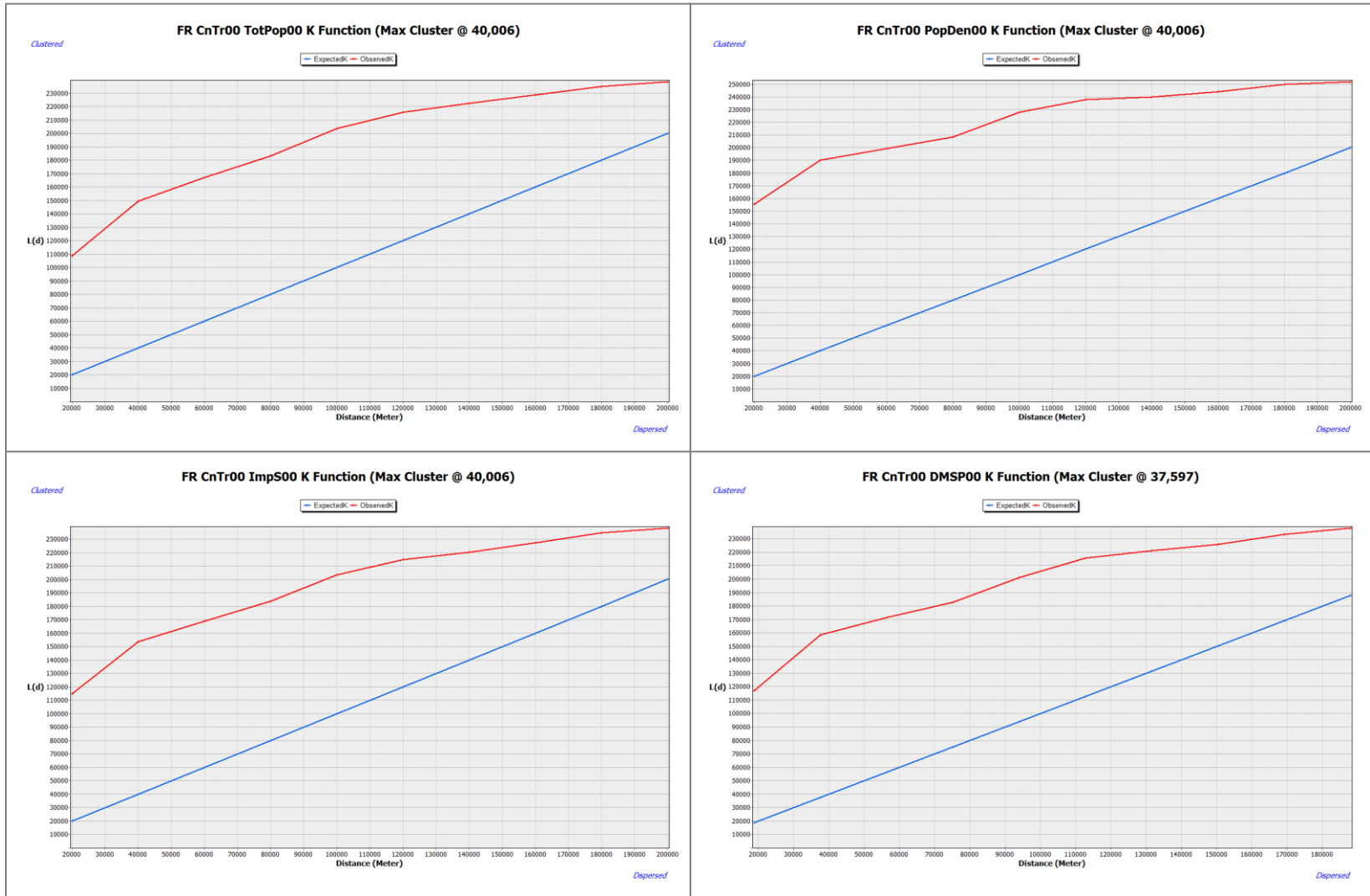
A.5. Ripley's K function results for the Florida megaregion



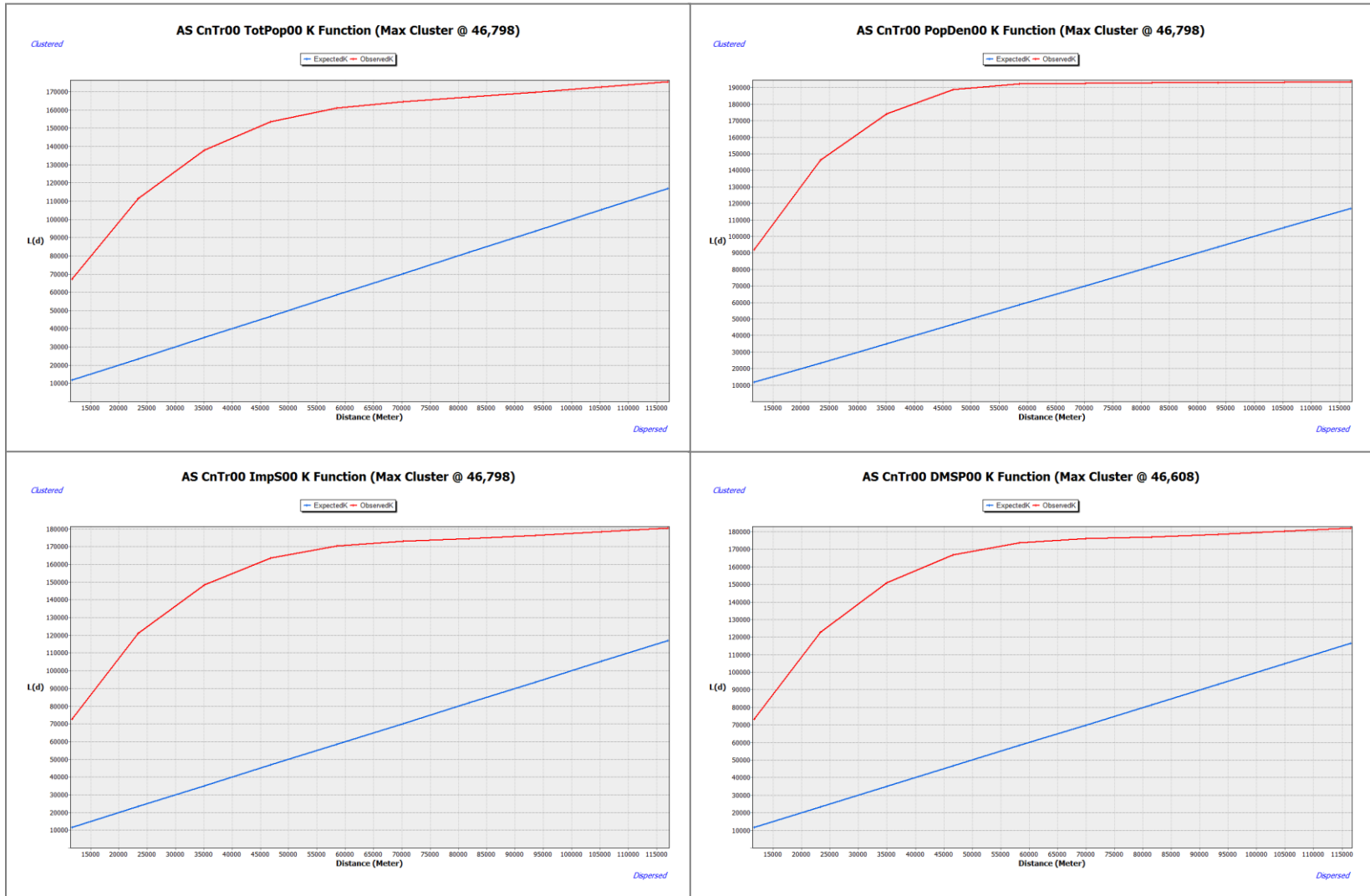
A.6. Ripley's K function results for the Gulf Coast megaregion



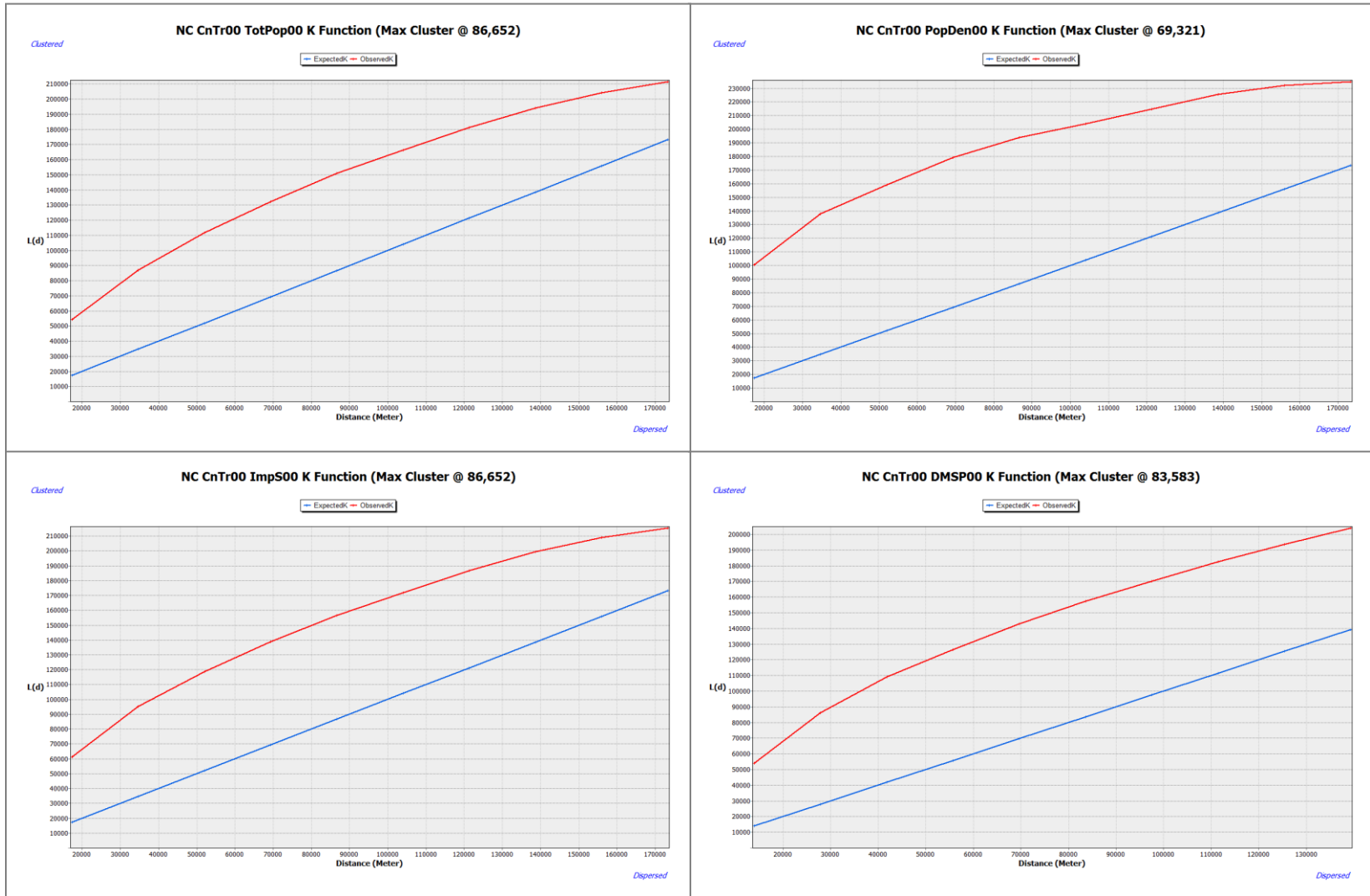
A.7. Ripley's K function results for the Front Range megaregion



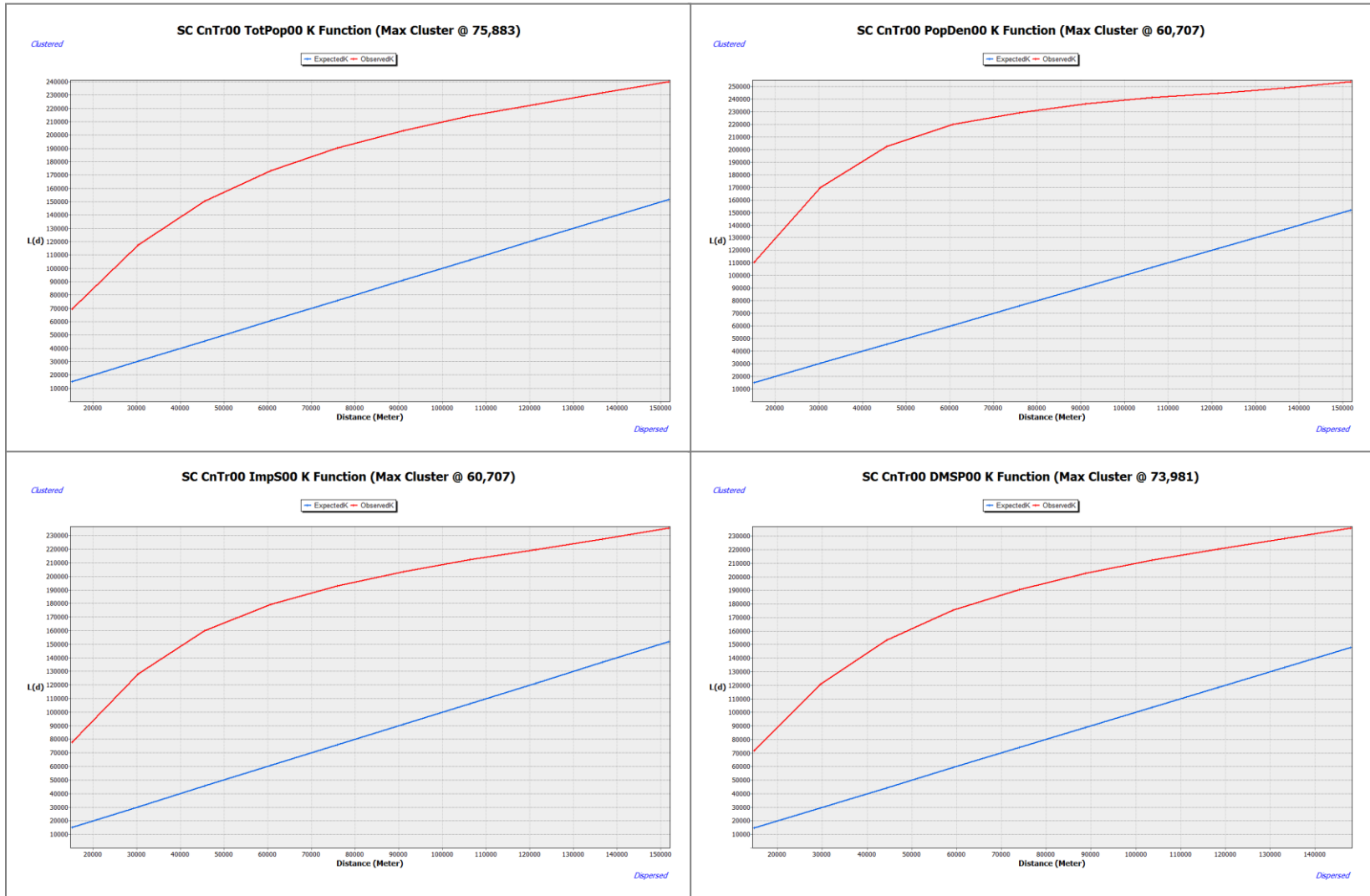
A.8. Ripley's K function results for the Arizona Sun Corridor megaregion



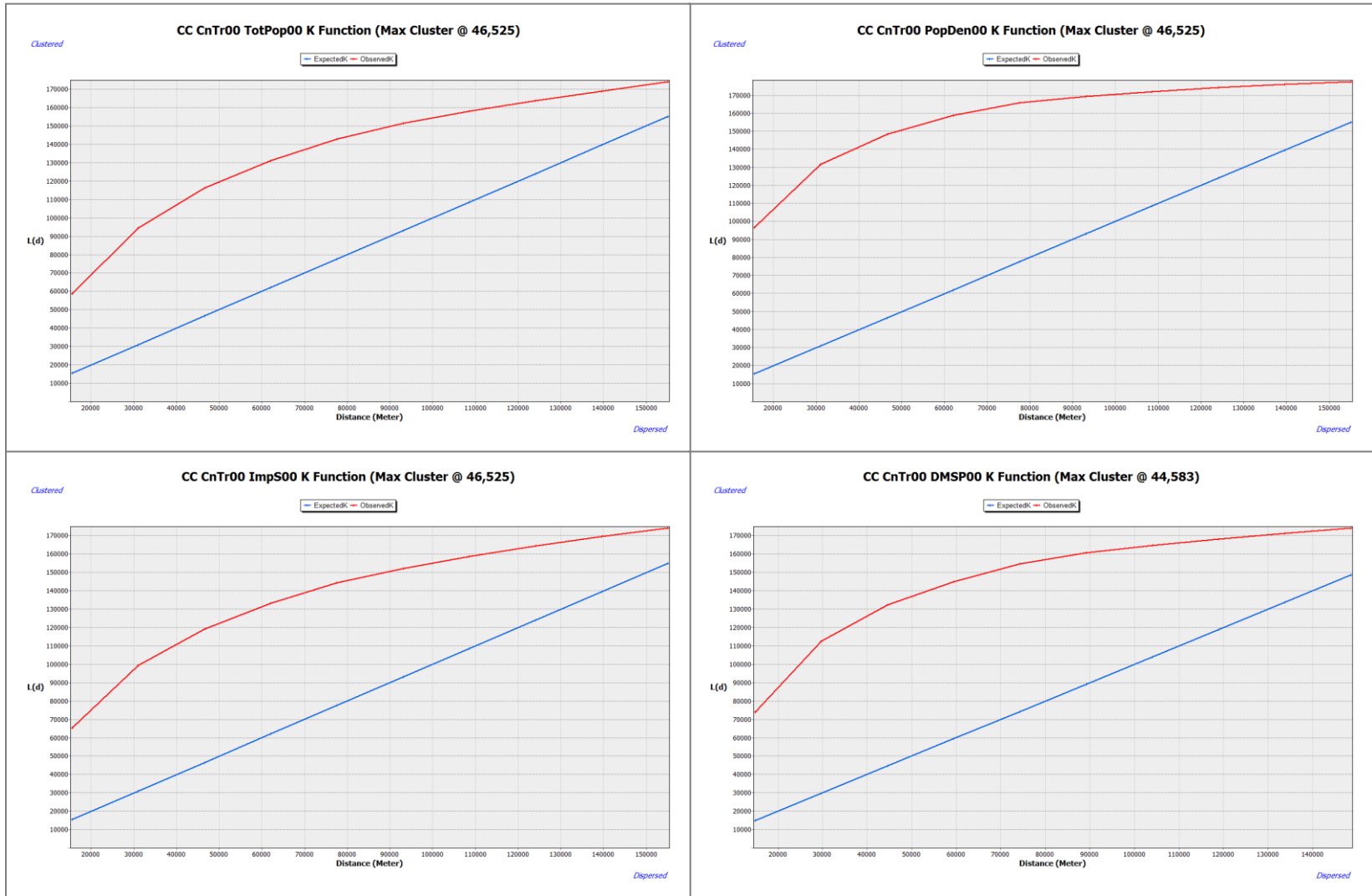
A.9. Ripley's K function results for the Northern California megaregion



A.10. Ripley's K function results for the Southern California megaregion

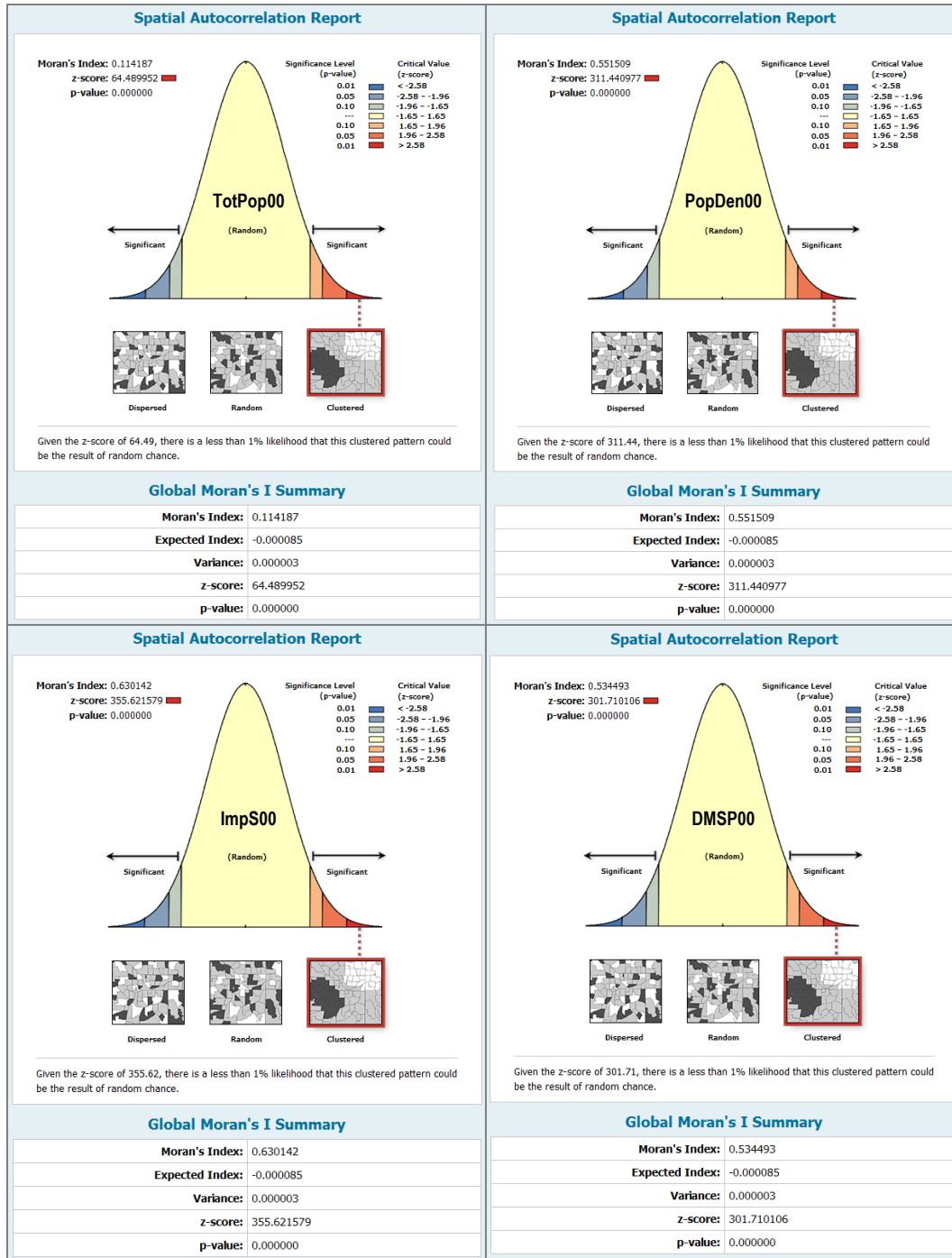


A.11. Ripley's K function results for the Cascadia megaregion

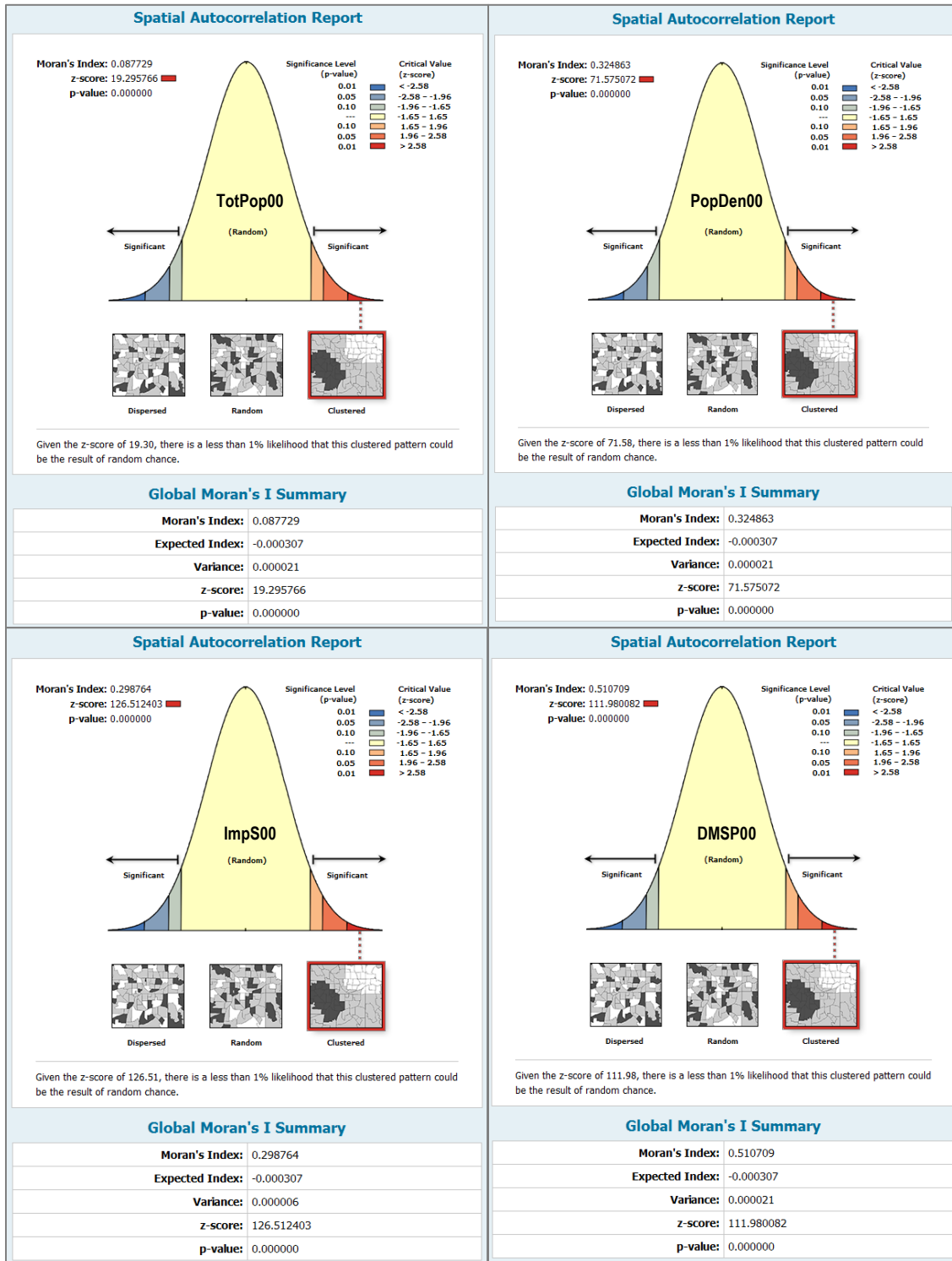


APPENDIX B

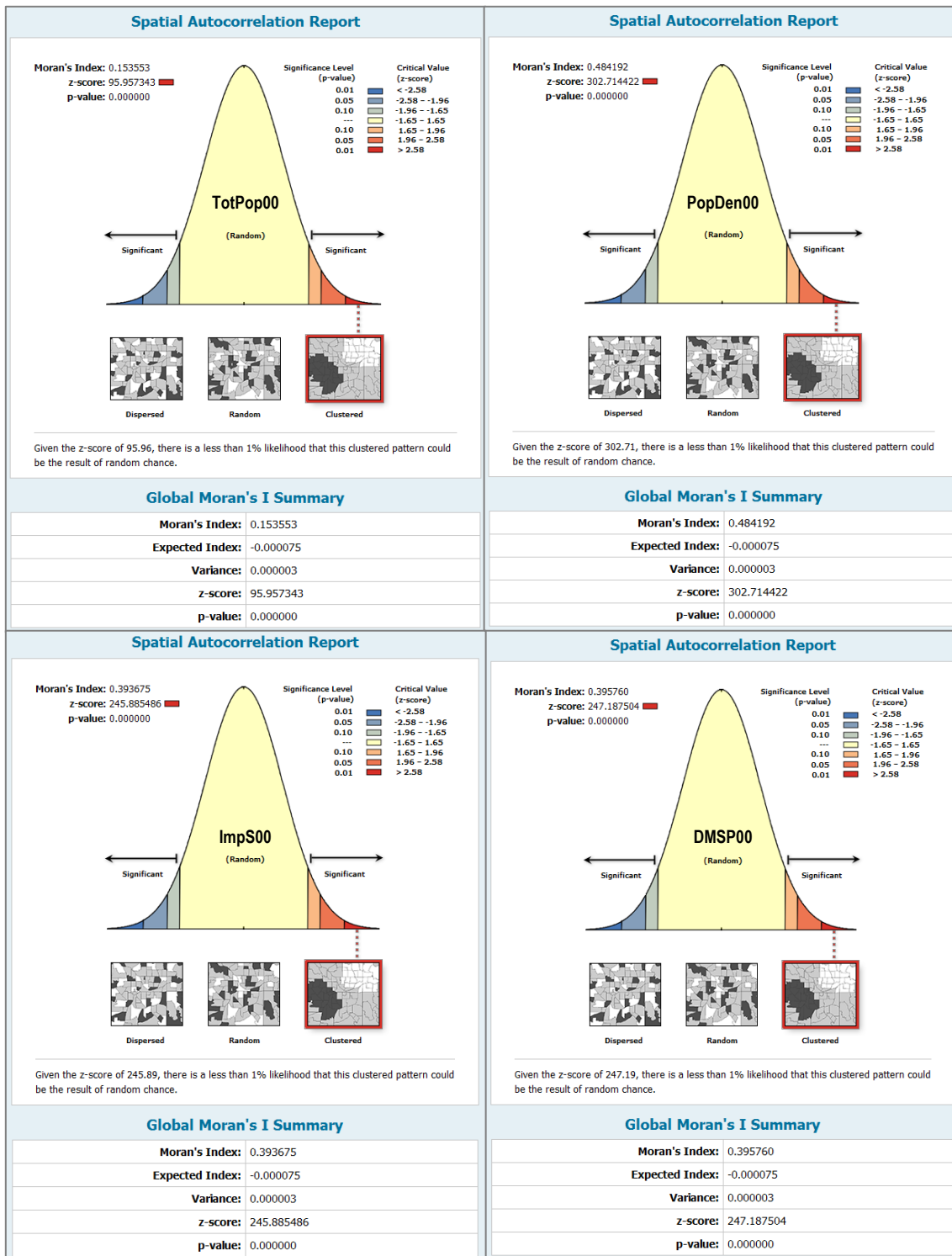
B.1. The spatial clustering pattern index results for the Northeast megaregion



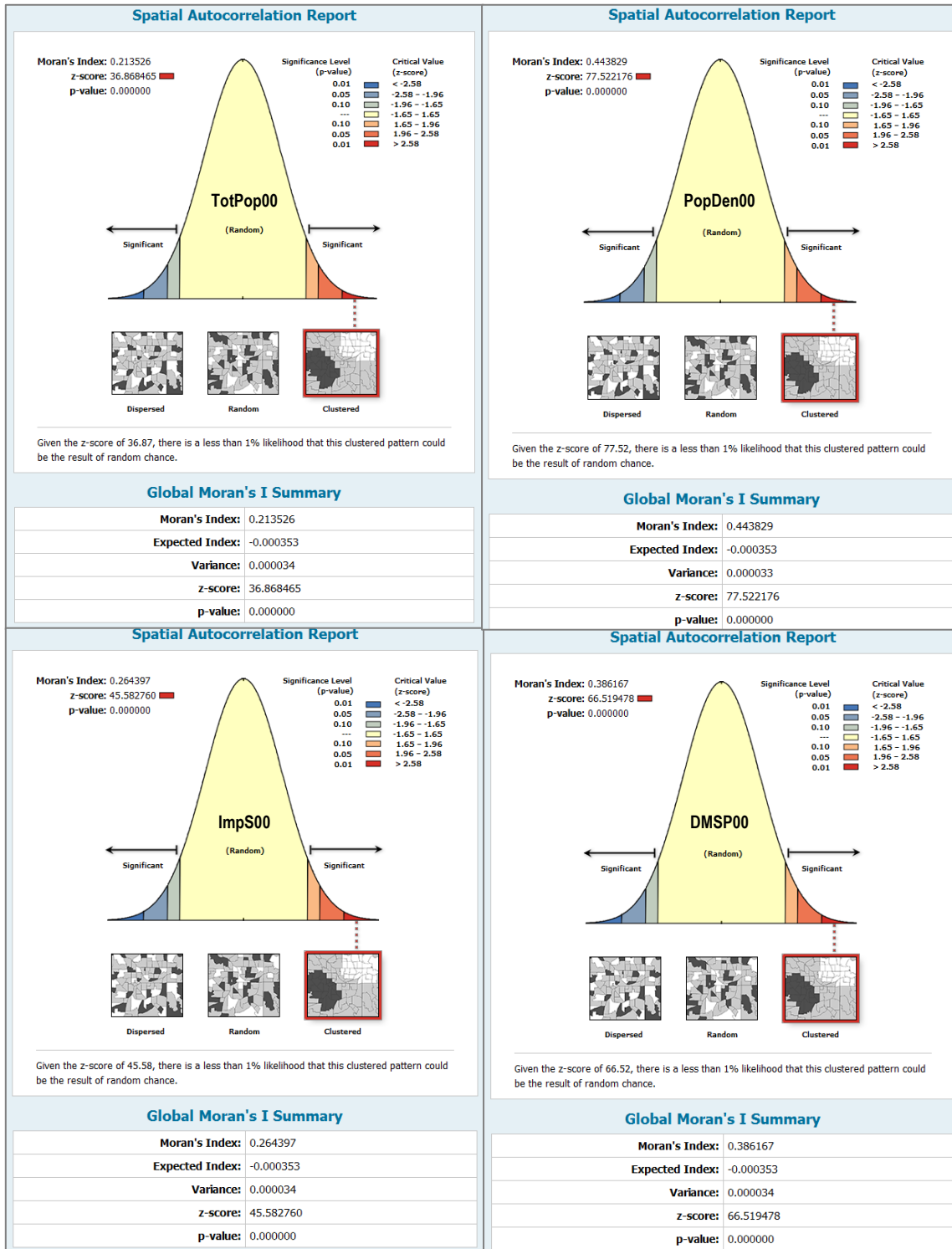
B.2. The spatial clustering pattern index results for the Texas Triangle megaregion



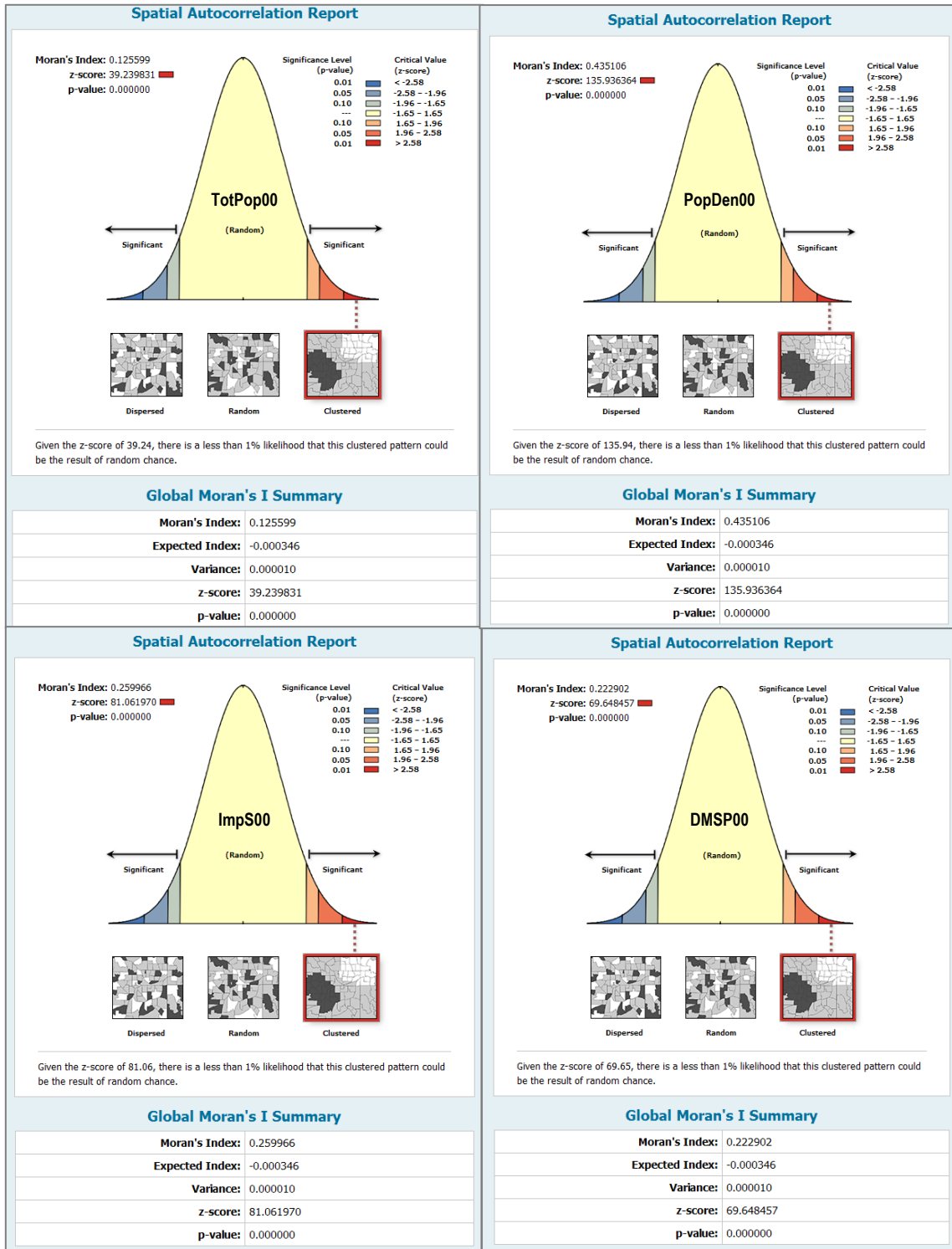
B.3. The spatial clustering pattern index results for the Great Lakes megaregion



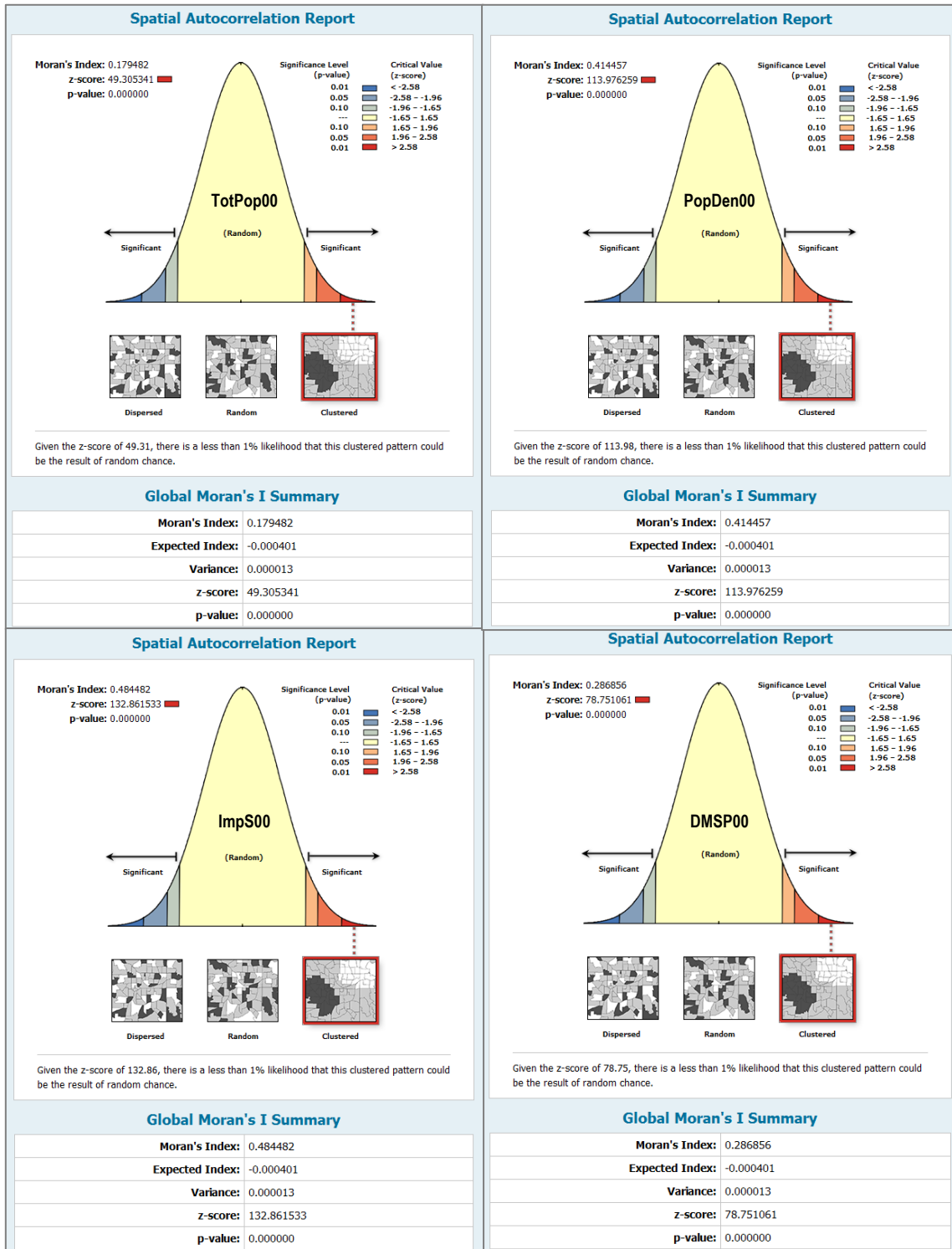
B.4. The spatial clustering pattern index results for the Piedmont Atlantic megaregion



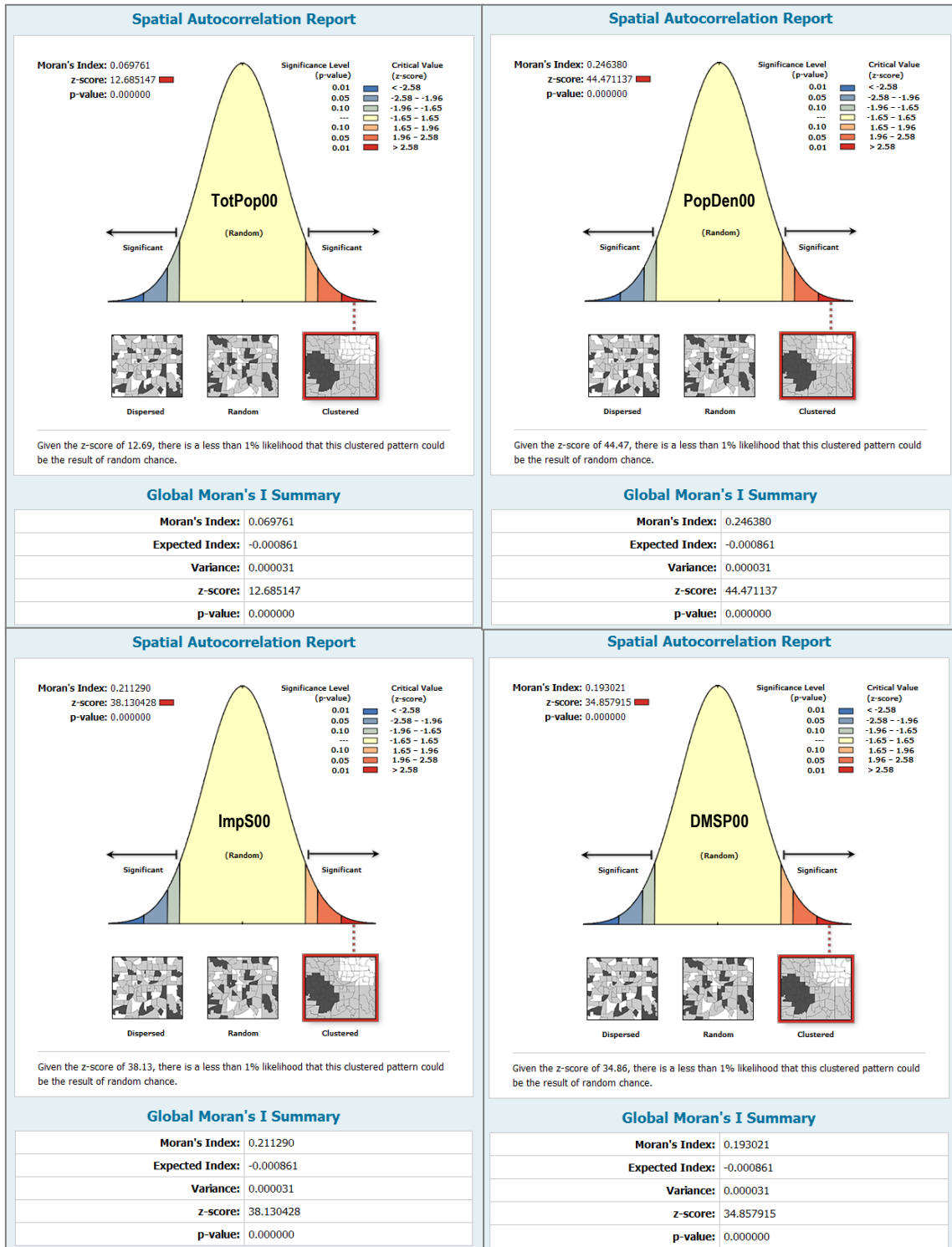
B.5. The spatial clustering pattern index results for the Florida megaregion



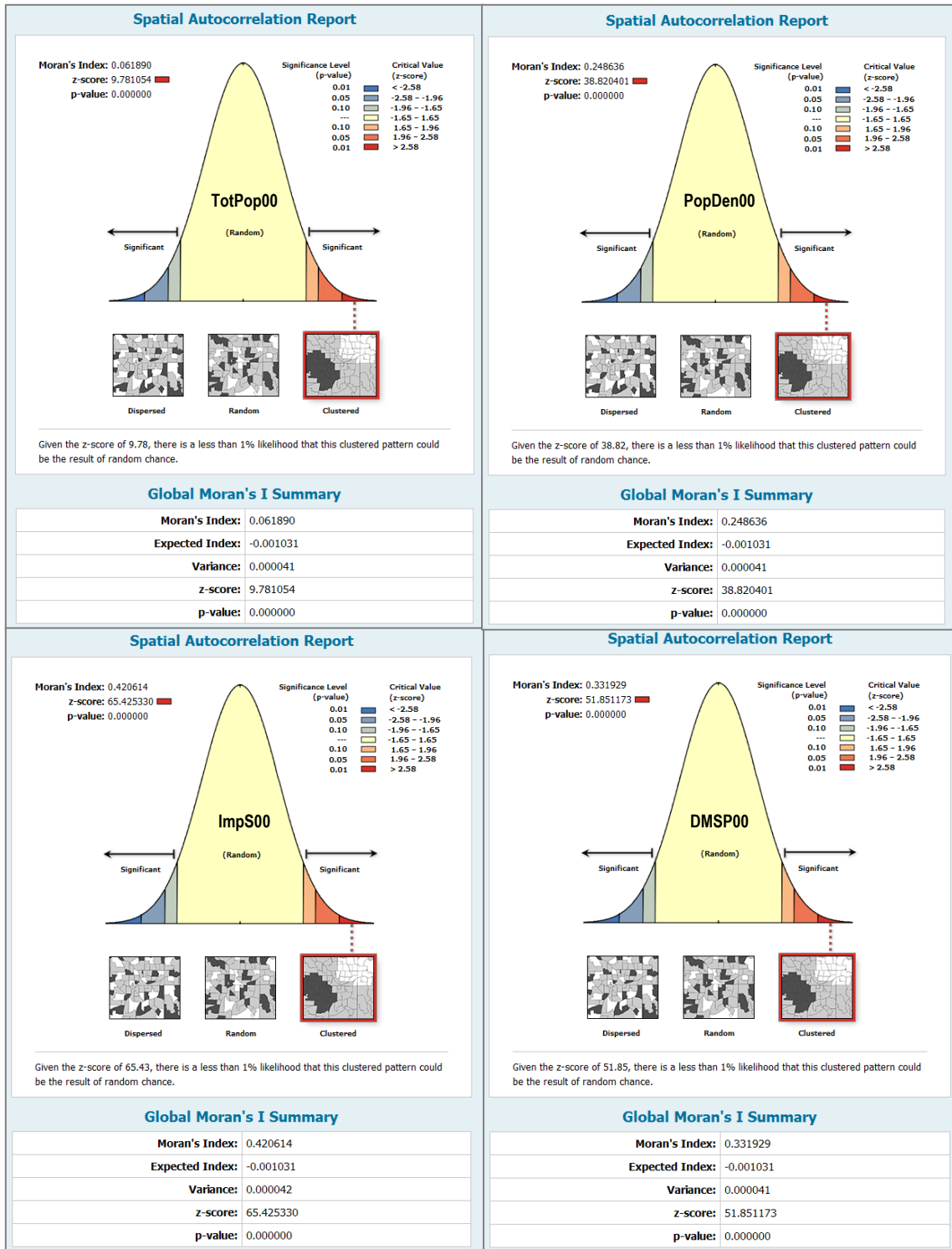
B.6. The spatial clustering pattern index results for the Gulf Coast megaregion



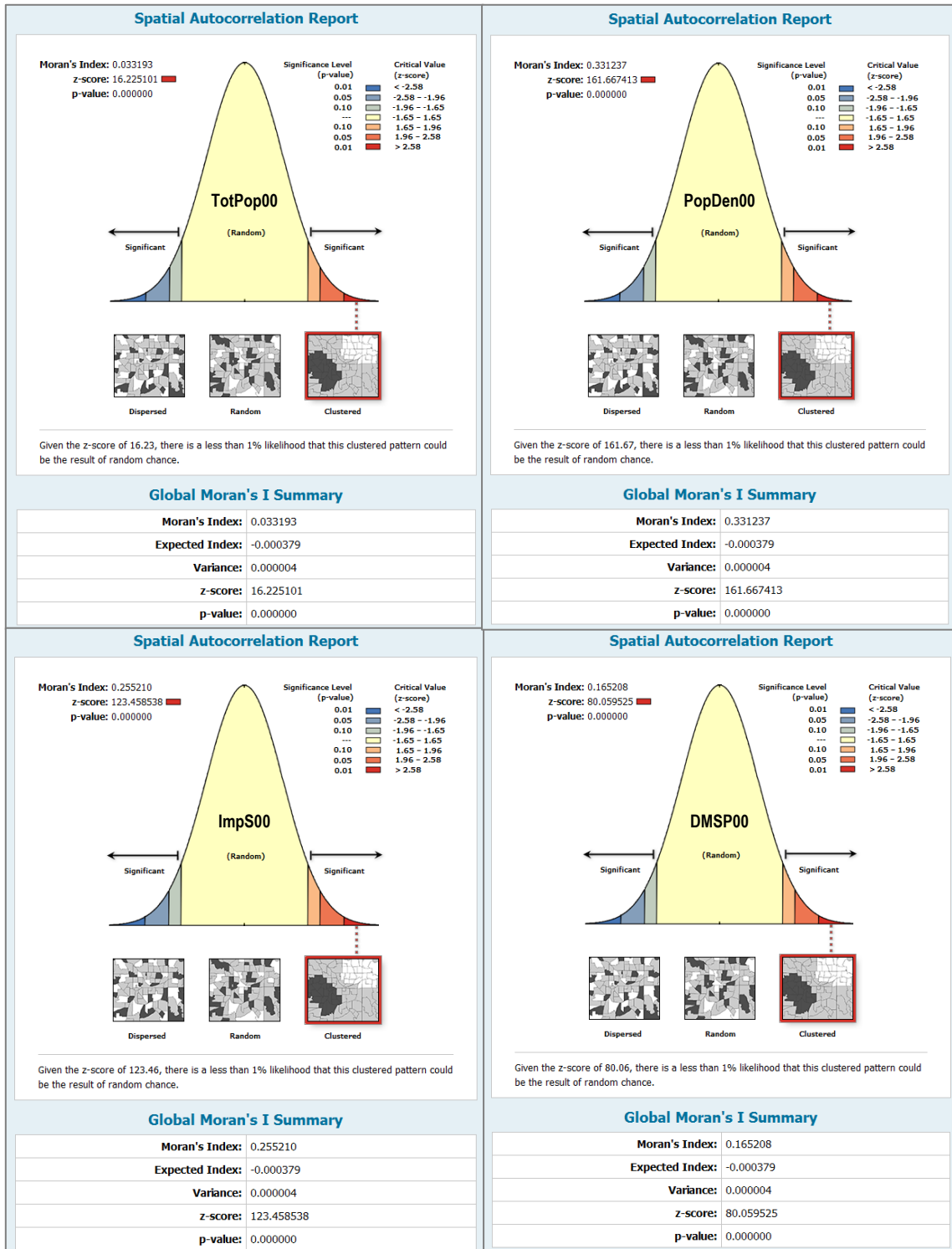
B.7. The spatial clustering pattern index results for the Front Range megaregion



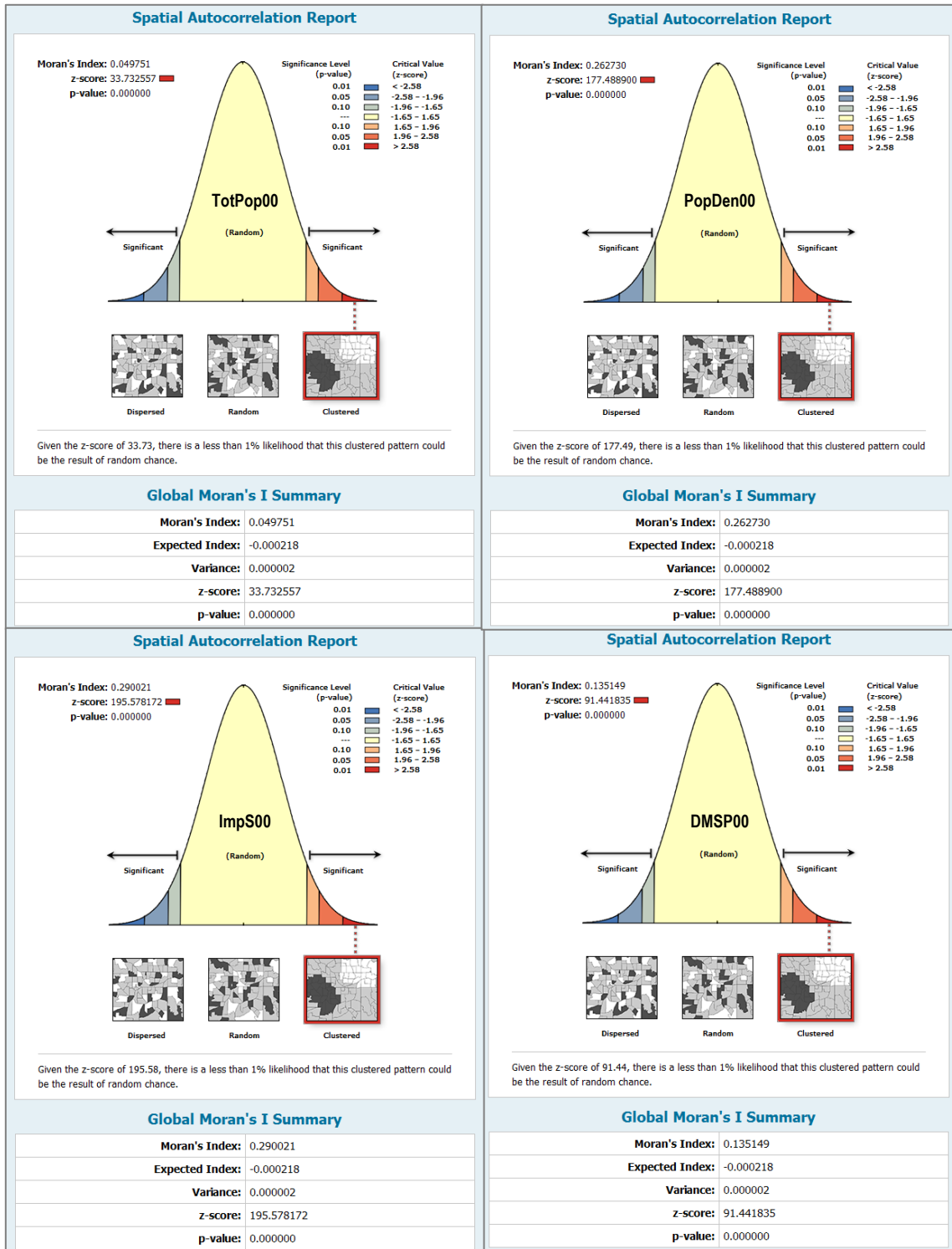
B.8. The spatial clustering pattern index results for the Arizona Sun Corridor megaregion



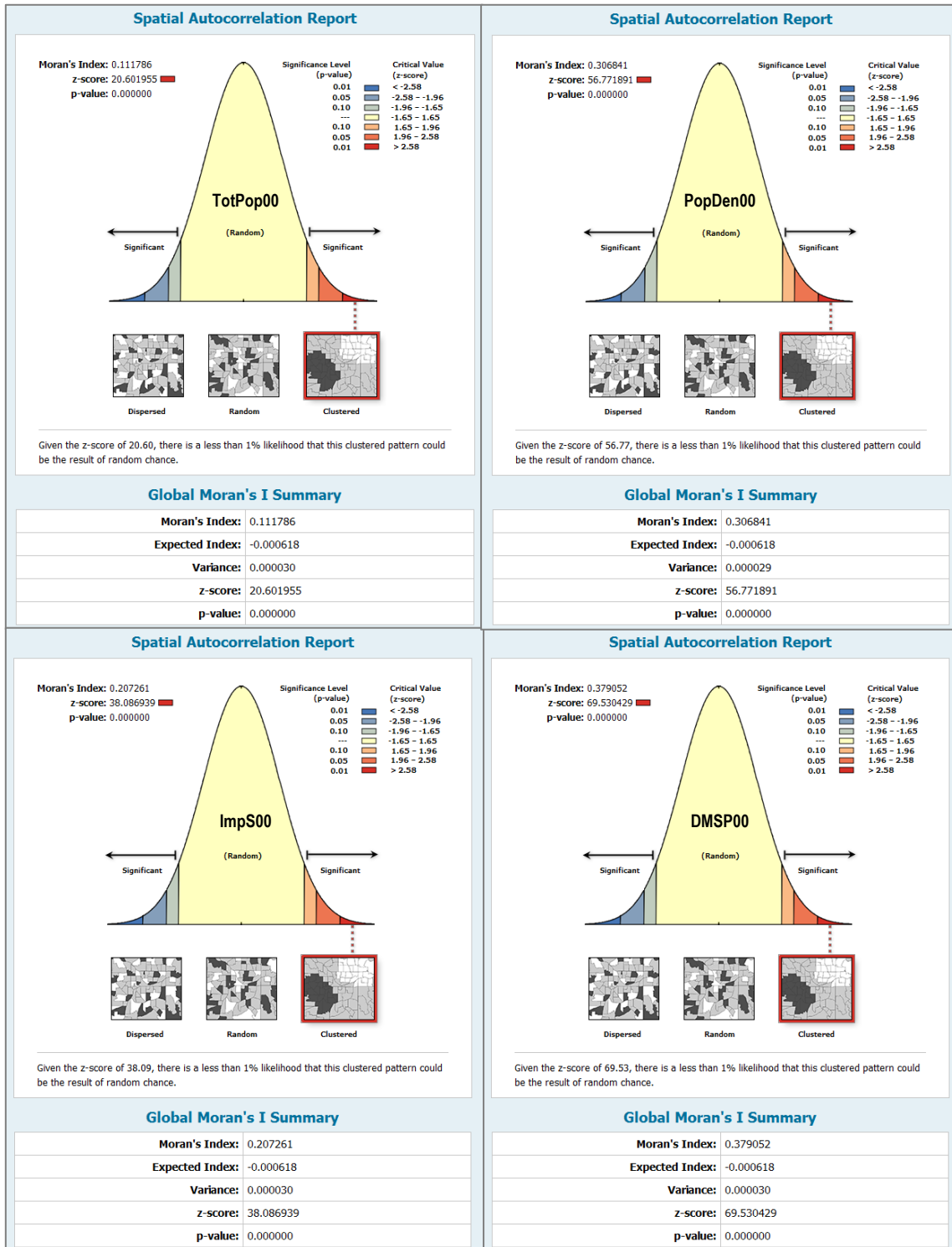
B.9. The spatial clustering pattern index results for the Northern California megaregion



B.10. The spatial clustering pattern index results for the Southern California megaregion



B.11. The spatial clustering pattern index results for the Cascadia megaregion



VITA

PERSONAL INFORMATION

Name: Youngho Ko

Email Address: youngho.ko@gmail.com

EDUCATION

B.A., Urban and Regional Planning, Handong University, S. Korea, 2004.

M.U.P., Texas A&M University, College Station, 2008.

Thesis: The Different Urban Efforts to Revitalize Urban Neighborhoods in US and UK: Comparative Case Study on Governmental Responses Focusing on Urban Neighborhood Revitalization.

EXPERIENCE

Assistant Researcher, Seoul Development Institute, S.Korea, 2005-06.

Research Internship, Korea Research Institute for Human Settlements, S.Korea, 2007.

Poster Presenter, Student Research Symposium, Texas A&M University, March 2007.

Paper Presenter, ACSP conference, Utah, October 2011.